

# PHOTONICA2011

International School and Conference on  
Photonics

29 August – 02 September 2011

Belgrade, Serbia

ABSTRACTS OF TUTORIAL, KEYNOTE  
AND INVITED LECTURES AND  
CONTRIBUTED PAPERS

*Editors*

Jovana Petrović, Milutin Stepić and Ljupčo Hadžievski

Vinča Institute of Nuclear Sciences

Belgrade, Serbia

Belgrade, 2011

ABSTRACTS OF TUTORIAL, KEYNOTE AND INVITED  
LECTURES AND CONTRIBUTED PAPERS  
of the  
International School and Conference on Photonics  
**PHOTONICA2011**

29 August – 02 September 2011  
Belgrade Serbia

*Editors*

Jovana Petrović  
Milutin Stepić  
Ljupčo Hadžievski

ISBN 978-86-7306-110-8

*Technical assistance*

Marija Petrović  
Petra Beličev  
Aleksandar Daničić  
Srđan Čortan

*Publisher*

Vinča Institute of Nuclear Sciences  
Mike Petrovića Alasa 12-14, P.O. Box 522  
11001 Belgrade, Serbia

*Printed by*

Printing office of the Vinča Institute of Nuclear Sciences

*Number of copies*

160

The International School and Conference on Photonics - PHOTONICA2011 is organized by the Vinča Institute of Nuclear Sciences ([www.vinca.rs](http://www.vinca.rs)), Institute of Physics, University of Belgrade ([www.phy.bg.ac.rs](http://www.phy.bg.ac.rs)), Faculty of Electrical Engineering, University of Belgrade ([www.etf.bg.ac.rs](http://www.etf.bg.ac.rs)), Faculty of Physics, University of Belgrade ([www.ff.bg.ac.rs](http://www.ff.bg.ac.rs)), Institute of Chemistry, Technology and Metallurgy, University of Belgrade ([www.ihtm.bg.ac.rs](http://www.ihtm.bg.ac.rs)), Faculty of Technical Sciences, University of Novi Sad ([www.ftn.uns.ac.rs](http://www.ftn.uns.ac.rs)) and Faculty of Sciences and Mathematics, University of Niš ([www.pmf.ni.ac.rs](http://www.pmf.ni.ac.rs)), with support of the **Ministry of Education and Science, Republic of Serbia**.

*The support from the sponsors of the Conference is gratefully acknowledged:*

1. SIEMENS
2. THORLABS
3. EKSMA OPTICS
4. EKSPLA
5. SWISSLION Takovo
6. Vinča Institute of Nuclear Sciences
7. Tourist Organization of Belgrade
8. Optical Society of America

The logo for Siemens, consisting of the word "SIEMENS" in a bold, teal, sans-serif font.The logo for Thorlabs, consisting of the word "THORLABS" in a bold, red, sans-serif font with a white outline.The logo for Ekspla, featuring a green asterisk-like symbol followed by the text "EKSPLA" in a bold, green, sans-serif font.The logo for Swisslion Takovo, consisting of the word "Swisslion" in red and "TAKOVO" in green, both in a sans-serif font.The logo for the Optical Society of America (OSA), consisting of the letters "OSA" in a bold, blue, sans-serif font with a registered trademark symbol.

## Scientific Committee

Aleksandra Maluckov, Serbia  
Arlene D. Wilson-Gordon, Israel  
Boris Malomed, Israel  
Branislav Jelenković, Serbia  
Dejan Milošević, Bosnia and Herzegovina  
Detlef Kip, Germany  
Dragan Indjin, United Kingdom  
Feng Chen, China  
Gaetano Mileti, Switzerland  
Giorgos Tsironis, Greece  
Goran Pichler, Croatia  
Ian Bennion, United Kingdom  
Jelena Radovanović, Serbia  
Kurt Hingerl, Austria  
Laurentius Windholz, Austria  
Ljupčo Hadžievski, Serbia  
Milivoj Belić, Qatar  
Nikola Burić, Serbia  
Paul Harrison, United Kingdom  
Radoš Gajić, Serbia  
Sergei Turitsyn, United Kingdom  
Slobodan Vuković, Serbia  
Stefka Cartaleva, Bulgaria  
Vladimir Škarka, France

## Organizing Committee

Ljupčo Hadžievski (Chair)  
Petra Beličev (Secretary)  
Milutin Stepić  
Milan Trtica  
Biljana Gaković  
Igor Ilić (Webmaster)  
Jovana Petrović  
Marija Petrović  
Aleksandar Daničić  
Branislav Jelenković  
Slobodan Vuković (OSA representative)  
Zoran Grujić (Webmaster)  
Jelena Radovanović  
Pedja Mihailović  
Jovan Elazar  
Bratislav Obradović  
Zoran Jakšić  
Miloš Živanov  
Aleksandra Maluckov

## Conference Topics

- Optical materials
- Metamaterials
- Photonic crystals
- Plasmonics
- Quantum optics
- Quantum informatics
- Ultracold systems
- Nonlinear optics
- Laser, laser spectroscopy
- Laser induced material modifications
- Biophotonics
- Optoelectronics and optocommunications
- Holography

## Preface

The **International School and Conference on Photonics - PHOTONICA**, is a biennial event held in Belgrade since 2007. The first meeting in the series was called ISCOM (International School and Conference on Optics and Optical Materials), but it was later renamed to Photonica to reflect more clearly the aims of the event as a forum for education of young scientists, exchanging new knowledge and ideas, and fostering collaborations between researchers working within emerging areas of photonic science and technology.

The Conference consists of oral presentations and vibrant poster sessions. The aim of the organizers is to provide a platform for discussing new developments and concepts within various disciplines of photonics by bringing together researchers from academia, government and industrial laboratories. In addition to the official program, the participants will also have plenty of opportunities to interact outside of the lecture theatre during the breaks and planned social events.

A particular educational feature of the program is provided through a series of tutorials specifically designed for students and scientists starting in the field. From our experience, they are an excellent introduction to the more specific topics covered by the regular talks.

This book contains abstracts of all presentations at the **3rd International School and Conference on Photonics - PHOTONICA2011**. During morning sessions 4 tutorial and 6 keynote speakers will give lectures to the benefits of students and young researches. 18 invited lectures and 17 oral presentations during afternoon sessions will present most recent results in their research fields. Students and young researches will present 116 poster presentations on their new results within the two afternoon poster sessions.

# Table of Contents

## Tutorial Lectures

T.1	Dynamics of dark solitons and vortex structures in Bose-Einstein Condensates <i>P.G. Kevrekidis</i>	18
T.2	Group IV Nanophotonics: From Silicon to Diamond <i>M. Lončar</i>	18
T.3	Terahertz technology and metamaterials <i>M. Hangyo</i>	19
T.4	Anderson localization of light <i>M. Segev</i>	20

## Keynote Lectures

K.1	Optical Airy beams and bullets <i>D. Christodoulides</i>	21
K.2	Waveguide lasers fabricated by Direct Laser Writing with femtosecond laser pulses <i>D. Jaque, A. Benayas, W. F. Silva, A. Ródenas, C. Jacinto, J. Vázquez de Aldana, F. Chen, Y. Tan, N.N. Dong, G. Lifante, E. Cantelar, R. R. Thomsom, G. A. Torchia and A. K. Kar</i>	22
K.3	Plasmonics for biosensing and metamaterials <i>V. P. Drachev</i>	22
K.4	Photonic crystals and quantum dots: from cavity QED, to single photon nonlinear optics and energy efficient information processing <i>J. Vučković, A. Majumdar, M. Bajcsy, E. Kim, A. Papageorge, A. Faraon, G. Shambat and B. Ellis</i>	23
K.5	Metamaterial surfaces at microwave frequencies <i>J. R. Sambles</i>	25
K.6	Novel integrated devices for all optical frequency conversion <i>R. Morandotti, L. Razzari, M. Ferrera, D. Duchesne, M. Peccianti, A. Pasquazi, S. Chu, B. E. Little and D. J. Moss</i>	26

## Invited Lectures

I.1	Spontaneous symmetry breaking in photonics and matter-wave optics <i>B. A. Malomed</i>	28
I.2	Computation and visualization of solutions to various generalized nonlinear Schrödinger equations <i>M. Belić, A. Sergeev, N. Aleksić and G. Chen</i>	28
I.3	Degenerate Quantum Gases manipulation on Atom Chips <i>F. S. Cataliotti</i>	29
I.4	Quasi static electromagnetic field generation in short pulse laser produced plasmas <i>K. Mima, T. Taguchi, T. Jhozaki, A. Sunahara, H. Nagatomo and H. Sakagami</i>	30

I.5	Inexpensive imaging at millimeter wave and terahertz frequencies using miniature neon lamp plasma focal plane arrays <i>N.S.Kopeika, A. Abramovich, O. Yadid-Pecht, Y. Yitzhaky, A. Levanon, D. Rozban, H. Joseph, A. Akram and A. Belenky</i>	30
I.6	Laser-induced modifications of transparent crystals and glasses: photo-excitation, thermodynamics, mechanical response <i>N.M. Bulgakova</i>	31
I.7	Ultrafast laser Parallel Processing of materials with Spatial Light Modulators <i>W. Perrie, D. Liu, Z. Kuang, S. P. Edwardson, E. Fearon, G. Dearden, K. Watkins, D. Karnakis, A. Kearsley and C. Moorhouse</i>	32
I.8	Optodynamics - Dynamic aspects of laser beam-surface interaction <i>J. Možina and J. Diaci</i>	33
I.9	Self-mixing interferometry with Vertical-Cavity Surface-Emitting Lasers: a new technology for biomedical sensing <i>A. D. Rakić, Y. L. Lim, S. J. Wilson and R. Kliese</i>	34
I.10	Revealing protein interactions with subcellular resolution: from physics to clinics <i>G. Vereb</i>	35
I.11	Enhance Persistent Luminescence of Nanoparticles for <i>In Vivo</i> Imaging <i>B. Viana, T. Maldiney, A. Lecointre, A. Bessière, M. Bessodes, D. Gourier, C. Richard and D. Scherman</i>	36
I.12	Nonlinear Superconducting Metamaterials <i>N. Lazarides and G. P. Tsironis</i>	37
I.13	Multipole approach for analytical modeling of metamaterials <i>A. Chipouline</i>	38
I.14	Atomic clocks: basic principles and applications; recent progress in vapor cell frequency standards <i>G. Miletì, C. Affolderbach, T. Bandi, F. Gruet, R. Matthey, D. Miletic and M. Pellaton</i>	38
I.15	Atomic magnetometers in fundamental and applied research <i>A. Weis, N. Castagna, M. Kasprzak, Z. Grujic, G. Bison and P. Knowles</i>	39
I.16	New nanostructure designs for the ultra-high-efficient solar cells <i>S. Tomić</i>	40
I.17	Record Performances in All-optical Signal Processing <i>N. Alic</i>	41
I.18	Advancements in imaging using terahertz quantum cascade lasers <i>P. Dean</i>	42

## Oral Presentations

### *Optical Materials*

O.OM.1	Using photonic crystal slabs to optimize quantum-well photo-detectors <i>R.Meisels, R. Brunner, O. Glushko, S. Kalchmair, R. Gansch and G. Strasser</i>	44
--------	--	----

## *Plasmonics*

- O.PL.1 Investigation of Ag nanoparticles' formation in soda-lime glass during nanosecond laser irradiation 45  
*A. Wolak, M. Grabić, O. Veron, J-P. Blondeau, N. Pellerin, M. Allix, S. Pellerin and K. Dzierżęga*

## *Nonlinear Optics*

- O.NO.1 On the problem of terawatt femtosecond pulse self - reflection from nonlinear focus and plasma in dielectrics 46  
*O. Khasanov, G. Rusetky, O. Fedotova, N. Aleksic and A. Sukhorukov*
- O.NO.2 Two color pump probe experiments at 4<sup>th</sup> generation X-ray light sources 47  
*N. Stojanovic, M. Gensch, F. Tavella, J. Feldhaus, B. Faatz, E. Schneidmiller and M.V. Yurkov*
- O.NO.3 Mobility of high-power solitons in saturable nonlinear photonic lattices 48  
*U. Naether, R. A. Vicencio and M. Stepić*

## *Optoelectronics and Optocommunications*

- O.OE.1 Determining Effective Refractive Index of Optical Slab Waveguide Based on Analytical and Finite Difference Method 49  
*A. Cetin, E. Ucgun and M. S. Kılıckaya*
- O.OE.2 Estimation of the uncertainty for a phase noise optoelectronic metrology system 50  
*P. Salzenstein, E. Pavlyuchenko, A. Hmima, N. Cholley, M. Zarubin, S. Galliou, Y. K. Chembo and L. Larger*
- O.OE.3 3D finite element modeling of optical microring resonators 51  
*B. Milanović, B. Radjenović and M. Radmilović-Radjenović*
- O.OE.4 A Simple Low-Coherence Interferometric Sensor for Absolute Position Measurement Based on Central Fringe Maximum Identification 52  
*L. Manojlovic, M. Zivanov, M. Slankamenac, D. Stupar, and J. Bajic*

## *Quantum Optics*

- O.QO.1 Nuclear quantum optics: Atoms and nuclei in a strong laser field 53  
*A.V. Glushkov*
- O.QO.2 Trajectory based interpretation of Poisson-Arago spot for photons and molecules 54  
*M. Davidović and M. Božić*
- O.QO.3 Spontaneous and blackbody-induced radiation transitions from Rydberg states in singly ionized calcium atoms 55  
*I.L. Glukhov and V.D. Ovsianikov*

## *Ultracold Systems*

- O.US.1 Dipolar Bose-Einstein Condensates with Weak Disorder 56  
*C. Krumnow and A. Pelster*

O.US.2	Parametric and Geometric Resonances of Collective Oscillation Modes in Bose-Einstein Condensates <i>I. Vidanović, H. Al-Jibbouri, A. Balaž and A. Pelster</i>	56
--------	--	----

### *Laser Induced Material Modification*

O.LIM.1	Influence of picosecond laser irradiation on nickel base superalloy surface microstructure <i>S. Petronic, D. Milanovic, A. Milosavljevic, M. Momcilovic and D. Petrusko</i>	57
O.LIM.2	Ultra-short pulse laser micro-processing of metals with radial and azimuthal polarization <i>O.J. Allegre, L. Mellor, S.P. Edwardson, W. Perrie, G. Dearden and K.G. Watkins</i>	58
O.LIM.3	Ultra-short Relativistic Photon and Particle Beams in High-Intensity Laser-Plasma Interaction <i>M.M. Škorić, Lj. Nikolić, Lj. Hadžievski and S. Ishiguro</i>	59

## **Poster Presentations**

### *Optical Materials*

P.OM.1	Sn/SiO <sub>2</sub> single crystals growth by hydrothermal method at high temperatures and pressures <i>I. Miron, D. H. Ursu, M. Miclau, R. Banica, M. Vasile and I. Grozescu</i>	61
P.OM.2	ZnO Nanowire emitters for tunable near-UV-Blue Light emitting diodes <i>B. Viana, O. Lupan and T. Pauporté</i>	62
P.OM.3	High power continuous-wave thin disk laser in Yb:CaGdAlO <sub>4</sub> <i>S. Ricaud, B. Weichelt, P. Goldner, B. Viana, P. Loiseau, A. Jaffres, A. Suganuma, M. Abdou-Ahmed, A. Voss, T. Graf, D. Ritz, E. Mottay, F. Druon and P. Georges</i>	63
P.OM.4	Influence of Na <sup>+</sup> ions on the dielectric spectra of double doped (YbF <sub>3</sub> , NaF):CaF <sub>2</sub> crystals <i>M. Stef and I. Nicoara</i>	64
P.OM.5	Analysis of imaging properties of microlenses based on the TESG layer elasticity <i>D. Vasiljević, B. Murić, D. Pantelić and B. Panić</i>	65
P.OM.6	Maximal Temperature Difference Determination in Pulse Infrared Thermography by Fitting Experimental Results with Numerical Simulation Curve <i>Lj. Tomić, J. Elazar and B. Milanovic</i>	66
P.OM.7	Enhancement of the photoluminescence properties of Al <sub>2</sub> O <sub>3</sub> -core/SnO <sub>2</sub> -shell nanowires by annealing in an oxidative atmosphere <i>C. Jin, S. Park, H. Kim and C. Lee</i>	67
P.OM.8	Enhancement of the photoluminescence properties of Ga <sub>2</sub> O <sub>3</sub> nanowires by In <sub>2</sub> O <sub>3</sub> coating <i>S. Park, C. Jin, H. Kim and C. Lee</i>	67

P.OM.9	A fiber-optic polarimetric demonstration kit <i>T. Eftimov, T. L. Dimitrova and G. Ivanov</i>	68
P.OM.10	Oblique Surface Waves at an Interface of Metal-dielectric Superlattice and an Isotropic Dielectric <i>S. M. Vuković, J. J. Miret, C. J. Zapata-Rodriguez and Z. Jakšić</i>	69
P.OM.11	Ab initio calculations of structural, electronic, optical and elastic properties of $K_3CrF_6$ <i>A. S. Gruia, C. N. Avram, N. M. Avram and M. G. Brik</i>	70
P.OM.12	Thermographic properties of $Sm^{3+}$ doped $GdVO_4$ phosphor <i>M.G. Nikolić, D. J. Jovanović, V. Đorđević, Ž. Antić, R.M. Krsmanović and M.D. Dramićanin</i>	70
P.OM.13	Thermographic properties of $Eu^{3+}$ and $Sm^{3+}$ doped $Lu_2O_3$ nanophosphor <i>R.M. Krsmanović, Ž. Antić, M.G. Nikolić, D. Jovanović, V. Đorđević and M.D. Dramićanin</i>	71
P.OM.14	Optical properties of $ZnAl_2O_4$ nanomaterials obtained by hydrothermal method <i>I. Miron, C. Enache, R. Banica, M. Vasile and I. Grozescu</i>	72
P.OM.15	Microlenses focal length control by chemical processing <i>B. Murić, D. Pantelić, D. Vasiljević and B. Panić</i>	72
P.OM.16	The model of exciton states in a nanocup in a magnetic field <i>V. Arsoski, N. Čukarić, M. Tadić and F.M. Peeters</i>	73
P.OM.17	Influence of the internal heterostructure to nonlinear absorption spectra for intersubband transitions in spherical quantum dot-quantum well nanoparticles <i>R. Kostić and D. Stojanović</i>	74
P.OM.18	Comparative study of crystal field parameters and energy levels scheme for the trivalent europium ion doped in $SrAl_2O_4$ and $SrIn_2O_4$ spinels <i>M. L. Stanciu and M. Vaida</i>	74
P.OM.19	Phonon Eigenvectors of Graphene at High-Symmetry Points of the Brillouin Zone <i>V. Damljanić, R. Kostić and R. Gajić</i>	75
P.OM.20	3d electron transitions in Co and Ni doped $MgSO_3 \cdot 6H_2O$ <i>P. Petkova</i>	75
P.OM.21	Visible and far IR spectroscopic studies of Co doped $(80-x)Sb_2O_3-20Na_2O-xWO_3$ glasses <i>P. Petkova, M.T. Soltani, S. Petkov, V. Nedkov and J. Tacheva</i>	76
P.OM.22	EPR parameters for $Co^{2+}$ doped in ZnO <i>R. Nistora</i>	76
P.OM.23	Vibronic interactions in excited states of $Mn^{2+}$ doped in $MF_2$ (M = Ca, Sr, Ba) crystals <i>M. Vaida</i>	77
P.OM.24	Electronic levels of $Cr^{2+}$ ion doped in II-VI compounds of ZnS – crystal field treatment <i>S. Ivaşcu and C.N. Avram</i>	78
P.OM.25	The parameters of free ions $Mn^{5+}$ and $Fe^{6+}$ <i>E.-L. Andreici and N.M. Avram</i>	78

P.OM.26	On the applicability of the effective medium approximation to the photoacoustic responses of multilayered structures	79
	<i>A. Popovic, Z. Soskic, Z. Stojanovic, D. Cevizovic and S. Galovic</i>	
P.OM.27	Interband optical absorption in a circular graphene quantum dot	80
	<i>M. Grujić, M. Zarenia, M. Tadić and F. M. Peeters</i>	
P.OM.28	Determination of surface minority carrier mobility in p-HgCdTe	80
	<i>V. Damnjanovic and J. Elazar</i>	
P.OM.29	Spectroscopic Ellipsometry and the Fano Resonance Modeling of Graphene Optical Parameters	81
	<i>A. Matković, U. Ralević, G. Isić, M. Jakovljević and R. Gajić</i>	
P.OM.30	Synthesis and characterization of graphene films by Hot Filament CVD	82
	<i>D. Stojanović, N. Woehrl and V. Buck</i>	

### *Metamaterials*

P.MM.1	Novel Design for Tunable Zeroth-Order Resonance in Epsilon-Near-Zero Channel: Theory and Experiment	83
	<i>M. Mitrovic and B. Jokanovic</i>	
P.MM.2	Enhancement of chemical sensors based on plasmonic metamaterials utilizing metal-organic framework thin films	84
	<i>Z. Jakšić, Z. Popović and I. Djerdj</i>	
P.MM.3	Variable angle ellipsometry and polarized reflectometry of the fishnet metamaterials	85
	<i>M. Jakovljević, G. Isić, B. Vasić, R. Gajić, I. Bergmair and K. Hingerl</i>	
P.MM.4	Modeling of tunneling times in anisotropic nonmagnetic metamaterials	86
	<i>I. Ilić, P.P. Beličev, J. Radovanović, V. Milanović and Lj. Hadžievski</i>	
P.MM.5	Mid-infrared semiconductor metamaterials utilizing intersubband transitions in quantum cascade laser structure	87
	<i>S. Ramović, J. Radovanović and V. Milanović</i>	

### *Plasmonics*

P.PL.1	Angular-dependent excitation of longitudinal surface plasmon polaritons in gold nanowires	88
	<i>O. A. Yeshchenko, I. M. Dmitruk and Y. Barnakov</i>	
P.PL.2	Size and temperature dependence of the surface plasmon resonance in silver nanoparticles	89
	<i>O. A. Yeshchenko, I. M. Dmitruk, A. A. Alexeenko, A. V. Kotko, J. Verdal and A. O. Pinchuk</i>	
P.PL.3	Tunable two-dimensional plasmonic crystals with semiconductor rods	90
	<i>B. Vasić and R. Gajić</i>	
P.PL.4	Hotspot Decorations for Metamaterial Arrays of Plasmonic Structures	90
	<i>V. K. Valev, A. V. Silhanek, Y. Jeyaram, D. Denkova, B. De Clercq, W. Gillijns, V. Petkov, O. A. Aktsipetrov, M. Ameloot, V. V. Moshchalkov and T. Verbiest</i>	

## *Nonlinear Optics*

P.NO.1	Plateau structures in laser-assisted and laser-induced processes <i>A. Čerkić, M. Busuladžić, E. Hasović, A. Gazibegović-Busuladžić, D. B. Milošević and W. Becker</i>	91
P.NO.2	Ellipticity dependence of the plateau structures in different atomic and molecular processes in strong laser field <i>A. Čerkić, M. Busuladžić, E. Hasović, A. Gazibegović-Busuladžić, S. Odžak and D. B. Milošević</i>	92
P.NO.3	Ionization rate for circularly polarized laser fields with modified ionization potential included <i>J.M. Stevanović, T.B. Miladinović, M.M. Radulović and V.M. Ristić</i>	93
P.NO.4	The energy of maximum number of photoelectrons during ionization of potassium and xenon atoms <i>T.B. Miladinović, J.M. Stevanović, M.M. Radulović and V.M. Ristić</i>	94
P.NO.5	Electric field effects on $D^0$ binding energies in CdTe/ZnTe spherical quantum dot <i>D. Stojanović and R. Kostić</i>	95
P.NO.6	Interface soliton complexes in system with one-site linked two-dimensional lattices <i>M. D. Petrović, G. Gligorić, A. Maluckov, Lj. Hadzievski and B. A. Malomed</i>	95
P.NO.7	Complexes of fundamental interface solitons in one-site coupled one-dimensional trilete lattices <i>M. Stojanović-Krasić, A. Maluckov, Lj. Hadzievski and B. A. Malomed</i>	96
P.NO.8	Exact spatio-temporal soliton solutions to the two-component co- and counter-propagating beams in Kerr-like media <i>N. Petrovic, H. Zahreddine and M. Belic</i>	97
P.NO.9	Dynamical instability of counterpropagating matter waves in optical lattices <i>S. Prvanović, D. Jović, R. Jovanović, A. Strinić and M. Belić</i>	97
P.NO.10	Boundary and finite size effects in highly nonlocal scalar nematic liquid crystals <i>A. Strinić, N. Aleksić, M. Petrović and M. Belić</i>	98
P.NO.11	Quantum dynamics of atomic ensembles in a laser pulse of definite shape: Chaos and optical bi-stability effects <i>O.Yu. Khetselius, G.P. Prepelitsa and A.A. Svinarenko</i>	98
P.NO.12	Multidimensional Ginzburg-Landau Equation in Nonlinear Optics Simulated with Split Step FDTD Method on Ultra Speed Hardware (GPU) <i>B. N. Aleksić, N. B. Aleksić, V. Skarka and M. Belić</i>	99
P.NO.13	Stability analysis of fundamental dissipative Ginzburg-Landau solitons <i>B. N. Aleksić, B. G. Zarkov, V. Skarka and N. B. Aleksić</i>	100
P.NO.14	Effect of FWM on High-Signal-Power Ultra DWDM-PONs with Standard SMFs <i>Z. Vujicic, N. B. Pavlovic and A. Teixeira</i>	101
P.NO.15	Interactions of gap solitons in double-periodic one-dimensional photonic superlattices with saturable nonlinearity <i>P.P. Beličev, I. Ilić and M. Stepić</i>	102

## *Lasers, Laser Spectroscopy*

- P.LS.1 AC Stark-shift in Double Resonance and Coherent Population Trapping in Wall-Coated Cells for Compact Rb Atomic Clocks 103  
*D. Miletic, T. Bandi, C. Affolderbach and G. Mileti*
- P.LS.2 Two-color photoionization of Helium through autoionization structures in XUV-FEL and laser fields 104  
*S.I. Themelis*
- P.LS.3 High-Power Metal Halide Vapour Lasers Oscillating in Deep Ultraviolet, Visible and Middle Infrared Spectral Ranges 104  
*K. A. Temelkov, S. I. Slaveeva, V. I. Kirilov, I. K. Kostadinov and N. K. Vuchkov*
- P.LS.4 Conversion of dark magneto-optical resonances to bright by controlled changes in the excitation parameters of the Rb D<sub>2</sub> line at linearly polarized excitation 105  
*L. Kalvans, M. Auzinsh, A. Berzinsh, R. Ferber, F. Gahbauer, A. Mozers and D. Opalevs*
- P.LS.5 Ground state Hanle resonances for measuring the longitudinal and transverse spin relaxation rates of cesium vapor in a paraffin-coated cell 106  
*N. Castagna and A. Weis*
- P.LS.6 Thermal memory influence on termoconducting component of photoacoustic response 107  
*M. Nestic, P. Gusavac, M. Popovic, Z. Soskic and S. Galovic*
- P.LS.7 Analysis of Fluorescence Emission Intensity and Lifetime of Rhodamine B in Ethanol and Tetrahydrofurane solvents 108  
*M.S. Rabasovic, D. Sevic, M. Terzic and B.P. Marinkovic*
- P.LS.8 Crossover resonances in Cs vapor confined in micrometric-thin cell 109  
*P. Todorov, D. Slavov, K. Vaseva, N. Petrov, A. Krasteva, D. Sarkisyan, S. Saltiel and S. Cartaleva*
- P.LS.9 Study of laser-pumped double-resonance clock signals using a micro-fabricated cell 110  
*M. Pellaton, C. Affolderbach, Y. Pétremand, N. F. de Rooij and G. Mileti*
- P.LS.10 Investigation of Color Balance Failure of offset printed images expressed by Color Difference in dependence of different Standard Illuminant Conditions 111  
*I. Spiridonov, M. Shopova, R. Boeva and M. Nikolov*
- P.LS.11 Terahertz pulse copropagation in ammonium vapors 112  
*S.Vidal, J.Degert, J. Oberlé, E.Freysz, O.Fedotova, G.Rusetsky and O.Khasanov*
- P.LS.12 Laser optics and spectroscopy of the cooperative electron - $\gamma$ - nuclear processes in molecular systems 113  
*A.V. Glushkov and A.A. Svinarenko*
- P.LS.13 The interpretation of the intensity of components of laser scattering by interaction with matter 114  
*Z. Fidanovski, M. Srečković, S. Ostojić, J. Ilić and M. Merkle*
- P.LS.14 Modeling of electron relaxation processes and the optical gain in magnet-field assisted THz quantum cascade laser 115  
*A. Daničić<sup>1</sup>, J. Radovanović<sup>2</sup>, V. Milanović<sup>3</sup>, D. Indjin<sup>3</sup> and Z. Ikonić<sup>3</sup>*

- P.LS.15 Development of an array of scalar and vector Cs magnetometers for a neutron EDM experiment 116  
*Z. Grujic, M. Kasprzak, P. Knowles and A. Weis*

### *Biophotonics*

- P.BP.1 Laser applications in retinopathy as invasive therapy and possibility of pre and post diagnostics by appropriate image processing 117  
*Z. Latinovic, A. Oros, M. Sreckovic, J. Ilic and P. Jovanic*
- P.BP.2 Stress and strain of dental abutment caused by the polymerization shrinkage of dental composite 118  
*T. Puskar, D. Vasiljevic, L. Blazic, D. Markovic, S. Savic-Sevic, B. Muric, D. Pantelic*
- P.BP.3 3D Solid model generation of a human maxillary premolar based on CT data 119  
*D. Vasiljević, I. Kantardžić, L. Blažić, M. Tasić and T. Puškar*
- P.BP.4 CT Scan-based finite element analysis of stress distribution in premolars restored with composite resin 120  
*I. Kantardžić, D. Vasiljević, L. Blažić, T. Puškar and M. Tasić*
- P.BP.5 Influence of photodiagnostic radiation on iron release by ferritin 121  
*L. Vladimirova and V. Kochev*
- P.BP.6 X-ray diffraction and FT-infrared spectroscopy in analyzing the hydroxyapatite for the application in dentistry 121  
*M. Đorđević, D. Jevremović, T. Puškar, A. Kovačević and G. Bogdanović*
- P.BP.7 Scattering of a laser beam in turbid media with sharply forward directed Henyey-Greenstein indicatrices 122  
*L. Gurdev, T. Dreischuh, I. Bliznakova, O. Vankov, L. Avramov and D. Stoyanov*
- P.BP.8 Comparison of beetroot extracts originating from several sites using Time Resolved Laser Induced Fluorescence Spectroscopy 123  
*M.S. Rabasovic, D. Sevic, M. Terzic and B.P. Marinkovic*
- P.BP.9 Study of the thermal denaturation of S-layer protein from *Lactobacillus salivarius* 124  
*L. Lighezan, R. Georgieva and A. Neagu*

### *Optoelectronics and Optocommunications*

- P.OE.1 Electric field enhancement in silicon slotted optical ring microresonators 125  
*B. Radjenović, B. Milanović, and M. Radmilović-Radjenović*
- P.OE.2 A simple fiber optic inclination sensor based on the refraction of light 126  
*J. Bajić, D. Stupar, A. Joža, M. Slankamenac and M. Živanov*
- P.OE.3 Tunneling times characterizing the electron transport through a multiple quantum well system with Rashba SOI 127  
*D.-M. Bălățeanu*
- P.OE.4 Monte Carlo simulation of Goos-Hänchen shifts in multimode step-index plastic optical fibers 127  
*M. S. Kovačević, A. Djordjevich and D. Nikezić*

P.OE.5	An analysis of modal dispersion in plastic optical fibers having W-shaped refractive index <i>M. S. Kovačević and A. Djordjevich</i>	128
P.OE.6	Explicit finite difference solution of the power flow equation in W-type optical fibers <i>A. Simović, S. Savović and A. Djordjevich</i>	128
P.OE.7	Calculation of the frequency response and bandwidth in step-index plastic optical fibers using the time-dependent power flow equation <i>B. Drljača, S. Savović and A. Djordjevich</i>	129
P.OE.8	FSR adjustment of silicone rib racetrack resonator <i>T. Keča, P. Matavulj, W. Headley and G. Mashanovich</i>	129
P.OE.9	Modeling of Carrier Dynamics in Multi-Quantum Well Semiconductor Optical Amplifiers <i>A. Totović, J.V. Crnjanski, M.M. Krstić and D.M. Gvozdić</i>	130
P.OE.10	Intersubband absorption in quantum dashes with various cross-section profiles <i>J.V. Crnjanski</i>	131
P.OE.11	Interface shape studies in Bridgman growth of multicrystalline silicon <i>O. Bunoiu, M. Stef, A. Popescu and D. Vizman</i>	132
P.OE.12	Modulation Response and Bandwidth of Injection-Locked Fabry-Perot Laser Diodes <i>A.G.R.Zlitni, M.M. Krstić and D.M. Gvozdić</i>	133
P.OE.13	Long-Period Gratings in PCF Fabricated by Fs Laser Pulses <i>M. D. Petrovic, A. Danicic, T. Allsop and J. Petrovic</i>	134
P.OE.14	Design of up-converters for silicon solar cells based on nonpolar a-plane GaN/AlGaIn quantum well structures <i>S. Radosavljević<sup>1</sup>, J. Radovanović, V. Milanović and S. Tomić</i>	134
P.OE.15	Evanescence field fiber-optic gas sensor using high index sol-gel nanoporous layer <i>N. Raicevic, A. Matthias, D. Kip and J. Deubener</i>	135

### *Photonic Crystals*

P.PC.1	Vortex solitons near boundaries of photonic lattices <i>D. Jović, R. Jovanović, C. Denz and M. Belić</i>	137
P.PC.2	Tunability of band gaps in the biopolymer photonic crystals <i>S. Savic-Sevic, D. Pantelic and B. Jelenkovic</i>	137
P.PC.3	Transition of Anderson localization behavior from one dimensional to two dimensional photonic lattices <i>D. Jović, M. Belić, C. Denz and Yu. S. Kivshar</i>	138

### *Holography*

P.HG.1	Reconstruction of silver-halide volume reflection holograms at the wavelengths of recording <i>B. Ivanov, M. Shopova, E. Stoykov and V. Sainov</i>	139
--------	---	-----

P.HG.2	Generation of sinusoidal fringes with a holographic phase grating and a phase-only Spatial light Modulator <i>N.Berberova, E. Stoykova and V. Sainov</i>	140
P.HG.3	High Resolution Solution Dot Matric Holograms Generation <i>B. Zarkov and D. Pantelić</i>	141
P.HG.4	Full-field stress analysis by holographic phase-stepping implementation of the photoelastic-coating method <i>T. Lyubenova, E. Stoykova, B. Ivanov, W.Van Paepegem, A. Degrieck and V. Sainov</i>	141

### *Quantum Optics*

P.QO.1	Free photon as a bound state system and consequence on electron <i>N.V.Delić, J.P. Šetrajić, S. Armačić, S. Cvetković, I.J. Šetrajić, V. Holodkov and B.Markoski</i>	142
P.QO.2	Radiation transitions from Rydberg states of lithium atoms in a blackbody radiation of environment <i>I.L. Glukhov and V.D. Ovsianikov</i>	143
P.QO.3	Simple analytical expressions for analysis of the phase-dependent electromagnetically induced transparency <i>J. Dimitrijević and D. Arsenović</i>	144
P.QO.4	Comparison of double- $\Lambda$ atomic scheme with single- and two-fold coupled transitions <i>D. Arsenović and J. Dimitrijević</i>	145
P.QO.5	A quantum phase operator on the von Neumann lattice <i>Lj. Davidović, M Davidović and M. Davidović</i>	146
P.QO.6	Narrowing of EIT resonance in the configuration of counter-propagation laser beams <i>I. S. Radojičić, Z. D. Grujić, M. M. Lekić, D. V. Lukić and B. M. Jelenković</i>	146
P.QO.7	Influence of Ramsey effects on Electromagnetically Induced Transparency and Slow Light in Hot Rubidium Vapor <i>S. N. Nikolic, N.M. Lucic, A.J. Krmpot, S.M. Cuk, M. Radonjic and B.M. Jelenkovic</i>	147
P.QO.8	Acoustic and visual display of photons: a demonstration device <i>T. L. Dimitrova, A. Lechkov, Ts. Grigorova and A. Weis</i>	148

### *Quantum Informatics*

P.QI.1	Constrained quantum dynamics and coarse-grained description of a quantum system of nonlinear oscillators <i>M. Radonjić, S. Prvanović and N. Burić</i>	149
--------	---	-----

### *Ultracold Systems*

P.US.1	Rb Magneto-Optical Trap and Temperature Measurement by Shaking of the Cold Cloud of Atoms <i>I.Temelkov, G. Dobrev, E. Dimova, A. Pashov, K.Blagoev and N. Vitanov</i>	150
--------	---	-----

P.US.2	Quantum Fluctuations in Dipolar Bose Gases <i>A. Lima and A. Pelster</i>	150
P.US.3	From spatially periodic states with lattice periodicity to states with the double lattice period in Bose-Einstein condensates in an optical lattice <i>G. Gligorić, A. Maluckov, Lj. Hadžievski and B. A. Malomed</i>	151

### *Laser Induced Material Modifications*

P.LIM.1	Microstructural changes of Nimonic-263 superalloy arisen by laser beam action <i>S. Petronić, A. Kovačević, A. Milosavljević and A. Sedmak</i>	152
P.LIM.2	Surface modification of Ti-based nanocomposite multilayer structures by laser beam irradiation <i>S. Petrović, B. Salatić, D. Peruško, M. Panjan, D. Pantelić, B. Gaković, B. Jelenković and M. Trtica</i>	153
P.LIM.3	Femtosecond laser ablation of alumina (Al <sub>2</sub> O <sub>3</sub> ) from a multilayered coating <i>B. Gaković, C. Radu, M. Zamfirescu, B. Radak, M. Trtica, S. Petrović, J. Stašić, M. Čekada and I.N. Mihailescu</i>	154
P.LIM.4	Laser based observation of water condensation on metal surface <i>A. Bizjak, D. Horvat and J. Možina</i>	155

### **Post-Deadline Contributions**

P.MM.6	Investigation of Group Delay in Transmission Lines Consisting of Reconfigurable Split-Ring Resonators <i>R. Bojanic, B. Jokanovic and V. Milosevic</i>	156
--------	---	-----

<b>Author Index</b>		158
---------------------	--	-----

# Tutorial Lectures

---

Tutorial Lectures T.1

## **Dynamics of dark solitons and vortex structures in Bose-Einstein Condensates**

P.G. Kevrekidis

*Department of Mathematics and Statistics, University of Massachusetts, Amherst, MA 01003, USA*  
e-mail: kevrekid@math.umass.edu

Our aim in these lectures is to give an over-arching methodology of how to approach the subject of dark solitons in quasi-one-dimensional and vortices in quasi-two-dimensional Bose-Einstein condensates (BECs). We will use a combination of analytical tools: in the near-linear, small density limit of the quantum harmonic oscillator, we will use bifurcation theory and Galerkin-type expansions; in the large density, so-called Thomas-Fermi limit, we will employ a particle-type approach and relevant ODE reductions that lead to equations for the dynamics of the coherent structures (solitons and vortices, respectively). These two analytical limits will be bridged by virtue of numerical continuation and bifurcation theory, as well as via direct numerical experiments that enable the full characterization of the mean-field approximation of the BEC system. These analytical and numerical results will be corroborated by direct comparisons with experimental results from the groups of M. Oberthaler and D. Hall, respectively. Additionally, the considerations will be generalized from the single-component (single-species) gases to that of multiple components and the setting of dark-bright and perhaps even vortex-bright solitary waves. Experimental comparisons in these will involve the work of the group of P. Engels. Connections with other areas such as nonlinear optics, integrability and dynamical systems theory will be highlighted along the way. A number of interesting directions for potential future study will also be presented.

Tutorial Lectures T.2

## **Group IV Nanophotonics: From Silicon to Diamond**

M. Lončar

*School of Engineering and Applied Science, Harvard University, Cambridge, MA 02138, USA*  
e-mail: loncar@seas.harvard.edu

Wavelength-scale optical resonators can enable on-chip manipulation of photons, and thus are important building blocks for optical- and quantum-communication systems. High quality factor (Q) photonic crystal (PhC) cavities, based on 2D photonic crystal architectures, have received a lot of attention as a promising platform for achieving these goals. However, recent work by our group[1,2,3] and others has demonstrated that 1D photonic crystal nanobeam cavities can also support ultra-high Q modes, on par with those found in 2D geometries. For example,  $Q=750,000$  was measured in a nanobeam cavity fabricated in silicon[1]. Owing to their tiny physical footprint, exactly the same as that of an optical waveguide, nanobeam resonators are ideally suited for application in densely

integrated photonics. Furthermore, by taking advantage of mechanical degrees of freedom of free-standing coupled nanobeam cavities, dynamically and continuously tunable/programmable optical filters can be realized[4]. External electrical or all-optical signals can be used to control the separation between such nanocavities, which in turn has a strong effect on their resonant wavelength. In my talk I will discuss application of photonic crystal nanobeam cavities in on-chip all-optical signal processing and bio-chemical sensing.

Single-crystalline diamond is another promising nanophotonic material platform. In particular, color centers in diamond have attracted significant attention as promising solid-state system for quantum communication and quantum information processing, as well as sensitive magnetometry. Performance of these systems can be significantly improved by embedding color centers within nanoscale optical devices including nanowires[5], nanoplasmonics[6] and all-diamond optical cavities. For example, in my talk I will describe a high-flux, room temperature, source of single photons based on an individual Nitrogen-Vacancy (NV) center embedded in a top-down nanofabricated, single crystal diamond nanowire[5].

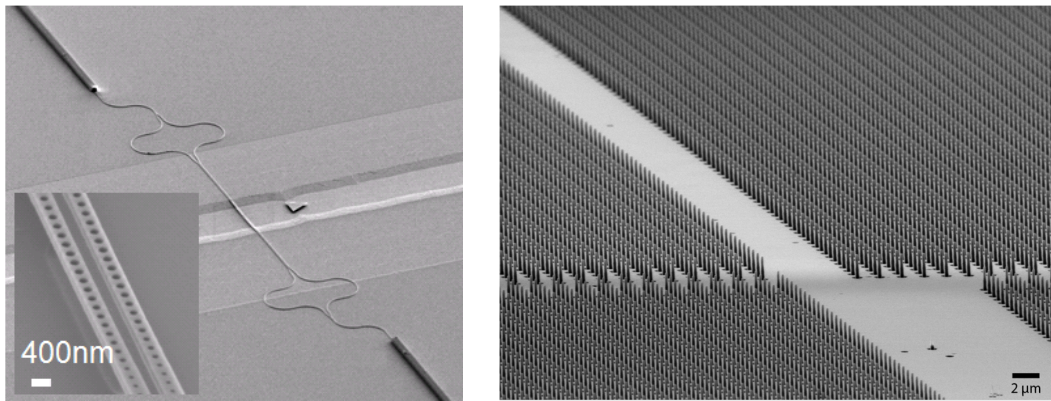


Figure. Programmable optical filter realized in silicon and Diamond nanowires.

#### REFERENCES

- [1] P. B. Deotare, M. W. McCutcheon, I. W. Frank, M. Khan, M. Lončar, APL 94, 121106 (2009).
- [2] M. W. McCutcheon, M. Lončar, Optics Express 16, 19136 (2008).
- [3] Q. Quan, P. B. Deotare, M. Lončar, Appl. Phys. Lett. 96, 203102 (2010).
- [4] I.W. Frank, P.B. Deotare, M.W. McCutcheon, M. Lončar, Opt. Exp. 18, 8705 (2010).
- [5] T.M. Babinec, B.M. Hausmann et al, Nature Nanotechnology 5, 195 (2010).
- [6] B. Hausmann, I. Bulu, T. M. Babinec, M. Khan, P. Hemmer, M. Loncar, CLEO (2010).

## Terahertz technology and metamaterials

M. Hangyo

*Institute of Laser Engineering, Osaka University*

*Suita, Osaka, Japan*

e-mail: hangyo@ile.osaka-u.ac.jp

Terahertz (THz) waves are electromagnetic waves between microwave and visible light in frequency and have been an unexploited frequency region until very recently. However, this frequency region has become the most rapidly growing electromagnetic wave region mainly owing to the development of the method of THz generation by using lasers. On the other hand, artificially sub-wavelength structured materials called metamaterials attract much attention. By suitably designing the structures, it is possible to obtain desired effective permittivity and permeability. Even negative permittivity and

permeability simultaneously is possible. In this case, the refractive index becomes negative. The THz wave region is the most suitable frequency region for developing metamaterials because the size of the elements (metaatoms) are of the order of several tens of microns and the required accuracy of them is about one micron, which is rather easy to access by modern fabrication technologies. In this tutorial lecture, at first I talk about the recent development of the THz technology and its various applications, and then, I talk about the metamaterials especially in the THz region.

THz wave pulses are emitted from devices such as semiconductor photoconductive antennas and nonlinear optical crystals by exciting them with femtosecond laser pulses. THz waves are also emitted from high-Tc superconductors. The THz spectroscopic system can be constructed by using these THz pulses and coherent detection of them. This system is called a THz time-domain spectroscopic system (THz-TDS). The THz spectroscopy and imaging have been applied to various fields as shown in Fig. 1 [1]. Nowadays, the THz-TDS has been routinely used in basic science such as condensed matter physics. Advanced spectroscopic systems such as magneto-optical and ellipsometric ones have also been developed. Since the papers and plastics transmit THz waves, THz waves can be used to find illicit drugs and explosives in mails.

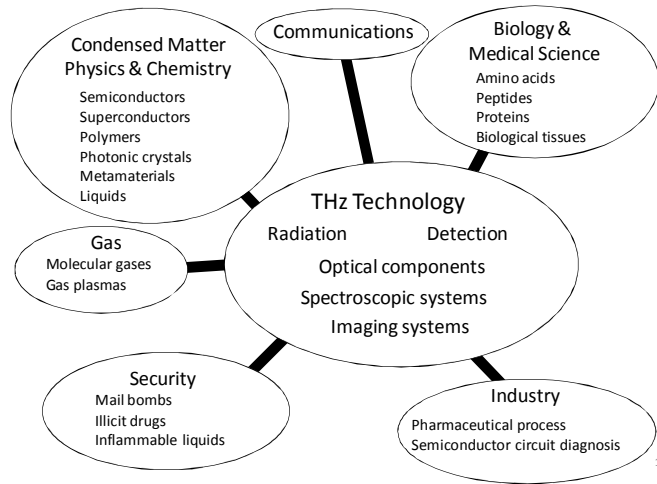


Fig. 1. Various applications of terahertz technology.

Metallic wire grids have been used as a polarizer or beam splitter in the THz region for long time. Since the period of the wires in them are much smaller than the wavelengths, the wire grids can be considered as a metamaterial. In this sense, metamaterials are realistic devices in the THz region. The planar metamaterials in the THz region are usually fabricated by photolithography. We proposed to use much easier and quick method for fabricating THz planar metamaterials using the super-fine ink-jet printing technology [2]. Metamaterials with negative permeability can be obtained usually by metallic split-ring resonators or their variations. We have realized negative permeability by utilizing the Mie resonances of the dielectric TiO<sub>2</sub> cubes.

REFERENCES

[1] M. Hangyo et al., *Int. J. Infrared and Millimeter Waves* 26, 1661 (2005).  
 [2] K. Takano et al., *Appl. Phys. Express* 3, 061701 (2010).

**Anderson localization of light**

M. Segev  
*Technion -Israel Institute of Technology, Haifa*  
*Haifa, Israel*  
 e-mail: msegev@tx.technion.ac.il

# Keynote Lectures

---

Keynote Lectures K.1

## Title Optical Airy beams and bullets

D. Christodoulides  
*CREOL-College of Optics and Photonics*  
*University of Central Florida*  
*Orlando, Florida 32816*  
demetri@creol.ucf.edu

We provide an overview of recent developments in the area of Airy beams and bullets. The possibility of using these new field arrangements in applications ranging from nonlinear optics and plasmonics to microparticle manipulation and ranging, will be discussed.

In recent years, the quest for non-spreading or non-diffracting optical beam configurations has been motivated by possible applications in diverse fields ranging from biology to atom optics. Lately our

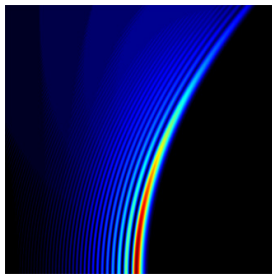


Fig. 1. Airy beams

group has explored the possibility of experimentally realizing non-spreading accelerating Airy beams in optics. This was done by exploiting the formal analogy between quantum wave mechanics and paraxial diffraction optics. We have demonstrated, that Airy beams can exhibit a host of interesting characteristics. More specifically, they resist diffraction while their main intensity maxima or lobes tend to self-bend and accelerate in free space along parabolic trajectories. This ballistic behavior persists over long distances in spite of the fact that the center of gravity of these wavepackets remains constant and eventually diffraction takes over. Figure 1 depicts quasi-diffractionless propagation of a finite-energy Airy beam where its “acceleration” dynamics are apparent. These intriguing properties of the Airy wavepackets put them in a category by themselves. In contrast to the already known families of non-diffracting fields they are possible in one-dimension, do not result from conical superposition, and are highly asymmetric. The peculiar features of Airy beams may find applications in near-field microscopy where their asymmetric intensity pattern could prove advantageous. Particle sorting (via optical gradient forces) along bent parabolic trajectories may be another fascinating direction. Versatile Airy spatio-temporal bullets (Fig. 2), resisting both diffraction and dispersion effects will be also discussed.

Figure 1 depicts quasi-diffractionless propagation of a finite-energy Airy beam where its “acceleration” dynamics are apparent. These intriguing properties of the Airy wavepackets put them in a category by themselves. In contrast to the already known families of non-diffracting fields they are possible in one-dimension, do not result from conical superposition, and are highly asymmetric. The peculiar features of Airy beams may find applications in near-field microscopy where their asymmetric intensity pattern could prove advantageous. Particle sorting (via optical gradient forces) along bent parabolic trajectories may be another fascinating direction. Versatile Airy spatio-temporal bullets (Fig. 2), resisting both diffraction and dispersion effects will be also discussed.

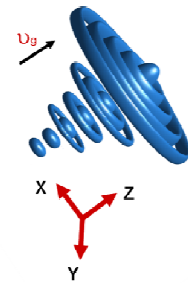


Fig.2. Airy bullets

## Waveguide lasers fabricated by Direct Laser Writing with femtosecond laser pulses

D. Jaque<sup>1</sup>, A. Benayas<sup>1</sup>, W. F. Silva<sup>2</sup>, A. Ródenas<sup>3</sup>, C. Jacinto<sup>2</sup>, J. Vázquez de Aldana<sup>4</sup>, F. Chen<sup>5</sup>, Y. Tan<sup>5</sup>, N.N. Dong<sup>5</sup>, G. Lifante<sup>1</sup>, E. Cantelar<sup>1</sup>, R. R. Thomsom<sup>3</sup>, G. A. Torchia<sup>6</sup> and A. K. Kar<sup>3</sup>

<sup>1</sup> *Departamento de Física de Materiales, Universidad Autónoma de Madrid, 28049 Madrid, Spain.*

<sup>2</sup> *Grupo de Fotônica e Fluidos Complexos, Instituto de Física, Universidade Federal de Alagoas, 57072-970 Maceió, Alagoas, Brazil*

<sup>3</sup> *School of Engineering and Physical Sciences, Heriot-Watt University, Edinburgh EH14 4AS, United Kingdom.*

<sup>4</sup> *Grupo de Óptica, Departamento de Física Aplicada, Facultad de Ciencias Físicas, Universidad de Salamanca, Salamanca 37008, Spain.*

<sup>5</sup> *School of Physics, Shandong University, Jinan 250100, People's Republic of China.*

<sup>6</sup> *Centro de Investigaciones Ópticas, CONICET-CIC, 1900 La Plata, Argentina erbia*

e-mail: daniel.jaque@uam.es

The fabrication of buried channel waveguides in laser gain media is nowadays reaching more and more attention. They constitute basic structures on which miniaturized lasers could be developed. Although there are several methods that have been already demonstrated to be valid for waveguide fabrication in laser gain media, the scientific community is still looking for new methods that can be incorporated in real mass production processes. In this sense Direct Laser Writing (DLW) with femtosecond laser pulses of waveguides has emerged as a revolutionary technique for waveguide fabrication that has been revealed to be almost universal as it has been already applied to a wide range of systems including glasses, glass-ceramics, transparent ceramics and laser crystals. The main advantages of the DLW waveguide is the associated reduced processing times, absence of previous sample preparation, true three dimensional capabilities and reduced manufacturing cost. In addition, it has been widely demonstrated, through confocal fluorescence imaging experiments, that DLW is a non destructive technique that preserves the original spectroscopic properties (and hence the laser ones) of the original system.

In this talk I will summarize the latest results obtained in the fabrication of multifunctional laser waveguides fabricated by DLW in a wide range of materials. In addition, special attention will be paid to elucidate the different physical mechanism that are beyond the permanent refractive index changes that are produce after the local irradiation with ultrafast laser pulses as well as to elucidate the resistance of these micro-structural modifications against time and temperature. Finally, the laser performance of the fabricated structures will be summarized and compared to those obtained from waveguides fabricated by different methods.

## Plasmonics for biosensing and metamaterials

V. P. Drachev

*Birk Nanotechnology Center and School of Electrical and Computer Engineering,  
Purdue University, West Lafayette, IN 47907, USA*

e-mail: vdrachev@purdue.edu

The recently emerged field of metamaterials promises a family of applications ranging from optical imaging with deeply sub-wavelength resolution to nanophotonics with the potential for much faster information processing. Artificially engineered materials with optical effective magnetism and negative refractive index employ the effect of circular currents in double layered plasmonic nanostructures separated by a dielectric spacer. Such a possibility has triggered intense basic and applied research on plasmonics over the past several years.

Also a progress in nanofabrication has led to significant achievements in well known plasmonic applications like surface-enhanced phenomena, and resulted in development of various new passive plasmonic components. Real-life applications require also active control to achieve signal switching, modulation, and amplification to compensate losses.

We will overview our experimental realizations of metamagnetics and negative index metamaterials for the visible range in both passive and active modes. We will discuss an example of plasmonic nanoantennas (pairs of metal particles, which can serve as emitters or receivers of electromagnetic radiation [1]) for photoluminescence kinetic parameters control and nonlinear materials engineering, experiments on a thermally tunable metamagnetic and imaging [2], and, finally, gain assisted negative index materials with no losses [3].

Experiments with aggregate nanostructures using bio-nanofabrication will be presented. It implies DNA-gold nanoparticle networks grown at cell surface marker sites with application in diagnostics of cancer cell lines. Profiling of human breast epithelial cells is performed to identify the membrane surface markers with surface-enhanced Raman scattering and dark field microscopy of plasmon resonances using DNA-hybridization-based gold nanoparticle networks.

In this talk we discuss combined, hyperspectral LSPRS imaging and SERS mapping using gold nanoparticle probes for multiplex profiling of human breast epithelial cells (HBECs) to identify the membrane surface markers. The plasmonic peak shift dependence on the DNA length and number of particles in aggregates is measured by the dark-field spectroscopy and can be extrapolated with a simple equation. A SERS signal of dye tag molecules is increased to the detectable level using DNA-assembled gold nanoparticle structures. The structure can be reversibly controlled by varying the temperature near DNA hybridization melting point. The detection is performed at demanding conditions of bio-sensing with Raman spectroscopy, such as long wavelength laser, low excitation power, and short measurement time. The feasibility of this approach is demonstrated for CD24 and CD44 receptors of three breast cancer cell lines (MCF-7, MDA-MB-231, and MDA-MB-468) [4].

#### REFERENCES

- [1] K.P. Chen, V.P. Drachev, J.D. Borneman, A.V. Kildishev, V.M. Shalaev, *Nano Letters* 10, 916 (2010).
- [2] S. Ishii, A. V. Kildishev, V. M. Shalaev, K.-P. Chen, V. P. Drachev, *Optics Letters* 36, 4, 451 (2011).
- [3] S. Xiao, V.P. Drachev, A.V. Kildishev, H.-K. Yan, U.K. Chettiar, V.M. Shalaev, *Nature* 466, 735 (2010).
- [4] K. Lee, V. P. Drachev, J. Irudayaraj, *ACS Nano*, 5, 2109 (2011).

Keynote Lectures K.4

### **Photonic crystals and quantum dots: from cavity QED, to single photon nonlinear optics and energy efficient information processing**

J. Vučković, A. Majumdar, M. Bajcsy, E. Kim, A. Papageorge, A. Faraon, G. Shambat and B. Ellis  
*Ginzton Laboratory and Department of Electrical Engineering, Stanford University,  
Stanford, CA 94305, USA  
e-mail: jela@stanford.edu*

Recent advances in nanofabrication have enabled the development of structures that can manipulate and localize light into volumes below a cubic optical wavelength with storage times of thousands of optical cycles. The emergence of such high quality nanophotonic structures has opened new opportunities for the study of light-matter interaction. For example, as a result of the localization of light within such ultra-small volume nano-resonators, large optical intensities can be achieved with

only a few photons coupled. Further, such a system also enables strong interaction between single atoms or atom-like quantum emitters (e.g. quantum dots) embedded within the cavity and single photons [1].

Such quantum emitters in optical nanocavities are interesting both as a testbed for fundamental cavity quantum electrodynamics (QED) experiments, as well as a platform for quantum and classical information processing. In addition to providing a scalable, on-chip, platform, these systems also enable large dipole-field interaction strengths, as a result of the localization of the field to very small optical volumes (as an example, for InAs quantum dots inside GaAs photonic crystal cavities, the vacuum Rabi frequency is on the order of 10s of GHz). As a result, system dynamics occurs on much faster time scales.

A single quantum emitter strongly coupled to an optical nanocavity can completely modify the cavity transmission, from transparent to opaque for an optical beam on the cavity resonance, as we have recently demonstrated in the InAs quantum dot/GaAs photonic crystal nanocavity system [1,2]. This implies that at the frequency corresponding to the empty cavity resonance there is now a dip, i.e., the cavity transmission dramatically changes. Moreover, we have shown that the cavity can be switched back to transparent if a control beam also shines on it, with control energies that can be as low as one photon per cavity photon lifetime [3]. We have also directly probed the ladder of dressed states of a strongly coupled quantum dot-cavity system and have employed its anharmonicity to demonstrate effects of photon blockade and photon induced tunneling, and to generate non-classical states of light [4]. Finally, we have also performed fast electrical control of the quantum dot strongly coupled to a cavity [5].

These demonstrations lie at the core of a number of proposals for quantum information processing, and could also be employed to build novel devices, such as optical gates operating at the single photon level and electro-optic modulators and switches with superior performance relative to state of the art devices.

For example, fast electrical control of a quantum dot strongly coupled to a cavity is important for switching and routing in quantum networks, but can also be employed in an electro-optic modulator controlled with sub-fJ energies (more than two orders of magnitude smaller than state of the art devices), while exhibiting modulation speeds exceeding 10's of GHz. [5] Moreover, a quantum dot-photonic crystal cavity laser with threshold current of 180nA has recently been demonstrated - the lowest threshold ever demonstrated in an electrically pumped semiconductor laser [6].

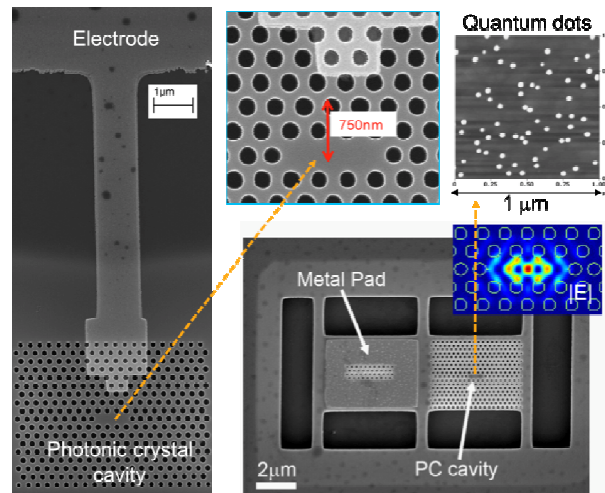


Fig. 1. Various quantum photonic devices based on InAs quantum dots embedded in GaAs photonic crystal nanocavities.

## REFERENCES

- [1] D. Englund, A. Faraon, I. Fushman, N. Stoltz, P. Petroff, J. Vuckovic, *Nature* 450, 7171, 857 (2007).
- [2] D. Englund, A. Majumdar, A. Faraon, M. Toishi, N. Stoltz, P. Petroff, J. Vuckovic, *Physical Review Letters* 104, 073904 (2010).
- [3] I. Fushman, D. Englund, A. Faraon, N. Stoltz, P. Petroff, J. Vuckovic, *Science* 320, 5877, 769 (2008).
- [4] A. Faraon, I. Fushman, D. Englund, N. Stoltz, P. Petroff, J. Vuckovic, *Nature Physics* 4, 859 (2008).
- [5] A. Faraon, A. Majumdar, H. Kim, P. Petroff, J. Vuckovic, *Physical Review Letters* 104, 047402 (2010).
- [6] B. Ellis, M. Mayer, G. Shambat, T. Sarmiento, E. Haller, J. S. Harris, J. Vuckovic, *Nature Photonics* 5, 297 (2011).

Keynote Lectures K.5

## **Metamaterial surfaces at microwave frequencies**

J. R. Sambles

*School of Physics, University of Exeter*

*Exeter, UK*

e-mail: j.r.sambles@exeter.ac.uk

Since the realization by Pendry and others [1] that by patterning metal surfaces with arrays of holes one may create ‘spoof’ or ‘designer’ surface plasmons at longer radiation wavelengths a substantial body of work has now appeared. Studies at microwave frequencies confirm experimentally the existence of these structurally-created surface waves [2], with more recent work ranging from these long wavelengths down through terahertz [3] and even into the visible [4]. In the visible domain a surface plasmon is the combined oscillation of the free electron charge density at the surface of a metal together with the highly localized electromagnetic field. At lower frequencies, as the electrons more readily respond to the driving frequency, this surface plasmon is much less localized in the dielectric half space, becoming essentially like a grazing photon and in the microwave domain such a surface wave is often referred to as a surface current. Pendry et al showed that the strong localization of the electromagnetic field in the dielectric (within a distance of the order of the wavelength) is recovered if the planar metal surface is patterned with a regular array of holes of size provided the frequency of interest is below the cut-off frequency of the holes. In actuality any structure at the surface of the metal which gives a localized resonance leads to a flat-banded dispersion which crosses the grazing photon light line and thereby creates a splitting into two distinct dispersion curves, one which is radiative and one which is non-radiative with ‘spoof’ surface plasmon character. This then opens up the potential for TE as well as TM surface waves [5] and the creation of surface waves on thin structures patterned with metal patches or ‘mushrooms’[6]. Further work has explored a range of surface structures studying guiding of these surface waves by lines of holes for example [7] or self-collimation with a laterally limited array [8]. This lecture will look at some recent developments in this area with particular reference to work at microwave frequencies.

## REFERENCES

- [1] J. B. Pendry, L. Martin-Moreno, F. J. Garcia-Vidal, *Science* 305, 847 (2004).
- [2] A. P. Hibbins, B. R. Evans, J. R. Sambles, *Science* 308, 5722 (2005) .
- [3] N. F. Yu, Q. J. Wang, M. A. Kats, J. A. Fan, S. P. Khanna, L. H. Li, A. G. Davies, E. H. Linfield, F. Capasso, *Nature Materials* 9, 730 (2010).
- [4] X. R. Huang, R. W. Peng, R. H. Fan, *Phys. Rev. Lett.* 105, 234901 (2010).
- [5] D. Sievenpiper, L. Zhang, R. F. J. Broas, N. G. Alexopolous and E Yablonovitch, *IEEE Trans. Microwave Theory Tech.* 47, 2059 (1999).

- [6] M. J. Lockyear, A. P. Hibbins and J. R. Sambles, Phys. Rev. Lett. 102, 073901 (2009).  
[7] L. F. Shen, X. D. Chen, X. F. Zhang, K. Agarwal, Plasmonics 6, 301 (2011).  
[8] S. H. Kim, T. T. Kim, S. S. Oh, J. E Kim, H. Y. Park, C. S. Kee, Phys. Rev. B 83, 165109 (2011).

## Novel integrated devices for all optical frequency conversion

R. Morandotti<sup>1</sup>, L. Razzari<sup>1</sup>, M. Ferrera<sup>1</sup>, D. Duchesne<sup>1</sup>, M. Peccianti<sup>1</sup>, A. Pasquazi<sup>1</sup>, S. Chu<sup>2</sup>,  
B. E. Little<sup>2</sup> and D. J. Moss<sup>3</sup>

<sup>1</sup>INRS-EMT, 1650 Boulevard Lionel Boulet, Varennes, Québec, Canada, J3X 1S2

Also with: Dipartimento di Elettronica, Università di Pavia, via Ferrata 1, 27100 Pavia, Italy

<sup>2</sup>Infinera Corp, 9020 Junction Dr, Annapolis, Maryland, USA 94089

<sup>3</sup>CUDOS, School of Physics, University of Sydney, New South Wales 2006 Australia

e-mail: morandot@emt.inrs.ca

Up to date, the world of electronics has always been an inexhaustible source of resources to satisfy the continuous request for larger bandwidth in communication systems. Unfortunately the bit rate limit of electronic devices (around 50 Gb/s) will soon be reached, and scientists and engineers are now struggling for alternative solutions. Among them, all-optical signal processing appears to be one of the most viable since it brings the promise to drastically increase the performances of transmission networks and, at the same time, to keep the associated costs low. However, in order to fulfill the goal of realizing all-optical agile communications systems and improve overall all-optical devices performances, it is mandatory to optimally perform fundamental network operations such as optical switching, data storage, ultrafast modulation, etc. In particular, wavelength conversion is required to realize wavelength division multiplexing systems capable of substantially increasing the bit rate by channeling the information on different frequency carriers. Recently ultra-low CW pump power (5mW) wavelength conversion based on Four Wave Mixing (FWM) has been reported in silicon micro-ring resonators. Nevertheless, it is of paramount importance to study other material systems, since silicon is well known to suffer from two-photon absorption (TPA) that in turn induces free carrier losses and may affect the performance of silicon based devices. In this work we first demonstrated, by means of C-MOS compatible Hydex ® glass based micro ring resonators, efficient wavelength conversion by FWM using ultra-low continuous-wave pump power (<5 mW, @1553.38nm). In this first set of experiments, we used rings whose Q factor was 65,000 and whose free spectral range was 575 GHz. By using the experimental value of the FWM efficiency we estimated the nonlinear refractive index ( $n_2$ ) of Hydex waveguides to be as much as five times larger than that of standard Silica, and the nonlinear  $\gamma$  parameter to be around 250 times higher than that of typical single mode glass fibers. Furthermore, the overall field enhancement factor of our device was shown to be  $\cong 1.4 \cdot 10^7$ , much larger than in semiconductor structures where losses tend to be in the order of several dB/cm.

Our results are comparable to the highest values reported to date in silicon ring resonators, and in addition they combine the advantages of ultra-low optical loss (0.06 dB/cm) with the absence of two-photon absorption (near  $\lambda=1.5\mu\text{m}$ ). We believe that these achievements may bring us a step forward in the quest to create very efficient all optical communication networks.

Furthermore, the possibility of creating novel frequency at very affordable power levels could open up an host of different applications beyond their use in telecommunication networks. For example, integrated multiple wavelength laser sources may be considered of great importance for applications as high-precision broadband sensing and spectroscopy, molecular fingerprinting, optical clocks, and attosecond physics. Even if they have recently been demonstrated in silica and single crystal micro-toroid resonators using parametric gain, for applications in telecommunications and optical interconnects, analogous devices in a fully integrated, CMOS compatible platform still do not exist.

While approaches such as silicon micro-ring resonators have been shown not to be ideal, other materials, such as Silicon nitride, have recently been proven to be a promising alternative platform for nonlinear optical devices since they exhibit negligible saturation effects due to multi-photon absorption, and this enabled the demonstration of efficient multi-wavelength optical parametric oscillation in integrated ring resonators.

In a second set of experiments, using rings with a higher Q factor, we succeeded in realizing a fully integrated, CMOS compatible, multiple wavelength source. We achieve CW optical “hyper-parametric” oscillation in a high quality factor ( $Q=1.2$  million) doped silica glass micro-ring resonator, with a differential slope efficiency above threshold of 7.4% for a single oscillating mode out of a single port, a CW threshold power as low as 54mW, and a controllable range of frequency spacing from 200GHz to more than 6THz. The low loss, design flexibility, and CMOS compatibility of this device will enable multiple wavelength sources for telecommunications, computing, sensing, metrology and other areas.

# Invited Lectures

---

Invited Lectures I.1

## Spontaneous symmetry breaking in photonics and matter-wave optics

B. A. Malomed

*Department of Physical Electronics, School of Electrical Engineering,  
Faculty of Engineering, Tel Aviv University, Tel Aviv 69978, Israel  
e-mail: malomed@eng.tau.ac.il*

Many important configurations in optical and matter-wave (Bose-Einstein-condensate) systems are based on settings with two parallel cores (waveguides), coupled by tunneling of photons or atoms. Basic models of such media amount to systems of linearly coupled equations with nonlinearities acting in each equation. A well-known example is the model of dual-core optical fibers or planar waveguides, which amounts to a system of linearly coupled nonlinear Schrödinger (NLS) equations. Similar models apply to BEC loaded into a set of parallel one- or two-dimensional tunnel-coupled traps. In such models, obvious symmetric soliton solutions lose their stability through symmetry-breaking bifurcations, when the total energy (norm) exceeds a certain critical value (i.e., the nonlinearity acting in the cores becomes strong enough). The bifurcations, which are typically of the sub- and supercritical types in the cases of the self-attractive and repulsive signs of the intrinsic nonlinearity, respectively, give rise to asymmetric solitons. These two types of the symmetry-breaking bifurcations are similar, severally, to the general phase transitions of the first and second kinds.

The talk aims to present an overview of basic models, results, and physical realizations of the symmetry-breaking phenomena in conservative and dissipative dual-core nonlinear media, including continual and discrete systems.

Invited Lectures I.2

## Computation and visualization of solutions to various generalized nonlinear Schrödinger equations

M. Belić<sup>1,2</sup>, A. Sergeev<sup>1</sup>, N. Aleksić<sup>2</sup>, G. Chen<sup>1</sup>

<sup>1</sup>*Texas A&M University at Qatar, P.O. Box 23874 Doha, Qatar*

<sup>2</sup>*Institute of Physics, University of Belgrade, P.O. Box 68 Belgrade, Serbia*

e-mail: milivoj.belic@qatar.tamu.edu

Numerical solutions to various generalized multidimensional nonlinear Schrödinger equations, including the paraxial wave equation, are very useful in many fields of physics. The reason is great importance of these equations as dynamical models in various fields and the lack of analytical solutions to them. What makes the problem of finding solutions to multidimensional nonlinear Schrödinger equations challenging is their inherent instability [1]. In such systems it is difficult to distinguish numerical instabilities from the real physical instabilities. One way out is to have at least *two independent* numerical packages that can treat the same system under the same conditions and

offer comparable solutions. The other is to have analytical solutions, to compare numerical solutions with (if and when analytical solutions are known). We utilize both ways. We have used the split-step beam propagation method in treating Schrödinger equations. We add to this a method based on the multidimensional finite-volume difference scheme. Hence, in this paper we present numerical computational results for several nonlinear optical processes governed by the generalized nonlinear Schrödinger and paraxial wave equations containing nonlinearities of various forms, using commercially available but suitably advanced numerical packages. The new numerical scheme is based on the parabolic marching in time with a finite-volume method, adapted from the heat diffusion equation in the computational fluid-dynamics software OpenFOAM [2]. We compare solutions obtained using this new method with the known numerical and analytical solutions of some generalized nonlinear Schrödinger equations and then proceed to find new solutions of other equations.

#### REFERENCES

- [1] C. Sulem and P. Sulem, *The nonlinear Schrödinger equation: Self-focusing and wave collapse* Springer, Berlin (2000).
- [2] OpenFOAM (<http://www.OpenFOAM.com>) is a free, open source computational fluid dynamics software package produced by a commercial company.

Invited Lectures      I.3

## **Degenerate Quantum Gases manipulation on Atom Chips**

F. S. Cataliotti

*LENS – Laboratorio Europeo di Spettroscopia Non-Lineare, Florence, Italy*

e-mail: [fsc@lens.unifi.it](mailto:fsc@lens.unifi.it)

Cold atomic systems in optical and magnetic potentials have been demonstrated as one of the most powerful tools for the investigation of quantum behavior in various model potentials, such as periodic potentials, reduced dimensionality potentials thanks to strong radial confinement, disordered potentials, and other more complex geometries. Precise knowledge of the model Hamiltonian, manipulation of its coupling constants, possibility of working with controllable disorder are some of the great advantages of atomic systems in optical and magnetic potentials which make them ideal tools for the realization of quantum models. The combination of optical potentials with magnetic and electrostatic fields varying on the scale of an optical wavelength opens even wider perspectives. The integration of cold atomic sources and electromagnetic field sources in the same device is a major frontier both for fundamental science and advanced technology where Europe has an important leadership.

I will discuss these devices, normally referred to as AtomChips, concentrating on the realization of a particular integrated matter wave interferometer where coherent coupling between the Bose-Einstein condensates in different Zeeman states is used to generate high-harmonic output signals with the enhanced sensitivity and maximum possible interferometric contrast. We have demonstrated a realisation of such an interferometer on an AtomChip providing a compact, easy-to-use, device.

Matter-wave interferometry is a powerful tool for high-precision measurements of the quantum properties of atoms, many-body phenomena and gravity. The most precise matter-wave interferometers exploit the excellent localization in the momentum space and coherence of the degenerate gases. Further enhancement of sensitivity and reduction of complexity are crucial conditions for success and widening of their applications. The device I discuss introduces a multi-path interferometric scheme that offers advances in both these aspects hence providing a new method for measurement of the light-atom and surface-atom interactions and enables application of simultaneous multi-parameter sensing schemes in the cold-atom interferometry.

## Quasi static electromagnetic field generation in short pulse laser produced plasmas

K. Mima<sup>1,2,3</sup>, T. Taguchi<sup>4</sup>, T. Jhozaki<sup>2</sup>, A. Sunahara<sup>2</sup>, H. Nagatomo<sup>2</sup> and H. Sakagami<sup>5</sup>  
<sup>1</sup> *The Graduate School for the Creation of New Photonic Industries, 1955-1, Kurematsu-cho, Nishi-ku, Hamamatsu, Shizuoka, Japan, 431-1202,*  
<sup>2</sup> *Institute of Laser Engineering, Osaka University,*  
<sup>3</sup> *IFN, University Polytechnica de Madrid,*  
<sup>4</sup> *Faculty of Engineering, Setunan University,*  
<sup>5</sup> *National Institute for Fusion Science*  
 e-mail: k.mima@gpi.ac.jp

Electron Magneto Hydrodynamics (EMHD) plays important roles in short pulse laser plasmas, magnetic field reconnection in MCF and space plasmas and magnetic field generation in astronomical plasmas when the space/time scales are much shorter than the ion scales and the time scale is much longer than the electron plasma frequency. The electro-magnetic fluctuations with frequencies much lower than the electron plasma frequency have structures like whistler waves. The turbulence of such electro-magnetic fluctuations is so called “whistler turbulence”. Examples of whistler turbulence are the turbulences predicted by the models of gamma ray burst and by the models for relativistic electron beam transport in ultra intense laser plasmas. The whistler turbulence also plays important roles in the collisionless magnetic reconnection in solar flare or magneto-sphere.

In this presentation, it is discussed that low frequency electro-magnetic fields are generated by the electromagnetic instabilities ( two stream Weibel instability ) and the thermo-electric effects. The self-generated electro-magnetic fields play important rolls in hot electron transport, ion acceleration and tera hertz radiation emission from laser plasmas.

The turbulence theory predicts that low frequency electromagnetic fluctuations in two dimension cascade to longer wave length modes through the non-linear interaction ( inverse cascade / self-organization). On the other hand, direction of magnetic fields becomes isotropic (Whistlerization). The theoretical analysis of the turbulence are applied to understand some simulation and experiment results. In some experiments, self-generated magnetic fields are self-organized to guide intense electron beams.

## Inexpensive imaging at millimeter wave and terahertz frequencies using miniature neon lamp plasma focal plane arrays

N.S.Kopeika<sup>1</sup>, A. Abramovich<sup>2</sup>, O. Yadid-Pecht<sup>3</sup>, Y. Yitzhaky<sup>1</sup>, A. Levanon<sup>1</sup>, D. Rozban<sup>1,2</sup>,  
 H. Joseph<sup>1</sup>, A. Akram,<sup>1,2</sup> and A. Belenky<sup>1</sup>  
<sup>1</sup>*Ben-Gurion University of the Negev, Beer-Sheva, Israel*  
<sup>2</sup>*Ariel University Center of Samaria, Ariel, Israel*  
<sup>3</sup>*University of Calgary, Calgary, Canada*  
 e-mail: kopeika@ee.bgu.ac.il

Millimeter wave (mmW) and terahertz (THz) imaging are subjects of immense interest because of unique applications in homeland security, biology, medicine, etc. Such systems, even though they usually do not contain focal plane arrays, are very expensive. Most mmW and THz imaging systems scan the image, thus detracting from the imaging speed. This is because focal plane arrays are usually not used because of detector price.

A solution for this problem is the use of miniature neon indicator lamps as detectors. They are quite inexpensive, costing about 50 cents each. Excellent responsivities and NEP have been obtained [1] in direct detection, with sensitivity improvement of about two orders of magnitude in heterodyne detection, depending on reference wave irradiance [2]. Speed of response is microsecond order and even less, depending on speed of electronics. Mechanism of detection is based on increase in free electron velocity in the gas discharge plasma, which increases the rate of ionization collisions of such free electrons with neutral gas atoms, thus increasing discharge current. These "signal" electrons are then swept by the substantial dc bias field towards the anode, and ionize many gas atoms along the way through collision processes, which gives rise to significant internal signal amplification [3]. Small focal plane arrays of 8X8 pixels have been developed, exhibiting good quality images [4] despite the small number of pixels, because of superresolution techniques. Such an 8X8 array has been used to obtain 32X32 pixel images at 100 GHz. Both conducting and dielectric objects have been imaged. A new 32X32 pixel array has recently been developed. Examples of imaging at 100 GHz, with and without superresolution, and calibration, are presented, including imaging of concealed objects. 8X8 and 32X32 pixel images are compared.

#### REFERENCES

- [1] A. Abramovich, N.S. Kopeika, D. Rozban, E. Farber, *Appl. Opt.* 46, 7207, (2007).
- [2] H. Joseph, A. Abramovich, N.S. Kopeika, A. Akram, D. Rozban, A. Levanon, *IEEE Sensors J.*, 2011, in press.
- [3] N.S. Kopeika, *IEEE Trans. Plasma Sci.* PS-6, 139, 1978.
- [4] D. Rozban, A. Levanon, H. Joseph, A. Akram, A. Abramovich, N.S. Kopeika, Y. Yitzhaky, A. Belenky, O. Yadid-Pecht, *IEEE Sensors J.*, 2011, in press.

Invited Lectures      I.6

### **Laser-induced modifications of transparent crystals and glasses: photo-excitation, thermodynamics, mechanical response**

N.M. Bulgakova<sup>1,2</sup>

<sup>1</sup>*Institute of Thermophysics SB RAS,  
Novosibirsk, Russia*

<sup>2</sup>*Optoelectronics Research Center, University of Southampton,  
Southampton, United Kingdom  
e-mail: nbul@itp.nsc.ru*

Ultrashort pulsed laser radiation applied to inorganic dielectric materials by focusing either on the surface or toward the bulk depth induces, depending on the irradiation conditions, different kinds of modifications such as formation of surface and volume periodic structures (nanogratings), densification and refractive index changes, formation of micro- and nanovoids, phase transitions such as amorphisation of crystalline materials, etc. Such modifications are already used in optoelectronics and photonics (optical signal transmission, optical beam manipulation, 3D writing of information, etc.) and also in microfluidics and the list of potential applications is rapidly expanding. In spite of growing technological applications of transparent materials and their paramount promises for using in optoelectronics and photonics, the fundamentals of laser-induced excitation of transparent crystalline materials and glasses have not sufficiently studied. This is conditioned by both the complexity of the processes in the laser-excited dielectrics and a great variety of compound transparent materials when even a small variation in atomic composition and structure changes dramatically material response to laser excitation. Successful development of applications based on laser-induced micro- and nanomodifications of transparent materials requires deep understanding of the whole chain of the intricate processes initiated in dielectrics by femtosecond laser pulses and extending up to millisecond time scale with formation of permanent mechanically deformed and/or chemically modified states.

This Lecture is dedicated to an outline of the processes taking place in transparent crystals and glasses under the action of ultrashort laser pulses. The spatiotemporal dynamics of laser-induced modifications will be analyzed which start from material photoionization with creation of seed free electrons followed by electron avalanche multiplication. This results in dense plasma formation accompanied by changing optical response of the laser-excited region toward metallization. The effects of self-focusing counteracted by scattering from the laser produced plasma upon propagation of the laser beam inside the bulk of a transparent material will be discussed. The aspects of warm dense matter and plasma collective behaviors will be touched. Special attention will be given to the thermal and mechanical effects which have yet been poorly studied for materials excited by ultrashort laser pulses. Swift heating of the photo-excited region occurring at picosecond timescale and corresponding pressure rise result in generation of the thermoelastic waves which, depending on the heating level and heat localization, can either completely dissipate, or lead to significant plastic deformations of the material, or even to mechanical damages in the form of micro- and nanovoids in the energy-release zone. The dynamics of the laser-induced processes will be illustrated by the results obtained in the frames of several modeling approaches, including those based on the non-linear Schrödinger equation, the Maxwell equations, the drift-diffusion approach, and the thermoelastoplastic stress analysis. The timescales of manifestation of the different processes will be defined, indicating the possibility of applying different modeling representations at different time spans.

A number of phenomena will be considered in detail such as charging of the dielectric surfaces culminating in Coulomb explosion, crater shaping, density redistribution upon waveguide writing; energy clamping effects. Finally, a short summary of several important experimental observations will be given which require explanations and adequate descriptions.

Invited Lectures I.7

## **Ultrafast laser Parallel Processing of materials with Spatial Light Modulators**

W. Perrie<sup>1</sup>, D. Liu<sup>1</sup>, Z. Kuang<sup>1</sup>, S. P. Edwardson<sup>1</sup>, E. Fearon<sup>1</sup>, G. Dearden<sup>1</sup>, K. Watkins<sup>1</sup>,  
D. Karnakis<sup>2</sup>, A. Kearsley<sup>2</sup> and C. Moorhouse<sup>3</sup>

<sup>1</sup> *Department of Engineering, University of Liverpool L69 3GQ, UK*

<sup>2</sup> *Oxford Lasers, Didcot, OX11 7HP, UK*

<sup>3</sup> *Coherent Scotland, Glasgow G20 OXA UK*

e-mail: wpfemto1@liv.ac.uk

Laser modification of materials with Ultrafast ( $\tau_p < 10\text{ps}$ ) laser pulses can demonstrate high precision by minimizing thermal diffusion during the pulse, coupling energy to the electronic system on a timescale shorter than the lattice heating time [1]. In metals, for example, this results in low threshold fluence  $F < 1\text{Jcm}^{-2}$  thus requiring only  $\mu\text{J}$  pulse energies while ultrafast (fs/ps) laser systems based on Regenerative amplifiers can provide mJ level pulses at kHz repetition rates. The need to severely attenuate pulse energies from mJ to  $\mu\text{J}$  results in very low throughput and waste of available laser output. Device fabrication can therefore take inordinately long to accomplish.

Spatial Light Modulators (SLM's) are dynamic diffractive optical elements, able to modulate an incoming wavefront through the application of Computer Generated Holograms (CGH's) to create any desired intensity distribution at the image plane of a lens. For example, an energetic fs/ps pulse can be diffractively split into many identical low energy spots in an arbitrary geometry and with the required fluence for precision micro-processing. As the intensity distribution at the lens image plane is the Fourier transform of the complex electric field after reflection on the SLM, the required CGH's can be calculated using Inverse Fourier Transforms (IFT's). Various algorithms (eg lens and gratings, Gerchberg-Saxton [2] for calculating the IFT's will be discussed and their relative merits in terms of

their accuracy and speed for producing a desired intensity patterns. Here, the degree of symmetry of the desired pattern is an important factor which can lead to unwanted intensity modulation.

We will demonstrate the use of phase only SLM's for highly parallel laser processing both on surfaces and inside optical materials through refractive index engineering. For example, high speed back contact opening for solar cells is shown by thin film removal of SiO<sub>2</sub> from Silicon at a rate of 1.6 10<sup>6</sup> contacts per second (1% area opening) so that a 5" wafer could be processed in ~ 2seconds. In addition, parallel refractive index modification of PMMA was employed to create efficient volume phase gratings with mm dimensions in minutes rather than hours. ( $\eta_{+1} > 75\%$ ). [3]

#### REFERENCES

- [1] B.N. Chichkov, C. Momma, S. Nolte, F. Alsvleben, A. Tunnermann, Appl. Phys. A. 63, 109 (1996).
- [2] G. Sinclair, J. Leach, P. Jordan, P. Gibson, E. Yao, Z. Laczik, M. Padgett, J. Courtial, Opt. Express 12, 1665 (2004).
- [3] D. Liu, Z. Kuang, W. Perrie, P.J. Scully, A. Baum, S.P. Edwardson, E. Fearon, G. Dearden, K.G. Watkins, Appl. Phys B, 101 8-7-823 (2010).

Invited Lectures I.8

## Optodynamics - Dynamic aspects of laser beam-surface interaction

J. Možina and J. Diaci  
*Faculty of Mechanical Engineering,  
University of Ljubljana,  
Ljubljana, Slovenia  
e-mail: janez.mozina@fs.uni-lj.si*

Laser interaction with matter can bring about a wide range of dynamic phenomena that can be observed on microscopic and macroscopic scales. Microscopic motion is e.g. associated with various waves (photo-acoustic, shock) that are generated during the laser-beam surface interaction and propagated in the surrounding media. These phenomena have been widely studied in order to understand the interaction processes and develop novel applications in several disciplines, such as non-destructive testing, spectroscopy, monitoring deexcitation processes and probing physical properties of materials [1]. Optodynamics has been defined as a new interdisciplinary research field representing a joint base for a variety of laser material processing and laser assisted medical applications [2]. Later a new propulsion concept was developed as an extreme example of laser induced mechanical motion in which thrust is produced as a reaction force of laser ablated material [3].

The contribution presents a synthesis of the results of original research in the area of laser material interaction and pulsed laser materials processing with a special emphasis on dynamic aspects of laser-beam surface interaction, which include the links between the laser material removal and the resulting material motion [4]. In view of laser material processing a laser beam is not only considered as a tool but also as a generator of information about the material transformation. The information is retained and conveyed by different kinds of optically induced mechanical waves. Several generation/detection schemes have been developed to extract this information especially in the field of non-destructive material evaluation. Blast and acoustic waves, which propagate in air surrounding the workpiece, have been studied using microphone detection as well as various set-ups of the laser beam deflection probe. Stress waves propagating through the workpiece have been studied using piezoelectric transducers and laser interferometers.

## REFERENCES

- [1] A.C. Tam, Rev. Mod. Phys., 58, 381 (1986).
- [2] J. Možina, R. Hrovatin, Prog. Nat. Sci. 6, S709 (1996).
- [3] C. Phipps et al., J. Prop. Power, 26, 609 (2010).
- [4] J. Možina and J. Diaci, Appl Phys B., DOI: 10.1007/s00340-011-4503-6.

Invited Lectures I.9

## **Self-mixing interferometry with Vertical-Cavity Surface-Emitting Lasers: a new technology for biomedical sensing**

A. D. Rakić, Y. L. Lim, S. J. Wilson and R. Kliese

*The University of Queensland, School of Information Technology and Electrical Engineering,  
Queensland 4072, Australia  
e-mail: rakic@itee.uq.edu.au*

Photonic technology has a history of significant contribution to biomedical research and practice. Revolutionary monitoring techniques such as pulse oximetry, transcutaneous gas monitoring and tissue spectrophotometry have all been predicated on developments in the underlying photonic devices.

In this paper, we introduce a compact sensing technology based on the self-mixing interferometer that uses Vertical-Cavity Surface-Emitting Laser (VCSEL) both for the emission and the detection of light. The self-mixing phenomenon occurs when the laser beam is partially reflected from an external target and injected back into the laser cavity [1]. The reflected light interferes or ‘mixes’ with the light inside the laser cavity and produces variations to the threshold gain, emitted power, lasing spectrum and the laser junction voltage. The reflected light can be frequency shifted, by means of Doppler effect, before being mixed with the original laser emission. The resulting output power variations are usually monitored by using the photodiode integrated within the laser package [2].

This phenomenon allows the laser to be used as an interferometric sensor incorporating the light source and the interferometer in one device thus significantly reducing the cost and the complexity of the sensing system. The homodyne (coherent) detection nature of this sensing scheme inherently provides very high sensitivity and consequently suffers minimal crosstalk between the channels in a free-space multichannel sensor implementation [3]. Self-mixing interferometry has been used to detect small displacements, change in the refractive index of materials, polarisation change and flow [4, 5]. In this paper we will outline several SM architectures with applications in biomedical sensing and imaging.

## REFERENCES

- [1] D. M. Kane, K. A. Shore, eds., *Unlocking Dynamical Diversity: Optical Feedback Effects on Semiconductor Lasers* (John Wiley & Sons Ltd, Chichester) (2005).
- [2] R. Kliese, Y. L. Lim, T. Bosch, A. D. Rakić, Opt. Lett. 35, 814 (2010).
- [3] Y. L. Lim, M. Nikolic, K. Bertling, R. Kliese, A. D. Rakic, Opt. Express, 17, 5517 (2009).
- [4] U. Zabit, R. Atashkhoei, T. Bosch, S. Royo, F. Bony, A. D. Rakic, Opt. Lett. 35, 1278 (2010).
- [5] Y. L. Lim, R. Kliese, K. Bertling, K. Tanimizu, P. A. Jacobs, A. D. Rakic, Opt. Express 18, 11720 (2010).

## Revealing protein interactions with subcellular resolution: from physics to clinics

G. Vereb

*Department of Biophysics and Cell Biology, University of Debrecen*  
e-mail: vereb@med.unideb.hu

Investigation of protein-protein interactions *in situ* in living or intact cells gains expanding importance as structure / function relationships proposed from bulk biochemistry and molecular modeling experiments require demonstration at the cellular level. Fluorescence resonance energy transfer (FRET) based methods are excellent tools for determining proximity and supramolecular organization of biomolecules at the cell surface or inside the cell. FRET measured on a cell-by-cell basis in flow cytometry, and with subcellular resolution in the microscope is has started to infiltrate basic research in cell biology. In fact, the number of publications exploiting FRET has doubled in the past five years. Yet, there is a hitherto unexploited possibility, that of transferring the knowledge gained in basic cellular models to the diagnostic level in molecular pathology. One salient example of such scenario is the case of multiform glioblastoma. Its treatment is frequently hampered by decreased radiosensitivity, which has been linked to overexpression of the ErbB1 / EGFR receptor tyrosine kinase.

In a model of glioblastoma expressing surplus ErbB1 we have identified that integrin  $\beta 1$  is also upregulated and decreasing radiosensitivity correlated with increasing ErbB1 and integrin  $\beta 1$  expression levels. As expected, increased expression of ErbB1 and integrin molecules was accompanied by increased ErbB1 – integrin  $\beta 1$  heteroassociation when measured by flow cytometric FRET. Interestingly, ErbB1 homoassociation decreased in parallel, in spite of the higher number of molecules in the cell membrane. Since the flow cytometric FRET approach yields average FRET values for each cell, and is restricted to assessing population statistics for one pair of molecules per sample, we have also implemented a microscopic two-sided FRET method which is based on labeling three molecular entities with three sequentially red-shifted dyes, such that first an acceptor photobleaching FRET measurement can be implemented on the more red-shifted pair, and consecutively the donor that remains intact in this procedure can serve as acceptor in a donor photobleaching protocol, using, as donor, the most blue-shifted fluorophor. This approach revealed that in pixels with higher ErbB1 – integrin  $\beta 1$  heteroassociation, ErbB1 homoassociation was lower, indicating a competition for association partners between these molecules. Furthermore, the shift towards heteroassociation was accompanied by a boosted PKB/Akt phosphorylation response to EGF, a possible explanation for greater radiation resistance in high expressing clones. For a clinical correlate, we have implemented acceptor photobleaching FRET on frozen tissue sections of grade II and IV clinical glioblastoma samples to further check the possible role of this ErbB1-integrin signaling axis. Grade IV tumors showed higher ErbB1 and integrin  $\beta 1$  expression levels and greater ErbB1 – integrin  $\beta 1$  heteroassociation than Grade II tumors. Of these parameters, the extent of molecular association was a single determinant of tumor grade in stepwise logistic regression. The revealed ErbB1 – integrin  $\beta 1$  heteroassociation raises the possibility of combining integrin blockers with kinase inhibitors in high grade glioblastoma.

### REFERENCES:

- [1] Vereb et al, *Methods Cell Biol* 75, 105 (2004).
- [2] Fazekas et al, *Cytometry A* 73, 209 (2008).
- [3] Roszik et al, *BMC Bioinformatics* 9, 346 (2008).
- [4] Roszik et al, *Cytometry A* 75, 761 (2009).

## Enhance Persistent Luminescence of Nanoparticles for *In Vivo* Imaging

B. Viana<sup>1\*</sup>, T. Maldiney<sup>2</sup>, A. Lecointre<sup>1</sup>, A. Bessière<sup>1</sup>, M. Bessodes<sup>2</sup>, D. Gourier<sup>1</sup>, C. Richard<sup>2</sup> and D. Scherman<sup>2</sup>

<sup>1</sup> *Laboratoire de Chimie de la Matière Condensée de Paris; Chimie-ParisTech, UPMC, Collège de France, CNRS UMR 7574, 11 rue Pierre et Marie Curie, 75231 Paris Cedex 05, France*

<sup>2</sup> *Unité de Pharmacologie Chimique et Génétique et d'Imagerie; CNRS, UMR 8151, Paris, F-75270 cedex France; Inserm, Faculté des Sciences Pharmaceutiques et Biologiques, Paris, F-75270 cedex France; Chimie Paristech, Paris, F-75231 cedex France, e-mail: bruno-viana@chimie-paristech.fr*

*In vivo* optical imaging, using photons as primary information, has witnessed several major improvements in the last decades. It was demonstrated that persistent luminescence nanoparticles could be used as sensitive optical probe for *in vivo* imaging, and that their biodistribution was highly dependent on both core diameter and global surface charge [1]. However, luminescence from these persistent luminescence nanoparticles was not intense enough to provide long-term monitoring of *in vivo* probes accumulation, unveiling the need to work on new nanomaterials with improved optical characteristics.

To better understand the origin of such phenomenon, we suggested a mechanism of persistent luminescence, with hole trap acting as recombination center. We then hypothesized that trivalent lanthanide ions could act as an efficient electron trap for persistent luminescence [2]. Several materials are then presented for such applications.

Starting from the hypothesis that controlling electrons trap depth could help to enhance the optical properties of persistent luminescence nanoparticles, we report the synthesis of several rare earth and transition metal doped nanoparticles. For instance divalent manganese, present in diopside silicate compounds, is at the origin of the red emission. We identify  $\text{Pr}^{3+}$  as the optimal electron trap in this host, which led to high performance nanomaterials, well excitable with UV light before injection in small animals and displaying the most intense afterglow in the near-infrared region. We managed to extract nanoparticles with narrow distribution from the initial polydisperse powder, and report their application for highly sensitive real-time *in vivo* bio-imaging. In some case it is possible to have an optical reexcitation under green/red emission in order to follow days after days the *in-vivo* nanoparticles distribution.

### REFERENCES

- [1] T. Maldiney, C. Richard, J. Seguin, N. Wattier, M. Bessodes, D. Scherman, *ACS Nano*. 5, 854 (2011).  
 [2] A. Lecointre, A. Bessière, B. Viana, D. Gourier, *Radiat. Meas.* 45, 497 (2010).

## Nonlinear Superconducting Metamaterials

N. Lazarides<sup>1</sup> and G. P. Tsironis<sup>1</sup>

<sup>1</sup>*Department of Physics, University of Crete, and FORTH,*

*P. O. Box 2208, 71003 Heraklion, Greece*

e-mail: nl@physics.uoc.gr

The term '*metamaterial*' usually refers to periodic arrangements of artificially structured elements designed to achieve advantageous and/or unusual electromagnetic properties. The interest in metamaterials originates from their great potential for novel applications in antennas, microwave devices, super-resolution imaging, cloaking and illusion devices, etc. The last decade, there have been many efforts to increase their performance and bring their operation frequency towards the optical [1,2]. However, significant losses place a strict limit on the performance of conventional metamaterials in the RF – Terahertz frequency range, hampering thus any progress toward their practical use [3,4]. Superconducting metamaterials provide a dramatic reduction of losses accompanied by inherent nonlinearity and extreme sensitivity to external fields [4,5].

Two-dimensional arrays of split-ring resonators (SRRs) made up of either low [6] or high [7,8] critical temperature superconducting material exhibit relative magnetic permeability less than one or even negative, and the ability to tune the frequency range at which this unique response occurs [9]. Moreover, the creation of a narrow tunnel barrier in the gap of each superconducting SRR brings the Josephson effect into play. These artificial *meta-atoms*, frequently referred to as 'Josephson junction rings', have much in common with the well-known in superconductivity radio-frequency superconducting interference devices (rf SQUIDs). It has been demonstrated that superconducting metamaterials composed of magnetically coupled rf SQUIDs, whose dominant nonlinearity is due to the Josephson effect, can operate as magnetic metamaterials exhibiting permeability oscillations and tunability as a function of an external magnetic field [10].

The combined effects of nonlinearity and discreteness may lead to the generation of nonlinear magnetic excitations in the form of dissipative discrete breathers, dynamically self-localized modes that may result from a delicate balance of the incident power due to the applied magnetic field and the intrinsic losses. The existence and stability of several types of discrete breathers, some of which may co-exist, has been demonstrated in a two-dimensional rf SQUID model based on equivalent circuits [11,12]. Discrete breathers break homogeneity by changing locally the magnetic response of the rf SQUID metamaterial from diamagnetic to paramagnetic (or vice versa). Moreover, wave transmission in small SQUID lattices reveals the presence of multistability and chaos [13].

### REFERENCES

- [1] C. M. Soukoulis, S. Linden, M. Wegener, *Science* 315, 47 (2007).
- [2] V. M. Shalaev, *Nature Photonics* 1, 41 (2007).
- [3] S. M. Anlage, *J. Opt.* 13, 024001 (2011).
- [4] N. I. Zheludev, *Science* 328, 582 (2010).
- [5] N. I. Zheludev, *Optics and Photonics News* 22, 30 (2011).
- [6] B. Jin et al., *Opt. Express* 18, 17504 (2010).
- [7] V. A. Fedotov *et al.*, *Opt. Express* 18, 9015 (2010).
- [8] J. Gu *et al.*, *Appl. Phys. Lett.* 97, 071102 (2010).
- [9] M. C. Ricci *et al.*, *IEEE Trans. Appl. Superconduct.* 17, 918 (2007).
- [10] N. Lazarides, G. P. Tsironis, *Appl. Phys. Lett.* 90, 163501 (2007).
- [11] N. Lazarides, G. P. Tsironis, M. Eleftheriou, *Nonlin. Phenom. Complex Syst.* 11, 250 (2008).
- [12] G. P. Tsironis, N. Lazarides, M. Eleftheriou, *PIERS Online* 5, 26 (2009).
- [13] M. Mattheakis, V. Rothos, N. Lazarides, G. P. Tsironis, in preparation.

## Multipole approach for analytical modeling of metamaterials

A. Chipouline

*Institute of Applied Physics, Friedrich Schiller University Jena, Max-Wien Platz 1, D-07743 Jena, Germany*  
e-mail: arkadi.chipouline@uni-jena.de

Metamaterials are composites consisting of artificial metaatoms/metamolecules with typical sizes less than the respective wavelengths. A key point of the metamaterials, which differs them principally from the natural one (at least in a visible wavelength range) is the magnetic response on an external electric field.

In this work we summarize the multipole expansion approach in order to describe analytically linear and nonlinear effective optical properties of passive metamaterials, and optical properties of metamaterials with gain. In order to validate our model, we applied the formalism for the split-ring resonator and the cut-wire structure and compare the results with rigorous numerical calculations. The proposed multipole approach has been applied to describe metamaterials with disorder. A new type of the second order nonlinearity – so called multipole nonlinearity – has been found to appear even for intrinsically linear metal, which the nano resonators consist of.

## Atomic clocks: basic principles and applications; recent progress in vapor cell frequency standards

G. Miletì, C. Affolderbach, T. Bandi, F. Gruet, R. Matthey, D. Miletic and M. Pellaton  
*Laboratoire Temps-Fréquence (LTF),  
Institute of Physics, Faculty of Sciences,  
University of Neuchâtel, Switzerland*  
e-mail: gaetano.mileti@unine.ch

This talk will start with a general introduction on atomic clocks, describing the main basic physical principles and reviewing their wide field of applications that range from fundamental physics experiments on ground and in space to practical devices used in everyday life, such as cell phones networks and satellite navigation systems.

In this introduction, we will also discuss some of the significant discoveries and innovations – in particular related to photonics - that have brought a step forward or sometimes a real “revolution” in the field of atomic clocks. Among those breakthroughs, one may mention the use of laser diodes in “traditional” microwave-based atomic clocks, the advent of laser cooling in primary frequency standards (atomic fountains) and, more recently, the impact of optical combs in a new generation of optically-based atomic frequency standards, which may even lead to a redefinition of the second.

In the second part of the presentation, we will focus on the particular case of vapor-cell atomic frequency standards, commonly referred to as “Rubidium clocks”, and present the main trends of this field of research [1].

Traditionally, the basic principle of cell standards has been microwave-optical Double Resonance (DR) using a plasma discharge lamp and isotopic filtering. With the advent of tunable laser diodes, the optical pumping process could be improved and/or refined, and Coherent Population Trapping (CPT) has emerged as possible alternative to DR as basic physical clock principle.

In general, two objectives are being pursued: (1) reaching excellent medium and long-term frequency stability (fractional frequency instability of the order or below  $10^{-14}$  at 1 day, which corresponds to approximately 1ns); (2) extreme miniaturization (1 cm<sup>3</sup>, 150mW) by exploiting modern micro fabrication techniques and assemblies. In the first case, high performance must be reached while maintaining a very low volume and power consumption (1 liter, 10 watts). In the second case, this stated reduction in size and power consumption has to be achieved while keeping an excellent performance, especially compared to quartz oscillators (fractional frequency instability of the order or below  $10^{-11}$  and frequency drifts on the same level per day, which corresponds to approximately 1 $\mu$ s at 1 day).

We will illustrate these two lines of research with some examples of on-going investigations related to high-performance atomic clocks for the future European satellite navigation system GALILEO (the European counterpart of GPS) and to chip-scale atomic clocks for telecommunications. In particular, we will report on the recent demonstration that gas-cell standards may reach similar performances of much bulkier devices in the short and medium term timescales [2, 3], and present the latest results on CPT in micro-fabricated Cesium cells for the first European chip-scale atomic clock [4, 5].

[1] J. Camparo, *Physics today*, Volume 60, Issue 11, p. 33 (2007).

[2] T. Bandi, C. Affolderbach, C. E. Calosso, and G. Mileti, *Electronics Letters*, 47, (12), 697 (2011).

[3] <http://telecom.esa.int/telecom/www/object/index.cfm?fobjectid=30855>

[4] D. Miletic, P. Dziuban, R. Boudot, M. Hasegawa, R. K. Chutani, G. Mileti, V. Giordano and C. Gorecki, *Electronics Letters*, 46, 15, 1069 (2010).

[5] <http://www.mac-tfc.eu/>

Invited Lectures I.15

## Atomic magnetometers in fundamental and applied research

A. Weis<sup>1</sup>, N. Castagna<sup>1</sup>, M. Kasprzak<sup>1</sup>, Z. Grujic<sup>1</sup>, G. Bison<sup>2</sup> and P. Knowles<sup>1</sup>

<sup>1</sup>*Physics Department, University of Fribourg, Fribourg, Switzerland*

<sup>2</sup>*Biomagnetisches Zentrum, Universitätsklinikum Jena, Jena, Germany*

e-mail:Antoine.weis@unifr.ch

The operation principle and performance of atomic magnetometers based on optically detected magnetic resonance (ODMR) in paraffin-coated alkali vapor cells will be discussed. Ground state spin orientation (vector polarization) is created via optical pumping with circularly polarized resonant laser radiation. The spin polarization is destroyed by an oscillating magnetic drive field (magnetic resonance). Since the optical properties of the medium (here, the absorption coefficient) depend on the medium's polarization, the same laser beam can be used to monitor polarization changes induced by the magnetic resonance process. Depolarization is most efficient when the frequency of the drive,  $\omega_{rf}$ , matches the Larmor frequency,  $\omega_L$ , of the precessing spins.

In the so-called  $M_x$ -geometry [1], the transmitted light intensity is modulated at the frequency  $\omega_{rf}$ . This can be used to operate the magnetometer as a phase-locked loop that forces the drive field to oscillate at the Larmor frequency. When the drive field oscillates along the direction of propagation of the laser beam, the device is a true scalar magnetometer whose oscillation frequency is proportional to the modulus of the external field, independent of its orientation.

We have developed compact magnetometer sensor heads that allow the design of multi-sensor arrays. Their construction will be presented, addressing in particular the high-quality paraffin-coated cells [2], of which we have produced >300 so far.

I will briefly review our previous measurement of dynamic field maps of the beating human heart recorded by a 21 sensor array operated in a second-order gradiometer configuration [3].

A modification of the same apparatus is currently used for magneto-relaxometry measurements on superparamagnetic nano-particles (SPIONs). After magnetization by exposure to an external magnetic field the relaxation of the magnetic field produced by the SPION's magnetization is recorded. The characteristics of this relaxation strongly depend on the particles environment, *viz.*, fast thermal relaxation in fluids and slow (up to minutes) Néel relaxation when the particles are bound to surfaces. The goal of these studies is the development of a new contact-free non-invasive biomedical imaging technique which allows the *in vivo* representation of biological entities (organs, tumors) to which the particles attach when covered with specific functional shells. First results will be shown.

On the more fundamental side we are part of a large collaborative effort searching for a permanent electric dipole moment in ultracold neutrons. This experiment calls for a precise monitoring and control of the temporal and spatial variations of a 1  $\mu$ T magnetic field in a large shielding volume [4]. I will discuss on how we solved the problems of operating a large number of sensors in high vacuum and near a high voltage carrying electrode.

Work funded by the SNSF projects 200020\_130480 and CRSII2\_130414/1.

#### REFERENCES

- [1] S. Groeger, J.-L. Schenker, R. Wynands, A. Weis, Eur. Phys. J. D. 38, 239 (2006).
- [2] N. Castagna, G. Bison, G. Di Domenico, A. Hofer, P. Knowles, C. Macchione, H. Saudan, and A. Weis, Appl. Phys. B96, 763 (2009).
- [3] G. Bison, N. Castagna, A. Hofer, P. Knowles, J.-L. Schenker, M. Kasprzak, H. Saudan, and A. Weis, Appl. Phys. Lett. 95, 173701 (2009).
- [4] P. Knowles, G. Bison, N. Castagna, A. Hofer, A. Mtchedlishvili, A. Pazgalev, and A. Weis, Nucl. Instrum. Meth. A611, 306 (2009).

Invited Lectures I.16

## **New nanostructure designs for the ultra-high-efficient solar cells**

S. Tomić

*Computational Science and Engineering Department, STFC Daresbury Laboratory, Cheshire WA4 4AD, UK*  
e-mail: stanko.tomic@stfc.ac.uk

Although several very accurate models exist to predict development of the PV market growth [1], it is still unclear why the penetration of PV produced electricity in the electricity supply system is so unsatisfactory? It was concluded that the main reason is the limited or poor utilization of the solar spectrum by present solar cells (SC) devices. It is obvious that a breakthrough technology is necessary now to solve this problem. One of the options proposed for better utilization of the sun spectra is the concept of intermediate band solar cell (IBSC) [2]. While the power efficiency of a single energy gap semiconductor SC is limited to 41% it is very challenging task to increase SC output voltage (and efficiency) without eventually degrading the photocurrent. One possible solution to this problem is that the limited efficiency can be exceeded by splitting the solar spectrum so that several sub-energy gap states can simultaneously convert a light energy from different spectral regions into electricity. Under ideal conditions, an efficiency of 63% can be achieved with a degree of flexibility in the value of the energy gaps and the intermediate band (IB) position. The higher efficiency is due to the fact that additional absorption, from valence band (VB) states to the IB and from the IB to the conduction band (CB) states, allows two photons with energies below the energy gap of the barrier material to be harvested in generating one electron-hole pair, in addition to those generated by direct VB-CB transitions. In this way the IBSC overcomes the problem of increasing the SCs photocurrent without degrading its voltage. Quantum nanostructures, such as quantum dots (QD), arranged in superlattice

arrays, can produce a narrow IB within the CB of the QD material and the energy gap of the barrier material.

In my lecture I will discuss recently developed model Hamiltonian for calculation of the electronic and optical structures of InAs/GaAs QD arrays [3]. Taking into account realistic QD shape, QD periodicity in the array, as well as effects such as band mixing between states in the conduction and valence band, strain and piezoelectric field, the model reveals the origin of the intermediate-band formation inside forbidden energy gap of the barrier material. Having established the interrelation between QD periodicity and the electronic structure across the QD array Brillouin zone, conditions will be identified for the appearance of pure zero density-of-states regions, that separate intermediate band from the rest of the conduction band. For one realistic QD array I will present all important absorption coefficients in IBSC [4], and most important, radiative and nonradiative scattering times (related to the polariton and Auger effects), and their effect on the overall efficiency of the device [5].

#### REFERENCES

- [1] A. Luque, A. Marti, *Electron. Lett.* 44, doi: 10.1049/el:20081154 (2008).
- [2] A. Luque, A. Marti, *Phys. Rev. Lett.* 78, 5014 (1997).
- [3] S. Tomić, A.G. Sunderland, I.J. Bush, *J. Mat. Chem.* 16, 1963 (2006).
- [4] S. Tomić, T.S. Jones, N.M. Harrison, *Appl. Phys. Lett.* 93, 263105 (2008).
- [5] S. Tomić, *Phys. Rev. B* 82, 195321 (2010).

Invited Lectures I.17

## **Record Performances in All-optical Signal Processing**

N. Alic

*California Institute of Telecommunications  
Jacobs School of Engineering, University of California San Diego  
e-mail: nalic@ucsd.edu*

The most prominent conclusion, as far as the applicability of photonics, at the turn of the century is that of shattering of the '*all optical dream*', zealously pursued in the decade(s) that preceded it. Indeed, many vocal proponents who tried to convince their peers that optics/photonics would completely push out electronics from optical transmission have been completely defeated by the emergence of e.g. electronic dispersion compensation and 100Gb/s transmission [1]. Nevertheless, optics still possesses advantages over the electronic processing in certain aspects, and in contrast to the non-objective pursuit of the unobtainium from the previous decade, a critical re-consideration of positive and negative properties of both processing domains does open a passage to a qualitatively better processing methodology - in terms of energy efficiency, agility and robustness.

Within the realm of all optical processing for a long time, there has been a debate among the practitioners regarding the best processing medium. This uncertainly, however is only a superficial one: A diligent survey of recently published work reveals that papers devoted to parametric processing in *high confinement silica fibers* significantly outnumber all other competing platforms put together [2]. Furthermore, silica based all optical processing holds records in the amount and gain-bandwidth product [3], breadth and efficiency of wavelength conversion [4, 3], optical sampling [2] and phase sensitive amplification, all-optical delays [5], as well as all-optical transmission impairments mitigation [6].

In this talk, we will give an overview of the activity and record results of the Photonics Systems group from the University of California San Diego. In addition to THz real time signal processing, penalty free signal multicasting and 0.5 PHz wavelength conversion [4], a particular emphasis will be devoted to high speed tunable laser sources. In particular, the laser tuning speed is set by the uncertainly

principle. In practice, however, the available tunable lasers reside orders of magnitude away from the fundamental limit. In effect, the practical limit is set by the cavity reconfiguration time which is required to be significantly faster (i.e. shorter) than the cavity photon life time. Recognizing this practical difficulty, our group has recently introduced a new approach capable of extending the tuning range and speed of tunable lasers by more than an order of magnitude, relying fully on the parametric physics [7].

Summarizing the above, a judicious choice of the processing domain, as well as the approach still offers a lot of potential to improving the signal integrity in both high speed transmission, and more significantly in non-telecom applications. A thoughtful combination of optical and electronic domain processing represents the only viable path towards the challenging requirements of the next generation systems and/or applications.

#### REFERENCES

- [1] C.R.S. Fludger, T. Duthel, J. Lightwave Technology 26, 1, 64 (2008).
- [2] S. Radic, Laser & Photonics Review 2, 6, 498 (2008).
- [3] A. Peric, S. Moro, N. Alic, Proc. FiO, paper FWW2, Rochester, NY (2010).
- [4] R. Jiang, N. Alic, S. Radic, J. Lightwave Technol. 25, 58 (2007).
- [5] N. Alic, E. Myslivets, S. Radic, J. Lightwave Technol. 28, 448 (2010).
- [6] B.P.-P. Kuo, E. Myslivets, A.O.J. Wiberg, J. Lightwave Technol. 29, 4, 516 (2011).
- [7] B.P.-P. Kuo, N. Alic, S. Radic, J. Lightwave Technol. 29, 410 (2011).

Invited Lectures I.18

## **Advancements in imaging using terahertz quantum cascade lasers**

P. Dean

*Institute of Microwaves and Photonics, School of Electronic and Electrical Engineering, University of Leeds,  
Leeds, LS2 9JT, UK  
e-mail: p.dean@leeds.ac.uk*

Since the first demonstration of imaging at terahertz (THz) frequencies [1], there has been a great deal of interest in terahertz (THz) imaging applications, particularly in the fields of non-destructive inspection, security screening and biomedicine. The suitability of THz radiation to such applications stems primarily from the transparency of many non-polar materials at THz frequencies. Furthermore, THz radiation is sensitive to absorption arising from molecularly-specific vibrational modes in a wide range of organic and inorganic chemicals including explosives and drugs-of-abuse.

In recent years, the quantum cascade laser (QCL) has attracted intense interest as a high-power, narrowband source for THz systems. The THz QCL is a compact, semiconductor heterostructure laser capable of emission from 1.2 to 5.0 THz, and with output powers exceeding 100 mW in continuous wave operation. In this lecture, recent advancements in the development of imaging and sensing systems based on THz QCL technology will be presented.

Diffuse reflectance imaging of concealed powdered samples using a THz QCL to identify differences in chemical composition is presented [2]. The sensitivity of this detection scheme to sub-surface absorption within samples is confirmed, and it is shown that the effective absorption coefficient of samples can be obtained from the measured backscattering cross-section through use of a scattering model based on the quasi-crystalline approximation. Results are compared with effective absorption coefficients obtained from THz time-domain spectroscopy measurements on pressed pellet samples, and show good agreement over the range of effective absorption coefficients studied [3]. The applicability of THz QCLs to spectroscopic imaging in a reflection geometry, which is most appropriate to real-world applications, is discussed.

The use of electrically-tuneable THz QCLs sources, based on a heterogeneous cascaded active region, to acquire multiple-frequency images in a transmission geometry is also presented [4]. Using this system, images of polycrystalline samples have been acquired at 3.05 THz and 3.24 THz in a single scan of the sample. It is demonstrated that the high-explosive PETN can be readily distinguished from common sugars by taking the difference-attenuation and difference-transmission images. Difference-intensity imaging at these frequencies, by combining amplitude modulation of the QCL bias with lock-in detection, is also demonstrated.

In addition, THz frequency imaging through use of a single QCL device for both generation and sensing of THz radiation is presented [5]. In this system, detection is achieved by utilising the effect of self-mixing in the QCL, and specifically by monitoring perturbations to the voltage across the QCL induced by light reflected from an external object back into the laser cavity. Self-mixing imaging offers high sensitivity, a potentially fast response, and a simple, compact optical design. Using this technique, high-resolution imaging as well as displacement sensing over a round-trip distance of 14 m through air have been demonstrated.

#### REFERENCES

- [1] B. B. Hu, and M. C. Nuss, *Opt. Lett.* 20, 1716 (1995).
- [2] P. Dean *et al.*, *Optics Express* 16, 5997 (2008).
- [3] P. Dean *et al.*, *J. Chem. Phys.* 134, 134304 (2011).
- [4] P. Dean *et al.*, *Optics Express* 17, 20631 (2009).
- [5] P. Dean *et al.*, *Opt. Lett.* 36, 2587 (2011).

# Oral Presentations

---

## *Optical Materials*

Oral Presentations – Optical Materials O.OM.1

### **Using photonic crystal slabs to optimize quantum-well photo-detectors**

R.Meisels<sup>1</sup>, R. Brunner<sup>1</sup>, O. Glushko<sup>1,2</sup>, S. Kalchmair<sup>3</sup>, R. Gansch<sup>3</sup> and G. Strasser<sup>3</sup>

<sup>1</sup>*Institute of Physics, Montanuniversitaet,  
Leoben, Austria*

<sup>2</sup>*Present address: Department of Material Physics, Montanuniversitaet,  
Leoben, Austria*

<sup>3</sup>*Center for Micro- and Nanostructures, TU Vienna,  
Vienna, Austria,*

e-mail: meisels@unileoben.ac.at

We present simulations in comparison to experimental results on free standing photonic crystal (PC) slabs fabricated from quantum well infrared photo-detectors (QWIPs). A typical application for QWIPs is thermal imaging. In order to build sensitive camera systems high signal-to-noise ratios are necessary. Additionally, the detection principle of QWIPs requires electrical field components perpendicular to the quantum wells. Surface normal incident radiation only has electrical field components parallel to the quantum well and therefore cannot excite electrons. Usually, grating couplers are used on the surface to diffract incident light to obtain an electric field component in growth direction. A more advanced possibility is to use PCs instead of a grating [1-4].

The active region of the QWIPs consists of multiple GaAs/AlGaAs quantum wells. The investigated devices were manufactured by growing an Al<sub>0.85</sub>Ga<sub>0.15</sub>As sacrificial layer on top of a GaAs substrate. On this layer 26 GaAs/Al<sub>0.3</sub>Ga<sub>0.7</sub>As quantum well layers were deposited forming the active region of the device. For the photonic crystal, holes were etched into these layers. By selective underetching a free standing photonic crystal slab (PCS) was formed, separated by an air layer between active region and the substrate.

Three-dimensional finite differences time domain (FDTD) calculations of the propagation of waves in the PCS-QWIP structure were performed. The wavelength dependence of the mean field component in growth direction  $\langle E_y^2 \rangle$  was determined, showing sharp peaks corresponding to resonances within the PCS. The resonances obtained at given wavenumbers show high agreement with the experimental results.

In addition we performed simulations for different refractive indices of the spacer below the PC from  $n_{sp} = 1$  (removed sacrificial layer) over  $n_{sp} = 2.9$  (original layer) to  $n_{sp} = 3.12$  (no index contrast). The simulation showed a strong response of the PC resonances to the variation of the refractive index. A decrease of the PC resonances by increasing the refractive index has been observed. An analysis of the modes from the  $E_y$  field distribution in the x-z plane yielded information about the shift of the resonances to lower wavenumbers with increasing refractive index. From the obtained simulations we

are able to conclude clearly, that the use of free standing photonic crystal slabs for QWIPs results in strong absorption enhancement, which is essential for high signal-to-noise ratios in these devices.

#### REFERENCES

- [1] S. Schartner et al., Appl. Phys. Lett. 89, 151107 (2006).
- [2] S. Schartner et al., Opt. Express 16, 4797 (2008).
- [3] S. Kalchmair et al., Appl. Phys. Lett. 98, 011105 (2011).
- [4] O. Glushko et al. (to be published).

## *Plasmonics*

Oral Presentations – Plasmonics O.PL.1

### **Investigation of Ag nanoparticles' formation in soda-lime glass during nanosecond laser irradiation**

A. Wolak<sup>1</sup>, M. Grabiec<sup>1</sup>, O. Veron<sup>2</sup>, J-P. Blondeau<sup>2</sup>, N. Pellerin<sup>3</sup>, M. Allix<sup>3</sup>, S. Pellerin<sup>4</sup> and K. Dzierżęga<sup>1</sup>

<sup>1</sup>*Marian Smoluchowski Institute of Physics, Jagiellonian University, Krakow, Poland*

<sup>2</sup>*PRISME Institute EA 4229, Université d'Orleans, France*

<sup>3</sup>*CEMHTI, CNRS/Université d'Orleans, France*

<sup>4</sup>*GREMI-Site de Bourges, Université d'Orleans/ CNRS, France*

e-mail: ola.sitko@uj.edu.pl

Nanocomposite materials containing noble metal clusters (MNPs) in dielectric matrices have been extensively studied due to their potential applications as photonic devices or nonlinear optical elements. The unique linear and non-linear optical properties of silver, gold or copper MNPs are related to coherent oscillations of conduction-band electrons in response to the electric field of electromagnetic radiation of light and accompanying strong electric fields generated at the surface of such nanoparticles. This resonant excitation is known as a localized surface plasmon resonance (LSPR) and appears in the visible and UV part of the absorption spectrum of MNPs. The LSPR characteristics like wavelength, intensity and spectral width strongly depend on the size and shape of the nanoparticle but also on its local environment.

Laser methods of MNPs precipitation has brought attention of research community as they can be space-selective so the growth and subsequent modification of these composites can be locally photoactivated.

In our experiments we studied precipitation and modification of silver nanoparticles in soda-lime glass, containing silver ions, as the result of nanosecond Nd:YAG laser irradiation of UV (335 nm), visible (532 nm) and near-infrared (1064 nm) wavelengths. Glass slides doped with silver ions in ion exchange process, were then irradiated by specific number of laser pulses. The laser irradiated area was simultaneously illuminated by a white light beam and imaged onto an entrance slit of the spectrograph equipped with an image intensified CCD camera (ICCD). Spatially resolved (across the laser beam) absorption spectra were measured on-line, after each laser pulse. This way we were able to follow the LSPR spectra in space – across the laser beam – and in time with laser pulses deposited on the sample. The LSPR spectra and their variations directly indicate formation and modification of silver nanoparticles during laser irradiation. Above some threshold fluence of the laser pulse and after a specific number of pulses silver ions are reduced to atoms which then migrate and form clusters of different sizes within the ion exchanged layer of the glass plate. Owing to spatial resolution of our measurements, we could study migration of silver clusters within the irradiated area. In each single

experiment precipitation process of silver nanoparticles began at the center of the irradiated area (where the laser intensity is the highest) and was spreading outwards with successive pulses. Finally, if the laser fluence was high enough, dark ring with substantial number of silver nanoparticles was formed around the laser irradiated area.

Experiments were performed with laser pulses of different energy and for samples with different initial concentrations of Ag ions. The latter was achieved by varying the time the glass plates were immersed in the molten salt bath of  $\text{NaNO}_3 - \text{AgNO}_3$  (10% mol) at temperature of 320 °C.

Our investigations reveal that the rate of NPs formation and modification but also their size and spatial distribution strongly depend on the characteristic of laser pulses – wavelength, fluence and number - as well as on the initial concentration of Ag ions.

#### REFERENCES

[1] J.-Ph. Blondeau, S. Pellerin, V. Vial, K. Dzierzega, N. Pellerin, C. Andreazza- Vignolle, Journal of Crystal Growth 311, 172 (2008).

## *Nonlinear Optics*

Oral Presentations – Nonlinear Optics O.NO.1

### **On the problem of terawatt femtosecond pulse self - reflection from nonlinear focus and plasma in dielectrics**

O. Khasanov<sup>1</sup>, G. Rusetsky<sup>1</sup>, O. Fedotova<sup>1</sup>, N. Aleksic<sup>2</sup> and A. Sukhorukov<sup>3</sup>

<sup>1</sup>*Scientific-Practical Material Research Centre of Belarus National Academy of Sciences  
19 P. Brovki, Minsk 220072 Belarus*

<sup>2</sup>*Institute of Physics Belgrade, University of Belgrade, Belgrade, Serbia*

<sup>3</sup>*Faculty of Physics, Moscow State University, Leninskie Gory, Moscow 119992 Russia  
e-mail: khasanov@ifttp.bas-net.by*

Model adequate to solve the nonlinear backscattering problem of terawatt femtosecond pulses from photoinduced plasma and nonlinear focus in Kerr media has been elaborated. Application of the nonlinear eikonal related to the pulsed beam phase increment along the propagation axis allows us to reduce Maxwell equation to the set of two coupled equations of non-linear Schrödinger type for forward and backward waves. Backscattering process is investigated in dependence on the ratio  $\alpha$  of input pulse power and critical one for self-focusing.

As is known, when the input pulse power exceeds the critical one it focuses in Kerr medium under propagation [1]. Its intensity increases and its radius decreases achieving the value less than wavelength. This process is accompanied with the plasma formation via the multiphoton absorption or tunnelling mechanisms. Near the nonlinear focus medium inhomogeneity becomes maximal. Maximum values of the longitudinal gradient of medium refraction index and plasma density are inherent to the nonlinear focus region. The very backscattering [2] of the incident pulse from such medium inhomogeneities is the origin of a backward wave. Note that the analysis of the forward pulse propagation and its self-reflection near the nonlinear focus requires nonparaxial approach. Elaborated model is appropriate to this propagation region. As analysis shows, the reflection coefficient from nonlinear focus depends on the  $\alpha$  value. In this work two regimes of backscattering from nonlinear focus namely including plasma and without it are compared. In the case of negligible influence of plasma the backscattered wave intensity does not exceed 5% of the forward one at  $\alpha < 20$ , and it can reach 10% and more at  $\alpha > 30$ . At this the backward wave beam radius becomes minimal and its

intensity is maximal at the distance of five wavelengths from the focus. At larger distances from nonlinear focus the backward wave beam defocuses essentially. The extent of this defocusing depends on the parameter  $\alpha$ . When the contribution from plasma becomes significant, the self-reflection scenario changes. The plasma arrests the forward wave pulse self-focusing at earlier stage then longitudinal gradient of refraction index. The minimal diameter of the forward wave pulse is about  $7\lambda$  that is essentially larger than in aforementioned case. For  $8 < \alpha < 20$  the reflection from plasma is 3 - 4 times more than the reflection from the nonlinear focus. Moreover, the backward wave beam width becomes minimal at the much shorter distance (about  $0.05\lambda$ ) from focus. At small distances from nonlinear focus the backward wave propagates in a waveguide formed by the forward wave pulse.

#### REFERENCES

- [1] R. W. Boyd, S. G. Lukishova, Y.R. Shen. Self-focusing: Past and Present Fundamentals and Prospects. Springer (2008).
- [2] J. Yu, D. Mondelain, G. Ange, R. Volk, S. Niedermeier, J. P. Wolf, J. Kasparian, R. Sauerbrey, Optics Letters. 26, 8 (2001).

Oral Presentations – Nonlinear Optics O.NO.2

### **Two color pump probe experiments at 4<sup>th</sup> generation X-ray light sources**

N. Stojanovic<sup>1</sup>, M. Gensch<sup>2</sup>, F. Tavella<sup>1</sup>, J. Feldhaus<sup>1</sup>, B. Faatz<sup>1</sup>, E. Schneidmiller<sup>1</sup> and M.V. Yurkov<sup>1</sup>  
*1 DESY, Notkestr. 85, 22607 Hamburg*  
*2 HZDR, Bautzner Landstr. 400, 01328 Dresden*  
e-mail: nikola.stojanovic@desy.de

In this paper we will present overview of photon science at 4<sup>th</sup> generation X-ray light sources. Presently two facilities, FLASH in Hamburg/Germany [1] and LCLS at Stanford/USA [2] are in operation and have opened new scientific possibilities reaching from ultrafast science to peak power experiments. The advantage of these large-scale facilities lies in their broad spectral range from the soft to hard X-ray regime, their tunability and the opportunity to generate ultra short pulses in the few 10 to few femtosecond regime. The facility at FLASH furthermore allows to generate intense pulses from the visible to the THz spectral range that are furthermore timed up to the X-ray pulses on a few femtosecond timescale [3].

In this paper we would like to discuss the opportunities of 4<sup>th</sup> generation X-ray light-sources on the example of FLASH in Hamburg with a particular emphasis in the topic of 2 color pump probe experiments.

#### REFERENCES

- [1] Ackermann, W. et al. , Nature Photon. 1, 336–342 (2007).
- [2] Emma, P. et al., Nature Photon. 4, 641 (2010).
- [3] F. Tavella, N. Stojanovic, G. Geloni, M. Gensch, Nat. Photon. 5, 162 (2011).

## Mobility of high-power solitons in saturable nonlinear photonic lattices

U. Naether<sup>1,2</sup>, R. A. Vicencio<sup>1,2</sup> and M. Stepić<sup>3</sup>

<sup>1</sup>*Departamento de Física, Facultad de Ciencias, Universidad de Chile, Santiago, Chile,*

<sup>2</sup>*Center for Optics and Photonics, Universidad de Concepción, Concepción, Chile*

<sup>3</sup>*Vinca Institute of Nuclear Sciences, Belgrade, Serbia*

e-mail: unaether@u.uchile.cl

Mobility of localized stationary solutions in the context of the discrete nonlinear Schrödinger (DNLS) equation is well known. For low powers, the energy barrier imposed by discreteness and nonlinearity (usually called Peierls-Nabarro (PN) potential [1]) remains small and solutions will move across the lattice by just giving them a judicious kick [2, 3]. For larger powers, the growing energy barrier inhibits mobility. However, for photorefractive media with saturable nonlinearity, corresponding to a s-DNLS [4] model, there are several points, where the energy difference between the two fundamental localized solutions - the one centered at one site (odd mode) and the one centered between two sites (even mode) - vanishes for different power values [4]. Close to these points, there are regions of stability exchange between the even and odd solutions. Since those regions exhibit bistability, the appearance of an intermediate asymmetric and unstable solution is inevitable[5]. Therefore the effective energy barrier will strongly depend on the intermediate solutions (IS). For saturable one-dimensional (1D) systems, this crucial issue has not been clearly identified yet. We believe this element could be one of the keys to experimentally observe, to the best of our knowledge for the first time, good soliton mobility in 1D nonlinear saturable photonic lattices.

When we consider the energy barrier the solution has to pass, hence including the IS, there is always a nonzero barrier to overcome in order to move a localized solution across the lattice. In fact, this barrier can be very small but it is always nonzero. Contrary to what is expected, the fundamental solutions remain immobile in the points of minimal effective energy barrier. If we kick an odd or even mode, we are putting in motion an immobile-defined solution, therefore there is always radiation from tails. As a consequence, the power of the moving solution is lower than the initial one. Using a constraint method [6,7] to identify the ISs and to describe a pseudo-potential landscape among all stationary modes, we can find the regions, where the effective energy barrier decreases, when power is lowered. We show, that they correspond to powers close to the bifurcation points, where the IS disappear.

To the best of our knowledge, mobility in this kind of systems was never predicted for a more realistic experimental input condition like gaussian input profiles. Previous simulations, starting from stationary solutions, observed good mobility [4-6,8]. However, saturable solutions are not well localized in the power-exchange regions and, furthermore, by increasing the power they become broader. Therefore, in an experiment, dynamics will be strongly determined by the power and shape of the chosen beam profile. Taking as input condition wide gaussian-like profile, we find different regions where mobility is enhanced. It is plausible to assume that this behavior corresponds to a manifestation of the continuously repeating bistable regions found for stationary solutions. Therefore, for even higher powers, we expect excellent mobility, in principle without limitations.

### REFERENCES

- [1] Yu.S. Kivshar, D.K. Campbell, Phys. Rev. E 48, 3077 (1993).
- [2] U. Peschel et.al., J. Opt. Soc. Am. B 19, 2637 (2003).
- [3] R.A. Vicencio, M.I. Molina, Yu.S. Kivshar, Opt. Lett. 28, 1942 (2003).
- [4] M. Stepić, D. Kip, Lj. Hadziievski, A. Maluckov, Phys. Rev. E 69, 066618 (2004); Lj. Hadziievski, A. Maluckov, M. Stepić, D. Kip, Phys. Rev. Lett. 93, 033901 (2004).
- [5] R.A. Vicencio, M. Johansson, Phys. Rev. E 73, 046602 (2006).
- [6] U. Naether, R.A. Vicencio, M. Johansson, Phys. Rev. E 83, 036601 (2011).

- [7] M.I. Molina, R.A. Vicencio, Yu.S. Kivshar, *Opt. Lett.* 31, 1693 (2006); C.R. Rosberg, D.N. Neshev, W. Krolikowski, A. Mitchell, R.A. Vicencio, M.I. Molina, Yu.S. Kivshar, *Phys. Rev. Lett.* 97, 083901 (2006).  
[8] T.R.O. Melvin, A.R. Champneys, P.G. Kevrekidis, J. Cuevas, *Phys. Rev. Lett.* 97, 124101 (2006).

## *Optoelectronics and Optocommunications*

Oral Presentations – Optoelectronics and Optocommunications O.OE.1

### **Determining Effective Refractive Index of Optical Slab Waveguide Based on Analytical and Finite Difference Method**

A. Cetin<sup>1</sup>, E. Uçgun<sup>2</sup> and M. S. Kılıçkaya<sup>1</sup>

<sup>1</sup>*Eskişehir Osmangazi University, Department of Physics, Eskişehir, Turkey*

<sup>2</sup>*Dumlupınar University, Department of Physics, Kütahya, Turkey*

e-mail: selamik@ogu.edu.tr

The simulation response of optical slab waveguide used in integrated optics needs numerical methods. These methods must be precise and useful in terms of memory capacity and time duration.

In this paper, according to these criteria, we present basic analytical and finite difference methods to determine effective refractive index of slab waveguide. Also, appropriate effective refractive index value is obtained with respect to number of grid point and number of matrix size. Finally, the validity of the obtained values by both methods is compared to using waveguide type.

#### REFERENCES

- [1] T. B. Koch, J. B. Davides, D. Wickramasinghe, *Electronics Letters*, 25 No. 8, 514 (1989).  
[2] C. L. Xu, W.P. Huang, *PIER*, 11, 1 (1995).  
[3] M. D. Feit, J. A. Fleck, Jr, *Applied Optics*, 19 No.13, 2240 (1980).  
[4] Y. Chung, N. Dağlı, 26 No. 8, 1335 (1990).  
[5] D. Marcuse, Academic Press, Boston (1991).  
[6] M. A. Matin, M. T. Benson, P. C. Kendall, M. S. Stern, *International Journal of Numerical Modelling: Electronic Networks, Devices And Fields* 7, 25 (1994).  
[7] N. M. Kassım, A. B. Mohammad, M. H. Ibrahim, *Jurnal Teknologi*, 42, 41 (2005).  
[8] M. Khalaj-Amirhosseini, *Transactions on Antennas and Propagation*, 54 No. 1, 130 (2006).  
[9] V. A. Popescu, N. N. Puscas, *Journal of Optoelectronics and Advanced Materials*, 8 No. 3, 1262 (2006).

## Estimation of the uncertainty for a phase noise optoelectronic metrology system

P. Salzenstein, E. Pavlyuchenko, A. Hmima, N. Cholley, M. Zarubin, S. Galliou, Y. K. Chembo and L. Larger  
*Centre National de la recherche Scientifique (CNRS), Franche Comté Electronique Thermique Optique Sciences et Technologies (FEMTO-ST),  
 32 avenue de l'Observatoire,  
 F25044 Besançon cedex, France  
 e-mail: patrice.salzenstein@femto-st.fr*

Recent progress in optoelectronics oscillators based on delay lines [1] or optics resonators [2,3] with modulation frequency in microwaves require low phase noise system. We first present a configuration of phase noise measurement system operating in X- band using a photonic delay line as a frequency discriminator. This system doesn't need any excellent frequency reference and works for any frequency between 8.2 and 12.4 GHz [4]. Oscillator frequency fluctuation is converted to phase frequency fluctuation through the delay line. The measured phase noise includes the DUT noise and the instrument background. Then the use of a cross correlation decrease the cross spectrum terms of uncommon phase noise as  $\sqrt{1/m}$ , where m is the average number. Using cross correlation on 500 averages, noise floor of the instrument  $\mathcal{L}(f)$  is respectively -150 and -170 dBc/Hz at  $10^1$  and  $10^4$  Hz from the 10 GHz carrier (-90 and -170 dBc/Hz including 2 km delay lines). Finally, the need is to determine uncertainty. There are two categories of uncertainties terms : "type A", statistic contribution such as repeatability and experimental standard deviation; "type B" due to various components and temperature control, but also to the asymmetry of the instrument. Uncertainty on  $\mathcal{L}(f)$  strongly depends on propagation of uncertainties through the transfer function. Elementary term of uncertainty for repeatability is found to be equal to 0.68 dB. Other elementary terms still have lower contributions. For instance, temperature effects, resolution of instruments are lower. Its leads to a global uncertainty of 1.58 dB at  $2\sigma$ . This calibration system is to be integrated in measurements means of the accredited laboratory to improve the Calibration Metrology Capabilities (CMC) of the national french metrology institute (LNE).

### REFERENCES

- [1] K. Volyanskiy, J. Cussey, H. Tavernier, P. Salzenstein, G. Sauvage, L. Larger, E. Rubiola, Journal of the Optical Society of America B, 25, 2140 (2008).
- [2] H. Tavernier, P. Salzenstein, K. Volyanskiy, Y. K. Chembo, L. Larger, IEEE Photonics Technology Letters, 22, 1629 (2010).
- [3] K. Volyanskiy, P. Salzenstein, H. Tavernier, M. Pogurmirskiy, Y. K. Chembo, L. Larger, Optics Express, 18, 22358 (2010).
- [4] P. Salzenstein, J. Cussey, X. Jouvenceau, H. Tavernier, L. Larger, E. Rubiola, G. Sauvage, Acta Physica Polonica A, 112, 1107 (2007).

### 3D finite element modeling of optical microring resonators

B. Milanović<sup>1</sup>, B. Radjenović<sup>2</sup> and M. Radmilović-Radjenović<sup>2</sup>

<sup>1</sup>Military Academy,

Pavla Jurišića Šturma 33, Belgrade, Serbia

<sup>2</sup>Institute of Physics, University of Belgrade,

Pregrevica 118, Belgrade, Serbia

e-mail:bradjeno@ipb.ac.rs

Microring resonators are frequency selective elements that can perform a variety of functions such as add/drop filtering, switching, and modulating in wavelength-division (WDM) systems. Their compact size and low-power-consuming property have enabled them to become a strong candidate as building blocks in the future photonic integrated circuits [1], [2]. Several methods are used for calculating the response of a microring resonator. One of the most widely accepted is semi-analytic coupled mode theory in time domain, implemented usually in two space dimensions (2D) [2], or rarely in 3D [3]. While 2D calculations are sufficient to explain concepts and phenomena, the full 3D simulations are necessary to determine the parameters of the devices intended to be used in real WDM systems. The Finite-Difference Time-Domain (FDTD) method is most popular simulation tool for that purpose, but due to its inherent weaknesses (stair casing error and numerical dispersion), other solutions are looked for.

Here we present the result of 3D frequency driven finite element simulations of an add/drop multiplexer configuration described in reference [4], where it was analyzed using FDTD method. The system, shown in Fig. 1, consists of a ring and two bus waveguides made silicon on SiO<sub>2</sub> substrate. In the calculations the first-order edge elements are used, and the computational domain is closed using standard perfectly matched layer method.

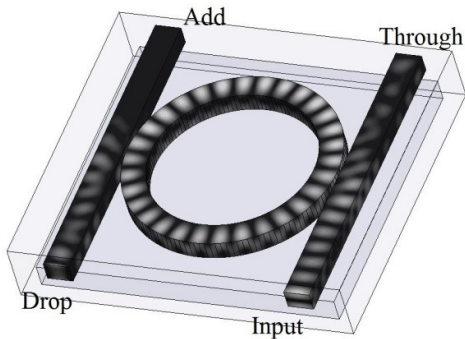


Figure 1.

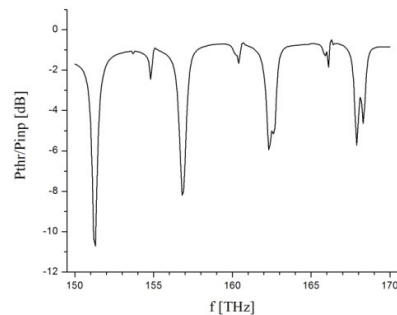


Figure 2.

The calculations are performed in a wide spectral range (150-170THz) with the step of 100GHz. In Fig.2 the transmission coefficient of the input bus (Input-Through) is shown, while in Fig. 1 the electric field distribution for the frequency of the first minimum in Fig. 2 (151.35 THz) is presented. The results are very similar to previous FDTD calculations [4].

#### REFERENCES

- [1] T. Benson, S. Boriskina, P. Sewell, A. Vukovic, S. Greedy, and A. Nosich, *Frontiers of Planar Lightwave Circuit Technology: Design, Simulation and Fabrication*, pp. 39-70, Springer (2005).
- [2] K. Hiremath, and M. Hammer, *Photonic Microresonator Research and Applications*. Springer Series in Optical Sciences, 156 . Springer Verlag, London, pp. 29-59 (2010).
- [3] R. Stoffer, K. R. Hiremath, M. Hammer, L. Prkna, and J. C tyroky, *Opt. Commun.* 256, 46 (2005).
- [4] M. Fujii, W. Freude, and P. Russer, *Proc. 19th Annual Rev. Progress in Appl. Comput. Electromagnetics*, 739, Monterey, CA. (2003).

## A Simple Low-Coherence Interferometric Sensor for Absolute Position Measurement Based on Central Fringe Maximum Identification

L. Manojlovic<sup>1,2</sup>, M. Zivanov<sup>2</sup>, M. Slankamenac<sup>2</sup>, D. Stupar<sup>2</sup>, and J. Bajic<sup>2</sup>

<sup>1</sup>Zrenjanin Technical College  
Zrenjanin, Serbia

<sup>2</sup>Faculty of Technical Sciences,  
University of Novi Sad, Serbia

e-mail: lazo.manojlovic@vts-zr.edu.rs

A simple low-coherence interferometric sensor for absolute position measurement based on central fringe maximum identification is presented. The channeled spectrum, captured by a commercial spectrometer, is analyzed using the algorithm based on fitting the calculated autocorrelation function of the captured optical power spectrum with the sum of two Gaussian functions. The position of the central fringe is obtained directly from the separation between two fitted Gaussian functions. In order to boost the precision of such a built sensing system the position of the maximum of the central fringe is identified by a simple algorithm. The system currently provides unambiguous measurement over a range of 200  $\mu\text{m}$  with a minimal error of better than 1.4 nm. In addition to this the sensor is characterized by a very small sensing head (bare single-mode fiber with the diameter of 125  $\mu\text{m}$ ) and by very high resistance to environmental influences, thus enabling the possibility of using very long down-lead sensing fiber.

### REFERENCES

- [1] R. J. Sandeman, *Appl. Opt.* 10, 1087 (1971).
- [2] U. Schnell, E. Zimmermann, R. Dändliker, *Pure Appl. Opt.* 4, 643 (1995).
- [3] L. M. Smith, C. C. Dobson, *Appl. Opt.* 28, 3339 (1989).
- [4] S. Taplin, A. Gh. Podoleanu, D. J. Webb, D. A. Jackson, *Electron. Lett.* 29, 896 (1993).
- [5] C. Boulet, M. Hathaway, D. A. Jackson, *Opt. Lett.* 29, 1602 (2004).
- [6] P. Hlubina, I. Gurov, V. Chugunov, *J. Mod. Opt.* 50, 2067 (2003).
- [7] P. Hlubina, *Opt. Comm.* 212, 65 (2002).
- [8] P. Hlubina, *J. Mod. Opt.* 51, 537 (2004).
- [9] J. Park, X. Li, *J. Lightw. Techn.* 24, 2473 (2006).
- [10] Y. J. Rao, D. A. Jackson, *J. Lightw. Techn.* 14, 592 (1996).
- [11] M. M. Brundavanam, N. K. Viswanathan, D. N. Rao, *Appl. Opt.* 47, 6334 (2008).
- [12] L. M. Manojlović, *Opt. Las. Eng.* 48, 486 (2010).

## Nuclear quantum optics: Atoms and nuclei in a strong laser field

A.V. Glushkov<sup>1,2</sup>

<sup>1</sup>*Odessa University, P.O.Box 24a, Odessa-9, Ukraine*

<sup>2</sup>*ISAN, Russian Academy of Sciences, Troitsk, Moscow reg., Russia*

e-mail: glushkov@paco.net

An energy approach [1] is used to study interaction of nuclei and atoms with an intense and super intense laser field, including high power X-,gamma-ray (raser, graser) pulses. Method bases on description of atom in a field by the  $k$ -photon emission and absorption lines. The lines are described by the QED moments of different orders, which can be calculated with the use of the Gell-Mann and Low S-matrix adiabatic formalism ( $T=0$ ). In relativistic version the Gell-Mann and Low formulae expresses an imaginary part of the energy shift  $\text{Im } E\{a\}$  through the QED scattering matrix, including interaction of atom with electromagnetic field and field of the photon vacuum. For any atomic level we calculate  $\text{Im } E\{a\}(\omega)$  as function of the laser pulse central frequency  $\omega$  (resonant curve). We calculate the moments for resonance, connected with concrete atomic a-p transition (a,p-discrete levels;  $k$  photons is absorbed). The ac Stark resonances energies and widths for a number of atoms (*H, Li, Tm, U* etc.) and different low-lying and Rydberg states [1] are obtained. The parameters of multi-photon resonance, ionization profiles in *Cs, Yb, Gd* atoms are found. We discovered a laser field effect of the giant broadening of widths for the Letokhov-Ivanov re-orientation decay autoionization resonances in *Tm* etc. This effect is firstly predicted for *U* atom and could be used in carrying out an optimal laser photoionization scheme of the uranium and other isotopes and nuclear isomers [1]. The actual application of energy approach is new consistent theory for resonant process of nuclear excitation by electron capture NEEC (NEET), in which a continuum electron is captured into a bound state of an ion with excitation of a nucleus. New data are obtained for electric and magnetic multipole E2, M1 transitions in *U, Yb, Gd, Tm*. Modelling nuclear ensembles in a super strong laser field provides opening the field of nuclear quantum optics and is carried out in our work too. A nuclear dynamic (AC) Stark shift of low-lying nuclear states due to off-resonant excitation by laser field ( $I \sim 10^{25} - 10^{35}$  W/cm<sup>2</sup>) is studied and is described within the operator perturbation theory and the relativistic mean-field (RMF) model for the nucleus [2]. The ac-Stark shifts of the same order as in typical quantum optical systems relative to the respective transition frequencies are feasible with state-of-the-art or near-future laser field intensities. The problem of creation of the high power monochromatic gamma radiation source is studied. The possible approach is based on the effect of discharge of meta-stable nuclei during negative  $\mu^-$  capture. A negative muon captured by a meta-stable nucleus may accelerate the discharge of the latter by many orders of magnitude [1,2]. For a certain relation between the energy range of the nuclear and muonic levels the discharge may be followed by the ejection of a muon, which may then participate in the discharge of the other nuclei. We present the results of modeling (within QED energy approach [2]) characteristics for discharge of a nucleus with emission of gamma quantum and further  $\mu^-$  conversion. The necessary parameters are now reached for example on the meson factory in Los-Alamos. The requirement of high stability of the states [ $T \sim 10(8)s$ ] and sufficiently high transition energy [ $>Z(2) \cdot 2.8keV$ ] transition limits a range of nuclei for observation of the effect. Our estimates show that the new high-energy transitions (with  $\mu^-$  conversion) can occur in a sample radiated by muons and any long-lived isomer with high-energy transitions can be used for observation of effect and creating high-energy gamma radiation source [1].

### REFERENCES

- [1] A.V.Glushkov, L.N. Ivanov, Phys. Lett. A. 170, 33 (1992); Preprint of ISAN, N AS1-3, Troitsk, (1992); A.V.Glushkov et al, Phys. Scripta. T135, 014022 (2009); Int.J.Quant.Chem. 104, 512, 562

(2005); 99, 889, 936 (2004); *Frontiers in Quantum Systems in Chem. and Phys.* (Berlin, Springer). 15,301 (2006); *ibid.* 18,505 (2008); *ibid.* 19,125 (2009); 22,131 (2011).  
[2] V.I.Gol'dansky, V.S.Letokhov, *JETP*. 78, 213 (1974); A.Glushkov, L.N.Ivanov, V.S.Letokhov, *Nuclear Quantum Optics*, Preprint ISAN, NAS-1, Troitsk, (1991); A.Glushkov et al, *Europ.Phys.J.* 160,195 (2008); T.Burvenich J.Evers, C.Keitel, *Phys.Rev.Lett.* 96,142501 (2006); *Phys. Rev. C* 74, 044601 (2007); A. Shahbaz, C. Muller, T.Burvenich, C.Keitel, *Nucl. Phys.* A821, 106 (2009).

Oral Presentations – Quantum Optics O.QO.2

## Trajectory based interpretation of Poisson-Arago spot for photons and molecules

M. Davidović<sup>1</sup> and M. Božić<sup>2</sup>

<sup>1</sup>*Faculty of Civil Engineering, University of Belgrade, Serbia*

<sup>2</sup>*Institute of Physics, University of Belgrade, Serbia*

e-mail: bozic@ipb.ac.rs

Feasibility of interference experiments with beams of one per one photon have motivated new theoretical approaches, supported by numerical evaluation, to electromagnetic energy flow lines behind diffraction gratings [1,2], a circular aperture and an opaque disc [3]. Interference pattern in the far field behind a grating [1], Talbot effect [2], well-known Poisson-Arago spot phenomenon [3] and four Arago-Fresnel laws governing the interference of polarized light [4] were explained in terms of EME flow lines. M. Gondran and A. Gondran put in the historical perspective [3] the EME based explanation of Poisson-Arago spot phenomena, by showing that EME flow lines provide a complementary answer to Fresnel's answer to the questions presented in 1818 by the French Academy "deduce by mathematical induction the movements of the rays during their crossing near the bodies". Davidović *et al.* [1] argued that EME flow lines (light rays) could be interpreted as photon trajectories. Recent experimental observation of average trajectories of single photons in a two-slit interferometer by Kocsis *et al.* [5] are supporting this argumentation, in our opinion.

According to Bohm's theory and its applications [6] matter-wave diffraction and interference are explicable using particle trajectories. The trajectories are in fact the lines of quantum mechanical current. There is an analogy between the equation of EME flow lines and the equation of flow lines of a quantum mechanical current [2]. Consequently, the forms of EME flow lines and the massive particle trajectories behind interference gratings are very similar and explain well interference patterns as a result of an accumulation of single particle events. Reisinger *et al.* recently reported [7] observation of Poisson-Arago spot using a beam of neutral deuterium molecules. In this paper we present trajectories of deuterium molecules diffracted by a circular disk and intensity distribution of molecules at various distances behind this disk. We compare our theoretical and numerical results with the experiment of Reisinger *et al.* [7].

### REFERENCES

- [1] M. Davidović, A. S. Sanz, D. Arsenović, M. Božić, S. Miret-Artés, *Phys. Scr.* T135, 014009 (2009).
- [2] A. S. Sanz, M. Davidović, M. Božić, S. Miret-Artés, *Ann. Phys.* 325, 763 (2010).
- [3] M. Gondran, A. Gondran, a) hal-00416055 version 1-11 Sep 2009; b) *Am. J. Phys.* 78, 598 (2010).
- [4] M. Božić, M. Davidović, T. L. Dimitrova, S. Miret-Artés, A. S. Sanz, A. Weis, *J. Russ. Laser Res.* 31, 117 (2010).
- [5] S. Kocsis, B. Braverman, S. Ravets, M. J. Stevens, R. P. Mirin, L. K. Shalm, A. M. Steinberg, *Science* 332, 1170 (2011).
- [6] A. S. Sanz, S. Miret-Artés, *J. Phys. A* 41, 435303 (2008).
- [7] T. Reisinger, A. A. Patel, H. Reingruber, K. Fladischer, W. E. Ernst, G. Bracco, H. I. Smith, B. Holst, *Phys. Rev. A* 79, 053823 (2009).

## Spontaneous and blackbody-induced radiation transitions from Rydberg states in singly ionized calcium atoms

I.L. Glukhov and V.D. Ovsianikov

*Department of Physics, Voronezh State University, Voronezh, Russian Federation*

e-mail: glukhovofficial@mail.ru

Singly ionized calcium may be treated as a system of an atomic core and an outer valence electron. The energy of the latter in a  $nl$ -state may be written in the hydrogen-like form

$$E_{nl} = -\frac{Z^2}{2\nu^2} \quad (1)$$

with the atomic core charge  $Z=2$  and  $\nu$ , the effective principal quantum number. For calculation of the rates of spontaneous and blackbody-radiation-(BBR)-induced decay and excitation from bound states in singly ionized calcium, the Fues' model potential (FMP) [1] may be used. As the FMP works better for higher states [1], then it gives more accurate wavefunctions for Rydberg levels.

The matrix elements of  $S$ - $P$  transitions, calculated in the FMP approach, were used for determining spontaneous decay rates  $P_{nl}^{sp}$  and lifetimes  $\tau_{nl}^{sp} = 1/P_{nl}^{sp}$  of the  $nS$ -series. The calculated lifetimes agree well with available data [2] (below 3% discrepancy). An asymptotic (for large values of the principal quantum number  $n$ ) approximation for the lifetimes of  $s$ -states (in ns) may be written as the  $n^3$  factor times a third-order polynomial of  $1/n$ :

$$\tau_{ns} = 75.19 \left(\frac{n}{10}\right)^3 \left(1 - \frac{4.657}{n} - \frac{26.91}{n^2} + \frac{321.2}{n^3}\right). \quad (2)$$

The  $S$ - $P$  matrix elements may also be used for determining the BBR-induced decay and excitation rates from highly excited (Rydberg) states of the  $nS$ -series. For sufficiently high Rydberg states the rates of the BBR-induced depopulation processes (decays and excitations  $-P_{ns}^{\text{dec(exc)}}$ ) may be comparable and even exceed the rates of spontaneous decays. The asymptotic presentation for the fractional decay (excitation) rate may be written as

$$R_{ns}^{\text{dec(exc)}}(T) = P_{ns}^{\text{dec(exc)}}(T) / P_{ns}^{\text{sp}} = \frac{a_0^{\text{dec(exc)}} + a_1^{\text{dec(exc)}}x + a_2^{\text{dec(exc)}}x^2}{n^2[\exp(0.315780x^3) - 1]}, \quad (3)$$

where  $x = \frac{100}{nT^{1/3}}$ . The  $a_i^{\text{dec(exc)}}$ -coefficients slightly depend on temperature and may be presented as

$$a_i^{\text{dec(exc)}} = b_{i0}^{\text{dec(exc)}} + b_{i1}^{\text{dec(exc)}} \left(\frac{100}{T}\right)^{1/3} + b_{i2}^{\text{dec(exc)}} \left(\frac{100}{T}\right)^{2/3}, \quad i=1,2,3, \quad (4)$$

where  $b_{ij}^{\text{dec(exc)}}$  are constant coefficients collected below in the table:

$i$	$b_{i0}^{\text{dec}}$	$b_{i1}^{\text{dec}}$	$b_{i2}^{\text{dec}}$	$b_{i0}^{\text{exc}}$	$b_{i1}^{\text{exc}}$	$b_{i2}^{\text{exc}}$
0	4.937	0.00936	0.1181	1.6264	-0.2176	0.1339
1	-5.903	2.936	-1.784	-2.4577	4.7826	-2.6020
2	0.1967	1.489	-0.5680	1.9599	-5.419	3.2622

With these coefficients, equations (3) and (4) give the values of  $R_{ns}^{\text{dec(exc)}}$  with an error below 3% for  $n>20$  and  $T$  from 100 to 3000 K.

### REFERENCES

- [1] N.L. Manakov, V.D. Ovsianikov, L.P. Papoport, Phys. Rep. 141, 319 (1986).  
 [2] Information system 'Electronic structure of atoms', Novosibirsk State University, <http://asd.nsu.ru>.

## **Dipolar Bose-Einstein Condensates with Weak Disorder**

C. Krumnow<sup>1</sup> and A. Pelster<sup>2,3</sup>

<sup>1</sup>*Institute for Theoretical Physics, Free University of Berlin, Germany,*

<sup>2</sup>*Department of Physics, University of Duisburg-Essen, Germany*

<sup>3</sup>*Department of Physics, University of Bielefeld, Germany*

e-mail: axel.pelster@fu-berlin.de

We consider a homogeneous polarized dipolar Bose-Einstein condensate in the presence of weak quenched disorder within mean-field theory at zero temperature. By solving at first perturbatively the underlying Gross-Pitaevskii equation and performing then disorder ensemble averages for physical observables, we show that the anisotropy of the two-particle interaction is passed on to both the superfluid density and the sound velocity.

### REFERENCES

[1] C. Krumnow, A. Pelster, eprint: arXiv:1103.2437, submitted for publication to Rapid Communication of Physical Review A.

## **Parametric and Geometric Resonances of Collective Oscillation Modes in Bose-Einstein Condensates**

I. Vidanović<sup>1</sup>, H. Al-Jibbouri<sup>2</sup>, A. Balaž<sup>1</sup> and A. Pelster<sup>3,4</sup>

<sup>1</sup>*Scientific Computing Laboratory, Institute of Physics Belgrade, University of Belgrade, Serbia*

<sup>2</sup>*Institute for Theoretical Physics, Free University of Berlin, Germany,*

<sup>3</sup>*Department of Physics, University of Duisburg-Essen, Germany*

<sup>4</sup>*Department of Physics, University of Bielefeld, Germany*

e-mail: antun.balaz@ipb.ac.rs

In this paper we analytically and numerically study nonlinear dynamics in Bose-Einstein condensates induced by a harmonic modulation of the interaction and by geometry of the trapping potential. To analytically describe BEC dynamics, we use perturbative expansion based on the Poincaré-Lindstedt analysis of a Gaussian variational ansatz [1], while in the numerical approach we use numerical solutions of a variational system of equations and of the full time-dependent Gross-Pitaevskii equation.

Harmonic modulation of the atomic  $s$ -wave scattering length a Bose-Einstein condensate of  ${}^7\text{Li}$  was achieved recently [2] via Feshbach resonance. Such modulation leads to a number of nonlinear effects, which we describe within our approach: mode coupling, higher harmonics generation and significant shifts in the frequencies of collective modes. In particular, analytic formulae for shifts in the frequencies of collective modes are derived and verified numerically for the case of spherically and axially symmetric condensates [3].

In addition to the strength of atomic interactions in BEC, geometry of the trapping potential [4, 5] is another key factor for the dynamics of the condensate, as well as for its collective oscillation modes. The asymmetry of the confining potential leads to important nonlinear effects, including the

resonances in the frequencies of collective oscillation modes of the condensate [6]. We study in detail such geometric resonances and derive explicit analytic results for frequency shifts for the case of axially symmetric condensate with 2-body and 3-body interactions. Analytically obtained results are verified by extensive numerical simulations.

**Acknowledgments:** The authors thank V. S. Bagnato for useful discussions. This work was supported in part by the Serbian Ministry of Education and Science under projects No. ON171017 and NAD-BEC, by DAAD - German Academic and Exchange Service under project NAD-BEC, and by the European Commission under EU FP7 projects PRACE-1IP, HP-SEE and EGI-InSPIRE.

#### REFERENCES

- [1] V. M. Pérez-García, H. Michinel, J. I. Cirac, M. Lewenstein, P. Zoller, Phys. Rev. Lett. 77, 5320 (1996).
- [2] S. E. Pollack, D. Dries, R. G. Hulet, K. M. F. Magalhães, E. A. L. Henn, E. R. F. Ramos, M. A. Caracanhas, V. S. Bagnato, Phys. Rev. A 81, 053627 (2010).
- [3] I. Vidanović, A. Balaž, H. Al-Jibbouri, A. Pelster, arXiv:1106.4686, Accepted for publication in Phys. Rev. A (2011).
- [4] V. I. Yukalov, V. S. Bagnato, Laser Phys. Lett. 6, 399 (2009).
- [5] G. Filatrella, B. A. Malomed, L. Salasnich, Phys. Rev. A 79, 045602 (2009).
- [6] F. Dalfovo, C. Minniti, L. P. Pitaevskii, Phys. Rev. A 56, 4855 (1997).

## *Laser Induced Material Modification*

Oral Presentations – Laser Induced Material Modification O.LIM.1

### **Influence of picosecond laser irradiation on nickel base superalloy surface microstructure**

S. Petronic<sup>1</sup>, D. Milanovic<sup>2</sup>, A. Milosavljevic<sup>3</sup>, M. Momcilovic<sup>2</sup> and D. Petrusko<sup>2</sup>

<sup>1</sup>*Innovation Center, Faculty of Mechanical Engineering,  
University of Belgrade, Serbia*

<sup>2</sup>*Vinca Institute of Nuclear Sciences,  
Belgrade, Serbia*

<sup>3</sup>*Faculty of Mechanical Engineering,  
University of Belgrade, Serbia*

e-mail: sanjapetronic@yahoo.com

Investigation was carried out on the nickel base superalloy – Nimonic 263, that are widely used at elevated temperatures and pressures. Nimonic 263 is a nickel based superalloy, thermo-mechanically treated, with excellent creep strength and oxidation resistance [1,2].

In the last few years the increasing availability of ultra short-pulsed lasers have opened up new possibilities and technologies. In the picosecond regimes [3] the laser-material interaction process is very different from that observed in the nanosecond regime.

In this paper, the samples were exposed to Nd<sup>3+</sup>:YAG pulsed laser, with wavelength of 1064nm and pulse duration of 170 ps. The estimated threshold damage was 2 mJ.

Different pulse energy and number of pulses were applied, in the air and helium enriched atmosphere. Spots obtained by laser interaction were observed by optical and scanning electron microscope and analyzed by energo-dispersive spectroscopy. Vickers microhardness tests were performed.

In this paper, the microstructural changes, arisen by different pulse energy and number of pulses, in the air and helium enriched atmosphere, were discussed with the aim to contribute to determination of optimal laser parameters in laser surface treatment process.

**Acknowledgements.** This work is supported by the Ministry of Science of the Republic of Serbia under contract TR-35040.

#### REFERENCES

- [1] N. Srinivasan, Y.V.R.K. Prasad, J. Mater. Proc. Technol 51, 171 (1995).
- [2] M. Maldini, G. Angella, V. Lupinc, Mat. Sci. Eng. A 462, 436 (2007).
- [3] M. Trtica, B. Radak, B. Gakovic, D. Milovanovic, D., Batani, T. Desai, Laser and Particle Beams. 27, 85 (2009).

Oral Presentations – Laser Induced Material Modification O.LIM.2

### **Ultra-short pulse laser micro-processing of metals with radial and azimuthal polarization**

O.J. Allegre, L. Mellor, S.P. Edwardson, W. Perrie, G. Dearden and K.G. Watkins  
*Laser Group, Department of Engineering, The University of Liverpool*  
*Liverpool*  
*L69 3GQ, UK*  
e-mail: O.Allegre@liv.ac.uk

The past two decades have seen significant developments in ultra-short pulse laser micro-processing. Thanks to the ultra-short timescale on which laser energy is coupled to the material, sub-micron precision processing can be achieved with very little thermal damage. As a result, industrial processes based on femtosecond and picosecond laser pulse durations are becoming increasingly widespread. Manufacturing applications include the very precise drilling of holes for fuel-injection nozzles, the processing of silicon wafers and the precise machining of medical stent devices [1].

Laser-material interactions are known to be strongly influenced by the polarization of the incident laser beam. In particular, polarization affects both the efficiency and the quality of ultra-short pulse micro-processes such as helical drilling and cutting. Thanks to their isotropic properties, circular polarized beams are chosen for most laser manufacturing applications, although they do not offer the best processing efficiencies [2]. The potential benefits of using radial and azimuthal polarizations for laser machining have been studied theoretically for several years, leading to predictions that the use of a radially polarized beam could enhance the efficiency of the cutting process by more than 50% compared to circular polarization [3]. However, producing these modes of polarization has been difficult until recently, making it complicated to verify these claims experimentally. Thanks to the latest technological developments in liquid-crystal devices such as spatial light modulators, it is now possible to produce such polarization modes in a relatively simple and cost effective manner.

In this work, a liquid-crystal spatial light modulator has been used to convert a linearly polarized femtosecond pulse laser beam to a radially, azimuthally and circularly polarized beam. The micro-processing properties of these modes of polarization have been investigated. Blind drilling, helical drilling and cutting tests have been carried out on metals such as stainless steel, copper and aluminium, generating micro-features of various depths and geometries. The resulting cutting profiles have been measured, demonstrating the effect polarization has on the process. Laser Induced Periodic Surface Structures (LIPSS) have also been investigated for the respective polarization modes.

These experiments did not confirm the 50% gain in efficiency when cutting metals with radial polarization, predicted by some of the early theoretical models. However, polarization emerged as a

powerful tool for optimizing ultra-short pulse laser micro-processing. Depending on the material, the geometry and depth of the machined structures, radial or azimuthal polarizations produced the best results, reducing ellipticity, improving the edge quality of the exit apertures and reducing the processing time, compared with more traditional polarizations such as circular. Azimuthal polarization was more efficient at cutting higher aspect-ratio features, due to its high reflectivity which allows a larger proportion of the beam energy to be channelled to the bottom of the structure. Radial polarization was better for cutting lower aspect-ratio features. To our knowledge, this work is the first to investigate the effects of radial and azimuthal polarizations on femtosecond laser micro-processing of metals.

#### REFERENCES

- [1] N.H. Rizvi, RIKEN Review 50, 107 (2003).
- [2] S. Nolte, C. Momma, G. Kamlage, A. Ostendorf, C. Fallnich, F. von Alvensleben, H. Welling, Appl. Phys. A 68, 563 (1999).
- [3] V.G. Niziev, A.V. Nesterov, J. Phys. D, Appl. Phys. 32, 1455 (1999).

Oral Presentations – Laser Induced Material Modification O.LIM.3

## Ultra-short Relativistic Photon and Particle Beams in High-Intensity Laser-Plasma Interaction

M.M. Škorić<sup>1</sup>, Lj. Nikolić<sup>2</sup>, Lj. Hadžievski<sup>3</sup> and S. Ishiguro<sup>1</sup>

<sup>1</sup>*National Institute for Fusion Science, Graduate University of Advanced Studies  
Toki-shi 509-5292, Japan*

<sup>2</sup>*University of Alberta, Canada*

<sup>3</sup>*Vinča Institute of Nuclear Sciences, Belgrade, Serbia*

e-mail: skoric.milos@nifs.ac.jp

Due to rapid progresses in high intensity lasers over last decades, based on the invention of the chirped pulse amplification (CPA) and advanced femtosecond techniques, it has become possible to drive electrons with relativistic energy, opening up new fields of relativistic nonlinear optics and plasma physics. Currently, a wide area of relativistic laser matter interactions is diverging in two main directions; the first, concerning a fast ignition concept in laser fusion, high energy density science and laboratory astrophysics, and the second, related to ultra high field science and acceleration of high energy particles and photon beams [1]. More recently, advancement of optical and plasma technology toward the attosecond regime, has opened up avenues of ultra-fast science, as sub-disciplines of atomic, molecular, solid-state physics and real time chemistry [2].

Here we discuss two different schemes for generation of intense ultra-fast, attosecond range photon and electron bunches in relativistic laser interaction with plasma targets. In relativistic plasmas it is often found that sub-femtosecond optical pulses are also accompanied by intense sub-femtosecond relativistic electron bunches. First, we explore a new concept for attosecond photon pulse generation by a reflection of a femtosecond laser pulse from a relativistic electron beam (REB) plasma. While most of the existing schemes for attosecond photon pulses require nonlinear high harmonics generation in ultra-relativistic intensity laser-plasmas, a proposed model operates in a linear regime, which could allow a low intensity laser system [3]. Analytical formulae for obliquely reflected pulse, predict temporal compression and intensity amplification, by the factor of  $2\gamma$  and  $4\gamma^2$ , respectively; where  $\gamma$  is the relativistic Lorentz factor of the REB plasma. We further test the feasibility by two-dimensional relativistic particle-in-cell (PIC) simulations. In many applications single attosecond pulse is preferred, so a half-cycle cosine is taken as an input laser pump. Agreement between PIC and analytical results is found, which predicts, for NIR laser pulse reflected from 5 MeV ( $\gamma \sim 10$ ) electron beam at a critical density, a pulse compression to 50 attosecond. Some ideas are proposed for future proof-of-principle experiments. Second, hollow cone-shaped solid plasma targets are investigated by

relativistic particle (PIC) simulations [4]. Introduced originally to enhance the electron transport in fast ignition targets, different geometries, such as: hollow cone, cone-wire and open-tip cone were explored. In addition, cone targets have shown a good potential for enhanced high optical harmonics generation of the reflected laser light which is of interest in many applications. Moreover, with optimized parameters, relativistic laser pulse interacting with an open cone solid plasma target can efficiently generate a train of forward propagating, ultra-short, attosecond electron bunches (sheets) with high relativistic energy ( $E > 10$  MeV), separated in space by  $\lambda/2$ .

#### REFERENCES

- [1] G.A. Mourou, et al., Plasma Phys. Contr. Fusion. 49, B667 (2007).
- [2] P.B. Corkum, F. Krausz, Nature Physics 3, 381 (2007).
- [3] M.M. Škorić, B. Stanić, Lj. Hadžievski, Lj. Nikolić, J. Plasma Phys. 75, 111 (2009).
- [4] <http://iopscience.iop.org/1742-6596/112/2/022086>

# Poster Presentations

---

## *Optical Materials*

Poster Presentations – Optical Materials P.OM.1

### **Sn/SiO<sub>2</sub> single crystals growth by hydrothermal method at high temperatures and pressures**

I. Miron<sup>1,2</sup>, D. H. Ursu<sup>1,2</sup>, M. Miclau<sup>2</sup>, R. Banica<sup>2</sup>, M. Vasile<sup>2</sup> and I. Grozescu<sup>1,2</sup>  
<sup>1</sup>"Politehnica" University of Timisoara, Romania

<sup>2</sup>National Institute for Research and Development in Electrochemistry and Condensed Matter,  
Timisoara, Romania  
e-mail: danielhoratiu@yahoo.com

$\alpha$ -quartz type materials are of major interest due to their piezoelectric properties [1]. At the moment, most perspective high temperature piezoelectric materials are single crystals of langasite family and gallium orthophosphate (GaPO<sub>4</sub>). However, the growth of this syngle crystals has some technical complexities [2]. Interest in growth of silicium dioxide single crystals with  $\alpha$ -quartz structure is connected to improvement of quality factor Q. Therefore, till now, the silicium dioxide single crystals were doped with Ge ions to improve this factor.

The present paper describes growth of silicium dioxide single crystals with  $\alpha$ -quartz structure doped with Sn ions. The growth of crystals was made by hydrothermal method at high temperature and pressure (420°C, 1500 bar). A chemical of 1.0M NaOH was used as mineralizer. Seeds were cut from synthetic quartz crystals. Nutrient material was prepared from synthetic quartz and there was loaded SnO<sub>2</sub> powder additive in proportions to quartz nutrient.

XRD spectra reveal that Sn/SiO<sub>2</sub> single crystals has an  $\alpha$ -quartz structure and EDAX measurements shows the closely stoichiometric composition with the precursor material. Also, obtained single crystals were investigated in terms of UV/VIS/NIR spectroscopy and FTIR spectroscopy for quality factor Q calculation.

This work was partially supported by the International Cooperation Project MNT-ERA.Net, Project No. MNT 7-027/2010, Acronym PIM-FCS.

This work was partially supported by the strategic grant POSDRU 107/1.5/S/77265, inside POSDRU Romania 2007-2013 co-financed by the European Social Fund – Investing in People.

#### REFERENCES

- [1] M. Miclau, N. Miclau, M. Poienar, I. Grozescu, Cryst. Res. Technol. 44, 6, 577 (2009).
- [2]. V.S. Balitsky, D.V. Balitsky, A.N. Nekrasov, L.V. Balitskaya, Journal of Crystal Growth 275, 807 (2005).

## ZnO Nanowire emitters for tunable near-UV-Blue Light emitting diodes

B. Viana<sup>1</sup>, O. Lupan<sup>2</sup> and T. Pauporté<sup>2</sup>

<sup>1</sup>Laboratoire de Chimie de la Matière Condensée de Paris, UMR 7574-CNRS- Chimie ParisTech -UPMC,  
11 rue P. et M. Curie, 75231 Paris cedex 05, France.

<sup>2</sup>Laboratoire d'Electrochimie, Chimie des Interfaces et Modélisation pour l'Energie (LECIME), UMR 7575  
CNRS, Chimie ParisTech, 11 rue P. et M. Curie, 75231 Paris, cedex 05, France.

e-mail : bruno-viana@chimie-paristech.fr

Nanowire (NW) based light emitting diodes (LEDs) have drawn large interest due to many advantages compared to thin film based devices. Marked improved performances are expected from nanostructured active layers for light emission. Nanowires can act as direct waveguides and favor light extraction without use of lens and reflectors. Moreover, the use of wires avoids the presence of grain boundaries and then the emission efficiency is boosted by the absence of non-radiative recombinations at the joint defects. The presentation will focus on the electrochemical deposition and hydrothermal techniques two cost-effective, low-temperature electrochemical or aqueous solution methods for growing zinc oxide (ZnO) nanorods on *p*-electrode of GaN-LEDs. ZnO is a promising wide band gap alternative material due to its many advantageous properties such as direct bandgap at 3.37 eV, large exciton binding energy of 60 meV at room temperature, instead of 25 meV for GaN base materials, and easy nanostructuring. Wires of high structural and optical quality have been epitaxially grown on *p*-GaN single crystalline substrates in order to produce low cost new LEDs.

After integration of the heterostructure in a LED device, a rectifying behaviour has been found with a forward current onset at 3V. The diodes emitted a unique UV-light peak centered at about 397 nm for either as-prepared or annealed samples. The emission turn-on voltage was 3.9 V for the hydrothermal and 4.2 V for the electrodeposition. Then the UV-emission was very bright at very low applied forward bias leading to a new generation of UV LEDs.

We have shown that the emission wavelength could be tuned and shift toward the violet-blue region by up to 40 nm by doping with Cu or Cd [3]. Our results clearly state the remarkable quality of the pure and doped-ZnO electrochemical materials and high quality of the ZnO-NWs/*p*-GaN interface. Near-UV and violet-blue sources can be combined with efficient phosphors for solid-state lighting in order to replace fluorescent light sources with long lifetimes and high energy saving.

### REFERENCES

- [1] O. Lupan, T. Pauporté, B. Viana., *Adv. Mater.*, 22 (30), 3298-3302, (2010).
- [2] O. Lupan, T. Pauporté, B. Viana, I. M. Tiginyanu, V. V. Ursaki, R. Cortès, *ACS Appl. Mater. Interfaces*, 2, 2083-2090, (2010).
- [3] Lupan O., Pauporté T., B. Viana., *Adv. Mater.*, on press.

## High power continuous-wave thin disk laser in Yb:CaGdAlO<sub>4</sub>

S. Ricaud<sup>1,4</sup>, B. Weichelt<sup>2</sup>, P. Goldner<sup>3</sup>, B. Viana<sup>3</sup>, P. Loiseau<sup>3</sup>, A. Jaffres<sup>3</sup>, A. Suganuma<sup>3</sup>,  
M. Abdou-Ahmed<sup>2</sup>, A. Voss<sup>2</sup>, T. Graf<sup>2</sup>, D. Ritz<sup>4</sup>, E. Mottay<sup>5</sup>, F. Druon<sup>1</sup> and P. Georges<sup>1</sup>

*1 Laboratoire Charles Fabry de l'Institut d'Optique, CNRS, Univ Paris-Sud, RD 128, 91127 Palaiseau, France*

*2 Institut für Strahlwerkzeuge (IFSW), Universität Stuttgart, Pfaffenwaldring 43 D-70569 Stuttgart, Germany*

*3 LCMCP Chimie Paristech 11 rue P. et M. Curie 75231 Paris, France*

*4 FEE GmbH, Struthstrasse 2, D-55743 Idar-Oberstein, Germany*

*5 Amplitude Systèmes, 6 allée du Doyen Georges Brus 33600 Pessac, France*

e-mail: bruno-viana@chimie-paristech.fr

The thin-disk laser design [1] allows the generation and the amplification of ultrashort pulses with very high efficiency, high output power and good beam quality [2]. Many interesting results were published using Yb:YAG crystal, leading to the generation of high power pulses up to 80 W [3] with a pulse duration around 1ps. Nevertheless, the emission cross section of Yb:YAG limits the generation of very short pulses, which explains the need of other materials. This is why investigating new thin-disk materials is an interesting point of view in order to generate shorter pulses with high average power.

In this point of view, Yb<sup>3+</sup>:CaGdAlO<sub>4</sub> has been recently demonstrated to be very interesting for the development of diode-pumped short-pulse modelocked lasers. First, it has the broadest and the flattest emission band of all the Yb:doped materials. Second, we measured the 2 at. % Yb:CALGO thermal conductivity at  $\sim 6.5 \text{ W} \cdot \text{K}^{-1} \cdot \text{m}^{-1}$  [4]. This high thermal conductivity allows high-power pumping. The generation of very short pulse has been demonstrated in mode-locked femtosecond oscillator with duration of 47 fs at 1050 nm [5].

Nevertheless, considering the good thermal properties of Yb:CALGO, the full potential of this crystal has not been exploited yet. This is why the thin disk structure with this crystal is very interesting to investigate.

Laser experiments were performed with 350  $\mu\text{m}$ -thick Yb<sup>3+</sup>:CaGdAlO<sub>4</sub> crystals, grown by the Czochralski technique and cut to have a polarization along the  $\sigma$  axis, and a propagation along the  $\pi$  axis. A 90 W fiber-coupled diode emitting at 980 nm has been used for the pump module. This pump module permitted 24 passes of the pump light through the crystal.

The first demonstration of laser operation with a thin-disk Yb:CALGO laser is presented. We have studied optical properties of crystals coming from different bowls, 2% or 3.5% doped, in CW regime and then spectral tunability have been investigated.

With this material, up to 30W, with a slope efficiency of 41% and an optical-to-optical efficiency of 32% have been obtained.

### REFERENCES

- [1] A. Giesen, et al., Appl. Phys. B 58, 365 (1994).
- [2] A. Giesen, et al., IEEE J. Sel. Top. Quantum Electron. 13, 598 (2007).
- [3] J. Neuhaus, et al., Opt. Express 16, 20530 (2008).
- [4] J. Boudeile, et al., Opt. Letters 32, 1962 (2007).
- [5] Y. Zaouter, et al., Opt. Letters 31, 119 (2006).

## Influence of Na<sup>+</sup> ions on the dielectric spectra of double doped (YbF<sub>3</sub>, NaF):CaF<sub>2</sub> crystals

M. Stef<sup>1,2</sup> and I. Nicoara<sup>1</sup>

<sup>1</sup>*Dept. of Physics, West University of Timisoara, 300223 Timisoara, Romania*

<sup>2</sup>*Alexandru Ioan Cuza University of Iasi, Bd. Carol I no. 11, 700506 Iasi, Romania*

e-mail: stef@quantum.physics.uvt.ro

When YbF<sub>3</sub> is dissolved in CaF<sub>2</sub> the Yb ions are in the trivalent state, consequently additional charge-compensating defects appear in the crystals. The local compensation, by pairing of Yb<sup>3+</sup> ions with an interstitial or substitutional F<sup>-</sup> ion, creates various crystal field symmetries of the Yb<sup>3+</sup> ions [1]. These types of charge compensation are the so-called isolated centers. As the concentration of the Yb<sup>3+</sup> ions increases, besides of the isolated centers additional complex defects (clusters) are present [2]. All these defects lead to a multisite structure of the absorption spectra. It has been observed [3] that alkali-metal codoping improves the multisite structure of the absorption spectrum and the laser performance of the crystals.

The goal of this work is to study the influence of Na<sup>+</sup> ions on the impurity-defect formation in YbF<sub>3</sub>-doped CaF<sub>2</sub> crystals, especially on the NN type defects with tetragonal symmetry (C<sub>4v</sub>). Ca<sub>1-x</sub>Yb<sub>x</sub>F<sub>2+x</sub> (x = 0.0007, 0.0017, 0.007, 0.0116) crystals with various NaF concentration (2.5-20mol%) were grown using the conventional Bridgman technique. Transparent colorless crystals were obtained in graphite crucible in vacuum (~ 10<sup>-1</sup> Pa) using a shaped graphite furnace [4].

Information on impurity-defect aggregates can be obtained from spectroscopic studies and dielectric relaxation technique [5]. The effect of Na<sup>+</sup> ions on the optical and dielectric spectra was studied. The dielectric spectra provide information about the type and number of the dipoles whose relaxation is observed [5]. Temperature and frequency dependence of the complex dielectric constant (the dielectric spectra) gives information about the relaxation processes and permits the determination of the activation energy for dipoles reorientation, the reciprocal frequency factor, τ<sub>0</sub>, of the relaxation time and the number of dipoles that contribute to the relaxation process.

The relaxation parameters and the number of the dipoles, N<sub>NN</sub>, that contribute to the dielectric relaxation have been determined from the dielectric spectra. The correlation between N<sub>NN</sub> and the optical spectra has been also discussed. From this study results that the Na<sup>+</sup> ions inhibit the clusters and the NN (C<sub>4v</sub>) type defects formation, but promote the NNN (C<sub>3v</sub>) defects that consist of substitutional Yb<sup>3+</sup> and interstitial Na<sup>+</sup> pairs. For high NaF concentration only the Na<sup>+</sup>-V<sub>F</sub> dipoles relaxation is observed. The reducing effect of the multisite structure of the broad <sup>2</sup>F<sub>7/2</sub> – <sup>2</sup>F<sub>5/2</sub> transition depends on the ratio of Na<sup>+</sup> to Yb<sup>3+</sup> ions concentrations.

Acknowledgement: This work was supported by the Sectorial Operational Programme for Human Resources Development “Trans-national network of integrated management for post-doctoral research in the field of Science Communication. Institutional construction (post-doctoral school) and fellowship Programme (CommScie)” POSDRU/89/1.5/S/63663.

### REFERENCES

- [1] C.R.A. Catlow, A.V. Chadwick, J. Corish, L.M. Moroney, A.N. O`Reilly, Phys. Rev. B 39, 1897 (1989).
- [2] V. Petit, P. Camy, J.-L. Doualan, X.Portier, R. Moncorgé, Phys. Rev. B 78, 085131 (2008).
- [3] L. Su et al., J. Crystal Growth 277, 264 (2005).
- [4] D. Nicoara and I. Nicoara, Mater. Sci. Eng. A 102, L1 (1988)
- [5] J. Fontanella and D. J. Treacy, J. Chem. Phys. 72, 2235 (1980).

## Analysis of imaging properties of microlenses based on the TESG layer elasticity

D. Vasiljević<sup>1</sup>, B. Murić<sup>1</sup>, D. Pantelić<sup>1</sup> and B. Panić<sup>1</sup>

<sup>1</sup>*Photonics center*

*Institute of Physics*

*University of Belgrade, Serbia*

e-mail: darko@ipb.ac.rs

Microlenses are increasingly used in various optical and biomedical applications. Microlenses are produced on tot'hema and eosin sensitized gelatin (TESG) layer [1]. Our standard microlenses are concave with parabolic profile. They are formed by focused 2<sup>nd</sup> harmonic Nd YAG laser (at 532 nm). Standard properties of such microlenses are presented in [2]. Image of the word microlens taken through one of such microlenses is given on Fig. 1.

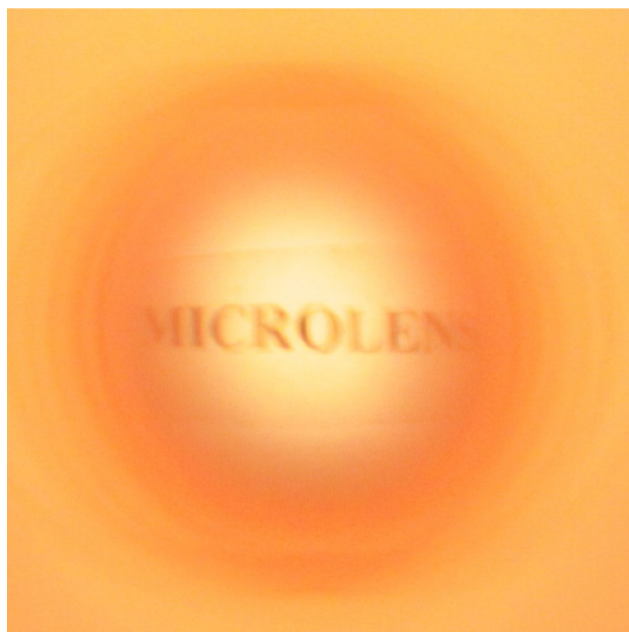


Fig. 1. Image of the word microlens taken through the microlens

For this research microlenses are written on a dog – bone shaped TESG layer. After production microlenses were stretched in one direction. As a result of stretching of microlenses, basic optical characteristics like the effective focal length were changed. The influence of TESG layer extensibility on imaging properties of microlenses were characterized by calculation of the RMS wavefront aberration, the modulation transfer function and the RMS and geometrical spot diagram.

### REFERENCES

- [1] B. Murić, D. Pantelić, D. Vasiljević, B. Panić, *Opt. Mater.* 30, 1217 (2008).
- [2] B. Murić, D. Pantelić, D. Vasiljević, B. Panić, *Appl. Optics* 46, 8527 (2007).

## **Maximal Temperature Difference Determination in Pulse Infrared Thermography by Fitting Experimental Results with Numerical Simulation Curve**

Lj. Tomić<sup>1</sup>, J. Elazar<sup>2</sup> and B. Milanović<sup>3</sup>  
<sup>1</sup>*Department of Electronic, Technical Test Center,  
 Belgrade, Serbian Armed Forces*  
<sup>2</sup>*School of Electrical Engineering,  
 University of Belgrade, Serbia*  
<sup>3</sup>*Military Academy,  
 Belgrade, Serbian Armed Forces*  
 e-mail:ljubisa.tomic@gmail.com

A special sample was prepared for the experiment, where on one side of an aluminum plate equally spaced grooves were produced, making a periodic defect structure with certain space frequency and certain depth [1]. The other side of the plate was illuminated by short light pulses and the temperature distribution on the same side was analyzed by pulse infrared thermography. Temperature distribution on the plate surface was also periodic, showing maxima above the grooves, i.e. defects, and minima where there were no defects.

Experimental results were obtained by a standard thermal imaging camera. The time history of the surface temperature after the absorption of a short light pulse is used to obtain information about the subsurface structure and the thermo-physical properties of the material. However, standard thermovision cameras do not offer the possibility of synchronizing the frame acquisition time with the heating light pulse, so it is often difficult to determine if the first obtained frame with increased temperature comes before or after the maximal temperature difference on the sample surface [2]. In addition, it is not possible to determine from the experimental results only if some of the frames comes exactly at the time of maximal temperature difference, which is essential for determination of defect size and depth. Therefore, it is necessary to fit the experimental points with a curve based on theory, and such a curve can be obtained by numerical simulation only.

In order to fit the experimental points with a curve based on theory a physical model was developed reflecting the sample properties. A computer program for simulation based on that model was written in MATLAB R2008a and 2D temperature field on the sample surface exposed to the heating light pulse was obtained for different values of absorption coefficient and different sizes and depths of the defect [3].

Only the central line normal to the grooves from each frame was used for the analysis. The noise was eliminated by filtering out all but the basic spatial frequency of the temperature distribution, and from there minimal and maximal temperatures on the surface were determined for that frame. Temperature difference obtained in such a way was plotted as a function of time at time points corresponding to the camera frame rate. These experimental results were then fitted with the curve obtained by numerical simulation using least square method as the criterion for the best fit [4].

Experimental and simulation results show excellent agreement. The simulation curve lies within the error bars for all experimental points on most frame trains obtained after different heating pulses. The maximal temperature difference and its time decay rate enabled determination of the depth dependent defect sizes which can be determined by the method, as well as material thermo- physical properties.

### REFERENCES

- [1] Lj. Tomić, J. Elazar, B. Milanović, Proc. Abstr. 3<sup>rd</sup> Conference MediNano 77, 18-19 October, Belgrade, Serbia 2010.  
 [2] Lj. Tomić, J. Elazar, B. Milanović, Proc. 54<sup>th</sup> ETRAN Conference, MO1.5-1-4, 2010.

[3] A. Darabi, Thèse, Université Laval Québec, 2000.

[4] C. Ibarra-Castanedo, M. Genest, P. Servais, X. Maldague, A. Bendada, NDT & E, 22 2007.

Poster Presentations – Optical Materials P.OM.7

## Enhancement of the photoluminescence properties of Al<sub>2</sub>O<sub>3</sub>-core/SnO<sub>2</sub>-shell nanowires by annealing in an oxidative atmosphere

C. Jin<sup>1</sup>, S. Park<sup>1</sup>, H. Kim<sup>1</sup> and C. Lee<sup>1</sup>

<sup>1</sup>*Department of Materials science and Engineering, Inha University, 253 Yonghyun-dong, Incheon 402-751, Republic of Korea*  
e-mail: cmlee@inha.ac.kr

We have fabricated Al<sub>2</sub>O<sub>3</sub>-core/SnO<sub>2</sub>-shell nanowires by thermal evaporation of Al powders and then coated Al<sub>2</sub>O<sub>3</sub> nanowires with SnO<sub>2</sub> by sputtering. We performed scanning electron microscopy (SEM), transmission electron microscopy (TEM), X-ray diffraction (XRD), energy-dispersive X-ray spectroscopy (EDXS), and photoluminescence (PL) spectroscopy to characterize the Al<sub>2</sub>O<sub>3</sub>-core/SnO<sub>2</sub>-shell nanowires. SEM analysis revealed that the nanowires were a few hundreds of nanometers in diameter and a few tens of micrometers in length. PL measurements at room temperature showed that Al<sub>2</sub>O<sub>3</sub> nanowires had a strong yellow emission band centered at 580 nm and a weak broad green emission band centered at around 680 nm. The major emission of core-shell nanowires was found to be enhanced by annealing in an oxidative atmosphere but degraded in a reductive atmosphere. In addition, the origins of these changes by annealing are discussed.

### REFERENCES

[1] C.M. Lieber, MRS Bull. 28, 486 (2003).

[2] M.H. Huang, S. Mao, H. Feick, H. Yan, Y. Wu, H. Kind, E. Weber, R. Russo, P. Yang, Science 292, 1897 (2001).

Poster Presentations – Optical Materials P.OM.8

## Enhancement of the photoluminescence properties of Ga<sub>2</sub>O<sub>3</sub> nanowires by In<sub>2</sub>O<sub>3</sub> coating

S. Park<sup>1</sup>, C. Jin<sup>1</sup>, H. Kim<sup>1</sup> and C. Lee<sup>1</sup>

<sup>1</sup>*Department of Materials science and Engineering, Inha University, 253 Yonghyun-dong, Incheon 402-751, Republic of Korea*  
e-mail: cmlee@inha.ac.kr

We have fabricated Ga<sub>2</sub>O<sub>3</sub>-core/In<sub>2</sub>O<sub>3</sub>-shell nanowires by thermal evaporation of GaN powders on Au-coated and then coated Ga<sub>2</sub>O<sub>3</sub> nanowires with In<sub>2</sub>O<sub>3</sub> by sputtering. Transmission electron microscopy (TEM) and X-ray diffraction (XRD) analyses revealed that the core was a Ga<sub>2</sub>O<sub>3</sub> single crystal with a monoclinic structure and that the shell was amorphous. Photoluminescence (PL) measurements at room temperature showed that uncoated Ga<sub>2</sub>O<sub>3</sub> nanowires had a blue emission band centered at approximately 480 nm. The intensity of the blue emission of Ga<sub>2</sub>O<sub>3</sub> nanowires increased with increasing the In<sub>2</sub>O<sub>3</sub> shell layer thickness. The highest emission intensity was obtained with a shell layer thickness of 10 nm. In addition, the origin of the PL intensity enhancement by SnO<sub>2</sub> coating is discussed.

### REFERENCES

[1] H. B. Xie, L. M. Chen, Y. N. Liu, K. L. Huang, Solid State Commun. 141, 12 (2007).

[2] L. Binet, D. Gourier, J. Phys. Chem. Solids 59, 1241 (1998).

## A fiber-optic polarimetric demonstration kit

T. Eftimov<sup>1</sup>, T. L. Dimitrova<sup>2</sup> and G. Ivanov  
*Faculty of Physics, University of Plovdiv “Paissi Hilendarski”*  
*Tzar Assen Str.24BG-4000 Plovdiv, Bulgaria*  
 e-mail: tldimitrova@abv.bg

Measuring the light polarization gives fundamental information about light and its interaction with the matter. The change of the light polarization is in the base of several experimental methods studying the properties, the structure and the composition of many nonorganic and organic materials. It has application in science, industry, medicine and pharmacy, food production etc.

We have built a simple and multifunctional fiber-optic polarimetric kit on the basis of highly birefringent single-mode fibers. The device is designed for demonstration experiments and for university laboratory exercises in optics and fiber optics.

The device is modular in order to enable plug-and-play options for different experiments. A 532 nm DPSS laser is used in combination with magnetically attached rotatable polarizer. Linearly polarized light can be launched along the fiber birefringence axis with the help of a tunable laser-to-fiber coupler having a rotatable receptacle. The magnetic attachments of the rotatable holders allow accommodation of various components. The sizes and the design of the set-up are appropriate to keep all components in case for better storage and transportation. The kit is easy for manipulation.

The kit is designed to demonstrate and measure some important properties and characteristics of highly birefringent fibers. It allows to locate birefringence axes and to preserve the polarization under eigenpolarization excitation. The fiber beatlength can be measured by introducing controlled perturbations along a direction non-coinciding with the birefringence axes. The principles of the fiber optic sensors can be demonstrated by measuring the fiber sensitivities to strain and temperature in the polarimetric response through crossed polarizer/analyzer with 45° input excitation.

The fiber-optic polarimetric kit allows to perform the following laboratory exercises: 1) Fiber excitation and numerical aperture; 2) Polarization preservation; 3) Polarization-sensitive fiberized interferometers.

The Gaussian distribution in the far-field can be observed by screen projection from the fiber output which also allows the determination of the mode-field diameter in the fibers.

Excitation polarization holding under eigenpolarization can be determined with a crossed analyzer at the fiber output. Excitation of both polarizations at the input of the fiber allows the observation of temperature and strain sensitivities by observing output intensity oscillations through a crossed analyzer.

The measurement of fiber beatlength and from it the magnitude of the birefringence is performed with eigenpolarization input. The fiber is lightly twisted and taped on the breadboard. A sharp edge transversally pressing the fiber introduces local mode coupling centers [1]. The edge is gently slid along the fiber and intensity oscillations are observed through crossed analyzer. Their period is the fiber beatlength.

A beamsplitter and a tunable mirror allow a fiber optic Michelson interferometer to be built. With eigen polarization excitation only interferometric responses to strain and temperature are observed, while with excitation of both polarizations the polarimetric response will be superimposed on the interferometric [2]. This will allow to observe fading of interference caused by changes of polarization along the fiber. Both conventional and photonic crystal fibers [3] can be used with this set-up.

#### Acknowledgements:

The authors thank the financial support of the SNF Scopes program (grant No. IZ73Z0–127942–1).

#### REFERENCES

- [1] T. Kortenski, T. Eftimov, *Journ. Mod. Optics*, 37(9), 1413, (1990).
- [2] D. Chadron, J. Huard, *J. Lightwave Technol.*, 4, 720, (1986).
- [3] T. Ritari, H. Ludvigsen, M. Wegmuller, M. Legré, and N. Gisin, J. R. Folkenberg and M. D. Nielsen, *Optics Express*, 12, 5931, (2004).

Poster Presentations – Optical Materials P.OM.10

## Oblique Surface Waves at an Interface of Metal-dielectric Superlattice and an Isotropic Dielectric

S. M. Vuković<sup>1</sup>, J. J. Miret<sup>2</sup>, C. J. Zapata-Rodriguez<sup>3</sup> and Z. Jakšić<sup>4</sup>

<sup>1</sup> *Institute of Physics, University of Belgrade, Pregrevica 118, 11080 Zemun, Serbia*

<sup>2</sup> *Department of Optics, Pharmacology and Anatomy, University of Alicante, P.O. Box 99, Alicante, Spain*

<sup>3</sup> *Department of Optics, University of Valencia, Dr. Moliner 50, 46100 Burjassot, Spain*

<sup>4</sup> *IHTM – Institute of Microelectronic Technologies and Single Crystals, University of Belgrade, Njegoševa 12, 11000 Belgrade, Serbia*

email: svukovic@ipb.ac.rs

We investigate existence and propagation of surface waves at an interface between semi-infinite isotropic dielectric, and semi-infinite plasmonic crystal cut normally to the constituent layers. The geometry of the problem allows for Dyakonov-like surface waves at the boundary of anisotropic uniaxial crystal with positive birefringence, and optical axis oriented along the boundary with isotropic dielectric [1, 2].

In dielectric-dielectric 1D superlattices there is always negative birefringence [3], and so, no Dyakonov surface waves are possible. The presence of metallic layers is crucial for positive birefringence which is necessary for existence of oblique surface waves. As an example we use plasmonic crystal with silver (thickness  $d_m = \text{nm}$ ), and GaAs (thickness  $d_d = \text{nm}$ ) stacking interfaced with fused silica. In the long-wavelength limit, at the vacuum wavelength  $\lambda = 1.55 \mu\text{m}$ , plasmonic crystal can be treated as a quasi-homogeneous but anisotropic medium with dielectric permittivity tensor components:  $\epsilon_z = 13.5 + i0.003$ ,  $\epsilon_x = \epsilon_y = 0.97 + i0.27$ , while the permittivity of fused silica is:  $\epsilon = 2.25$ . Therefore, the existence condition for Dyakonov surface waves  $\epsilon_z > \epsilon > \epsilon_x$  is satisfied [1]. Moreover, the introduction of metal-dielectric metamaterial instead of natural anisotropic uniaxial crystal reveals substantial increase of the range of propagation angles:  $35^\circ < \varphi < 70^\circ$ . However, in contrast to the classical Dyakonov problem, due to the presence of metallic layers dispersion and dissipation are non-negligible here. In order to see the influence of dissipation which is represented via imaginary parts of dielectric permittivity tensor components, one has to calculate the so called “figure of merit”. That means the ratio of real and imaginary parts of the wavevector representing in fact, the distance (number of wavelengths) over which the mode can propagate without serious attenuation. Our calculations show that the figure of merit is always greater than 10 in the whole range of angles where the oblique surface waves do exist. However, the figure of merit increases towards the smaller angles of propagation, getting to very high values, and therefore, almost negligible dissipation. We also study the effect of finite number of periods [4], and localization of modes near the edges of plasmonic crystal.

#### REFERENCES

- [1] M. I. Dyakonov, *Soviet Physics JETP* 67, 714 (1988).
- [2] D. Artigas and L. Torner, *Phys. Rev. Lett.* 102, 043903 (2009).
- [3] D. Artigas and L. Torner, *Phys. Rev. Lett.* 94, 013901 (2006).
- [4] S. M. Vukovic, Z. Jaksic, and J. Matovic, *J. Nanophotonics* 4, 041770 (2010).

## Ab initio calculations of structural, electronic, optical and elastic properties of $K_3CrF_6$

A. S. Gruia<sup>1</sup>, C. N. Avram<sup>1</sup>, N. M. Avram<sup>1,2</sup> and M. G. Brik<sup>3</sup>

<sup>1</sup> Faculty of Physics, West University of Timisoara, V. Parvan 4, Timisoara 300223, Romania

<sup>2</sup> Academy of Romanian Scientists, Independentei Street 54, Bucharest 050094, Romania

<sup>3</sup> Institute of Physics, University of Tartu, Riia 142, Tartu 51014, Estonia

e-mail: gruia@physics.uvt.ro

$K_3CrF_6$  has attracted recently considerable interest due to the high site symmetry of  $Cr^{3+}$  ion and  $[CrF_6]^{3-}$  complex [1 and reference therein]. The aim of this study is to present the results of the *ab initio* calculations (with the use of the CASTEP module [2] and the CRYSTAL09 computer program [3]) of the optimized crystal structure, band structure, density of states (DOS), optical and elastic properties of  $K_3CrF_6$ . Both generalized gradient approximation (GGA) with the Perdew–Burke–Ernzerhof functional [4] and local density approximation (LDA) with the Ceperley–Alder–Perdew–Zunger parameterization [5] were used in all calculations for the sake of consistency. The electronic configurations were  $2s^22p^5$  for the fluorine,  $3s^23p^63d^54s^1$  for chromium, and  $4s^23p^64s^1$  for potassium. *Ab initio* calculations of the density of states allowed evaluating contribution of each ion into the calculated bands. In addition, the spin-polarized calculations allowed for finding difference between densities of the spin-up and spin-down states of 6-fold coordinated  $Cr^{3+}$  ion. To the best of the authors' knowledge, there are no experimental data on the band structure, elastic constants and absorption spectrum function for this host, so the present work is the first theoretical study of this kind, and the theoretically obtained results could be suggestions for future experiments.

### REFERENCES

- [1] M. G. Brik, K. Ogasawara. Phys.Rev., B74, 045105 (2006).
- [2] M. D. Segall *et al*, J. Phys.: Condens. Matt. 14, 2717 (2002).
- [3] R. Dovesi *et.al*, CRYSTAL09 (2009), CRYSTAL09 User's Manual, University of Turin, Turin (2010).
- [4] J. P. Perdew, K. Burke, M. Ernzerhof, Phys. Rev. Lett. 77, 3865 (1996).
- [5] D. M. Ceperley, B. J. Alder, Phys. Rev. Lett. 45, 566 (1980).

## Thermographic properties of $Sm^{3+}$ doped $GdVO_4$ phosphor

M.G. Nikolić, D. J. Jovanović, V. Đorđević, Ž. Antić, R.M. Krsmanović and M.D. Dramićanin

Vinca Institute of Nuclear Sciences, Belgrade, Serbia

e-mail: radenka@vinca.rs

Phosphor based thermometry utilizes the emission properties of phosphor particles for assessing temperature. Phosphors are considered thermographic if they exhibit emission-changing characteristics with temperature. Main investigations in phosphor thermometry involves one of two types of analysis: the lifetime decay method or the intensity ratio method. The latter has been widely accepted since it eliminates a number of errors coming from fluctuations of the excitation light source, temperature changes of excitation bands and non-uniform dopants concentrations [1], and has been used in this study.

The lanthanide ions activated orthovanadate *phosphors* have considerable practical applications in devices involving the artificial production of light, such as cathode ray tubes, lamps, and x-ray detectors [2]. In particular gadolinium vanadate has been extensively studied in the field of lasers due

to its stable physical and chemical properties [3]. The temperature dependence of emission intensities for three samples of  $\text{GdVO}_4:\text{Sm}^{3+}$  (0.5, 1 and 2 mol.% Sm), prepared by the high temperature solid-state method, is presented in this work. We investigated the possibility for  $\text{GdVO}_4:\text{Sm}^{3+}$  usage in phosphor thermometry by observing temperature changes of trivalent samarium transitions from  $^4\text{F}_{3/2}$  and  $^4\text{G}_{5/2}$  energy levels to the ground state. Measurements were recorded from room temperature up to 820 K, showing that  $\text{GdVO}_4:\text{Sm}^{3+}$  is a new, promising high temperature thermographic phosphor of very good sensitivity.

#### REFERENCES

- [1] N. Ishiwada, T. Ueda, Takeshi Yokomori, J. Bio. Chem. Lumin., DOI 10.1002/bio.1237.
- [2] H. Xin, L.X. Lin, J.H. Wu, B. Yan, J. Mater. Sci: Mater Electron, DOI: 10.1007/s10854-011-0308-y.
- [3] K. S. Shim, H. K. Yang, B. K. Moon, B. C. Choi, J. H. Jeong, J. H. Kim, J. S. Bae, K. H. Kim, Curr Appl Phys. 9, S226 (2009).

Poster Presentations – Optical Materials P.OM.13

### **Thermographic properties of $\text{Eu}^{3+}$ and $\text{Sm}^{3+}$ doped $\text{Lu}_2\text{O}_3$ nanophosphor**

R.M. Krsmanović, Ž. Antić, M.G. Nikolić, D. Jovanović, V. Đorđević and M.D. Dramićanin  
*Vinca Institute of Nuclear Sciences, Belgrade, Serbia*  
e-mail: radenka@vinca.rs

Knowing that lutetium oxide has high chemical stability and temperature resistance, we investigated possibility for its usage in high-temperature phosphor thermometry. The temperature-dependent photoluminescence emission of  $\text{Lu}_2\text{O}_3:\text{Eu}^{3+}$  (3at.% Eu) and  $\text{Lu}_2\text{O}_3:\text{Sm}^{3+}$  (1at.% Sm) were examined using the intensity ratio method [1, 2]. Two lines are considered appropriate for intensity ratio method if they both have strong emission intensity in the whole temperature range, and if their intensity ratio gives high temperature resolution.

The photoluminescence spectra were collected under excitation light of a 450 W Xenon lamp on the Fluorolog-3 Model FL3-221 (Horiba Jobin-Yvon) spectrofluorometer system ( $\lambda_{\text{exc}}(\text{Lu}_2\text{O}_3:\text{Eu}) = 393$  nm,  $\lambda_{\text{exc}}(\text{Lu}_2\text{O}_3:\text{Sm}) = 406$  nm), elevating the temperature gradually from room temperature to 850 K. Variation of emission intensity with increasing temperature is monitored for main transitions of  $\text{Eu}^{3+}$  and  $\text{Sm}^{3+}$  ions, aiming to detect the intensity ratio of the highest gradient and linearity over the entire temperature range. We also tested the lifetime decay response in the same temperature region.

Our experimental results demonstrate the performance of  $\text{Eu}^{3+}$  and  $\text{Sm}^{3+}$  doped  $\text{Lu}_2\text{O}_3$  as high temperature thermographic phosphors of very good sensitivity.

#### REFERENCES

- [1] S.A. Wade, S.F. Collins, G.W. Baxter, J. Appl. Phys. 94, 4743 (2003).
- [2] A.H. Khalid, K. Kontis, Sensors 8, 5673 (2008).

## Optical properties of ZnAl<sub>2</sub>O<sub>4</sub> nanomaterials obtained by hydrothermal method

I. Miron<sup>1,2</sup>, C. Enache<sup>3</sup>, R. Banica<sup>2</sup>, M. Vasile<sup>2</sup> and I. Grozescu<sup>1,2</sup>

<sup>1</sup>"Politehnica" University of Timisoara, Romania

<sup>2</sup>National Institute for Research and Development in Electrochemistry and Condensed Matter, Timisoara, Romania

<sup>3</sup>Institute of Chemistry Timisoara of Romanian Academy, Romania

e-mail:mironiasmina@gmail.com

Nanocrystalline zinc aluminate with a normal spinel structure are widely used as catalytic and electronic materials [1–3]. Besides, as a wide band gap semiconductor (3.8 eV), ZnAl<sub>2</sub>O<sub>4</sub> spinels can be used as transparent conductor, dielectric material, and optical material [4,5].

Nanocrystalline zinc aluminate (ZnAl<sub>2</sub>O<sub>4</sub>) particles with a spinel structure were prepared by hydrothermal method with a post treatment at different temperatures. For preparation of zinc aluminate nanoparticles zinc nitrate hexahydrate and aluminium nitrate nonahydrate were used as precursors. Nanocrystalline ZnAl<sub>2</sub>O<sub>4</sub> were investigated in terms of XRD and SEM/EDAX techniques. The XRD spectra shows that obtained zinc aluminate nanoparticles has a spinel structure and EDAX measurements reveals the purity of material. Optical properties of nanocrystalline zinc aluminates were investigated by UV/VIS/NIR spectroscopy and PL measurements.

This work was partially supported by the strategic grant POSDRU/88/1.5/S/50783, Project ID50783 (2009), co-financed by the European Social Fund – Investing in People, within the Sectorial Operational Programme Human Resources Development 2007-2013.

### REFERENCES

- [1] W. Streck, P. Dreen, E. Lukowiak, J. Wrzyszczyk, M. Zawadzki, P. Pershukovich, *Spectrochim. Acta*, A 54, 2121(1998).
- [2] R. Roesky, J. Weiguny, H. Bestgen, U. Dingerdissen, *Appl. Catal., A Gen.* 176, 213 (1999).
- [3] I. Futoshi, G. Naoyuki, M. Masashi, US Patent 5561089, (1996).
- [4] N.J. Van der Laag, M.D. Snel, P.C.M.M. Magusin, G. de With, *J. Eur. Ceram. Soc.* 24, 2417 (2004).
- [5] A.R. Phani, M. Passacantando, S. Santucci, *Mater. Chem. Phys.* 68, 66 (2001).

## Microlenses focal length control by chemical processing

B. Murić, D. Pantelić, D. Vasiljević and B. Panić

*Institute of Physics,*

*Belgrade, Serbia*

e-mail: muric@ipb.ac.rs

Microlenses are increasingly used in different optical and biomedical applications [1, 2]. Transparent, aspheric, concave microlenses (individual or array) were produced on the tot'hema and eosin sensitized gelatin layer (TESG), by 2<sup>nd</sup> harmonic Nd:YAG laser [3, 4, 5]. Tot'hema is an oral solution assigned for treatment of human anemia [6]. Produced microlenses were additionally chemically processed. The microlens focal length of 400 μm was obtained after isopropyl alcohol processing. We have shown that the focal length of microlenses can be easily and precisely controlled by varying potassium alum concentration – focal length can be increased up to three times. After alum processing

microlenses retain their mechanical and optical properties indefinitely and are not affected by environmental influences like UV light, humidity or temperature. The temperature range was extended after alum processing.

This method quickly and directly produces high quality, transparent, concave microlenses (individual or array) on a cheap, easy available and low toxic material - the fact which can be rarely found in the literature.

#### REFERENCES

- [1] C.P.B. Siu, H. Zeng, Mu Chiao, *Opt. Express* 15, 11154 (2007).
- [2] S. Calixto, V.P. Minkovich, I.T. Gomez, *Appl. Opt.* 45, 6463 (2006).
- [3] B. Murić, D. Pantelić, D. Vasiljević, B. Panić, *Opt. Mat.* 30, 1217 (2008).
- [4] B. Murić, D. Pantelić, D. Vasiljević, B. Panić, *Appl. Opt.* 46, 8527 (2007).
- [5] B. Murić, D. Pantelić, D. Vasiljević, B. Panić, B. Jelenković, *Appl. Opt.* 48, 3854 (2009).
- [6] [http://www.vidal.fr/Medicament/tot\\_hema-16626.htm](http://www.vidal.fr/Medicament/tot_hema-16626.htm).

Poster Presentations – Optical Materials P.OM.16

### **The model of exciton states in a nanocup in a magnetic field**

V. Arsoski<sup>1</sup>, N. Čukarić<sup>1</sup>, M. Tadić<sup>1</sup> and F.M. Peeters<sup>2</sup>

<sup>1</sup>*School of Electrical Engineering,  
University of Belgrade, Serbia*

<sup>2</sup>*Department of Physics, University of Antwerp,  
Antwerp, Belgium*

e-mail: arsosk@etf.bg.ac.rs

The magnetic-field dependence of the single electron and hole states in a nanocup [1], which is composed of a ring (the nanocup rim) that surrounds a disk (the nanocup bottom), is theoretically determined. The calculations were done for the strained (In,Ga)As/GaAs system. The strain distribution is determined from the model of isotropic strain using the inclusion theory [2]. The single particle states are extracted from the effective-mass model, whereas an exact diagonalization approach is employed to compute the states of the neutral exciton [3]. Furthermore, the hole energy levels determined by means of the single-band model are compared with those extracted from Luttinger-Kohn model and some differences are found. The strain is found to favor the spatial localization of the heavy holes inside the disk, that lead to a separation of the electron and the hole like in a type-II band alignment. Therefore, strain increases the polarization of the exciton, which is beneficial for the appearance of the excitonic Aharonov-Bohm (AB) effect. When the nanocup bottom is thin, the oscillator strength for exciton recombination exhibits small AB oscillations with magnetic field. The results of our calculations show that the excitonic AB effect could occur in properly designed experimental nanorings fabricated by means of the Stranski-Krastanov growth [4-7].

#### REFERENCES

- [1] N. A. J. M. Kleemans et al., *Phys. Rev. B* 80, 155318 (2009).
- [2] J. H. Davies, *J. Appl. Phys.* 84, 1358 (1998).
- [3] M. Tadić, N. Čukarić, V. Arsoski, F.M. Peeters, arXiv:1003.0467 (unpublished).
- [4] A. O. Govorov, S. E. Ulloa, K. Karrai, R. J. Warburton, *Phys. Rev. B* 66, 081309 (2002).
- [5] M. D. Teodoro et al., *Phys. Rev. Lett.* 104, 086401 (2010).
- [6] F. Ding, N. Akopian, B. Li, U. Perinetti, A. Govorov, F. M. Peeters, C. C. Bof Bufon, C. Deneke, Y. H. Chen, A. Rastelli, O. G. Schmidt, V. Zwiller, *Phys. Rev. B* 82, 075309 (2010).
- [7] R. Okuyama, M. Eto, H. Hyuga, *Phys. Rev. B* 83, 195311 (2011).

## **Influence of the internal heterostructure to nonlinear absorption spectra for intersubband transitions in spherical quantum dot-quantum well nanoparticles**

R. Kostić and D. Stojanović

*University of Belgrade, Serbia*

*Institute of Physics, P. O. BOX 68, 11080 Belgrade, Serbia*

e-mail: rkostic@ipb.ac.rs

In this paper, we present results of our investigation of electronic spectra and optical properties of one-electron spherical quantum dot-quantum well (QDQW) structure. Investigated QDQW system consists of CdSe core surrounded by ZnS shell, CdSe shell and capped by material of a very high electron potential barrier compared to CdSe i.e. CdSe/ZnS/CdSe structure. Eigen energies and corresponding wave functions were calculated using effective mass approximation.

We focused to one-electron ground (1s) and the first three excited states. For allowed transitions we have calculated oscillator strengths and linear and third-order nonlinear intersubband optical absorption coefficients for various structures i.e. different CdTe core radius, ZnS shell (barrier) width and CdSe shell width. Behavior of this specific QDQW system is determined by CdSe and ZnS properties (effective masses and conductance band offset) and structure composition. Change in core and shells dimensions induces a change in electron wave function, followed by significant change in energy of state. This change in electron localization, at geometries characteristic for each state, reflects to transitions that include this state. As a result optical properties of this system are greatly dependent on the QDQW structure.

## **Comparative study of crystal field parameters and energy levels scheme for the trivalent europium ion doped in SrAl<sub>2</sub>O<sub>4</sub> and SrIn<sub>2</sub>O<sub>4</sub> spinels**

M. L. Stanciu and M. Vaida

*Faculty of Physics, West University of Timisoara, 3200223*

*Timisoara, Romania*

e-mail: stanciumarialetitia@yahoo.com

Strontium aluminate (SrAl<sub>2</sub>O<sub>4</sub>) and the indium aluminate (SrIn<sub>2</sub>O<sub>4</sub>) spinels have been proven to be efficient host materials, which offer the possibility of generating broadband emission after doping with rare earth trivalent ions [1]. By doping them with Eu<sup>3+</sup> ions, Eu<sup>3+</sup> will substitute the aluminum ions and the indium ions in the two crystals, in six fold coordination with oxygen ions; having a monoclinic site symmetry. No charge compensation is necessary.

The present work is devoted to the comparative study of the crystal field parameters (CFPs) and energy levels scheme for the trivalent europium ion doped in SrAl<sub>2</sub>O<sub>4</sub> and SrIn<sub>2</sub>O<sub>4</sub> spinels, in the frame of the superposition model of the crystal field [2]. Using the intrinsic parameters for Eu<sup>3+</sup>-O<sup>2-</sup> bonds [3-5], and the geometry structure of the each crystal, we modeled the CFP<sub>s</sub> and simulated the low-lying energy levels schemes. In order to give the reliable CFP<sub>s</sub> we made the standardization of the monoclinic H<sub>CF</sub> of each system using the relations from [6].

The obtained results are discussed and compared with the experimental data [7-9].

## REFERENCES

- [1] F.C. Palilla, A.K. Levine, M.R. Tomkus, J. Electrochem. Soc. 115, 642 (1968).
- [2] D. J. Newman, B. Ng. Rep. Prog. Phys. 52, 699 (1989).
- [3] J. Newman, Aust. J. Phys. 30, 315 (1977).
- [4] S. Vishwamittar, P. Puri, J. Chem. Phys. 61, 3720 (1974).
- [5] W. C. Zheng, H. N. Dong, S. Y. Wu, T. Sheng, Physica B 344, 103 (2004).
- [6] Czeslaw Rudowicz, J. Chem. Phys. 84 (9), 5045 (1986).
- [7] Paulo J.R. Montes, Mario E.G. Valerio, Gustavo de M. Azevedo, Nucl. Instr. and Meth. in Phys. Res. B 266, 2923 (2008).
- [8] C. E. Rodriguez-Garcia, N. Perea-Lopez, G. A. Hirata, S. P. DenBaars, J. Phys. D: Appl. Phys. 41, 092005 (2008).
- [9] Zhiping Yang, Jing Tian, Shaoli Wang, Guangwei Yang, Xu Li, Panglai Li, Materials Letters 62, 1369 (2008).

Poster Presentations – Optical Materials P.OM.19

## Phonon Eigenvectors of Graphene at High-Symmetry Points of the Brillouin Zone

V. Damljanović<sup>1</sup>, R. Kostić<sup>1</sup> and R. Gajić<sup>1</sup>

<sup>1</sup>Institute of Physics, Pregrevica 118, 11080

Belgrade, Serbia

e-mail: damlja@ipb.ac.rs

We have determined phonon eigenvectors of graphene at high symmetry points ( $\Gamma$  and K) of the Brillouin zone. For the point K we used Wigner's method of group projectors. For the  $\Gamma$  point we applied an alternative, simpler method. We compare our results with those obtained by other, more conventional methods which are published in the literature [1-3].

## REFERENCES

- [1] M.S. Dresselhaus, G. Dresselhaus, A. Jorio, Group theory, Springer Verlag, Berlin (2008).
- [2] C. Mapelli, C. Castiglioni, G. Zerbi, K. Müllen, Phys. Rev. B 60, 12710-12725 (1999).
- [3] M. Mohr, J. Maultzsch, E. Dobardžić, S. Reich, I. Milošević, M. Damnjanović, A. Bosak, M. Kirsch, C. Thomsen, Phys. Rev. B 76, 035439 (2007).

Poster Presentations – Optical Materials P.OM.20

## 3d electron transitions in Co and Ni doped MgSO<sub>3</sub>·6H<sub>2</sub>O

P. Petkova<sup>1</sup>

<sup>1</sup>Shumen University "Konstantin Preslavsky", 115 Universitetska street, 9712 Shumen, Bulgaria

e-mail: Petya232@abv.bg

Absorption spectra of magnesium sulfite hexahydrate (MgSO<sub>3</sub>·6H<sub>2</sub>O), doped with Co and Ni have been studied in the spectral region 1,46-3,82 eV. The investigations have been carried out with linear polarized light  $E\parallel c$ ,  $E\perp c$  ( $c$  is the optical axis of MgSO<sub>3</sub>·6H<sub>2</sub>O) which propagates in the direction (1210). The Co structure manifests in the spectral region 2,07-3,1 eV and the Ni structures manifest in the spectral region 1,46-3,82 eV. The peculiarities of the Jahn-Teller effect and spin-orbit interaction in dependence of the impurity ions in the crystal lattice of MgSO<sub>3</sub>·6H<sub>2</sub>O are analyzed and discussed. The electron transitions in Co<sup>2+</sup> and Ni<sup>2+</sup> ions are determined for  $E\parallel c$ ,  $E\perp c$ . The crystal field parameter  $Dq$  and Racah parameters  $B$  and  $C$  are also calculated.

## REFERENCES

- [1] G. Giorgi, G. Lyutov, L. Lyutov, Bulg. Chem. Communications 43, 236 (2011).  
[2] Zh. Bunzarov, I. Iliev, T. Dimov, P. Petkova, Ts. Kovachev, L. Lyutov, Y. Tzoukrovski, Proc. of SPIE, 7501, 75010X (2009).

Poster Presentations – Optical Materials P.OM.21

### Visible and far IR spectroscopic studies of Co doped (80-x)Sb<sub>2</sub>O<sub>3</sub>-20Na<sub>2</sub>O-xWO<sub>3</sub> glasses

P. Petkova<sup>1</sup>, M.T. Soltani<sup>2</sup>, S. Petkov<sup>1</sup>, V. Nedkov<sup>1</sup> and J. Tacheva<sup>1</sup>

<sup>1</sup>Shumen University „Konstantin Preslavsky”, 115 Universitetska street, 9712 Shumen, Bulgaria  
<sup>2</sup>Department of Physics, Faculty of sciences and engineering sciences, University of Biskra, Algeria  
e-mail:Petya232@abv.bg

We are investigated the absorption of the glasses (80-x)Sb<sub>2</sub>O<sub>3</sub>-20Na<sub>2</sub>O-xWO<sub>3</sub> (x % mol of WO<sub>3</sub>) in the spectral regions 21053-13333 cm<sup>-1</sup> and 2000-8000 cm<sup>-1</sup>. The samples are doped with 0.05 % mol of Co<sub>3</sub>O<sub>4</sub> from x = 10 % until x = 40 %. On the basis of the comparison with [1, 2, 3], the observed absorption bands are due to the Co-impurity. The absorption band of glasses in the visible spectral region does not contain information about the exactly energy position of Co-levels. Therefore, we are calculated the second derivative of absorption. It is established that Co<sup>2+</sup>-ions are surrounded by distorted tetrahedral coordination in the investigated glasses. The energy level structure of the Co<sup>2+</sup> ion in the samples is also presented. We are calculated the crystal field parameter Dq and the Racah parameters B and C.

## REFERENCES

- [1] C. Ballhausen, Introduction to Ligand Field Theory (McGraw-Hill Book Company), 339 (1964).  
[2] H. Keppler, American Mineralogist 77, 62 (1992).  
[3] A. El-Kheshen, F. El-Batal, S. Marzouk, Indian Journal of Pure & Applied Physics 46, 225 (2008).

Poster Presentations – Optical Materials P.OM.22

### EPR parameters for Co<sup>2+</sup> doped in ZnO

R. Nistora

Faculty of Physics, West University of Timisoara, 300223  
Timisoara, Romania.

e-mail: nistora\_ramona@yahoo.com

ZnO is a semiconductor with a wide band gap (3.3 eV), large exciton binding energy (60 meV), n-type conductivity, abundant in nature and environmentally friendly. These characteristics make this material attractive for many applications, such as solar cells, optical coatings, photo catalysts, electrical devices, antibacterial coatings, active medium in UV semiconductor lasers and in gas sensors [1, 2, 3]. In ZnO each Zn<sup>2+</sup> ion is tetrahedral surrounded by O ions, with a slight distortion to C<sub>3v</sub> symmetry along the c-axis of the crystal. If a Zn<sup>2+</sup> ion is substituted by a transition metal ion the electronic structure of the partly filled d shell can be described by ligand field theory for distorted tetrahedral complexes. In Td symmetry, the e orbital are lower in energy than the t<sub>2</sub> orbital [4]. The aim of this paper is to present two methods of calculation the spin Hamiltonian parameters of Co<sup>2+</sup> doped in ZnO. First method is based on the higher order perturbation and second one use the complete diagonalization of the spin-Hamiltonian of the system. I will calculate also the EPR parameters for Co<sup>2+</sup> doped in ZnO in DFT method. The results are discussed and compared with experimental data [5] and a good agreement is observed.

## REFERENCES

- [1] Pivin J.C., Socol G., Mihailescu I., Berthet P, Singh F, Patel MK, et al., 517. 916 (2008).
- [2] Sato K, Katayama-Yoshida H., Jpn. J. Appl. Phys 39, 555 (2000).
- [3] Manjula G. Nair, M. Nirmala, K. Rekha, A. Anukaliani, Materials Letters 65, 1797 (2011).
- [4] Karin Fink, Chemical Physics 326, 297 (2006).
- [5] N. Volbers, H. Zhou, C. Knies, D. Pfisterer, J. Sann, D.M. Hofmann, B.K. Meyer, Appl. Phys. A 88, 153 (2007).

Poster Presentations – Optical Materials P.OM.23

## **Vibronic interactions in excited states of $Mn^{2+}$ doped in $MF_2$ ( M = Ca, Sr, Ba) crystals**

M. Vaida

*Faculty of Physics, West University of Timisoara*

*Timisoara, Romania*

e-mail: vaida.mirela@yahoo.com

$MF_2$  (M=Ca, Sr, Ba) doped with  $Mn^{2+}$  ions have been matter of great interest because of their relevance as scintillators, phosphors and in general for understanding basic properties of the optical materials [1]. Doped crystals are attractive since  $Mn^{2+}$  occupies the cation site of the fluorite structure with eightfold coordination.

The aim of this work is to present the crystal field analysis of the  $[MF_8]^{6-}$  complex in the static and vibronic interactions in the dynamic crystal field. The modeling of the crystal field parameters and simulated energy levels scheme is presented in exchange charge [2] and superposition models [3]. The electron-phonon interaction of the bivalent manganese ion doped in  $MF_2$  was studied, using the single configurational coordination model. Some physical quantities associated with the normal vibration modes  $a_{1g}$ ,  $e_g$ , and  $t_{2g}$  of the  $[MF_8]^{6-}$  complex, coupled with electron states of  $Mn^{2+}$ , like the electron-vibration constants, the Stokes shifts, the Huang-Rhys factors and the Jahn-Teller stabilization energy were calculated. The obtained results are discussed and compared with experimental data.

## REFERENCES

- [1] B. P. Sobolev, et. al., Scintillator and phosphor materials, 348, Pittsburgh (1994).
- [2] B. Z. Malkin, in: A.A. Kaplyanskii, B. M. Macfarlane (Eds.). Spectroscopy of Solids Containing Rare-Earth Ions, North - Holland, Amsterdam, 33 (1987).
- [3] D.J. Newman, B. Ng, Rep. Prog. Phys. 52, 699 (1989).

## Electronic levels of $\text{Cr}^{2+}$ ion doped in II-VI compounds of ZnS – crystal field treatment

S. Ivaşcu and C.N. Avram

*Department of Physics, West University of Timisoara, V. Parvan 4, Timisoara 300223, Romania*  
e-mail: simonaivascu@yahoo.com

II-VI compounds are frequently studied materials since of their important applications [1], but the detailed nature of the electronic properties associated with the transition-metal ions doped in such host materials are not still understood. The aim of present paper is to report our theoretical analysis on the modeling of the crystal field parameters of  $\text{Cr}^{2+}$  doped in II-VI host matrix ZnS, ZnSe, and simulate its energy levels scheme. The fine structure of the energy levels and the Jahn-Teller interactions have been taken into account. For this, first we calculate the parameters of the free  $\text{Cr}^{2+}$  ion taken into account the fine interactions [2] and then investigated the influence of these fine interactions on the energy levels of the doped ions in above crystals. The vibronic Jahn-Teller coupling constants have been calculated in the exchange charge model of crystal field [3, 4]. The linear vibronic coupling constants are numerically calculated for each case of the Jahn-Teller interactions and all considered types such interaction are expected to give information on the new peculiarities of the absorption and emission bands, as well as of non-radiative transitions between the electronic states of impurity ions. The obtained results were discussed, compared with similar obtained results in literature and with experimental data.

### REFERENCES

- [1] S. Adachi, Properties of Semiconductor Alloys: Group-IV, III-V and II-VI Semiconductors, Wiley (2009).  
[2] A. M. Lenshin, E. N. Irinyakov, Optics and Spectroscopy 100, 368 (2006).  
[3] B. Z. Malkin, in: A.A. Kaplyanskii, B.M. Macfarlane (Eds.), Spectroscopy of Solids Containing Rare-Earth Ions, North-Holland, Amsterdam, (1987).  
[4] S. I. Klokishner, B. S. Tsukerblat, O. S. Reu, A.V. Pali, S. M. Ostrovsky, Chem.Phys., 316, 83 (2005).

## The parameters of free ions $\text{Mn}^{5+}$ and $\text{Fe}^{6+}$

E.-L. Andreici<sup>1</sup> and N.M. Avram<sup>1,2</sup>

<sup>1</sup> *Department of Physics, West University of Timisoara, V. Parvan 4, Timisoara 300223, Romania*

<sup>2</sup> *Academy of Romanian Scientists, Independentei Street 54, Bucharest 050094, Romania*

e-mail: n1m2marva@yahoo.com

In most cases, among all the interactions occurring in a free many-electron atom, only the strongest interactions are taken into account, such as the electrostatic repulsion of electrons and the spin-orbit. The analysis of the behavior of iron-group ions in crystals, using a free-ion Hamiltonian, that involves terms with only four parameters ( $B$ ,  $C$ ,  $\xi$  and  $\alpha$ ) seems to be erroneous since it is incapable of predicting correctly the levels of even a free ion [1]. Such calculations may lead to wrong conclusions concerning the crystal-field effects and the electron-phonon interaction. In this paper we present the results of calculation the parameters which characterize the free ions of  $\text{Mn}^{5+}$  and  $\text{Fe}^{6+}$  with  $3d^2$  configuration out of full shells. The effective Hamiltonian of the free ions taken into account all interactions besides the spin-orbit, the relativistic interactions spin-spin, orbit-orbit, spin-other-orbit interactions and linear correlation effect [1,2]. In such way, each from above free ions will be characterized by seven parameters:  $B, C$  (Racah),  $\xi$  (spin-orbit interaction),  $\alpha$ ,  $\beta$ , ( linear configuration

interaction) and  $M^0$ ,  $M^2$ (Marvin integrals) .The values for these parameters are obtained by fitting experimental data with the minimum value of the r m s error. The final results are discussed .

#### REFERENCES

- [1] A.M.Leushin and E.N.Irinyakov, Optics and spectroscopy 100, 326 (2006).
- [2] Î.N. Irinyakov, PhD thesis (unpublish).

Poster Presentations – Optical Materials P.OM.26

### **On the applicability of the effective medium approximation to the photoacoustic responses of multilayered structures**

A. Popovic<sup>1</sup>, Z. Soskic<sup>2</sup>, Z. Stojanovic<sup>3</sup>, D. Cevizovic<sup>3,4</sup> and S. Galovic<sup>3,4</sup>

<sup>1</sup>*IUNO-LUX NS d.o.o., Belgrade, Serbia*

<sup>2</sup>*Faculty of Mechanical Engineering Kraljevo,  
University of Kragujevac, Kraljevo, Serbia*

<sup>3</sup>*Vinca Institute of Nuclear Sciences,  
University of Belgrade, Belgrade, Serbia*

<sup>4</sup>*Joint Institute for Nuclear Research, Bogoliubov Laboratory of Theoretical Physics,  
Dubna, Russia*

e-mail: soskic.z@mfkv.kg.ac.rs

If the model of photoacoustic response of an investigated system contains many unknowns parameters, like it is the case with multilayered samples, than the inverse procedures for determination of the parameters are highly sensitive to the experimental noise. This problem cannot be solved by development of experimental setup or data acquisition, but by improvement of theoretical approach. In this paper is analyzed the applicability of the effective medium theory to the multilayered samples. It has been shown that the theory is not applicable in general. The explicit expressions for the effective values of thermal diffusivity, relaxation time, and conductivity in some special cases have been derived.

#### REFERENCES

- [1] T. Tominaga, K. Ito, Jpn. J. Appl. Phys., Part 1, 27, 2392 (1988).
- [2] A.M. Mansanares, A.C.Bento, H.Vargas, Phys.Rev.B, 42, 4477 (1995).
- [3] M.D. Dramicanin, Z.D. Ristovski, V. Djokovic, S. Galovic, Appl. Phys. Lett , 73, 321 (1998).
- [4] A. Salazar, A. Sanchez-Lavega, J.M. Terron, J. Appl. Phys., 84, 3031 (1998).
- [5] H. Hu, X. Wang, X. Xu, J. Appl. Phys., 86, 3953 (1999).
- [6] G. G. de la Cruz, Yu. G. Gurevich, Phys, Rev. B, 51, 2188 (1998).
- [7] S. Galovic, D. Kostoski, Proc. XLVII ETRAN conference, Herceg-Novi, June 8-13, (2003).
- [8] Yu.G. Gurevich, G. N. Logvin, G. G. de la Cruz, G.E. Lopez, Int. J. Therm. Sci, 42, 63 (2003).
- [9] M.Madariaga, A.Salazar, J. Appl. Phys., 101, 103534 (2008).
- [10] J. Ordenez-Miranda, J.J. Alvarado-Gill, Int. J. Therm. Sci, 48, 10 (2009).

## Interband optical absorption in a circular graphene quantum dot

M. Grujić<sup>1</sup>, M. Zarenia<sup>2</sup>, M. Tadić<sup>1</sup> and F. M. Peeters<sup>2</sup>

<sup>1</sup>*School of Electrical Engineering,  
University of Belgrade, Serbia*

<sup>2</sup>*Department of Physics, University of Antwerp,  
Antwerp, Belgium*

e-mail: marko.grujic@etf.bg.ac.rs

We present the fully analytical theory of the Dirac fermionic states in a circular graphene quantum dot. It has been established that the electron and hole states in graphene nanostructures are strongly dependent on the edge topology. For instance, for a zigzag termination in triangular and hexagonal graphene quantum dots, there arises a band of zero-energy edge-localized states [1-3]. In the present study, the Dirac-Weyl equation is solved for the case of an applied perpendicular magnetic field. We study differences between the results for zigzag and infinite-mass boundary conditions. The Landau levels are found to form due to a transition from the edge dominated confinement at low magnetic fields to the magnetic-field dominated confinement at high magnetic fields. The quantum-dot states which form the zero-energy Landau level are found to become pseudo-spin polarized for both adopted boundary conditions. However, the band of the zero-energy states appear in the energy spectrum for only the zigzag boundary condition. The differences in the electronic structure for the two boundary conditions are found to affect interband absorption spectra. As a matter of fact, much larger absorption is found for the infinite-mass boundary condition than for the zigzag boundary condition. Those differences are explained to arise from different electron-hole and intervalley symmetries for the two cases. Moreover, selection rules for interband transitions are determined and discussed.

### REFERENCES

- [1] K. Nakada, M. Fujita, G. Dresselhaus, M. S. Dresselhaus, Phys. Rev. B 54, 17954 (1996).
- [2] H. P. Heiskanen, M. Manninen, J. Akola, New J. Phys. 10, 103015 (2008).
- [3] M. Wimmer, A. R. Akhmerov, F. Guinea, Phys. Rev. B 82, 045409 (2010).

## Determination of surface minority carrier mobility in p-HgCdTe

V. Damnjanovic<sup>1</sup> and J. Elazar<sup>2</sup>

<sup>1</sup>*Faculty of Mining and Geology,  
University of Belgrade, Serbia*

<sup>2</sup>*Faculty of Electrical Engineering,  
University of Belgrade, Serbia*

e-mail: damnjanovic@rgf.bg.ac.rs

Mercury cadmium telluride ( $\text{Hg}_{1-x}\text{Cd}_x\text{Te}$ ) is a very important semiconductor material for infrared (IR) detection and infrared thermal imaging. Due to its unique properties, it has many advantages comparing to other semiconductors. It can be seen as a pseudo binary compound,  $(\text{HgTe})_{(1-x)}(\text{CdTe})_x$ , with an arbitrary proportion of components. The semiconductor bandgap can change continuously from -0.3 to 1.6 eV, depending on the parameter  $x$ , covering almost the entire IR band [1]. A variety of different photosensitive devices can be built from  $\text{Hg}_{1-x}\text{Cd}_x\text{Te}$ . However, the well-known  $\text{Hg}_{1-x}\text{Cd}_x\text{Te}$  surface (or interface with other materials, instability) can significantly influence device characteristics, so its surface passivation becomes a necessity. It seems that passivation plays a more important role as the device complexity increases.

Surface carrier mobility differs substantially from their bulk mobility [2]. It is determined by carrier scattering on phonons, charge centers and surface micro-roughnesses, all of which can be influenced by passivation process [3,4]. Operation of some semiconductor devices, like MISFETs, critically depends on minority carrier surface mobility, therefore it's investigation is important.

A special MIS sample was prepared for  $\text{Hg}_{1-x}\text{Cd}_x\text{Te}$  minority carrier surface mobility investigation. Semiconductor was a bulk grown  $\text{Hg}_{1-x}\text{Cd}_x\text{Te}$  monocrystal, with  $x = 0.215 - 0.34$ , vacancu doped with  $p \approx 10^{16} - 8 \times 10^{15} \text{ cm}^{-3}$  and with the bulk mobility of  $\mu_n \approx 250-400 \text{ cm}^2\text{V}^{-1}\text{s}^{-1}$  at 77 K. Two electrodes were deposited at different levels of MIS structure - one at the insulator layer and the other at the upper metal layer. Both electrodes are adequately biased to stop the majority carriers current. An ac voltage is applied on the electrode attached to the metal layer with the frequency  $f$  corresponding to the low frequencies  $C/V$  structure characteristics and the produced current  $J$  was measured.

$J/f$  was plotted against  $f$  and the minority carrier surface mobility  $\mu_n$  was determined from the characteristic point (second drop of the  $J/f$ ) on the obtained diagam. Values for  $\mu_n$  were in the range  $20 \times 10^3 \text{ cm}^2\text{V}^{-1}\text{s}^{-1}$  for 77 K and  $2 \times 10^3 \text{ cm}^2\text{V}^{-1}\text{s}^{-1}$  for 120 K.

We would like to thank RD&P Center „Orion“ for providing excellent experimental facilities.

#### REFERENCES

- [1] A. Rogalski, Rep. Prog. Phys. 68, 2267 (2005).
- [2] R. K. Bhan, V. Dhar, Opto-electronics review. 12, 213 (2004).
- [3] V. Damnjanovic, V. P. Ponomarenko, J. M. Elazar, Semicond. Sci.and Tech. 24, 025003 (2009).
- [4] V. Damnjanovic, V. P. Ponomarenko, J. M. Elazar, Semicond. Sci.and Tech. 22, 137 (2007).

Poster Presentations – Optical Materials P.OM.29

## Spectroscopic Ellipsometry and the Fano Resonance Modeling of Graphene Optical Parameters

A. Matković<sup>1,§</sup>, U. Ralević<sup>1,§</sup>, G. Isić<sup>1</sup>, M. Jakovljević<sup>1</sup> and R. Gajić<sup>1</sup>  
<sup>1</sup> Institute of Physics, University of Belgrade, Pregrevica 118, P.O. Box 68,  
11080 Belgrade, Serbia

<sup>§</sup> Both authors contributed equally

e-mail: amatkovic@ipb.ac.rs, uros@ipb.ac.rs

We investigate the optical response of graphene via spectroscopic ellipsometry in the UV and visible ranges. Samples are made by micromechanical exfoliation of graphenium flakes [1], and are resting on top of the Si/SiO<sub>2</sub> substrate. Graphene's dispersion relation [2,3] shows that density of states function has a logarithmic van Hove singularity corresponding to transitions at the  $M$  point of the Brillouin zone. Theoretically this results in an infinite real part of optical conductivity [4]. It manifests itself as an intense absorption in the ultraviolet part of the spectrum [5,6,7]. In the nearest-neighbor tight-binding model, this peak is symmetrical and located at around 5.2eV [8,9]. In reality the single particle model is not sufficient to describe this effect [8]. The strong electron-hole interaction present at this singularity introduces an energy downshift and asymmetry of the resonant peak. The observed excitonic resonance is explained phenomenologically with a Fano model of a strongly coupled excitonic state and a band continuum [6,7]. The parameters of this model are extracted from our spectroscopic ellipsometry measurements. The exciton binding energy is calculated as the difference between the resonant and the saddle point energies.

This work is supported by the Serbian Ministry of Science through Projects OI 171005, III 45018, and by the EU FP7 project NIM NIL (gr. a. no 228637 NIM NIL: www.nimnil.org). We are grateful to K. Novoselov and S. Anisimova for their help regarding graphene exfoliation.

## REFERENCES

- [1] K. S. Novoselov, D. Jiang, F. Schedin, T. J. Booth, V. V. Khotkevich, S. V. Morozov, A. K. Geim, Proc. Natl. Acad. Sci. U.S.A. 102, 10451 (2005).
- [2] P. R. Wallace, Phys. Rev. 71, 9 (1946).
- [3] A. H. Castro Neto, F. Guinea, N. M. R. Peres, K. S. Novoselov, A. K. Geim, Rev. Mod. Phys. 81, 109 (2009).
- [4] T. G. Pedersen, Phys. Rev. B 67, 113106 (2003).
- [5] V. G. Kravets, A. N. Grigorenko, R. R. Nair, P. Blake, S. Anissimova, K. S. Novoselov, A. K. Geim, Phys. Rev. B 81, 155413 (2010).
- [6] D.-H. Chae, T. Utikal, S. Weisenburger, H. Giessen, K. v. Klitzing, M. Lippitz, J. Smet, Nano Lett. 9, 358 (2011).
- [7] K. F. Mak, J. Shan and T. F. Heinz, Phys. Rev. Lett. 106, 046401 (2011).
- [8] L. Yang, J. Deslippe, C.-H. Park, M. L. Cohen, and S. G. Louie, Phys. Rev. Lett. 103, 186802 (2009).
- [9] T. Stauber, N. M. R. Peres and A. K. Geim, Phys. Rev. B 78, 085432 (2008).

Poster Presentations – Optical Materials P.OM.30

## Synthesis and characterization of graphene films by Hot Filament CVD

D.Stojanović, N. Woehrl and V. Buck  
*Faculty of Physics,*  
*University of Duisburg-Essen, Germany*  
e-mail: danka.etf@gmail.com

Graphene has many unique properties that make it an ideal material for researches as well as for potential applications [1]. Several approaches have been successfully developed to produce graphene. Industrial applications make it desirable to develop deposition methods that enable the deposition of graphene on large areas. In this study graphene films are deposited on copper substrate [2] by using hot filament CVD, and characterized by Raman spectroscopy which is a nondestructive technique, applied to determine the structural and electronic properties of carbon nanostructures films. Three samples of graphene on copper substrate have been produced and designated as type A, B and C, according to the preparation conditions. Experiments were conducted at temperatures 800 and 1000 °C, gas pressure of 500 Torr, and exposure times 1, 5 and 30 minutes. Raman spectroscopy was used to evaluate the quality of the graphene layers (G peak), obtain information about defects (D peak) and numbers of layers (2D peak) [3]. Relative intensity  $I(D)/I(G)$  indicates similar size of grain and similar degree of defects in all three samples and  $I(G)/I(2D)$  has average values higher than one which indicates us that it is probably few-layer graphene [4].

## REFERENCES

- [1] Zhenhua Ni, Yingying Wang, Ting Yu, Zexiang Shen, Nano Res., Vol. 1, pp. 273 (2008).
- [2] Xuesong Li, Weiwei Cai, Jinho An, Seyoung Kim, Junghyo Nah, Dongxing Yang, Richard Piner, Aruna Velamakanni, Inhwa Jung, Emanuel Tutuc, Sanjay K. Banerjee, Luigi Colombo, Rodney S. Ruoff, Science 324 (2009).
- [3] F. Molitor, D. Graf, C. Stampfer, T. Ihn, K. Ensslin, Raman Imaging and Electronic Properties of Graphene in Advances in Solid State Physics 47, Ed. R.Haug, Springer (2008).
- [4] Matthew O'Brien, Barbara Nichols, CVD Synthesis and Characterization of Graphene Thin Films, U.S. Army Research Laboratory (2010).

## Novel Design for Tunable Zeroth-Order Resonance in Epsilon-Near-Zero Channel: Theory and Experiment

M. Mitrovic and B. Jokanovic  
*Institute of Physics,  
Belgrade, Serbia  
e-mail:miranda@ipb.ac.rs*

In the past few years there has been an increased interest in metamaterials with relative dielectric permittivity close to zero (ENZ,  $\epsilon$ -near-zero metamaterials). In 2006 Silveirinha and Engheta [1] proposed the structure for energy tunneling using two parallel plate waveguides connected by a very narrow channel. They suggested that ENZ materials can improve transmission efficiency of waveguides with sharp bends or discontinuities and concentration of energy in a small subwavelength cavity. However, these theoretical studies did not take into account real losses in dielectrics and in metal plates as it was analyzed in our previous work [2].

In this work we propose a novel and simple design of  $\epsilon$ -near-zero (ENZ) channel operating in frequency range 3.95-5.85 GHz. It consists of two input foam waveguides mounted on dielectric substrate that also serves as an ENZ channel. For ENZ channel we chose a standard microwave dielectric substrate with Cu-cladding on both sides which provides precise thicknesses in the range of 0.1÷1.5 mm and a small loss tangent (0.0009 to 0.003). Waveguide sections are made from ROHACELL dielectric foam, which is easy to cut and shape.

Many papers about ENZ waveguides published so far [3-6], emphasized that frequency of energy tunnelling, i.e. zeroth-order resonance (ZOR) is independent on channel length, which is not the case with Fabry-Perot resonance. It was shown that frequency of ZOR is fixed by dielectric permittivity of the channel ( $\epsilon_{rch}$ ) and by waveguide width  $a$  ( $f_{ZOR} \cong f_{TE_0}^{ch} = c/2a\sqrt{\epsilon_{rch}}$ ).

In this paper we also propose the way how to change ZOR frequency using two longitudinal slots placed at the metallic plate of the channel (top or bottom). It is shown that position and length of the slots affect the tuning sensitivity of the channel. In a difference to orthogonal slots (placed orthogonally to wave propagation), which extensively radiate, longitudinal slots are almost non-radiative. That is the main difference between ENZ channel and classical waveguides where both type of slots radiate.

By using longitudinal slots, ZOR resonance can be changed in tuning range of 12.55% while at the same time, Fabry-Perot resonance is shifted for 10.61%. Our simulations include the real characteristics of dielectrics and metals used in ENZ channel in order to compare directly measured and simulated characteristics. Experimental measurements are expected in the near future.

### REFERENCES

- [1] M. G. Silveirinha, N. Engheta, Phys. Rev. Lett. 97, 157403 (2006).
- [2] M.Mitrović, B.Jokanović, Microwave Review 16-2, pp. 8-13 (2010).
- [3] B. Edwards, A. Alù, M. E. Young, M. G. Silveirinha, N. Engheta, Phys. Rev. Lett. 100, 033903 (2008).
- [4] R. Liu, Q. Cheng, T. Hand, J. J. Mock, T. J. Cui, S. A. Cummer, D. R. Smith, Phys. Rev. Lett. 100, 023903 (2008).

- [5] D. V. B. Murthy, A. Corona-Chávez, J. L. Olvera-Cervantes, Progress In Electromagnetics Research 15, pp 65-74 (2010).
- [6] H. Lobato-Morales, A. Corona-Chávez, D. V. B. Murthy, J. Martinez-Brito, L. G. Guerrero-Ojeda, 2010 IEEE MTT-s International Microwave Symposium Digest, pp. 1644-1647.

## Enhancement of chemical sensors based on plasmonic metamaterials utilizing metal-organic framework thin films

Z. Jakšić<sup>1</sup>, Z. Popović<sup>2</sup> and I. Djerdj<sup>3</sup>

<sup>1</sup>*Institute of Chemistry, Technology and Metallurgy,  
University of Belgrade, Serbia*

<sup>2</sup>*Department of Chemistry, Faculty of Science,  
University of Zagreb, Horvatovac 102A, 10000 Zagreb, Croatia*

<sup>3</sup>*Ruđer Bošković Institute,  
Bijenička 54, 10000 Zagreb, Croatia  
e-mail:jaksa@nanosys.ihm.bg.ac.rs*

Surface plasmon resonance-based devices belong to the most convenient and ultrasensitive label-free chemical or biological sensors. A generalization of these devices are sensors based on plasmonic metamaterials [1], where one is able to utilize the "Catalyst Plus" concept [2] to improve the adsorption of the targeted analyte. To this purpose one designs a hybride structure that simultaneously represents an ordered metal-dielectric medium with metamaterial properties and a porous medium with pores representing the building blocks of the metamaterial. Adsorption is greatly enhanced in pores owing to the large effective surface, and this in turn causes larger changes of refractive index due to the presence of adsorbed analyte, thus modulating evanescent wave propagation and facilitating chemical detection at lower levels of analyte concentration.

We chose metal-organic frameworks (MOF) as a convenient platform for metamaterial-based hybrid structures. They are a relatively recently introduced concept and represent 1D, 2D or 3D crystalline compounds, typically porous, which simultaneously contain metal ions or ion clusters and organic molecules. Their pores ensure especially large effective surface for adsorption [3]. They were also proposed for storage of different guest molecules like carbon dioxide or hydrogen [4]. The use of MOF materials for the improvement of analyte adsorption in surface plasmon resonance-based sensors was described in [5].

We considered theoretically and experimentally a strategy to enhance metamaterial-based plasmonic sensors by combining the concepts of metamaterial sensors and MOF materials. To this purpose one introduces one or more layers consisting of MOF nanocrystals into metamaterial sensor structure. The simplest approach is to use dip or drop coating of metamaterial scaffold with MOF nanocrystal emulsion. The scaffolds we investigated included metal-containing freestanding, self-supported ultrathin membranes and sandwich structures with nanoaperture arrays. Regarding materials, we investigated the applicability of four different inorganic-organic hybrid (MOF) compounds, including  $\text{VO}(\text{C}_6\text{H}_5\text{COO})_2$ ,  $\text{V}_4\text{O}_4(\text{OH})_2(\text{O}_2\text{CC}_6\text{H}_4\text{CO}_2)\cdot\text{DMF}$ ,  $\text{VO}(\text{C}_{10}\text{H}_7\text{COO})_2$   $\text{VO}(\text{C}_{14}\text{H}_9\text{COO})_2$  [6].

It is our conclusion that the preferential concentration of analytes within the MOF pores may ensure improved adsorption and thus large sensor signal enhancement compared to non-functionalized structures. In addition to that, one may obtain increased selectivity by introducing plasmonic material nanoparticles or by utilizing other functionalizing materials like catalysts or various ligands.

### REFERENCES

- [1] Z. Jakšić, S. Vuković, J. Matovic, D. Tanasković, Materials 4, 1 (2011).
- [2] Z. Jakšić, O. Jakšić, Z. Djurić, C. Kment, J. Opt. A: Pure Appl. Opt. 9 S377 (2007).

- [3] J. Rowsell, E. Spenser, J. Eckert, J.A. K. Howard, O. M. Yaghi, *Science* 309, 1350 (2005).  
[4] B. Wang, A. P. Cote, H. Furukawa, M. O'Keeffe, O. M. Yaghi, *Nature* 453, 207 (2008).  
[5] L. E. Kreno, J. T. Hupp, R. P. Van Duyne, *Anal Chem.* 82, 8042 (2010).  
[6] I. Djerdj, M. Cao, X. Rocquefelte, R. Černý, Z. Jagličić, D. Arčon, A. Potočnik, F. Gozzo, M. Niederberger, *Chem. Mater.* 21, 3356 (2009).

Poster Presentations – Metamaterials P.MM.3

## **Variable angle ellipsometry and polarized reflectometry of the fishnet metamaterials**

M. Jakovljević<sup>1</sup>, G. Isić<sup>1,2</sup>, B. Vasić<sup>1</sup>, R. Gajić<sup>1</sup>, I. Bergmair<sup>3</sup> and K. Hingerl<sup>4</sup>

<sup>1</sup>*Institute of Physics,*

*Pregrevica 118, Belgrade, Serbia*

<sup>2</sup>*School of Electronic and Electrical Engineering*

*University of Leeds, LST 9JT, United Kingdom*

<sup>3</sup>*Functional Surfaces and Nanostructures, PROFACTOR GmbH,*

*Im Stadgut A2, 4407 Steyr-Gleink, Austria*

<sup>4</sup>*Center for Surface and Nanoanalytics,*

*Johannes Kepler University, Altenbergerstr. 69, Linz, Austria*

e-mail: milka@ipb.ac.rs

The optical properties of the fishnet metamaterials in near infrared and optical frequencies were studied. The angular dependence of the polarized reflection and ellipsometric spectra were simulated and discussed. The dispersion of the surface plasmon polaritons[1,2], localized resonance at the cut-off frequencies [3] and the Wood's anomalies [2] were observed in the ellipsometric spectra. The calculated field distributions at the characteristic resonances revealed the nature of the certain modes.

This work is supported by the Serbian Ministry of Science under project No. OI171005. We also acknowledge funding by the European Community's 7th Framework Program under grant agreement no 228637 NIM\_NIL ([www.nimnil.org](http://www.nimnil.org)). I. B. and K. H. acknowledge the Austrian NANO Initiative (FFG and bmvit) for funding this work partially by the NILmeta project within the NILaustria project cluster ([www.NILaustria.at](http://www.NILaustria.at)).

### REFERENCES

- [1] T. Li, S. M. Wang, H. Liu, J. Q. Li, F. M. Wang, S. N. Zhu, X. Zhang, *J. Appl. Phys.*, 103, 023104 (2008).  
[2] R. Ortuno, C. Garcia-Meca, F. J. Rodriguez-Fortuno, J. Marti, A. Martinez, *Phys. Rev. B*, 79, 075425 (2009).  
[3] A. Mary, S. G. Rodrigo, F. J. Garcia-Vidal, L. Martin-Moreno, *Phys. Rev. Lett.*, 101, 103902 (2008).

## Modeling of tunneling times in anisotropic nonmagnetic metamaterials

I. Ilić<sup>1</sup>, P.P.Beličev<sup>1</sup>, J. Radovanović<sup>2</sup>, V. Milanović<sup>2</sup> and Lj. Hadžievski<sup>1</sup>

<sup>1</sup>*Vinča Institute of Nuclear Sciences,  
Belgrade, Serbia*

<sup>2</sup>*School of Electrical Engineering,  
University of Belgrade, Serbia  
e-mail:igori@vin.bg.ac.rs*

The effects of electromagnetic wave tunneling through a low-refractive-index barrier have received much attention in recent years. Part of this attention is focused on calculating times needed for the electromagnetic wave to tunnel through such barrier. Most widely used tunneling times are dwell time, which is related to electromagnetic energy propagation through the barrier, and group delay, which is related to the wave phase propagation. So far, these tunneling times have been calculated for linear non-absorptive non-dispersive [1], linear absorptive dispersive [2], nonlinear non-absorptive non-dispersive [3] and nonlinear absorptive dispersive materials [4]. Also, impact of the Goos-Hänchen shift on these times has been calculated [5].

In this paper, we present theoretical and numerical research on tunneling times in anisotropic media. We derive expressions for calculating tunneling times in layered periodic material, which expresses anisotropic properties due to its structure. Numerical calculations of these expressions have been performed on new type of anisotropic metamaterial [6], showing strong impact of anisotropy on tunneling times through such structure.

### REFERENCES

- [1] H. G. Winful, *Phys. Rev. E* 68, 016615 (2003).
- [2] I. Ilić, P. P. Beličev, V. Milanović, J. Radovanović, *J. Opt. Soc. Am. B* 25, 1800 (2008).
- [3] G. Isić, V. Milanović, J. Radovanović, Z. Ikonić, D. Indjin, P. Harrison, *Phys. Rev. A* 77, 033821 (2008).
- [4] P. P. Beličev, I. Ilić, V. Milanović, J. Radovanović, Lj. Hadžievski, *Phys. Rev. A* 80, 023821 (2009).
- [5] I. Ilić, P. P. Beličev, V. Milanović, J. Radovanović, Lj. Hadžievski, *Phys. Lett. A* 375, 1357 (2011).
- [6] A. J. Hoffman, L. Alekseyev, S. S. Howard, K. J. Franz, D. Wasserman, V. A. Podolskiy, E. E. Narimanov, D. L. Sivco, C. Gmachl, *Nat. Mater.* 6, 946 (2007).

## Mid-infrared semiconductor metamaterials utilizing intersubband transitions in quantum cascade laser structure

S. Ramović, J. Radovanović and V. Milanović

<sup>1</sup>*School of Electrical Engineering,*

*University of Belgrade, Serbia*

e-mail: sabina\_ramovic@yahoo.com

The enormous interest in metamaterials originates from the possibility of engineering the effective medium parameters (permeability and permittivity) and thus controlling the transmission and the reflection of impinging electromagnetic waves in a prescribed manner. Motivation for analyzing this type of materials lies in the fact that the majority of proposed and experimentally demonstrated metamaterials is based on metallic inclusions and exhibit high optical losses which are detrimental to their performance and limit the applicability [1-3]. One of the major challenges at present is to reduce the optical losses [1-5] and a promising research directions involves trying to compensate the losses by adding gain, i.e. designing active metamaterials. The idea is to replace metallic components by low-dimensional semiconductor quantum structures, such as quantum cascade laser or quantum amplifier, where substantial gain may be achieved via carrier injection [1,2,6,7]. This would enable all-semiconductor metamaterial realization, which relies on using the well established technology of epitaxial growth and incorporation into existing optical semiconductor devices. Particular attention is paid to the left-handed materials, also called negative-refraction media, since the directions of energy flow and the phase velocity are opposite therein, leading to unusual properties described by a negative index of refraction [3].

We have analyzed metamaterials made of very thin semiconductor layers, whose composition corresponds to GaAs/AlGaAs quantum cascade laser, placed in a very strong external magnetic field (15T – 40T) to maximize the optical output. The role of the magnetic field is to assist the attainment of sufficient population inversion, necessary to effectively manipulate the permittivity. By discretizing the in-plane electron motion, external magnetic field influences all the relevant relaxation processes in the structure [8-10]. This enables one to control and to tune the value of the complex dielectric permittivity so to fulfill the negative refraction conditions [11]. Apart from illustrating the influence of magnetic field magnitudes on the permittivity and metamaterial's features, effects of varying electron surface densities and the operating temperature have been presented as well.

### ACKNOWLEDGEMENTS

This work was supported by the Ministry of Science (Republic of Serbia), ev. no.III 45010.

### REFERENCES

- [1] P. Ginzburg, M. Orenstein, J. Appl. Phys. 104, 063513 (2008).
- [2] P. Ginzburg, M. Orenstein, J. Appl. Phys. 103, 083105 (2008).
- [3] V. M. Shalaev, Nat. Photonics 1, 41 (2007).
- [4] J. B. Pendry, Opt. Express 11, 755 (2003).
- [5] C. M. Soukoulis, S. Linden, M. Wegener, Science 315, 47 (2007).
- [6] J. Faist, F. Capasso, D. L. Sivco, C. Sirtori, A. L. Hutchinson, A. Y. Cho, Science 264, 553 (1994).
- [7] C. Gmachl, F. Capasso, D. L. Sivco, A. Y. Cho, Rep. Prog. Phys. 64, 1533 (2001).
- [8] J. Radovanović, A. Mirčetić, V. Milanović, Z. Ikonić, D. Indjin, P. Harrison, R.W. Kelsall, Semicon. Sci. Technol. 21, 215 (2006).
- [9] J. Radovanović, V. Milanović, Z. Ikonić, D. Indjin, P. Harrison, J. Appl. Phys. 97, 103109 (2005).
- [10] A. Daničić, J. Radovanović, V. Milanović, D. Indjin, Z. Ikonić, J. Phys. D: Appl. Phys. 43, 045101 (2010).
- [11] V.A.Podolskiy, E. E.Narimanov, Phys. Rev B 71, 201101R (2005).

**Angular-dependent excitation of longitudinal surface plasmon polaritons in gold nanowires**

O. A. Yeshchenko<sup>1\*</sup>, I. M. Dmitruk<sup>1</sup> and Y. Barnakov<sup>2</sup>

<sup>1</sup> *Physics Department, National Taras Shevchenko Kyiv University, Kyiv, Ukraine*

<sup>2</sup> *Norfolk State University, Norfolk, USA*

e-mail: yes@univ.kiev.ua

Extinction spectra of parallel gold nanowires (diameter – 28 nm, length – 9  $\mu\text{m}$ ) in porous alumina were studied in spectral range of 360 – 1200 nm. The spectra were measured at various angles of incidence  $\theta$  of exciting light beam. Here,  $\theta$  is the angle between the propagation direction of exciting beam and the axis of nanowire.

The extinction spectra contain two bands. First, T-band is caused by the excitation of the transversal oscillations of the free electrons, i.e. longitudinal surface plasmon (SP) mode in Au nanowire. Second, L-band is caused by longitudinal surface plasmon modes of nanowire. The spectral position of L-band changes non-monotonically with  $\theta$ : it red shifts at the increase of  $\theta$  from 0 to 30<sup>0</sup> and blue shifts at the increase of  $\theta$  from 30 to 70<sup>0</sup>. The bandwidth changes with change of  $\theta$  non-monotonically as well: it has maximum at  $\theta = 30^0$ , and has smaller values at lower and higher incidence angles.

The longitudinal surface plasmon modes in long metallic nanowires have the character of surface plasmon polaritons (SPP) propagating along the axis of nanowire. SPPs are reflected from the ends of the nanowire, and the standing SPP waves arise. Thus, the nanowire acts as optical resonator. The theoretical calculations show that  $\theta = 30^0$  is the angle at which the most efficient excitation of the longitudinal SPP occurs. At this condition the axial SPPs are excited that propagate along the nanowire axis. This mode has lowest energy and damping. At other angles of incidence the non-axial SPP modes are excited that propagate angle-wise to wire axis. Non-axial modes have the higher energies and damping that explains the observed dependencies of L-band characteristics on  $\theta$ .

## Size and temperature dependence of the surface plasmon resonance in silver nanoparticles

O. A. Yeshchenko<sup>1\*</sup>, I. M. Dmitruk<sup>1</sup>, A. A. Alexeenko<sup>2</sup>,  
A. V. Kotko<sup>3</sup>, J. Verdal<sup>4</sup> and A. O. Pinchuk<sup>4</sup>

<sup>1</sup> *Physics Department, National Taras Shevchenko Kyiv University,  
2/1 Akademik Glushkov prosp., 03127 Kyiv, Ukraine*

<sup>2</sup> *Laboratory of Technical Ceramics and Silicates, Gomel State Technical University,  
48 October prosp., 246746 Gomel, Belarus*

<sup>3</sup> *I.M. Frantsevich Institute for Problems of Materials Science, 3 Krzhizhanovsky str., 03680 Kyiv, Ukraine*

<sup>4</sup> *Department of Physics and Energy Sciences, University of Colorado at Colorado Springs,  
1420 Austin Bluffs Pkwy, Colorado Springs, Colorado 80933, USA  
e-mail: yes@univ.kiev.ua*

The dependences of the surface plasmon energy were studied for silver nanoparticles in the size range 11–30 nm and in the temperature interval 293–650 K.

The energy of SPR in silver nanoparticles embedded in silica glass host matrix depends on the size and the temperature of the nanoparticles. Our experiments exhibit the nonlinear red shift of the SPR as the size of the nanoparticles decreases. The increase of the surface scattering rate of the free electrons causes the red shift of the SPR energy as the particle size decreases.

As the temperature of the sample increases, the SPR red shifts. The volume thermal expansion of the nanoparticles leads to red shift of the SPR. As the temperature of the particle increases, the volume of the nanoparticle increases and the density of the free electrons decreases. The lower electron density leads to the lower plasma frequency of the electrons and subsequently to the red shift of the SPR. The red shift of SPR with the increase of temperature is linear for large (25 nm and 30 nm) silver nanoparticles and becomes nonlinear (superlinear) for smaller nanoparticles (17 nm, 11 nm). The nonlinearity of the dependence of SPR energy on temperature becomes stronger for smaller nanoparticles (17 nm, 11 nm). These two effects can be rationalized by the dependence of the coefficient of the volume thermal expansion on the size and temperature of the nanoparticles. The coefficient of the volume thermal expansion increases when the nanoparticle size decreases and with the increase of the temperature of the nanoparticle.

Spill-out and electronic environmental effects were considered as possible mechanisms of the shift of SPR as the temperature and size of the nanoparticles changes. The calculations of the SPR shift caused by these two effects show that it is negligibly small.

## Tunable two-dimensional plasmonic crystals with semiconductor rods

B. Vasić and R. Gajić

*Institute of Physics, University of Belgrade, Pregrevica 118, P. O. Box 68,  
11080 Belgrade, Serbia  
e-mail: bvasic@ipb.ac.rs*

We theoretically investigate tunable two-dimensional plasmonic crystals with semiconductor rods at terahertz frequencies. The tuning of the plasmonic crystals is achieved by changing charge carrier concentration in the rods [1], [2]. In this way, it is possible to achieve either tunable photonic band-gaps [3] or tunable effective refractive index [4]. The tunable photonic band-gaps arise due to the localized plasmonic resonances in individual rods when electric field is normal to them or due to negative effective permittivity when the electric field is parallel to the rods. The tunable effective refractive index can be obtained within allowed bands. This is applied to graded plasmonic crystals for the implementation of tunable gradient refractive index structures.

### REFERENCES

- [1] P. Halevi, F. Ramos-Mendieta, Phys. Rev. Lett. 85, 1875 (2000).
- [2] C.-S. Kee, H. Lim, Phys. Rev. B 64, 121103(R) (2001).
- [3] J. Leon, T. Taliercio, Phys. Rev. B 82, 195301 (2010).
- [4] M. D. Goldflam, T. Driscoll, B. Chapler, O. Khatib, N. Marie Jokerst, S. Palit, D. R. Smith, H.-T. Kim, M. Di Ventra, D. N. Basov, arXiv:1103.5729v1 (2011).

## Hotspot Decorations for Metamaterial Arrays of Plasmonic Structures

V. K. Valev<sup>1</sup>, A. V. Silhanek<sup>2</sup>, Y. Jeyaram<sup>2</sup>, D. Denkova<sup>2</sup>, B. De Clercq<sup>3</sup>, W. Gillijns<sup>2</sup>, V. Petkov<sup>4</sup>,  
O. A. Aktsipetrov<sup>5</sup>, M. Ameloot<sup>3</sup>, V. V. Moshchalkov<sup>2</sup> and T. Verbiest<sup>1</sup>

<sup>1</sup> *Molecular Electronics and Photonics, INPAC, Katholieke Universiteit Leuven, Celestijnenlaan 200 D, B-3001 Leuven, Belgium.*

<sup>2</sup> *Nanoscale Superconductivity and Magnetism, Pulsed Fields Group, INPAC, Katholieke Universiteit Leuven, Celestijnenlaan 200 D, B-3001 Leuven, Belgium.*

<sup>3</sup> *University Hasselt and transnational University Limburg, BIOMED, Agoralaan building C, B-3590 Diepenbeek, Belgium.*

<sup>4</sup> *Dept. Metallurgy and Materials Engineering, Katholieke Universiteit Leuven, Kasteelpark Arenberg 44, B-3001, Leuven, Belgium.*

<sup>5</sup> *Department of Physics, Moscow State University, 11992 Moscow, Russia.  
e-mail: v.k.valev@fys.kuleuven.be*

In the past ten years, a new class of materials has emerged and it has attracted a lot of attention due to its counterintuitive optical behavior and revolutionary potential applications – metamaterials. Metamaterials are materials engineered for displaying unusual electromagnetic properties and they have been associated with negative refractive index [1, 2], invisibility [3], light-based nanocircuits [4-6], etc. Most of these spectacular phenomena are based on surface plasmon resonances – the property whereby, in metallic nanostructures, light can collectively excite the electron population at surfaces. However, in mapping the plasmonic patterns on the surfaces of nanostructures, the diffraction limit of light remains an important obstacle. Here we demonstrate that this limit can essentially be removed. We have studied nanostructures made of nickel and palladium, deposited by electron beam lithography in different geometrical patterns, including the G-shaped design that we proposed previously [7-10]. We show that, upon illuminating nanostructures, the resulting surface plasmon pattern is imprinted on the structures themselves allowing for subsequent imaging with Scanning Electron Microscopy and

Atomic Force Microscopy (AFM). The resulting resolution of plasmon pattern imaging can therefore, in principle, be brought down to that of the AFM. Our results open a new avenue for studying plasmonic patterns at the nanoscale [11].

This work is supported by FWO, VAP projects and Methusalem Program by the Flemish Government.

#### REFERENCES

- [1] V.G. Veselago, *Sov. Phys. Usp.*, 10, 4, 509 (1968).
- [2] R.D. Smith, J.B. Pendry, M.C.K. Wiltshire, *Science*, 305, 788 (2004).
- [3] D. Schurig, et al., *Science*, 314, 977 (2006).
- [4] N. Engheta, A. Salandrino, A. Alù, *Phys. Rev. Lett.*, 95, 095504 (2005).
- [5] N. Engheta, *Science*, 317, 1698 (2007).
- [6] C. Walther, et al., *Science*, 327, 1495 (2010).
- [7] V. K. Valev, et al., *Nano Lett.*, 9, 3945 (2009).
- [8] V. K. Valev, et al., *Phys. Rev. Lett.*, 104, 127401 (2010).
- [9] V. K. Valev, et al., *Opt. Express* 18, 8286-8293 (2010).
- [10] V. K. Valev, et al., *ACS Nano*, 5, 91-96 (2011).
- [11] V. K. Valev, et al., *Phys. Rev. Lett.*, in press (2011).

## *Nonlinear Optics*

Poster Presentations – Nonlinear Optics P.NO.1

### **Plateau structures in laser-assisted and laser-induced processes**

A. Čerkić<sup>1</sup>, M. Busuladžić<sup>2</sup>, E. Hasović<sup>1,3</sup>, A. Gazibegović-Busuladžić<sup>1</sup>,  
D. B. Milošević<sup>1,3</sup> and W. Becker<sup>3</sup>

<sup>1</sup>*Faculty of Science, University of Sarajevo, Zmaj od Bosne 35, 71000 Sarajevo, Bosnia and Herzegovina*

<sup>2</sup>*Medical Faculty, University of Sarajevo, Čekaluša 90, 71000 Sarajevo, Bosnia and Herzegovina*

<sup>3</sup>*Max-Born Institut, Max-Born Strasse 2a, 12489 Berlin, Germany*

e-mail: mustafabusuladzic@bih.net.ba

Different nonlinear processes can occur when atoms or molecules are exposed to an intense laser field [1, 2]. Generally, these processes can be categorized into two main groups: laser-assisted processes and laser-induced processes [1]. In the first group belong phenomena, which can occur without influence of a laser field. The presence of a strong laser field enriches the structure of their characteristic spectra [3]. On the other hand, the laser-induced processes can happen only in the presence of a laser field and they usually require a threshold value of the number of absorbed laser photons. In this paper we are interested in two processes: laser-assisted electron-atom scattering (LAS) and high-order above-threshold ionization (HATI). Their electronic spectra are characterized by two plateaus. The first plateau is due to direct scattering (ionization), where the scattered (ionized) electron goes directly to the detector. The second plateau is a consequence of the rescattering, since the laser field may drive a previously scattered (ionized) electron back to its atom (parent ion). Finally, the rescattered electrons can be accelerated to high energies. The plateaus manifest themselves as broad ranges of the energy spectrum in which the photoelectron yield is practically constant. On the high energy end, these ranges are terminated by abrupt cutoffs.

We present quantum-mechanical LAS theory and show how the rescattering effects can be described within the second Born approximation [3]. Also, we will use two versions of the atomic (molecular) strong-field approximation (SFA) in order to describe HATI process [4-8]. In the improved strong-field approximation (ISFA), which describes HATI, the rescattering of the ionized electron on the

parent ion is described within the first-order Born approximation. More recently, we have introduced the low-frequency approximation (LFA) for atomic HATI [5] as well as for molecular HATI in few-cycle laser pulses. In the LFA theory the first-order Born approximation for the elastic rescattering amplitude is replaced by the exact scattering amplitude taken on the energy shell. Our theory is in good agreement with available experimental data for atomic (molecular) HATI with long [8, 9] and ultrashort laser pulses.

Sponsorship has been provided by the Alexander von Humboldt Foundation and funding by the German Federal Ministry of Education and Research in the framework of the Research Group Linkage Programme.

#### REFERENCES

- [1] D. B. Milošević, F. Ehlotzky, *Adv. At., Mol., Opt. Phys.* 49, 373 (2003).
- [2] M. Lein, *J. Phys. B* 40, R135 (2007).
- [3] A. Čerkić, D. B. Milošević, *Phys. Rev. A* 75, 013412 (2007).
- [4] M. Okunishi, T. Morishita, G. Prümper, K. Shimada, C. D. Lin, S. Watanabe, K. Ueda, *Phys. Rev. Lett.* 100, 143001 (2008).
- [5] Z. Chen, A. T. Le, T. Morishita, C. D. Lin, *Phys. Rev. A* 79, 033409 (2009).
- [6] A. Čerkić, E. Hasović, D. B. Milošević, W. Becker, *Phys. Rev. A* 79, 033413 (2009).
- [7] M. Busuladžić, A. Gazibegović-Busuladžić, D. B. Milošević, W. Becker, *Phys. Rev. Lett.* 100, 203003 (2008); *Phys. Rev. A* 78, 033412 (2008).
- [8] D. B. Milošević, W. Becker, M. Okunishi, G. Prümper, K. Shimada, K. Ueda, *J. Phys. B* 43, 015401 (2010).
- [9] M. Okunishi, R. Itaya, K. Shimada, G. Prümper, M. Busuladžić, A. Gazibegović-Busuladžić, D. B. Milošević, W. Becker, *Phys. Rev. Lett.* 103, 043001 (2009).

Poster Presentations – Nonlinear Optics      P.NO.2

### **Ellipticity dependence of the plateau structures in different atomic and molecular processes in strong laser field**

A. Čerkić<sup>1</sup>, M. Busuladžić<sup>2</sup>, E. Hasović<sup>1,3</sup>, A. Gazibegović-Busuladžić<sup>1</sup>,  
S. Odžak<sup>1</sup> and D. B. Milošević<sup>1,3</sup>

<sup>1</sup>*Faculty of Science, University of Sarajevo, Zmaj od Bosne 35, 71000 Sarajevo, Bosnia and Herzegovina*

<sup>2</sup>*Medical Faculty, University of Sarajevo, Čekaluša 90, 71000 Sarajevo, Bosnia and Herzegovina*

<sup>3</sup>*Max-Born Institut, Max-Born Strasse 2a, 12489 Berlin, Germany*

e-mail: mustafabusuladzic@bih.net.ba

The study of atomic and molecular processes in strong fields has attracted a lot of attention during last decades (see the recent reviews [1-3] and references therein). Particular attention has been devoted to high-order laser-induced processes: high-order harmonic generation (HHG) and high-order above-threshold ionization (HATI). These phenomena can occur only in the presence of a strong laser field. They are of great interest for deeper understanding of the laser-matter interaction. Both of them can be described using the so-called three-step model. In the first step, atom or molecule is ionized. During this process the irradiated system absorbs more photons than is necessary for ionization. This is the so-called above-threshold ionization (ATI). In the second step, the electron is driven back by the laser field and revisits its parent atomic (molecular) ion. For the HHG process, in the third step, the electron recombines with the parent ion and a high-energy photon is emitted, while for HATI the laser driven electron backscatters off the parent ion and can be accelerated to high energies.

There are also processes, which can occur without the influence of the laser field. The presence of a strong laser field enriches the structure of their characteristic spectra [4]. One of them is the laser-assisted electron-atom scattering (LAS). All mentioned phenomena are characterized by a plateau

which finishes by an abrupt cutoff. In the most papers different processes were investigated in a linearly polarized field. In the last few years some exciting features of the spectra of different processes in an elliptically polarized laser field were found [5, 6].

In this paper we present an appropriate quantum-mechanical theory in order to describe laser-induced and laser-assisted processes with emphasis on elliptically polarized strong laser field [7-9]. The features of the high-energy regions of spectra and their cutoffs are analyzed in detail for different values of ellipticity, laser intensities and various atomic and molecular species.

Sponsorship has been provided by the Alexander von Humboldt Foundation and funding by the German Federal Ministry of Education and Research in the framework of the Research Group Linkage Programme.

#### REFERENCES

- [1] A. Becker and F. H. M. Faisal, *Adv. At., Mol., Opt. Phys.* 38, R1-R56 (2005).
- [2] M. Lein, *J. Phys. B: Adv. At., Mol., Opt. Phys.* 40, R135-R173 (2007).
- [3] C. D. Lin, A.T. Le, Z. Chen, T. Morishita, R. R. Lucchese, *J. Phys. B* 43, 122001 (2010).
- [4] A. Čerkić, D. B. Milošević, *Phys. Rev. A* 75, 013412 (2007).
- [5] T. Kanai, S. Minemoto, H. Sakai, *Phys. Rev. Lett.* 98, 053002 (2007).
- [6] X. Zhou, R. Lock, W. Li, N. Wagner, M. M. Murnane, H. C. Kapteyn, *Phys. Rev. Lett.* 100, 073902 (2008).
- [7] M. Busuladžić, A. Gazibegović-Busuladžić, D. B. Milošević, *Phys. Rev. A* 80, 013420 (2009); *Laser Phys.* 20, 1001 (2010).
- [8] S. Odžak, D. B. Milošević, *Phys. Rev. A* 82, 023412 (2010); *J. Phys. B* 44, 125602 (2011).
- [9] A. Čerkić et al., (in preparation)

Poster Presentations – Nonlinear Optics P.NO.3

### **Ionization rate for circularly polarized laser fields with modified ionization potential included**

J.M. Stevanović, T.B. Miladinović, M.M. Radulović and V.M. Ristić  
*Department of Physics, Faculty of Science, Kragujevac University,*  
*Kragujevac, Serbia*  
e-mail: jasnas@kg.ac.rs

During the ionization of atoms with low-frequency laser fields, the tunneling ionization occurs for values of Keldysh parameter  $\gamma \ll 1$ . One of the most used theories is ADK (Ammosov-Delone-Krainov) theory, which was developed both for linearly and circularly polarized laser fields. Here is examined the influence of modified ionization potential on ionization rate in ADK theory for the case of circularly polarized laser field. The studied atoms are K, Na, Li and Cs; they are ionized by CO<sub>2</sub> laser in the intensity regime between  $10^{14}$  W / cm<sup>2</sup> and  $10^{16}$  W / cm<sup>2</sup>. It is found that ionization rates of atoms with similar values of ionization potential behave in similar manner; also, the influence of modified ionization potential on ionization rates is much stronger as laser intensities increase.

#### REFERENCES

- [1] L.V. Keldysh, *Sov. Phys. JETP* 20, 1307 (1965).
- [2] A.M. Perelomov, V.S. Popov, M.V. Terent'ev, *Sov. Phys. JETP* 23, 924 (1966).
- [3] V.M. Ammosov, N.B. Delone, V.P. Krainov, *Sov. Phys. JETP* 64, 1191 (1986).
- [4] N.B. Delone, V.P. Krainov, *Physics-Uspekhi* 41, 469 (1998).
- [5] V.M. Ristić, T.B. Miladinović, M.M. Radulović, *APP A* 116, 504 (2009).
- [6] D. Bauer, *Phys. Rev. A* 55, 2180 (1997).

- [7] E. Gubbini, Multiple Ionization of Heavy Atoms in Super Strong Laser Fields, PhD dissertation (2004).  
 [8] D. Bauer, Theory of Laser-Matter Interaction, Max-Planck Institute, Heidelberg (2002).  
 [9] L.D. Landau, E.M. Lifshitz, Quantum Mechanics: Non-Relativistic Theory, 3<sup>rd</sup> ed. Butterworth-Heinemann, London, (1991).  
 [10] A.S. Kornev, E.B. Tulenko, B.A. Zon, Phys. Rev. A 68, 043414 (2003).  
 [11] V.M. Ristić, T.B. Miladinović, J.M. Stevanović, APP A 119, 761 (2011).

Poster Presentations – Nonlinear Optics P.NO.4

## The energy of maximum number of photoelectrons during ionization of potassium and xenon atoms

T.B. Miladinović, J.M. Stevanović, M.M. Radulović and V.M. Ristić  
*Department of Physics, Faculty of Science, Kragujevac University,*  
*Kragujevac, Serbia*  
 e-mail: tanja.miladinovic@gmail.com

Two formulas for energy at which the maximum number of ejected photoelectrons is detected are examined; one is  $E_{\max}$  with non-zero momentum included in both exponent and pre-exponent part of expression, and the other is  $E_{\max \text{ App}}$  which represents a previous formula, but approximated for higher intensity laser fields. It is analyzed which formula gives the numerical values closest to the experimental values obtained in this area of research, concerning tunnel ionization of K and Xe atoms by linearly polarized laser fields.

It is found that formula  $E_{\max}$  gives satisfactory results in a wide range of laser field intensities, for both atoms; for intensity  $4 \times 10^{12} \text{ W/cm}^2$  it is  $E_{\max} = 9.046 \text{ eV}$  in the case of potassium atom. Also, for Xe atom,  $E_{\max}$  appears at intensity  $5 \times 10^{13} \text{ W/cm}^2$ , while in experiment it was determined that this value occurs at  $7.5 \times 10^{13} \text{ W/cm}^2$ . Formula for  $E_{\max \text{ App}}$  is applicable for higher laser intensities; it is also consistent with one for  $E_{\max}$  at range of field intensities  $10^{15} - 10^{16}$ .

### REFERENCES

- [1] L.V. Keldysh, Sov. Phys. JETP 20, 1307 (1965).  
 [2] M.V. Ammosov, N.B. Delone, V.P. Krainov, Sov. Phys. JETP 64, 1191 (1986).  
 [3] V.P. Krainov, W. Xiong, S.L. Chin, Laser Phys. 2, 467 (1992).  
 [4] W. Xiong, S.L. Chin, Sov. Phys. JETP 99, 481 (1991).  
 [5] A.M. Perelomov, V.S. Popov, Sov. Phys. JETP 25, 336 (1967).  
 [6] S.L. Chin, G. Farkas, F. Yergeau, J. Phys. B 16, L223 (1983).  
 [7] F. Yergeau, S.L. Chin, P. Lavigne, J. Phys. B: At. Mol. Phys. 20, 723 (1987).  
 [8] W. Xiong, F. Yergeau, S.L. Chin, P. Lavigne, J. Phys B: At. Mol. Opt. Phys. 21, L159 (1998).  
 [9] S. Augst, D. Strickland, D.D. Meyerhofer, S.L. Chin, J.H. Eberly, Phys. Rev. Lett. 63, 2212 (1989).  
 [10] V.P. Krainov, V.M. Ristić, Zh. Eksp. Teor. Fiz. 101, 1479 (1992).  
 [11] N.B. Delone, I.Yu. Kiyan, V.P. Krainov, Laser Phys. 3, 312 (1993).

## Electric field effects on $D^0$ binding energies in CdTe/ZnTe spherical quantum dot

D. Stojanović and R. Kostić

*University of Belgrade, Serbia*

*Institute of Physics, P. O. BOX 68, 11080 Belgrade, Serbia*

e-mail:dusanka@ipb.ac.rs

Binding energy of neutral ( $D^0$ ) hydrogenic impurity located at the center of the CdTe/ZnTe spherical quantum dot in the external electric field has been investigated.

Calculations for the case without field are performed under the effective mass approximation on the basis of exact solution of the Schrödinger and Poisson equations. Eigenfunctions are expressed in terms of the Whittaker and Coulomb wave functions. Results for  $D^0$  impurity energies of ground  $1s$ , and excited  $2p$  states strongly depend on CdTe/ZnTe QD size if QD radius is less than one effective Bohr radius.

Stark shift energy levels and their wave functions in external electric field were determined based on variational calculations scheme within the effective mass approximation. The results show the hydrogenic impurity binding energy dependence on the dot radius and the external electric field strength.

### REFERENCES

[1] M. Kirak, S. Yılmaz, M. Sahin, M. Gencaslan, J. App. Phys. 109, 094309 (2011).

## Interface soliton complexes in system with one-site linked two-dimensional lattices

M. D. Petrović<sup>1</sup>, G. Gligorić<sup>1,2</sup>, A. Maluckov<sup>3</sup>, Lj. Hadzievski<sup>1</sup> and B. A. Malomed<sup>4</sup>

<sup>1</sup>*Vinca Institute of Nuclear Sciences, Belgrade, Serbia*

<sup>2</sup>*Max-Planck-Institut für Physik komplexer Systeme, Dresden, Germany*

<sup>3</sup>*Faculty of Sciences and Mathematic, University of Niš, Serbia*

<sup>4</sup>*School of Electrical Engineering, Faculty of Engineering, Tel Aviv University, Israel*

e-mail: marijap@vinca.rs

Formation, stability and dynamical properties of the soliton complexes formed of fundamental solitons pinned at linkage site in the system with one-site coupled two-dimensional lattices are investigated. The system can be realized in terms of Bose-Einstein condensates, and may occur in a range of artificially built discrete nonlinear media. The model of wave propagation in the system is extension of the previously established one [1] which accounts local modification of the potential of the lattices caused by the inter-lattice coupling between the linked sites. This is mathematically described by the system of the discrete nonlinear Schrödinger equations:

$$\begin{aligned} i d\varphi_{n,m}/dt + \varphi_{n+1,m} + \varphi_{n-1,m} + \varphi_{n,m+1} + \varphi_{n,m-1} - 4\varphi_{n,m} + \varepsilon\psi_{n,m}\delta_{n,0}\delta_{m,0} + |\varphi_{n,m}|^2 \varphi_{n,m} &= \zeta\varphi_{n,m}\delta_{n,0}\delta_{m,0} \\ i d\psi_{n,m}/dt + \psi_{n+1,m} + \psi_{n-1,m} + \psi_{n,m+1} + \psi_{n,m-1} - 4\psi_{n,m} + \varepsilon\varphi_{n,m}\delta_{n,0}\delta_{m,0} + |\psi_{n,m}|^2 \psi_{n,m} &= \zeta\psi_{n,m}\delta_{n,0}\delta_{m,0} \end{aligned}$$

written here in rescaled form, where coefficient  $\zeta$  accounts for the additional local potential acting at the linkage sites. The last is proposed to be of the order of the inter-site coupling parameter  $\varepsilon$ .

We study consequences of the additional feedback effect on the properties of the interface soliton complexes. This is quantitatively measured by the ratio between coefficients  $\zeta$  and  $\varepsilon$ . The main goal is to see if the modification of the lattice coupling at the linkage sites reflects on the symmetry breaking, which was previously discovered in the system formed of two locally linked two-dimensional lattices. We use the variation approximation and numerical methods [1] to find the parameter regions of existence and stability of the localized symmetric, asymmetric and antisymmetric soliton complexes pinned to the linkage site.

The spontaneously symmetry-breaking pitchfork bifurcation of the supercritical type is found, which destabilizes the symmetric complexes and simultaneously creates stable asymmetric ones, as well as the areas of the bistability between the antisymmetric modes and either symmetric or asymmetric ones. The bifurcation parameter values and boundaries of the bistability area depend on the ratio between coefficients  $\zeta$  and  $\varepsilon$ , but the properties of the soliton complexes will not be qualitatively affected by the additional effect.

#### REFERENCES

[1] M. D. Petrović, G. Gligorić, A. Maluckov, Lj. Hadžievski, B. A. Malomed, submitted to PRE.

Poster Presentations – Nonlinear Optics P.NO.7

### **Complexes of fundamental interface solitons in one-site coupled one-dimensional trilete lattices**

M. Stojanović-Krasić<sup>1</sup>, A. Maluckov<sup>1</sup>, Lj. Hadžievski<sup>2</sup> and B. A. Malomed<sup>3</sup>

<sup>1</sup> *Faculty of Sciences and Mathematics, Niš, Serbia*

<sup>2</sup> *Vinca Institute of Nuclear Sciences, Belgrade, Serbia*

<sup>3</sup> *School of Electrical Engineering, Faculty of Engineering, Tel Aviv University, Israel*  
e-mail: marijastojanovickrasic@gmail.com

The complexes formed from the fundamental interface solitons in the system of three one-site coupled semi-infinite one-dimensional nonlinear lattices are investigated. This system may be realized in nonlinear optics and Bose-Einstein condensates. The wave propagation is modeled by the system of three discrete Schrödinger equations with cubic nonlinearity. The formation, stability and dynamics of symmetric and asymmetric complexes of fundamental solitons centered at the interface are investigated by variational and numerical approach. Both of them show that two asymmetric and two antisymmetric branches exist in the entire parameter space, while four asymmetric complexes and the symmetric one can be found below some critical value of the inter-lattice coupling parameter. The symmetric solution branch loss of stability accompanied with appearance of one stable and the other unstable asymmetric branches is related to the symmetry-breaking bifurcation in the trilete system. At the bifurcation point the antisymmetric branch is getting stabilized against oscillatory perturbations.

Direct simulations demonstrate that unstable symmetric complexes are transformed into robust oscillating localized interface breathing complexes by radiating away a part of their power. On the other hand, the unstable asymmetric complexes form breathers traveling away from the interface across the lattice. Dynamics of the surface modes can be related to the competition between the repulsion from the interface and the intra-lattice attractive interactions.

#### REFERENCES

[1] M. Stojanović, A. Maluckov, Lj. Hadžievski, and B. A. Malomed, *Physica D* in press.

[2] M. Heinrich, R. Keil, F. Dreisow, A. Tünnermann, S. Nolte, A. Szameit, *New Journal of Physics* 12, 113020 (2010).

## Exact spatio-temporal soliton solutions to the two-component co- and counter-propagating beams in Kerr-like media

N. Petrovic<sup>1,2</sup>, H. Zahreddine<sup>1</sup> and M. Belic<sup>1</sup>

<sup>1</sup>*Texas A&M University at Qatar,  
Education City, Doha, Qatar*

<sup>2</sup>*Institute of Physics,  
Belgrade, Serbia*

e-mail: nikola.petrovic@qatar.tamu.edu

We apply techniques that were developed in [1] and extended in [2-4], i.e. the F-expansion method using Jacobi elliptic functions combined with the principle of harmonic balance, to find exact spatio-temporal soliton solutions to the two component optical systems in Kerr-like media. We consider both co- and counter-propagating beam geometries. We obtain novel solutions for  $c=3$ , where  $c$  is the cross-phase mixing parameter of the two beams, that display interaction between the two beams. We also obtain that Manakov systems, i.e.  $c=1$ , cannot be expressed through Jacobi elliptic functions in this way.

### REFERENCES

- [1] M. Belic, N. Petrovic, W. Zhong, R. Xie, G. Chen, L. Yi, Phys. Rev. Lett. 101, 0123904 (2008).
- [2] N. Petrovic, M. Belic, W. Zhong, R. Xie, G. Chen, Opt. Lett. 34, 1609 (2009).
- [3] N. Petrovic, M. Belic, W. Zhong, Phys. Rev. E 81, 016610 (2010).
- [4] N. Petrovic, M. Belic, W. Zhong, Phys. Rev. E 83, 026604 (2011).

## Dynamical instability of counterpropagating matter waves in optical lattices

S. Prvanović<sup>1</sup>, D. Jović<sup>1,2</sup>, R. Jovanović<sup>1,2</sup>, A. Strinić<sup>1,2</sup> and M. Belić<sup>2</sup>

<sup>1</sup>*Institute of Physics, P.O. Box 57, 11001 Belgrade, Serbia*

<sup>2</sup>*Texas A&M University at Qatar, P.O. Box 23874 Doha, Qatar*

e-mail: strinic@ipb.ac.rs

We investigated the interactions of two-component counterpropagating Bose-Einstein condensate (BECs) when illuminated by laser beams that form optical lattices, producing periodic external potentials. Our approach is similar to the one given in [1]. The question of stability or robustness of matter waves is addressed by numerical analysis of sufficiently long propagation. By analyzing the temporal evolution of two counterpropagating condensates in the periodic potential we shall be able to conclude how to pick characteristic parameters in order to stabilize them. It is well known that an optical lattice formed by laser beams, with corresponding periodic potential, can stabilize an otherwise unstable BEC, but we are interested in stability of propagation of solitonic solutions. We study the interaction of two counterpropagating (CP) condensates that are initially confined to the so-called pancake shape [2, 3] and propagate head-on along the square optical lattice. In this manner we numerically consider the evolution of two BECs for which it is possible to take separated wave functions. We show how the proper choice of characteristic parameters of involved waves can stabilize BEC during the propagation. We investigated time evolution of counterpropagating Bose-Einstein condensate (BEC) in two dimensional square and hexagonal optical lattices.

### REFERENCES

- [1] T. Maytevarunyoo, B. A. Malomed, Physical review A 74, 033616 (2006).
- [2] E. A. Ostrovskaya, Yu.S. Kivshar, Phys. Rev. Lett. 93, 160405 (2004).
- [3] B. J Dabrowska et al., J. Opt. B: Quantum Semiclass. Opt. 6, 423, (2004).

## Boundary and finite size effects in highly nonlocal scalar nematic liquid crystals

A. Strinić<sup>1,2</sup>, N. Aleksić<sup>1,2</sup>, M. Petrović<sup>1,2</sup> and M. Belić<sup>2</sup>

<sup>1</sup> *Institute of Physics, P.O. Box 57, 11001 Belgrade, Serbia*

<sup>2</sup> *Texas A&M University at Qatar, P.O. Box 23874 Doha, Qatar*

e-mail: strinic@ipb.ac.rs

We investigate numerically solitons in a highly nonlocal three dimensional (3D) scalar nematic liquid crystal (NLC) in the presence of an externally applied bias voltage. We calculate fundamental (shape-invariant) soliton profiles by using modified Petviashvili's method. We present main results concerning boundary and finite size effects on solitons in uniaxial NLCs.

## Quantum dynamics of atomic ensembles in a laser pulse of definite shape: Chaos and optical bi-stability effects

O.Yu. Khetselius<sup>1</sup>, G.P. Prepelitsa<sup>1</sup> and A.A. Svinarenko<sup>1</sup>

<sup>1</sup> *Odessa University, P.O.Box 24a,*

*Odessa-9, Ukraine*

e-mail: nuclei08@mail.ru

Present paper has for an object (i) to carry out numerical quantum computation of a temporal dynamics of populations' differences at the resonant levels of atoms in a large-density medium in a nonrectangular form laser pulse and (ii) to determine possibilities that features of the effect of internal optical bi-stability at the adiabatically slow modification of effective field intensity appear in the sought dynamics. It is known that the dipole-dipole interaction of atoms in dense resonant mediums causes the internal optical bi-stability at the adiabatically slow modification of radiation intensity. The experimental discovery of bi-stable cooperative luminescence in some matters, in crystal of Cs<sub>3</sub>Y<sub>2</sub>Br<sub>9</sub>Yb<sup>3+</sup> particularly, showed that an ensemble of resonant atoms with high density can manifest the effect of optical bistability in the field of strong laser emission. The Z-shaped effect is actually caused by the first-type phase transfer. On basis of the modified Bloch equations, we simulate numerically a temporal dynamics of populations' differences at the resonant levels of atoms in the field of pulse with the nonrectangular  $ch^{-1}t$  form. Furthermore, we compare our outcomes with the similar results, where there are considered the interaction between the ensemble of high-density atoms and the rectangularly- and sinusoidally-shaped pulses. The modified Bloch equations, which describes the interaction of resonance radiation with the ensemble of two-layer atoms subject to dipole-dipole interaction of atoms, are as follows:

$$\begin{aligned} \frac{dn}{d\tau} &= \frac{i2\mu T_1}{\hbar} (E^* P - P^* E) + (1-n) \\ \frac{dP}{d\tau} &= \frac{i2\mu T_1 n}{\hbar} - PT_1 \frac{1-i(\delta+bn)}{T_2}, \end{aligned} \quad (1)$$

where  $n = N_1 - N_2$  are the populations' differences at the resonant levels,  $P$  is the amplitude of atom's resonance polarization,  $E$  is the amplitude of effective field,  $b = 4\pi\mu^2 N_0 T_2 / 2\hbar$  is the constant of dipole-dipole interaction,  $T_1$  is the longitudinal relaxation time,  $\delta = T_2(\omega - \omega_{21})$  is the offset of the frequency  $\omega$  of effective field from the frequency of resonance transition  $\omega_{21}$ ,  $N_0$  is the density of resonance atoms,  $\mu$  is the dipole moment of transition,  $\tau = t/T_1$ . Analytical solution (1) cannot be found in general case. So, the numerical modeling has been carried out [1]. The temporal dynamics for the populations' differences at the resonant levels of atoms in a nonrectangular form pulse field:

$$E(\tau) = |E_0|^2 ch^{-1} \frac{\pi\tau T_1}{T_2} \quad (2)$$

has been defined. In the numerical experiment  $\tau$  varies within  $0 \leq \tau \leq T_p/T_1$  and  $T_p$  is equal to  $10T_1$ . It is known from general examination of set (1) that on the assumption of  $b > 4$  and  $b > |\delta|$  with  $\delta < 0$  (the long-wavelength offset of incident light frequency is less than Lorenz frequency  $\omega_L = b/T_2$ ) and if the intensity of light field has certain value ( $I_0 = 4|E_0|^2 \mu^2 T_1 T_2 / h^2$ ) then there are three positive stationary states  $n_i$  (two from them with maximal and minimal value of  $n$  are at that stable). This can be considered as evidence and manifestation condition of the internal optical bistability effect in the system. A fundamental aspect lies in the advanced possibility that features of the effect of internal optical bi-stability at the adiabatically slow modification of effective field intensity for pulse of  $ch^{-1}t$  form, in contrast to the pulses of rectangular form, appear in the temporal dynamics of populations' differences at the resonant levels of atoms.

#### REFERENCES

- [1] A.V.Glushkov, O.Yu. Khetselius, A.A.Svinarenko, G.P.Prepelitsa, Coherence and Ultrashort Pulsed Emission, Ed. Darte F. J. (Intech, Vienna). 159 (2010); O.Yu. Khetselius, Physica Scripta, T135, 014023 (2009); A. V. Glushkov, A.A. Svinarenko et al., Int.J.Quant. Chem. 99, 889 (2004).

Poster Presentations – Nonlinear Optics P.NO.12

### **Multidimensional Ginzburg-Landau Equation in Nonlinear Optics Simulated with Split Step FDTD Method on Ultra Speed Hardware (GPU)**

**B. N. Aleksić<sup>1</sup>, N. B. Aleksić<sup>1</sup>, V. Skarka<sup>2</sup> and M. Belić<sup>3</sup>**

<sup>1</sup>*Institute of Physics Belgrade, University of Belgrade, Belgrade, Serbia*

<sup>2</sup>*Laboratory of Photonic, University of Angers, Angers, France*

<sup>3</sup>*Texas A&M University at Qatar, Doha, Qatar*

e-mail: branislav.aleksic@ipb.ac.rs

Ginzburg-Landau (GL) is a generic name for a class of basic models of nonlinear science, with a wide range of applications. They combine most fundamental features that underlie pattern formation in nonlinear media: linear and nonlinear dissipation, gain, nonlinearity, and diffraction and/or dispersion. Much research is invested in simulating GL equation and efficiency implementation on hardware. To make simulation more accurate and to speed up execution time, many numerical methods and hardware were developed. A recent development in computational science is the use of video graphics cards for numerical problems, because of high parallelization capabilities and low cost. The Graphical Processing Units (GPU) are structured to have many moderate speed Arithmetic Logical Units (ALU) arranged in a very efficient hardware orientation. For some problems, the GPUs have the potential to speed up computations by a factor of over one hundred. The other advantage of using GPUs is that simulations can be implemented without requiring too much extra code development time. On the basis of that, we concentrate our efforts on the parallelization of numerical methods for solving GL equation on a GPU. Beside achieving higher execution speed, we also improved the numerical algorithm. We noticed that traditional finite difference time domain (FDTD) method is not precise enough and made some improvement. It consists in implementing a split step method with improved accuracy. Simulations were performed in two and three spatial dimensions. This algorithm is also implemented on CPU, to compare with the GPU. Results are presented visually and discussed extensively, to achieve the best solution for the given problem.

#### REFERENCES:

- [1] Jason Sanders, Edward Kandrot - *CUDA by Example*, Addison-Wesley (2010).  
 [2] Dennis Sullivan - *Electromagnetic Simulation Using The FDTD Method*, Wiley-IEEE Press (2000).

- [3] J.M. Alcaraz-Pelegrina, P. Rodriguez-Garcia, *Computer Physics Communications* 182, 7 (2011).  
 [4] I Wayan Sudiarta, D J Wallace, *J. Phys. A, Math. Theor.* 40 (2007).  
 [5] N.N. Akhmediev, A.A. Ankiewicz -*Dissipative Solitons*, (Springer, Berlin), (2005).

## Stability analysis of fundamental dissipative Ginzburg-Landau solitons

B. N. Aleksic<sup>1</sup>, B. G. Zarkov<sup>1</sup>, V. Skarka<sup>1,2</sup> and N. B. Aleksic<sup>1</sup>

<sup>1</sup>*Institute of Physics, University of Belgrade, Pregrevica 118, 11001 Belgrade, Serbia*

<sup>2</sup>*Laboratory of Photonic, University of Angers, 2, boulevard Lavoisier, 49045 Angers, France*

e-mail: branslav.aleksic@ipb.ac.rs

A wide class of systems, ranging from nonlinear optics, plasma physics, and fluid dynamics to superfluidity, superconductivity, and Bose-Einstein condensates, can be modeled by complex Ginzburg-Landau equations [1, 2]. In nonlinear optics, the two-dimensional complex cubic-quintic Ginzburg-Landau equation for the normalized complex envelope of the electrical field  $E$  reads

$$i \frac{\partial E}{\partial z} + (1 - i\beta) \left( \frac{\partial^2 E}{\partial x^2} + \frac{\partial^2 E}{\partial y^2} \right) + (1 - i\varepsilon) |E|^2 E - (\nu - i\mu) |E|^4 E - i\delta E \quad (1)$$

Parameter  $\nu$  is positive and without loss of generality can be taken as  $\nu=1$ . The stability of the pulse background involves the linear loss, thus, the parameter  $\delta$  must be positive. Parameters  $\varepsilon$  and  $\mu$  are associated with cubic gain and quintic loss terms respectively. Term with  $\beta$  in Eq. (1) corresponds to diffusion of the field. This equation has stable solutions corresponding to localized solitonic structures. A spatial soliton is completely localized in all transverse dimensions whenever diffraction is compensated by nonlinearity [3]. In dissipative systems, the solitonic structure can be preserved if appropriate gain match linear and nonlinear losses. In Ref. [3] we extended variation method in order to establish stability domain in space of parameters for radially symmetric two-, and three-dimensional solitons. In subsequent papers the stability of asymmetric Gauss beam is analyzed and the selforganization of dissipative solitons is established [4, 5].

In this paper a stability analysis of the Ginzburg-Landau system is performed using variation method. Growth rates for radially symmetric and asymmetric perturbations of fundamental steady state solutions of cubic-quintic Ginzburg-Landau equation are found. The region for small gain parameter  $\varepsilon$  of the obtained stability domain corresponds to negative growth rates for both radially symmetric and asymmetric perturbations. Therefore, the stability of fundamental dissipative solitons is established. In the region with big  $\varepsilon$  fundamental steady state solutions are unstable to the asymmetric perturbations while they are stable to the symmetric ones. Analytical results are confirmed by exhaustive numerical simulations.

### REFERENCES

- [1] N.N. Akhmediev, A.A. Ankiewicz, *Dissipative Solitons*, (Springer, Berlin), (2005).  
 [2] I. S. Aranson, L. Kramer, *Rev. Mod. Phys.* 74, 1 (2002).  
 [3] V. Skarka, and N.B. Aleksic, *Phys. Rev. Lett.* 96, 013903 (2006).  
 [4] N.B. Aleksic, V. Skarka, D.V. Timotijevic, D Gauthier, *Phys. Rev. A* 75, 061802(R) (2007).  
 [5] V. Skarka, D.V. Timotijevic, N.B. Aleksic, *J. Opt. A: Pure Appl. Opt.* 10, 075102 (2008).

## Effect of FWM on High-Signal-Power Ultra DWDM-PONs with Standard SMFs

Z. Vujicic<sup>1</sup>, N. B. Pavlovic<sup>1</sup> and A. Teixeira<sup>1,2</sup>

<sup>1</sup>*Instituto de Telecomunicações, Campus Universitário de Santiago, 3810-193 Aveiro, Portugal.*

<sup>2</sup>*Nokia Siemens Networks, Amadora, Portugal.*

e-mail: zoran.vujicic1@gmail.com

Extended reach Ultra Dense Wavelength Division Multiplexing (UDWDM) systems, operating at multi gigabit rates with large number of densely spaced channels [1], require high input powers in order to bridge long distances without Signal-to-Noise Ratio (SNR) deterioration. Due to the high powers, the impact of the Four-Wave Mixing (FWM) can be significant even in Single Mode Fibers (SMF) [2]. Therefore, it is important to investigate the effects of FWM in SM fibers for the conditions of high powers and low channel spacing.

It has been shown that the power of the new (idler) wave generated through FWM between the pump and signal waves does not depend solely on the FWM efficiency, but also on the conditions of the optical power transfer within the process [3]. Thus, we investigated the FWM idler power evolution along the standard SM fiber in extended reach UDWDM-PON scenario. The impact of the signal input power on properties of optical power transfer within the FWM process and consequent idler gain characteristics are analyzed for the case of high power limits. The investigation was conducted following the FWM model presented in [3].

In our simulations, we considered 0.08nm (~11GHz) channel spacing between the signal and the pump waves, aiming at emulating the UDWDM scenario. The pump power was kept constant at 0.1W (20dBm), while the signal power was varied by 1 dB from 20dBm to 17dBm. To emphasize the power transfer dynamics within the FWM process, we considered the case of zero attenuation since it does not influence the direction of the process. As the idler wave experiences periodic amplification and deamplification, depending on the direction of optical power transfer governed by the relative phase mismatch between the waves, it exhibits a sinusoid spatial distribution along the fiber length. As expected, the results suggest a strong dependency of the idler spatial distribution amplitude on the signal input power. It is evident from the results that the growth of the signal power led to the increase of the frequency of power transfer sinusoid and the decrease of its amplitude. Thus, it was shown that the growth of the signal input power is followed by the idler gain drop-off.

We have shown that the signal power increase of 3dB was followed by the idler power distribution and pump depletion amplitude decrease of 0.23dB (2.4mW) and 10.3dB (9.5mW), respectively. This behavior can be explained by noting that the signal input power highly affects both the frequency and amplitude of the sinusoid that governs the relative phase evolution along the fiber [3, 4]. This is confirmed in our simulations by exploring the effect of signal power increase on the relative phase spatial distribution along fiber length. The results further suggest that, for sufficiently high signal power limits, the idler gain drop-off exhibited saturation. This approach can thus be used for the purpose of FWM mitigation in extended reach UDWDM systems.

### REFERENCES

- [1] H. Suzuki, M. Fujiwara, N. Takachio, K. Iwatsuki, T. Kitoh, T. Shibata, *Photonics Technology Letters, IEEE*, 14, 405 (2002).
- [2] F. Forghieri, R. W. Tkach, A. R. Chraplyvy, in *Optical Fiber Telecommunications IIIB*, I. P. Kaminow and T.L.Koch, Eds. San Diego, CA, USA: Academic Press, pp. 69-114, (1997).
- [3] K. Inoue and T. Mukai, "Signal wavelength dependence of gain saturation in a fiber optical parametric amplifier," *Opt. Lett.*, vol. 26, pp. 10-12, (2001).
- [4] G. Cappellini and S. Trillo, "Third-order three-wave mixing in single-mode fibers: exact solutions and spatial instability effects," *J. Opt. Soc. Am. B*, vol. 8, pp. 824-838, (1991).

## **Interactions of gap solitons in double-periodic one-dimensional photonic superlattices with saturable nonlinearity**

P.P. Beličev, I. Ilić and M. Stepić  
*Vinča Institute of Nuclear Sciences, Belgrade, Serbia*  
 e-mail: petrab@vinca.rs

Light propagation in various photonic lattices consisting of nonlinear waveguide arrays whose characteristics nowadays may be controlled during fabrication process practically at will represent an active research field. Uniform photonic lattices are periodic structures exhibiting band gap structure with stop and pass bands. Several unique phenomena such as discrete diffraction, diffraction management, gap solitons, Tamm oscillations and Landau-Zener tunneling are seminally observed in such systems [1]. Gap solitons in lossless lattices are strongly localized structures which may occur in the case when dispersive and nonlinear effects are mutually balanced. Except in uniform lattices, gap solitons are investigated in lattices with deliberately induced defects [2,3], in binary arrays in which either the width of individual channels [4,5] or the distance between adjacent channels [6] alters periodically. Both types of above mentioned binary lattices may be regarded as superlattices [7] in which additional periodicity opens a new mini-gap in which light propagation is not allowed. Interestingly, gap solitons may be also observed in Bose-Einstein condensates in optical superlattices [8] and in diatomic lattices [9].

In this contribution, we explore theoretically light propagation in one-dimensional binary waveguide array consisting of double-channel cells where all channels are identical but spacing between two adjacent channels in the cell and two adjacent cells differs. We focus on media with saturable defocusing nonlinearity such as photovoltaic lithium niobate crystal and use simplified discrete model [10] to derive the corresponding dispersion relation. The existence of the new mini-gap in which the nonlinear energy localization is possible, giving the rise of the so-called symmetric gap solitons, is shown. The anti-symmetric solutions exist in the regular gap. Field envelope of the first type of solutions changes its phase between cells, while it remains in phase inside the cell. On the other hand, anti-symmetric field envelope has out-of-phase relation from site to site. Analysis show that anti-symmetric localized structures stay stable during the propagation for lower powers, while for higher powers they propagate in the form of breather preserving its original structure. In the case of symmetric localized modes, direct simulation describes breather-like behavior of the obtained solutions with smaller oscillations in amplitude for structures which are “deeper” in the mini-gap, whereas the increase of power necessary for light localization leads to its corruption. In addition, we study numerically the parallel interactions between different types of gap solitons [11], looking for nonlinear all-optical switching in such double-periodic photonic lattices. Depending on the type of interacting solitons, attracting and repulsive interactions can be observed leading to fusion of two solitons into single one or forcing them to change their propagation course through the lattice.

### REFERENCES

- [1] F. Lederer et al., Phys. Rep. 463, 1 (2008).
- [2] W. Królikowski and Yu. S. Kivshar, JOSA B 13, 876 (1996).
- [3] L. M. Molina and R. A. Vicencio, Opt. Lett. 31, 966 (2006).
- [4] A. A. Sukhorukov and Yu. S. Kivshar, Opt. Lett. 27, 2112 (2002).
- [5] R. Morandotti et al., Opt. Lett. 29, 2890 (2004).
- [6] R. A. Vicencio and M. Johansson, Phys. Rev. A 79, 065801 (2009).
- [7] Y. J. He, W. H. Chen, H. Z. Wang, B. A. Malomed, Opt. Lett. 32, 1390 (2007).
- [8] P. J. Y. Louis, E. A. Ostrovskaya, Yu. S. Kivshar, Phys. Rev. A 71, 023612 (2005).
- [9] Yu. S. Kivshar and N. Flytzanis, Phys. Rev. A 46, 7972 (1992).
- [10] M. Stepić et al., Phys. Rev. E 69, 066618 (2004).
- [11] M. Stepić et al., Phys. Rev. E 74, 046614 (2006).

**AC Stark-shift in Double Resonance and Coherent Population Trapping in Wall-Coated Cells for Compact Rb Atomic Clocks**

D. Miletic, T. Bandi, C. Affolderbach and G. Mileti  
*Laboratoire Temps-Fréquence (LTF), Université de Neuchâtel*  
*Neuchâtel, Switzerland*  
e-mail: danijela.miletic@unine.ch

The AC Stark shift (light-shift) is the frequency shift of atomic energy levels due to interaction between oscillating electric field (light) and the induced atomic dipole moment. This light shift is one of the main sources of instability in atomic clocks on medium - to long - term time scales [1]. We experimentally studied the light-shift in two different schemes for Rb gas-cell clocks: Double Resonance (DR) clock scheme, where light shift comes from monochromatic optical excitation and Coherent Population Trapping (CPT) clock scheme, where light shift comes from the multi-frequency optical excitation.

Our experimental setup allowed us to measure and study the AC Stark shift in both clock schemes. Light from a compact laser head [2] is frequency-stabilized to the Rb D1 transition (795 nm) and passes through an Electro-Optical Modulator (EOM). Before irradiating the resonance cell, the laser beam is linearly polarized, and has a diameter of 5 mm. The vapor cell is cylindrical, 14 mm long and has 14mm diameter, contains pure 87-Rb, and its inner walls are coated with paraffin. This cell is placed in a magnetron-type microwave cavity. The volume of the total physics package, including two layers of magnetic shielding, is approximately 1 litre. DR or CPT signals are obtained by injecting the microwave signal either directly into the microwave cavity or into an Electro-Optical Modulator (EOM) for creating a multi-frequency laser spectrum, respectively.

We precisely measure the light shift as a function of laser intensity and frequency in both the DR and CPT clock schemes. This shift depends on the spectrum of the optical radiation and may be expressed by the two coefficients  $\alpha$  and  $\beta$ , often referred to as the intensity light-shift coefficient ( $\alpha$ ) and the frequency light-shift coefficient ( $\beta$ ) [3]. Under typical operating conditions, the intensity light-shift and the frequency light-shift are  $1.5 \times 10^{-11} (\mu\text{W}/\text{cm}^2)^{-1}$  and  $3 \times 10^{-11}/\text{MHz}$ , respectively, and are of comparable value for both DR and CPT.

Acknowledgments: This work was supported by the Swiss National Science Foundation (project 200020\_130381) and the European Space Agency (ESA). We thank our colleagues from LTF-UniNe for their contributions to this work.

REFERENCES

- [1] C. Cohen-Tannoudji, J. Dupont-Roc, Phys. Rev. A 5, 968 (1972).
- [2] C. Affolderbach, G. Miletic, Rev. of Scien. Instr. 76, 073108, (2005).
- [3] W. Happer, Rev. Mod. Phys. 44, 169 (1972).

## Two-color photoionization of Helium through autoionization structures in XUV-FEL and laser fields

S.I. Themelis  
 Department of Applied Sciences,  
 Technological Educational Institute of Chalkis,  
 34400 Psahna, Greece  
 e-mail: sthemelis@teihal.gr

Coherent short wavelength (XUV and beyond) radiation sources of some intensity and short pulse duration, such as the accelerator based FEL (Free Electron Laser), open the way for the exploration of highly excited multielectron states well beyond the standard single photon absorption probe technique. The combination and synchronization of such sources with optical lasers of ultrashort duration, and possibly controllable phase, may for the first time allow the study of the coupling between highly excited states. One can thus realistically contemplate the coupling of Auger or multiply excited states which would provide a rather unique probe of such highly correlated configurations offering the ultimate test of degree of validity of theoretical approaches and calculations [1].

In this study, we discuss the dynamics of the two-photon resonant ionization of helium involving two autoionizing states in the presence of two-color laser fields. The ground state is coupled to the  $2s2p\ ^1P^o$  autoionizing state, through a laser with frequency  $\omega_1$ . A second laser, with frequency  $\omega_2$ , couples the  $2s2p\ ^1P^o$  state to the  $3s^2\ ^1S$  autoionizing state. The laser coupling between the doubly excited states is shown to lead to modifications of the Beutler-Fano profile and the appearance of an Autler-Townes doublet. This double resonance effect between autoionizing states can be observed at moderate laser intensities easily attainable by currently operated sources [2].

### REFERENCES

- [1] P. Lambropoulos and P. Zoller, Phys. Rev. A 24, 379 (1981).  
 [2] M. Drescher, *et al.*, Nature 419, 803 (2002).

## High-Power Metal Halide Vapour Lasers Oscillating in Deep Ultraviolet, Visible and Middle Infrared Spectral Ranges

K. A. Temelkov<sup>1</sup>, S. I. Slaveeva<sup>1</sup>, V. I. Kirilov<sup>2</sup>, I. K. Kostadinov<sup>3</sup> and N. K. Vuchkov<sup>1</sup>  
<sup>1</sup>*Institute of Solid State Physics, Bulgarian Academy of Sciences  
 Sofia, Bulgaria*  
<sup>2</sup>*Faculty of Mathematics and Informatics,  
 University of Sofia, Bulgaria*  
<sup>3</sup>*Pulsligh”t Ltd.,  
 Sofia, Bulgaria*  
 e-mail: temelkov@issp.bas.bg

High-power gas-discharge laser sources, oscillating from deep ultraviolet (DUV) to middle infrared (MIR) spectral ranges, are objects of great interest, because of a wide variety of applications, concerning with laser-matter interaction and laser-induced phenomena in laser surgery, microbiology, high-precision processing of different materials, high-density optical recording of information, modification of various materials and etc. [1]. Nowadays excimer lasers are generally used as light sources in the DUV range. Demand for high beam quality and laser linewidth is high, and increasing. The good spatial structure of the laser beam is generally important for the good quality image

projected, while the narrow linewidth would reduce the chromatic aberrations. Due to the broad gain curve and the naturally short (around 20 ns) laser pulse duration, the excimer lasers can neither reach the spatial structure nor the linewidth required. Their wide application is also impeded by their cost and considerable overheads. Recently, by means of a free electron laser (FEL) with variable wavelength between 3 and 20  $\mu\text{m}$ , it has been found that the laser radiation at 6.45  $\mu\text{m}$  is the most effective tool for soft tissue and bone ablation with minimal thermal damage and smear layer [2]. While the use of the FEL has shown much promise for surgical applications in viable clinical systems, further advances are inhibited by its size, cost, and considerable overheads.

Metal and metal halide vapour lasers are very perspective for application, because of the possibility to oscillate in different spectral ranges – from DUV to MIR. High beam quality and narrow-linewidth are inherent for metal vapor lasers. DUV and MIR laser systems, which are based on powerful high-beam-quality long-lifetime DUV Ne-CuBr and MIR He-SrBr<sub>2</sub> lasers excited in nanosecond pulsed longitudinal discharge, are developed, patented and studied. Optimal discharge conditions, such as active zone diameter, vapor pressure, buffer-gas pressure, electrical excitation scheme parameters, average input power, pulse repetition frequency, are found. The highest output laser parameters are obtained for the DUV Cu<sup>+</sup> and 6.45- $\mu\text{m}$  Sr atom lasers, respectively. These lasers equipped with optical systems for control of laser radiation parameters, such as laser beam divergence, laser intensity distribution, etc. are applied in a series of applications, such as microhole drilling in glass, polymers and semiconductors, laser-induced modification of conducting polymer and metal-polymer layers, as well as photoluminescence and determination of linear optical properties of new materials, as alternative laser sources of the excimer and free electron lasers, which could not reach either the spatial structure or the emission linewidth, or the relevance of the metal vapour lasers.

A MOPA system, which is based on the high-beam-quality high-power CuBr vapour laser and is equipped with an optic system for laser beam control and with X-Y stage controlled by adequate software as well, is developed and used in high-precision micromachining of samples made of Nickel and tool steel.

#### REFERENCES

- [1] R. Salimbeny, Pulsed Metal Vapour Lasers, ed. C. E. Little, N. V. Sabotinov (Dordrecht: Kluwer Academic Publishers), 229 (1996).
- [2] J. M. Auerhammer, R. Walker, A. F. G. van der Meer, B. Jean, Appl. Phys. B 68, 111 (1999).

Poster Presentations – Laser, Laser Spectroscopy P.LS.4

### **Conversion of dark magneto-optical resonances to bright by controlled changes in the excitation parameters of the Rb D<sub>2</sub> line at linearly polarized excitation**

L. Kalvans, M. Auzinsh, A. Berzinsh, R. Ferber, F. Gahbauer, A. Mozers and D. Opalevs  
*Laser Centre.*

*University of Latvia, Riga, Latvia*  
e-mail: linards.kalvans@lu.lv

Magneto-optical resonances observed in the laser induced fluorescence of alkali metal vapors [1,2], caused by zero-field level-crossing can be dark or bright [3] depending on the particular hyperfine transition selected by the exciting laser radiation. If the total atomic angular momentum of the ground state ( $F_g$ ) is greater than or equal to the total atomic angular momentum of the excited state ( $F_e$ ) the resonance is expected to be dark. In the opposite case ( $F_g < F_e$ ) a bright resonance is expected. These simple rules hold while distinct hyperfine transitions are resolved under Doppler broadening. If the

latter condition is not fulfilled the observed resonance would be influenced by all of the overlapping hyperfine transitions.

If Rubidium atoms are confined in a vapor cell at a room temperature and the  $D_2$  line is excited, only the ground state hyperfine level can be unambiguously selected, while the structure of the excited state remains unresolved. In this situation the influence of "bright" or "dark" transitions on the total resonance signal can be controlled by tuning the excitation frequency over the wide Doppler profile. In this way, a dark resonance can be "converted" to bright resonance simply by changing the excitation frequency [4]. Moreover the bright resonance, which typically has a very low contrast, seems to become dark when the excitation power density is increased. The polarization axis of the linearly polarized exciting radiation and the controlled magnetic field are mutually perpendicular.

Both experimental results and theoretical calculations obtained by a model, based on the optical Bloch equations are presented. The theoretical model has been successfully applied to describe similar resonances observed at  $D_1$  excitation of Rubidium [4] and other systems. The model accounts for energy shifts of the magnetic sublevels and mixing among hyperfine levels in the presence of a magnetic field. Averaging over the different velocity groups and their respective frequency shifts due to the Doppler effect is also performed.

The study is supported by the Latvian State Research Program Grant No. 2010. 10-4/VPP-2/1, the ERAF project No. 2010/0242/2DP/2.1.1.1.0/APIA/VIAA/036, and the ESF project No. 2009/0223/1DP/1.1.1.2.0./09/APIA/VIAA/008.

#### REFERENCES

- [1] J.-C. Lehmann and C. Cohen-Tannoudji, C.R. Acad. Sci. Paris Ser. IV 258, 4463 (1964).
- [2] R. W. Schmieder, A. Lurio, W. Happer, A. Khadjavi, Phys. Rev. A 2, 1216 (1970).
- [3] G. Alzetta, A. Gozzini, L. Moi, G. Orriols, Il Nuovo Cimento B 36, 5 (1976).
- [4] M. Auzinsh et al., Phys. Rev. A 79, 053404 (2009).

Poster Presentations – Laser, Laser Spectroscopy P.LS.5

## **Ground state Hanle resonances for measuring the longitudinal and transverse spin relaxation rates of cesium vapor in a paraffin-coated cell**

N. Castagna and A. Weis  
*Physics Department, University of Fribourg,  
Fribourg, Switzerland  
e-mail: natascia.castagna@unifr.ch*

In 1924 W. Hanle discovered the effect, named after him, in which a static external magnetic field depolarizes the resonance fluorescence from atoms in an atomic vapor [1]. The effect was later explained in terms of the interplay of excited state spin polarization created by absorption of polarized radiation, the precession of the associated magnetization in the magnetic field, and relaxation induced by the decay of the excited state and/or by collisions.

Almost half a century later, Dupont-Roc and colleagues discovered a related effect in the ground state, in which spin polarization is created by optical pumping [2]. In these experiments one measures the power of a (circularly or linearly) polarized resonant light beam traversing an atomic vapor. The ground state Hanle effect manifests itself as a level crossing resonance, which is observed as a resonant change of the transmitted power, when the magnitude of a (suitably oriented) applied magnetic field  $B$  is scanned across  $B=0$ .

In recent years the ground state Hanle effect has received a renewed interest, when interpreted in terms of coherent population trapping (CPT), electromagnetically induced transparency/absorption (EIT/EIA). To our knowledge, no theoretical treatment has been presented in the literature which describes the dependence of the Hanle resonance lineshapes (amplitude, width) for arbitrary field geometries, nor how the experimental parameters can be used to infer the longitudinal and transverse relaxation rates of the medium's orientation and alignment.

We have studied ground state Hanle resonances using circularly polarized light in the weak intensity limit, in which the atoms undergo only a single optical pumping cycle. We will present equations which describe the dependence of the amplitudes and widths of the resonances for arbitrary magnetic field orientations, and show how the longitudinal ( $\gamma_1$ ) and transverse ( $\gamma_2$ ) spin relaxation rates can be inferred from the resonance parameters.

We made measurements in which a longitudinal/transverse magnetic field (with respect to the laser beam's propagation) was scanned. The characteristic change of the resonance amplitude and width as a function of discrete values of a weak transverse/longitudinal field yields consistent determinations of  $\gamma_1$  and  $\gamma_2$ . The intrinsic values of these rates are obtained by a linear extrapolation to zero laser power. In this way we determine the relaxation parameters that characterize a given cell (at a given temperature).

We will discuss the pros and cons of this technique compared to the optically detected magnetic resonance method which we have used in the past for the quality control of more than 300 paraffin-coated cells produced in our laboratory [3].

#### REFERENCES

- [1] W. Hanle, Z. Phys. 30, 93 (1924).
- [2] J.C. Lehmann, C. Cohen-Tannoudji, Comptes Rend. 258, 4463 (1964), and J. Dupont-Roc, S. Haroche, C. Cohen-Tannoudji, Phys. Lett. 28A, 638 (1969).
- [3] N. Castagna *et al.*, Appl. Phys. B 96, 763 (2009).

Poster Presentations – Laser, Laser Spectroscopy P.LS.6

### **Thermal memory influence on thermoconducting component of photoacoustic response**

M. Nesic<sup>1</sup>, P. Gusavac<sup>2</sup>, M. Popovic<sup>1</sup>, Z. Soskic<sup>3</sup> and S. Galovic<sup>1</sup>

<sup>1</sup>*Vinca Institute of Nuclear Sciences,  
Belgrade, Serbia*

<sup>2</sup>*School of Electrical Engineering,  
University of Belgrade, Serbia*

<sup>3</sup>*Faculty of Mechanical Engineering,  
University of Kragujevac, Kraljevo, Serbia*

e-mail: mioljub@gmail.com

In this work, a model of thermoconducting component of the photoacoustic (PA) response is derived, which includes thermal memory properties of the examined material and its fluid environment. A comparison is made between the derived model and the classic one, which neglects the influence of thermal memory. It has been shown that, at modulation frequencies lower than certain critical frequency of the light source, these models tend to overlap, while, at higher frequencies, noticeable differences occur. The cutoff frequency depends on heat propagation velocity through the sample and its thickness.

Our results limit the validity domain of the classic model, offering, at the same time, the possibility of obtaining thermal memory properties using PA effects at frequencies above the critical one.

#### REFERENCES

- [1] S. Galovic, Z. Soskic, D. M. Todorovic, A. Mendez-Vilas, J. Diay (Eds.) *Microscopy: Science, Technology, Applications and Educations*, Formatex Research Center, Badajoz, Spain (2010).
- [2] H. Vargas, L.C.M. Miranda, Photoacoustic and related photothermal techniques. *Physic. Rep.* 161, 45 (1998).
- [3] M. Terasina, N. Hirota, S.E. Braslavsky, A. Mandelis, S.E. Bialkowski, G.J. Diebold, R.S.D. Miller, D. Fournier, R.A. Palmer, A. Tam, *Pure Appl. Chem.* 76, 1083 (2004).
- [4] P. M. Nikolić, D.M. Todorović, Serbian Academy of Sciences and Arts Department of Technical Sciences Book 40, monographs vol. DCXLVIII, Belgrade (2001).
- [5] A. Rosencwaig, *J. Appl. Phys.* 51, 2210 (1980).
- [6] F. McDonald, G. Westel, *J. Appl. Phys.* 49, 2313 (1978).
- [7] Allan Rosencwaig, Allen Gersho, *J. Appl. Phys.* 47, 64 (1976).
- [8] S. Galovic, D. Kostoski, *J. Appl. Phys.* 95, 2063 (2003).
- [9] I.A. Novikov, *J. Appl. Phys.* 81, 1067 (1997).
- [10] S. Galovic, Z. Stojanovic, D. Cevizovic, M. Popovic, *J. Microsc.* 232, 558 (2008).
- [11] M. Popovic, Z. Stojanovic, S. Galovic, *Hem. Ind.* 61, 66, (2007).
- [12] S. Galovic, PhD thesis, Belgrade, (2003).

Poster Presentations – Laser, Laser Spectroscopy P.LS.7

### **Analysis of Fluorescence Emission Intensity and Lifetime of Rhodamine B in Ethanol and Tetrahydrofurane solvents**

M.S. Rabasovic<sup>1</sup>, D. Sevic<sup>1</sup>, M. Terzic<sup>2</sup> and B.P. Marinkovic<sup>1</sup>

<sup>1</sup>*Institute of Physics,  
University of Belgrade, Serbia*

<sup>2</sup>*Faculty of Science,  
University of Novi Sad., Serbia*

e-mail: bratislav.marinkovic@ipb.ac.rs

A number of earlier reports have examined the fluorescence emission of the laser dye Rhodamine B [1-5]. A nonlinear absorption of Rhodamine B in methanol and water has been investigated extensively [6]. Srinivas et al. [6] performed also lifetime measurements of the first excited state of Rhodamine B in water and methanol and they observed that the fluorescence lifetimes were much smaller in water (about 1.4 ns) than in methanol (about 2.6 ns).

M. Fikry et al. [3] described the fluorescence characteristics of the thin film samples of Rhodamine B when polymethylmethacrylate (PMMA) is used as a host medium, as well as Rhodamine B dissolved in ethanol and tetrahydrofurane (THF). In this paper, using the Time Resolved Laser Induced Fluorescence (TR-LIF) spectroscopy, we have extended the study presented in [3], analyzing the fluorescence lifetime of Rhodamine B in ethanol and THF solvents, including the effect of solution concentration.

The time resolved fluorescence emission spectra of Rhodamine B in ethanol and tetrahydrofurane solvents were acquired using a streak camera (Hamamatsu model C4334-01). Pulsed light excitation is provided by a tunable Nd-YAG OPO laser system (Vibrant model 266 made by Opotek, Inc.). The OPO is excited with the fourth harmonic of the Brilliant laser at 266 nm. The output level at 266 nm is 50 mJ, with pulse duration of about 5 ns and repetition rate of 10 Hz. After passing through the OPO pulse length could be reduced to around 1 ns, the energy is about 5 mJ. The output of the OPO can be continuously tuned over a spectral range from 320 nm to 475 nm.

A detailed description and some of the preliminary results of our experimental set up are published recently [7-9].

#### REFERENCES

- [1] M. Ishikawa, M. Watanabe, T Hayakawa, M. Koishi Anal. Chem.67, 511 (1995).
- [2] P. Zhao, S. Rodriguez, J. Fluoresc. 7, 121 (1997).
- [3] M. Fikry, M.M. Omar, L.Z. Ismail, J. Fluoresc. 19, 741 (2009).
- [4] Y. Takahashi, T. Yamanaka, K. Uchida, J. Luminisc. 62, 299 (1994).
- [5] D. Madge, G.E. Rojas, P.G. Seybold, Photochemistry and Photobiology 70,737 (1999).
- [6] N.K.M.N. Srinivas, S.V. Rao, D.N. Rao, J. Opt. Soc. Am. B 20,2470 (2003).
- [7] M. Terzic, B.P. Marinkovic, D. Sevic, J. Jureta, A.R. Milosavljevic, Facta Universitatis, Series Phys. Chem. Technol. 6, 105 (2008).
- [8] M.S. Rabasovic, D. Sevic, M. Terzic, S. Savic Sevic, B. Muric, D. Pantelic, B.P. Marinkovic Acta Physica Polonica A 116, 570 (2009).
- [9] D. Sevic, M.S. Rabasovic, B.P. Marinkovic, to appear in IEEE Transactions on Plasma Science, Vol. 39, Special Issue of Images in Plasma Science, (2011).

Poster Presentations – Laser, Laser Spectroscopy P.LS.8

### **Crossover resonances in Cs vapor confined in micrometric-thin cell**

P. Todorov<sup>1</sup>, D. Slavov<sup>1</sup>, K. Vaseva<sup>1</sup>, N. Petrov<sup>1</sup>, A. Krasteva<sup>1</sup>, D. Sarkisyan<sup>2</sup>, S. Saltiel<sup>3</sup>  
and S. Cartaleva<sup>1</sup>

<sup>1</sup>*Institute of Electronics, Bulgarian Academy of Sciences, Sofia, Bulgaria*

<sup>2</sup>*Institute for Physical Research, National Academy of Sciences of Armenia, Ashtarak-2, 378410, Armenia*

<sup>3</sup>*Sofia University, Faculty of Physics, 5 J. Bourchier boulevard, 1164 Sofia, Bulgaria*  
e-mail:petkoatorov@yahoo.com

The development of a new type of cell for atomic spectroscopy, so called Extremely Thin Cell (ETC, with thickness of a few microns and less) was first demonstrated by D. Sarkisyan et al. [1]. The most important characteristic of this type of cell is the anisotropy of its dimensions: typically, the transversal dimensions are about four orders of magnitude larger than the cell thickness. Due to this space anisotropy and to the very small cell thickness atoms confined in the cell can be distinguished in respect to their velocity component along the laser beam direction of propagation. The cell thickness is in order of the irradiating light wavelength, which for Cs D<sub>2</sub> – line is  $\lambda=852$  nm.

Recently it has been demonstrated [2] that in the ETC absorption and fluorescence spectrum, the single beam spectroscopy of the open atomic transitions shows interesting features, especially when increasing the cell thickness up to almost 3 micrometers. When laser irradiating the ETC strongly saturates the atomic transition, one observes dips in the fluorescence and absorption profiles. The dips have a width smaller than that of the sub-Doppler profile of the hyperfine transition.

In this work we present our recent experimental results related to further enhanced cell thickness, comparing ETC with thickness of about 5 $\mu$ m (precisely 6 $\lambda$ ) with a cell with thickness  $\sim$ 19 $\mu$ m (22 $\lambda$ ). We demonstrate that for the cell with thickness 6 $\lambda$ , in the absorption and fluorescence profiles a narrow velocity selective optical pumping deep appears when irradiating three F<sub>g</sub> = 3  $\rightarrow$  F<sub>e</sub> = 2, 3, 4 hyperfine transitions by resonant laser light. F<sub>g</sub> denotes the quantum number of the ground state and F<sub>e</sub> - the excited state of Cs D<sub>2</sub> – line. We also show that for this cell the crossover resonances are not observable in the explored irradiating intensity range. While using the cell with thickness 22 $\lambda$  we also observe velocity selective optical pumping deeps at the hyperfine transition centers, in addition some crossover resonances are already present having better contrast in thin cell reflection spectrum.

The narrow resonances in  $6\lambda$  cell are very convenient for building simple and robust frequency reference because they are obtained by single beam irradiating the ETC, which is different from Saturated Absorption (SA) scheme, where one needs two overlapped beams. In  $22\lambda$  cell we observe together with hyperfine transitions resonances their crossover resonances except the crossover resonance between  $F_g = 4 \rightarrow F_e = 3$  and  $F_g = 4 \rightarrow F_e = 5$  transitions, which masks  $F_g = 4 \rightarrow F_e = 4$  resonance in SA scheme. Hence, the thin cell with thickness  $22\lambda$  offers us a perspective to build a frequency reference with the maximum possible frequency markers for Cs  $D_2$  – line.

Presented results contribute to the further advancement in fundamental studies of saturation and optical pumping in extremely thin vapor layers.

Authors are grateful for the partial supports by the Bulgarian NCSR (grant № DMU 02/17 – 18.12.2009 and grant № DO 02-108/22.05.2009).

#### REFERENCES

- [1] D. Sarkisyan, D. Bloch, A. Papoyan, M. Ducloy, *Opt. Commun.* 200, 201 (2001).  
 [2] Stefka Cartaleva, Solomon Saltiel, Armen Sargsyan, David Sarkisyan, Dimitar Slavov, Petko Todorov, Kapka Vaseva *J. Opt. Soc. Am. B* 26, 1999 (2009).

Poster Presentations – Laser, Laser Spectroscopy P.LS.9

### **Study of laser-pumped double-resonance clock signals using a micro-fabricated cell**

M. Pellaton<sup>1</sup>, C. Affolderbach<sup>1</sup>, Y. Pétremand<sup>2</sup>, N. F. de Rooij<sup>2</sup> and G. Mileti<sup>1</sup>

<sup>1</sup>*Laboratoire Temps-Fréquence (LTF)  
 Université de Neuchâtel (UniNE), Switzerland*

<sup>2</sup>*Institute of Microengineering (IMT)  
 Ecole Polytechnique Fédérale de Lausanne (EPFL), Switzerland  
 e-mail: gaetano.mileti@unine.ch*

We present our microwave spectroscopic studies on laser-microwave double-resonance signals, obtained from a micro-fabricated Rb vapor cell. This study concentrates on the characteristics and systematic shifts of the ground-state “clock transition” in  $^{87}\text{Rb}$  ( $|F_g=1, m_F=0\rangle \rightarrow |F_g=2, m_F=0\rangle$ ), and represents a first step towards a miniature atomic clock based on the double-resonance scheme [1].

The micro-fabricated cell is realized using anodic bonding [2]. Its inner dimensions are 5 mm diameter and 2 mm height (volume  $< 40 \text{ mm}^3$ ). The cell is filled with metallic Rb and an appropriate mixture of Nitrogen and Argon as buffer gases, which allows us to observe an inversion temperature (of temperature shift). Double-resonance signals are obtained using pump light from a compact, frequency-stabilized laser head [3], with the laser frequency locked to the  $|F_g=2\rangle \rightarrow |F_e=1\rangle$  transition (Rb D1 line at 795nm), while the microwave field is applied to the atoms using a magnetron-type cavity [4].

Double-resonance clock signals with nearly 2% of contrast and a linewidth of 7.4 kHz (FWHM) are obtained. This sets a signal-to-noise limit of  $1.8 \cdot 10^{-11} \tau^{-1/2}$  for the stability of a Rb atomic clock based on this approach. Our measured clock stability shows a short-term stability of  $2 \cdot 10^{-11} \tau^{-1/2}$ , in good agreement with the signal-to-noise limit, and meeting typical requirements for miniaturized atomic clocks.

We also have studied systematic shifts of the resonance frequency, due to, e.g., the light shift (AC Stark shift) and temperature effects, which are among the main sources of clock instabilities at longer timescales. At integration times of  $\tau \geq 1000 \text{ s}$ , we find a clock stability on the order of  $10^{-11}$ , limited by

light-shift effects ( $\approx 10^{-9}/\mu\text{W}$  level) and temperature shifts. The instability due to temperature shifts can still be reduced by at least a factor of 10 by optimization of the cell contents. Detailed results will be presented at the conference.

Acknowledgement: This work was supported by the Swiss National Science Foundation (grant CRSI20\_122693/1) and the European Space Agency (ESA). We thank F. Gruet, P. Scherler, and M. Durrenberger for their contributions to the realization of the hardware.

#### REFERENCES

- [1] A. M. Braun et al., Proc. of the 39<sup>th</sup> Precise Time and Time Interval (PTTI) Meeting, Long Beach CA, USA, p. 233 (2007).
- [2] J. Di Francesco et al., Proc. SPIE Vol. 7720, 77201T (2010).
- [3] S. Micalizio et al., Proc. of the European Frequency and Time Forum (EFTF), ESA-ESTEC, Noordwijk, The Netherlands, (2010).
- [4] G. Mileti et al., Proc. of the European Frequency and Time Forum (EFTF), ESA-ESTEC, Noordwijk, The Netherlands, ESA-SP340, p. 515 (1992).

Poster Presentations – Laser, Laser Spectroscopy P.LS.10

### **Investigation of Color Balance Failure of offset printed images expressed by Color Difference in dependence of different Standard Illuminant Conditions**

I. Spiridonov, M. Shopova, R. Boeva and M. Nikolov  
*University of Chemical Technology and Metallurgy, Department of Printing Arts, Pulp and Paper  
Sofia, Bulgaria*  
e-mail: mariana\_k\_sh@abv.bg

One of the biggest problems in color reproduction processes are color shifts occurring when the images are viewed under different illuminants. Process ink colors and their combinations that match under one light source will often appear different under the other. Many people incorrectly refer to this phenomenon as metamerism. This problem is referred as Color Balance Failure or Color Inconstancy. According ISO standards ICC color profiling assumes the print is viewed under CIE D50 lighting. With most pigment sets (CMYK inks solid and/or used together) the gray gradient and all colors shifts considerably when viewed under different illuminants.

The main goals of this research are investigation and determination of Color Balance Failure (Color Inconstancy) of offset printed images expressed by Color Difference in dependence of different standard illuminant conditions. For experiment were chosen three of most commonly used in practice illuminants – CIE D50 natural horizon daylight with color temperature 5003 K; CIE F2 cool white fluorescent, 4230K; CIE A typical Tungsten-filament lighting, 2856 K. A special test form that have been used contains different control strips and measurement components include test chart TC6.02 with about 1000 color patches with different percent combinations of Cyan, Magenta, Yellow and Black. The papers, printing inks and printing presses used in experiment are some of most commonly used in practice for producing of high quality color reproductions. A spectrophotometer/densitometer of type SpectroEye and X-Y SpectroScan of GretagMachbeth has been used for measuring of optical density and the color characteristics in the CIE Lab color system.

A series of colorimetric and densitometric measurements were performed for different combinations of C, M, Y, K in single, double, triple and quadruple overprint for high tones, middle tones and dark tones.

For estimating of Color Balance Failure for all above mentioned measurements it have been calculated the color difference in dependence of standard illuminants CIE D50, CIE F2, CIE A. The results achieved are important from scientific and practical point of view.

For a first time a methodology is suggested and implemented for examination and estimating of color shifts by studying a big number of color changes in various ink combinations for different illuminants.

**Keywords:** Color difference, Color Balance Failure, Standard Illuminant, Image quality

#### REFERENCES

- [1] ISO 3664:2009, Viewing conditions - Graphic technology and photography. Viewing conditions – Graphic technology and photography
- [2] ISO 12647-2:2004, Graphic technology - Process control for the production of half-tone colour separations, proof and production prints - Part 2: Offset lithographic processes
- [3] ISO 13656, Graphic technology - Application of reflection densitometry and colorimetry to process control or evaluation of prints and proofs
- [4] CIE 15:2004 Colorimetry
- [5] CIE Standard; CIE Colorimetric illuminants, ISO/CIE 10526 – 1991 (CIE S001-1986)
- [6] CIE International Lighting Vocabulary, item 845-02-59, CIE 17.4 – 1987

Poster Presentations – Laser, Laser Spectroscopy P.LS.11

### Terahertz pulse copropagation in ammonium vapors

S.Vidal<sup>1</sup>, J.Degert<sup>1</sup>, J. Oberlé<sup>1</sup>, E.Freysz<sup>1</sup>, O.Fedotova<sup>2</sup>, G.Rusetsky<sup>2</sup> and O.Khasanov<sup>2</sup>

1. *Centre de Physique Moléculaire Optique et Hertzienne, UMR-CNRS 5798, Université Bordeaux I, 351 course de Liberation, Talence 33400 France*
2. *Scientific-Practical Material Research Centre, Belarus National Academy of Sciences, 19 Brovki str., Minsk 220072 Belarus*  
e-mail: olfe@ifftp.bas-net.by

Terahertz (THz) spectral region attracts much attention of scientists anticipating its importance for solutions of many problems, for example, such as biomedical diagnostics, law enforcement, environment monitoring, characterization of complex molecules, nanostructures, metamaterials, etc. Since the THz frequency range corresponds to the inverse of femtosecond pulse duration, femtosecond lasers have been widely used to generate broadband single-cycle THz waves. As a result the broadband THz pulse covering many rotational transitions in molecular vapors may excite simultaneously multiple transient coherent signals [1]. However, many applications for ultrahigh-speed optoelectronic devices and THz time-domain spectroscopy require not only single-cycle THz pulse generation or cw THz sources, but also arbitrary THz waveform generators. Therefore the development of schemes of the THz pulse shaping is timely. In the work [2] the effective method of THz pulse shaping which consists in synthesis of THz pulses via optical rectification of shaped laser pulses has been developed. At this one can produce mono- an many-cycle pulses that have strong peak powers able to reach several tens of milliwatts.

In this work we consider the propagation of THz pulses resonant with lowest rotational levels in ammonia vapors (in particular, 0.6 THz and 1.2 THz) and estimate experimental realization of pulse propagation in solitonic regime. We also demonstrate the possibility of simulton propagation of two color THz pulses accounting for many involved transitions. At this, simulton formation is available for pulses of comparable (equal) as well as different intensity in dependence on preliminary preparation of the medium. More intensive pulse may be two- and even three-humped while the weak pulse is one-humped and its area may be much less than  $2\pi$ . The more-humped intensive pulse the weaker the second one. The stability of the coupled state of two pulses is provided by that the two-humped pulse makes the medium transparent for the one-humped pulse. Moreover we investigate the conditions of

interchanneling of two copropagating THz pulses with different frequencies in ammonia vapors. The form and intensity of such pulses are estimated and the origin of pulse interchanneling is discussed.

#### REFERENCES

- [1] H. Harde, D.R. Grischkowsky, JOSA B, 8, 1642 (1991).  
 [2] C. D'Amico, M. Tondusson, J. Degert, E. Freysz, Opt. Express. 17, 592 (2009).

Poster Presentations – Laser, Laser Spectroscopy P.LS.12

### Laser optics and spectroscopy of the cooperative electron $\gamma$ - nuclear processes in molecular systems

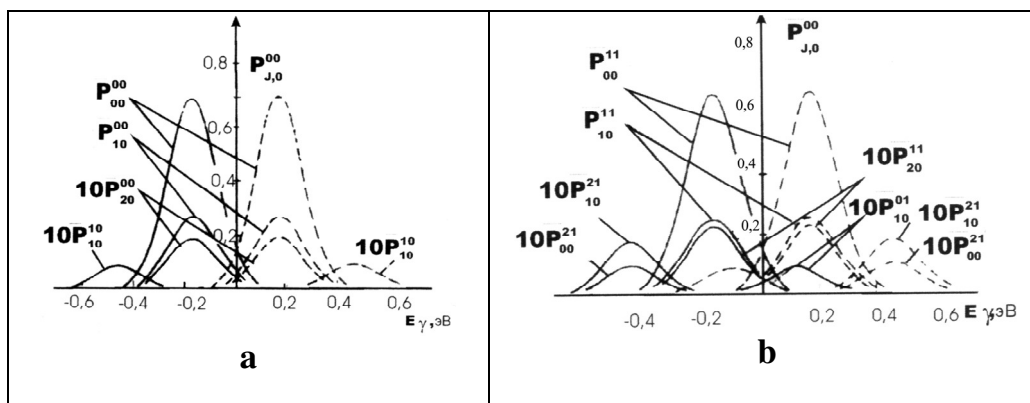
A.V. Glushkov<sup>1,2</sup> and A.A. Svinarenko<sup>1</sup>

<sup>1</sup>Odessa University, P.O.Box 24a,  
 Odessa-9, Ukraine

<sup>2</sup>ISAN, Russian Academy of Sciences,  
 Troitsk, Moscow reg., Russia

e-mail: glushkov@paco.net

A new class of problems has been arisen in the modern quantum optics and spectroscopy and connected with modelling of the co-operative laser-electron-nuclear phenomena in the molecular systems [1,2]. It includes a calculation of the probabilities and energies of the mixed  $\gamma$ -optical quantum transitions in molecules, intensities of the complicated  $\gamma$ -transitions due to the changing of the molecular excited states population under action of laser radiation, quantum calculation of a system “laser-nucleus-electron shells of a molecule” [2]. Due to the emission or adsorption of the nuclear  $\gamma$ -quantum in molecular system there is changing the electron vibration-rotation molecular states. We developed new quantum approach to calculation of electron-nuclear  $\gamma$  transition spectra (set of vibration satellites) of nucleus in a molecule, based on the density functional (DF) formalism and energy approach (S-matrix formalism of Gell-Mann and Low) [1]. Decay and excitation probability are linked with imaginary part of the atom (molecule) - field system. Calculation results of electron-nuclear  $\gamma$ -transition spectra of the nucleus in some diatomic and multiatomic molecules are presented. As illustration in figures a and b the spectrum of emission and adsorption of nucleus  $^{127}\text{I}$  ( $E_\gamma=203\text{keV}$ ) in molecule of  $\text{H}^{127}\text{I}$  is presented (the initial state of molecule: (a)  $v_a=0, J_a=0$ ; b)  $v_a=1, J_a=0$ ). Estimates are made for vibration-nuclear transition probabilities for number of molecules: diatomics, 3-atomic  $\text{XY}_2$  ( $D_{\infty h}$ ), 4-atomic  $\text{XY}_3$  ( $D_{3h}$ ), 5-atomic  $\text{XY}_4$  ( $T_d$ ), 7-atomic  $\text{XY}_6$  ( $O_h$ ) ones.



#### REFERENCES

- [1] V.S.Letokhov, V.G.Minogin, JETP. 69, 1569 (1975); 70, 794 (1976); L.N.Ivanov, V.S.Letokhov, JETP. 93, 396 (1987); A.V.Glushkov, L.N.Ivanov, Phys.Lett.A 170,33 (1992); A.V.Glushkov,

L.N.Ivanov, V.S.Letokhov, Preprint of Institute for Spectroscopy of the USSR Academy of Sciences, ISAN, N AS-1, Troitsk, (1991).

[2] A.V. Glushkov, O.Yu. Khetselius, A.V.Loboda, A.A.Svinarenko, *Frontiers in Quantum Systems in Chemistry and Physics, Ser. Progress in Theoretical Chemistry and Physics* (Berlin, Springer). 18, 523 (2008); A.Glushkov, O.Khetselius, S.Malinovskaya, *Europ.Phys.J.*160, 195 (2008); *Molec.Phys.* 108, 1257 (2008); A.V.Glushkov, O.Yu. Khetselius, A.A.Svinarenko, G.P.Prepelitsa, In: *Coherence and Ultrashort Pulsed Emission*, Ed. Darte F. J. (Intech, Vienna). 159 (2010).

Poster Presentations – Laser, Laser Spectroscopy P.LS.13

## The interpretation of the intensity of components of laser scattering by interaction with matter

Z. Fidanovski<sup>1</sup>, M. Srećković<sup>2</sup>, S. Ostojić<sup>3</sup>, J. Ilić<sup>4</sup> and M. Merkle<sup>2</sup>

<sup>1</sup>*School of computing, Union University, Belgrade, Serbia*

<sup>2</sup>*Faculty of Electrical Engineering, Belgrade, Serbia*

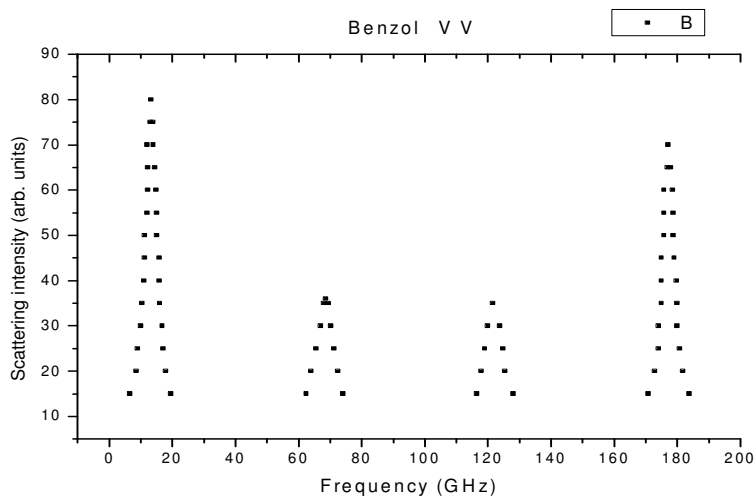
<sup>3</sup>*Faculty of Technology and Metallurgy, Belgrade, Serbia*

<sup>4</sup>*Faculty of Mechanical Engineering, Belgrade, Serbia*

e-mail: zfidanovski@raf.edu.rs

Light scattering, as an optical method, is very efficient in experimental estimation of many quantities in various fields. The scattered laser beams give the description of a scattering medium, i.e. it is the response of a medium to a certain light impact – the response that contains certain information about the matter. The measurement of scattered light properties offers many optical, acoustical, dielectric, thermodynamic and other data about the scattering medium.

Brillouin spectroscopy in various modifications and with different laser types has become a measurement technique in acoustics long time ago. It enables more detailed and more exhaustive knowledge of the acoustic properties of a matter, beside of optical data.



A series of Rayleigh-Brillouin spectra are recorded for set of organic solutions and their mixtures. The equipment used in spectrum recording enables the measurement of four components of scattered laser intensity  $I_{hh}$ ,  $I_{hv}$ ,  $I_{vv}$  and  $I_{vh}$ . The ratios of the width of different lines, as well as their distance, are determined for Rayleigh-Brillouin spectra. According to Brillouin shifts, the velocity of hypersound, and absorption coefficients of analyzed fluids can be calculated. There are numerous softwares for processing of data obtained in laser interaction (scattering) with matter in various fields,

created with different programming tools. The analysis of obtained spectra is performed, i.e. the examination of which distribution (Gaussian or Lorentzian) explains or support better the experimentally obtained diagrams (Fig.1).

## **Modeling of electron relaxation processes and the optical gain in magnet-field assisted THz quantum cascade laser**

A. Daničić<sup>1</sup>, J. Radovanović<sup>2</sup>, V. Milanović<sup>3</sup>, D. Indjin<sup>3</sup> and Z. Ikonić<sup>3</sup>

<sup>1</sup>*Vinca Institute of Nuclear Sciences,  
Belgrade, Serbia*

<sup>2</sup>*School of Electrical Engineering,  
University of Belgrade, Serbia*

<sup>3</sup>*School of Electronic and Electrical Engineering,  
University of Leeds, UK*

e-mail: aleksandar\_danicic@vin.bg.ac.rs

We present a detailed model for calculating the optical gain of quantum cascade laser that operates in the terahertz spectral range [1-6], when subjected to a strong magnetic field, as well as the total relaxation rates due to the emission of LO phonons and interface roughness scattering [5,6], as a function of the applied field. When the magnetic field is applied in the direction perpendicular to the plane of the layers, each energy state is split into series of discrete Landau levels, which are magnetically tunable and it is therefore possible to control the modulation of the population inversion, and consequently the optical gain, just by varying the magnetic field [3,5, 7-13]. In this model, the gain is obtained by solving the full system of rate equations, from which one can calculate the carrier densities of each level. The simulations are performed on a system that comprises two-well design quantum cascade laser that operates at 4.6 THz [2], implemented in GaAs/Al<sub>0.15</sub>Ga<sub>0.85</sub>As. Numerical results are presented for magnetic field values from 0.1T up to 20T, while the band nonparabolicity is taken into account.

### ACKNOWLEDGEMENTS

This work was supported by the Ministry of Science (Republic of Serbia), ev. no.III 45010.

### REFERENCES

- [1] N. Péré-Laperne, L. A. de Vaultier, Y. Guldner, G. Bastard, G. Scalari, M. Giovannini, J. Faist, A. Vasanelli, S. Dhillon, C. Sirtori, Appl. Phys. Lett. 91, 062102 (2007).
- [2] S. Kumar, C. W. I. Chan, Q. Hu and J. Reno, Appl. Phys. Lett. 95 14110 (2009).
- [3] A. Wade, G. Fedorov, D. Smirnov, S. Kumar, B. S. Williams, Q. Hu, J. L. Reno, Nature Photon. 3, 41 (2009).
- [4] G. Scalari, M. I. Amanti, C. Walther, R. Terazzi, M. Beck, J. Faist, Opt. Express 18, 8043 (2010)
- [5] A. Leuliet, A. Vasanelli, A. Wade, G. Fedorov, D. Smirnov, G. Bastard and C. Sirtori, Phys. Rev. B 73, 085311 (2006).
- [6] T. Unuma, M. Yoshita, T. Noda, H. Sakaki and H. Akiyama, J. Appl. Phys. 93, 3 (2003).
- [7] I. Savić, N. Vukmirović, Z. Ikonić, D. Indjin, R. W. Kelsall, P. Harrison, V. Milanović, Phys. Rev. B 76, 165310 (2007).
- [8] I. Savić, Z. Ikonić, N. Vukmirović, D. Indjin, P. Harrison, V. Milanović, Appl. Phys. Lett. 89, 011109 (2006).
- [9] Y. Chen, N. Regnault, R. Ferreira, B.-F. Zhu, G. Bastard, Phys. Rev. B 79, 235314 (2009).
- [10] J. Radovanović, V. Milanović, Z. Ikonić, D. Indjin, P. Harrison, J. Appl. Phys. 97, 103109 (2005).
- [11] J. Radovanović, A. Mirčetić, V. Milanović, Z. Ikonić, D. Indjin, P. Harrison, R. W. Kelsall, Semicon. Sci. Technol. 21, 215 (2006).

[12] A. Daničić, J. Radovanović, V. Milanović, D. Indjin, Z. Ikonić, *J. Phys. D: Appl. Phys.* **43**, 045101 (2010).

[13] C. Becker, A. Vasanelli, C. Sirtori and G. Bastard, *Phys. Rev. B* **69**, 115328 (2004).

Poster Presentations – Laser, Laser Spectroscopy P.LS.15

## Development of an array of scalar and vector Cs magnetometers for a neutron EDM experiment

Z. Grujic<sup>1</sup>, M. Kasprzak<sup>1</sup>, P. Knowles<sup>1</sup>, and A. Weis<sup>1</sup>

<sup>1</sup>*Department of Physics, University of Fribourg,*

*CH-1700 Fribourg, Switzerland*

e-mail: zoran.grujic@unifr.ch

The existence of a nonzero permanent electric dipole moment (EDM) of the neutron is a question of primary importance in fundamental particle physics. For neutrons precessing in a small constant magnetic field, an EDM is detectable via a proportional shift that a static electric field (applied parallel or anti-parallel) to the magnetic field it induces in the precession frequency. This frequency shift is measured by Ramsey's method of time separated oscillating fields applied to stored ultracold neutrons. The experimental goal is to achieve an EDM sensitivity of  $10^{-28}$  e·cm, needed to advance the field. To achieve this precision, the measurement and control of the offset magnetic field and all its spatial and temporal gradients has to be done with sensitivity below  $100$  fT/Hz<sup>1/2</sup>. For this purpose, an array of optically pumped atomic Cs magnetometers has been developed at Fribourg University.

The magnetometers are based on double resonance in an anti-relaxation (paraffin) coated, spherical vacuum cells containing Cs vapour at ambient temperature [1]. The vapor is magnetized by optical pumping with circularly polarized laser light on the  $F_g = 4 \rightarrow F_e = 3$  D<sub>1</sub> transition at 894 nm. The precession of the magnetization around offset magnetic field is driven by small magnetic rf field oscillating at the Larmor frequency. The spin precession induces a modulation of the light intensity, whose phase with respect to the oscillating field is measured. Magnetic field changes are then monitored as changes of that phase.

The present magnetometer system, installed at the Paul Scherrer Institute (Switzerland), consists of 12 vacuum compatible sensors, of which four are high voltage compatible. The system is in constant evolution in order to adapt it to the operating environment of the nEDM experiment and to improve its sensitivity. Recently, the sensor geometry has been modified to provide true scalar devices [2]. Currently we are working on the development of vector magnetometers based on the techniques proposed in [3]. Progress of this work shall be presented.

### REFERENCES

[1] N. Castagna, G. Bison, G. Di Domenico, A. Hofer, P. Knowles, C. Macchione, H. Saudan, A. Weis, *Appl. Phys. B* **96**, 763 (2009).

[2] A. Weis, "rf projection phase error in Cs OPMs", Internal report, University of Fribourg.

[3] E. B. Alexandrov et al., *Meas. Sci. Technol.* **15**, 918 (2004).

## **Laser applications in retinopathy as invasive therapy and possibility of pre and post diagnostics by appropriate image processing**

Z. Latinovic<sup>1</sup>, A. Oros<sup>2</sup>, M. Sreckovic<sup>1</sup>, J. Ilic<sup>3</sup> and P. Jovanic<sup>4</sup>

<sup>1</sup>*Faculty of Electrical Engineering, University of Belgrade, Bulevar Kralja Aleksandra 73, Belgrade, Serbia*

<sup>2</sup>*University Eye Clinic, Clinical Center of Vojvodina, Hajduk Veljkova 1, 21000 Novi Sad, Serbia*

<sup>3</sup>*Faculty of Mechanical Engineering, University of Belgrade, Kraljice Marije 16, Belgrade, Serbia*

<sup>4</sup>*Institute of Multidisciplinary Studies, Belgrade, Serbia*

e-mail: esreckov@etf.rs

Retinopathy of Prematurity (ROP) is a leading cause of blindness in children. The ROP is a disease that occurs in premature infants and affects the blood vessels of the developing retina. The unique feature of ROP relates to its occurrence only in premature infants with immature and incompletely vascularized retina. We reduce the blindness from ROP by appropriate screening and effective diode laser treatment (diode red 810nm). Ocular fundus photos are performed as a part of ROP screening. During screening examination, the RetCam3, equipped with 130° lens, is used to obtain the color images of both eyes. In all cases of active posterior ROP the laser treatment is performed. In those infants the fundus images are taken in sessions of laser treatment and it is repeated one or two weeks later. The goal of each imaging session is to obtain clear and focused images of all parts of the ocular fundus. The images are stored on the RetCam3 computer hard drive.

This paper attempts to compare certain methods of quantifying results of several stages of the pathological eye conditions in clinical practice based on RetCam image records. The first image processing is related to the application of color analysis by the program Matcad. It is scrutinized if the increased or decreased presence of certain colors in an image of a full eye or specific parts of the eye indicates the degree/severity of the disease (pathological state). Another approach is the implementation of the program Image J. The third quantification belongs to fractional analysis where several approaches are executed related to the application of different filtrations. Herein it is addressed the analysis of concrete examples and analysis of different utility levels of processing technique. In particular, some issues of interaction of the three laser types with eye tissue in various operating modes (ex. Q-switched lasers and others) are particularly discussed.

## Stress and strain of dental abutment caused by the polymerization shrinkage of dental composite

T. Puskar<sup>1</sup>, D. Vasiljevic<sup>2</sup>, L. Blazic<sup>1</sup>, D. Markovic<sup>1</sup>, S. Savic-Sevic<sup>2</sup>, B. Muric<sup>2</sup>, D. Pantelic<sup>2</sup>

<sup>1</sup>*Faculty of Medicine - School of Dentistry, University of Novi Sad,  
Vojvodina Dental Clinic, Hajduk Veljkova 12, Serbia*

<sup>2</sup>*Institute of Physics, Photonics Center, University of Belgrade  
Pregrevica 118, Zemun, Serbia*

e-mail: tatjanapuskar@yahoo.com

Resin composites are widely used as a core build up restorations of endodontically treated teeth prior to a crown placement [1]. Besides many favorable characteristics, resin composite core build up restorations have the potential to generate deformation and stresses of dental tissues due to polymerization contraction. Contraction stress resulting from polymerization shrinkage could be potentially a serious problem for surrounding tooth tissues [2, 3]. A total amount of resulting stress and strain depends on many factors and cannot be determined in a simple manner [4].

The primary aim of this study was detecting and recording the deformation of an abutment teeth prepared for a full ceramic crown during dental composite core build up polymerization using real time holography. The second aim was to calculate stress and strain induced using finite element analysis (FEA) on the previously created mathematical models.

**Materials and methods:** Five intact maxillary first incisors were endodontically treated and prepared for all-ceramic restoration, as a standard procedure [1]. Deformation of the hard dental tissues during polymerization of resin composite core build up was recorded and measured using real time holographic interferometry. The interference pattern was recorded with a CCD camera. Interferograms were analyzed by counting fringes during illumination. One fringe was equivalent to approximately 532 nm deformation. The mechanical model of the abutment, containing the prepared cavity, was done as a solid model with complex geometry in the program for solid modeling SolidWorks according to the literature data (*Solid Works Corporation, USA*). Stress and strain of the dental tissue were calculated using FEA in software Abaqus (SIMULIA, Dassault Systems S.A., USA).

**Results:** The deformation of dental hard tissue due to light-induced polymerization process of dental composite core build up was recorded. During polymerization, the fringes appeared at the top of the abutment teeth and started to travel down towards the root. The maximum deformation was attained at the end of the illumination process. The greatest value of the dental hard tissue deformation was 8.5  $\mu\text{m}$ . The numerical calculation of an internal stress was performed, based on holographic deformation measurement. The mechanical model was meshed and FEA showed that the greatest Von Mises stress was found on the abutment teeth cavity inner edges and corners (4.15 MPa). Von Mises stress in the entire coronal tissue was in range from 1.3 MPa to 4.15 MPa. The stress values found were lower if compared to the literature data stress values which could cause a damage of an abutment tissue [5].

**Conclusion:** The deformation of the dental tissue found and the stress calculated by FEA could not cause a damage of the abutment.

### REFERENCES

- [1] S. Rosenstiel, M. Land, J. Fujimoto, Contemporary fixed prosthodontics, Mosby 275 (2006).
- [2] H.Y. Chen, J. Manhart, R. Hickel, K.H. Kunzelmann, Dent. Mater. 17, 253 (2001).
- [3] D. Pantelić, L. Blažić, S. Savić-Šević, B. Murić, D. Vasiljević, B. Panić, I. Belić, Opt. Express, 15, 6823 (2007).
- [4] J.L. Ferracane JL, Dent. Mater. 21, 36 (2005).
- [5] J.H. Kinney, S.J. Marshall, G.W. Marshall, Crit. Rev. Oral. Biol. Med. 14, 13 (2003).

### 3D Solid model generation of a human maxillary premolar based on CT data

D. Vasiljević<sup>1</sup>, I. Kantardžić<sup>2</sup>, L. Blažić<sup>2</sup>, M. Tasić<sup>3</sup> and T. Puškar<sup>2</sup>

<sup>1</sup>Photonics Center,

Institute of physics,

University of Belgrade, Serbia

<sup>2</sup>School of Dentistry,

Faculty of Medicine,

University of Novi Sad, Serbia

<sup>3</sup>College of Applied Sciences Tehnikum Taurunum,

Belgrade, Serbia

e-mail:darko@ipb.ac.rs

Among all the performances of a dental materials and tooth structures, their mechanical properties can be investigated either experimentally or with numerical simulations. In the other hand, any *in vivo* experiment or clinical trial performed could be ethically questionable, very expensive and/or time consuming. According to that, a development of the mathematical model of tooth structures is very desirable.

The first step made in the development of the 3D complex tooth mathematical model, was using the literature data in order to build the simplified mathematical model [1]. This simplified mathematical model can be used in calculation of various types of stress and strain in the tooth structures generated by different therapeutic procedures [2]. Calculation of stress and strain is usually done in programs for the finite element analysis.

In this paper, development of the 3D solid model of the human maxillary premolar based on CT data is presented. The first step was a scanning procedure of the extracted upper second premolar by Sensation 64 Cardic CT scanner (Siemens, Germany). The scannes were written in the series of files in DICOM file format. The program AMIRA (Visage Imaging, USA) was used for analysis and forming input data for the program SolidWorks (SolidWorks Corp. USA). The program SolidWorks is well known program for construction of a 3D solid models and finite element analysis. All of mayor tooth tissues and surrounding structures were modeled: enamel, dentin, pulp, peridental ligament and cortical bone. In the finite element analysis the linear static analysis was used, and all of the tooth structures were represented by Young's modulus of elasticity and Poisson's ratio.

#### REFERENCES

- [1] T. Puškar, D. Vasiljević, D. Marković, D. Jevremović, D. Pantelić, S. Savić – Šević, B. Murić, *Srpski arhiv za celokupno lekarstvo* 138, 19 (2010).  
 [2] D. Pantelić, L. Blažić, S. Savić-Šević, B. Murić, D. Vasiljević, B. Panić, I. Belić, *Opt. Express* 15, 6823 (2007).

## CT Scan-based finite element analysis of stress distribution in premolars restored with composite resin

I. Kantardžić<sup>1</sup>, D. Vasiljević<sup>2</sup>, L. Blažić<sup>1</sup>, T. Puškar<sup>1</sup> and M. Tasić<sup>3</sup>

<sup>1</sup>University of Novi Sad, Faculty of Medicine, School of Dentistry, Novi Sad, Serbia

<sup>2</sup>University of Belgrade, Institute of Physics, Belgrade, Serbia

<sup>3</sup>College of Applied Sciences Tehnikum Taurunum, Belgrade, Serbia

e-mail: ivanakantardzic@gmail.com

Mechanical properties of a dental restorative material influence stress distribution during mastication in both, the remaining tooth structure and restorative material as well [1]. An investigation of these properties can be done experimentally [2] and numerically [3]. Due to the fact that *in vitro* and *in vivo* experiments may be quite expensive and ethically questionable, the use of a 3D solid tooth models and numerical simulations became a valuable tool for saving time and money spent in laboratory and/or clinical research [4].

The aim of this study was to investigate an influence of the restorative material with different modulus of elasticity on stress distribution in the 3D solid tooth model using a finite element analysis (FEA). Computed tomography (CT scan) data of the human maxillary second premolar was used for the 3D solid model generation. Tooth reconstruction with four different composite resins: modulus of elasticity of 6.7 GPa (Gradia Direct Posterior, GC, Japan), 9.5 GPa (Herculite XRV, Kerr Corp, USA), 14.1 GPa (Charisma, Heraeus Kulzer, Germany) and 21 GPa (Filtek Z100, 3M ESPE, USA) for MOD (mesio-occluso-distal) cavity restoration was simulated in SolidWorks 2009 software (Dassault Systèmes SolidWorks Corp, USA). Each model was subjected to a resulting force of 200 N directed to occlusal surface and stress distribution and maximal von Mises stresses were calculated using finite element analysis.

The stresses in the enamel and dentin did not vary much with changing modulus of elasticity of the composite resin. In contrast, maximal von Mises stresses in restorative material increased (6.7-12.2 MPa) with increasing the composite resin modulus of elasticity. For all the models, stresses were concentrated at the loading point and at the cervical region of palatal surface. This is in accordance with clinical experience in MOD restored premolars, where palatal cusp fractures more often than buccal.

The results showed that tooth reconstruction with the low modulus composite resin material provided more favorable biomechanical performance in restoring premolar with MOD cavity. On the other hand, the restorative material modulus of elasticity did not influence the stress distribution pattern. These findings proved the numerical simulation is a useful method for investigation tooth biomechanics after different restorative procedures.

### REFERENCES

- [1] W. Jiang, H. Bo, G. YongChun, Ni. LongXing, J. Prosthet Dent 103, 6 (2010).
- [2] P. Soares, P. Santos-Filho, L. . Martin, C. Soares, J. Prosthet Dent 99, 30 (2008).
- [3] P. Soares, P. Santos-Filho, L. . Martin, C. Soares, J. Prosthet Dent 99, 114 (2008).
- [4] P. Ausiello, P. Franciosa, M. Martorelli, D. Watts, Dent. Mater (2011),  
doi:10.1016/j.dental. 2010.12.001.

## Influence of photodiagnostic radiation on iron release by ferritin

L. Vladimirova and V. Kochev

*Sofia University, Faculty of Physics, Department of Atomic physics, Sofia, Bulgaria*

e-mail: vladimirova@phys.uni-sofia.bg

The influence of radiation used for photodiagnosis of skin diseases on iron release by ferritin is investigated in this work.

The ferritins are family of iron storage proteins and play a key role in biochemical transformations between iron and oxygen. The processes are exceptionally important for all living organisms. The iron stored within the ferritin as a mineral core of insoluble crystal is in the form of Fe(III). It is well known, however, that the core can be reduced by visible light as well as by near IR or UV with subsequent release of Fe(II), the last being dangerous agent. This work considers the induction of Fe(II) release from ferritin under exposure to photodiagnostic radiation with wavelength 635 nm. The quantity of the reduced iron in the solution is determined by the method of potentiometric titration. This technique already was proved to be a reliable tool for detection of Fe(II).

## X-ray diffraction and FT-infrared spectroscopy in analyzing the hydroxyapatite for the application in dentistry

M. Đorđević<sup>1</sup>, D. Jevremović<sup>1</sup>, T. Puškar<sup>2</sup>, A. Kovačević<sup>3</sup>, G. Bogdanović<sup>4</sup>

<sup>1</sup>*University Business Academy, School of Dentistry, Pančevo, Serbia*

<sup>2</sup>*University of Novi Sad, School of Medicine, Department of Dentistry, Novi Sad, Serbia*

<sup>3</sup>*Institute of Physics, University of Belgrade, Belgrade, Serbia*

<sup>4</sup>*Oncology Institute of Vojvodina, Sremska Kamenica*

e-mail: aleksander.kovacevic@ipb.ac.rs

Spectroscopic techniques, like ultraviolet-visible (UV-VIS), infrared (IR), X-ray diffraction (XRD) and Fourier-transform infrared (FTIR), are attractive analytical methods commonly used in materials science, and for bio-materials and biological tissues [1, 2]. The methods are non-contact, non-destructive, providing the information on the composition of the sample and on the structure. Due to its short wavelength, XRD provide the best resolution. In FTIR, beams with different combinations of wavelengths propagate consecutively through a sample and from recorded spectra of each transmitted beam the information on the sample is derived.

Hydroxyapatite (HAP) is the inorganic matrix of bone tissue [3]. Among many bioactive materials in dentistry, it can be used as bone substitute or as a pulp capping material. It strengthens soften dentine at the application site and induces the formation of the barrier of solid dental tissue without major destruction of the pulp tissue below. HAP bioactivity could be influenced by the surrounding conditions such as saliva presence. XRD can be used for analyzing the crystallographic structure, chemical composition and physical properties of HAP [4]. The degree of change in all HAP particles cannot be determined by solely one spectroscopic method; therefore a combination of different methods of different resolutions from different areas of the electromagnetic spectrum (from X to IR) should be used. In this work, the aim is to determine - by using XRD and FTIR - the structural, morphological and chemical changes of HAP induced by artificial saliva.

**Materials and methods.** Ten HAP samples, each of 0.5 g, have been exposed to artificial saliva for 35 days. XRD patterns (Siemens 50 rd) of the samples have been recorded at regular intervals in order

to determine the structural changes. Simultaneously, the FTIR spectrum of HAP solution in artificial saliva was recorded by Perkin-Elmer FTIR 403.

**Results.** XRD and FTIR analyses have shown that the artificial saliva induces the activation of HAP. Both the dissociation of calcium ions into the surrounding solution and the increase in free phosphorous ions concentration on the sample surface were evidenced by FTIR analysis. At the same time, there was a considerable degree of degradation of the basic crystalline structure of HAP (amorphization) as evidenced by XRD.

**Conclusion.** Using the combination of X-ray diffraction and FT-infrared spectroscopy, it was possible to obtain the data on changes occurring in the HAP-saliva system, under which it is possible to set the hypothetical mechanisms of HAP activation induced by saliva

**Acknowledgements.** The work is supported by the Ministry of Science of the Republic of Serbia under the contract III45016.

#### REFERENCES

- [1] C. M. Botelho, M. A. Lopes, I. R. Gibson et al., *J. Mater Sci.* 13, 1123 (2001).
- [2] F. H. Jones, *Surf. Sci. Rep.* 42, 75 (2001).
- [3] C.-C. Yang, C.-T. Lin, S.-J. Chiu, *Desalination* 233, 137 (2008).
- [4] B. S. Clausen, *Catalysis Today* 39, 293 (1998).

Poster Presentations – Biophotonics P.BP.7

### **Scattering of a laser beam in turbid media with sharply forward directed Henyey-Greenstein indicatrices**

L. Gurdev, T. Dreischuh, I. Bliznakova, O. Vankov, L. Avramov, and D. Stoyanov  
*Institute of Electronics, Bulgarian Academy of Sciences,  
72 Tsarigradsko chaussee, Sofia 1784, Bulgaria  
e-mail: tanjad@ie.bas.bg*

Optical tomography of biological tissues is a rapidly expanding research area that is expected to provide powerful non-invasive, non-radioactive methods for early diagnosis of human tissue diseases. The numerous variants of optical tomography being developed at present (see [1-3] and references therein) require knowledge of the optical properties of the tissues and the laws governing the radiative transfer within the investigated biological objects. This fact conditions the intensive investigations performed last years on the propagation of light inside turbid media which simulate real biological media (e.g., [4-6]).

In this work the propagation is investigated theoretically of a continuous laser beam through homogeneous tissue-like turbid media such as diluted emulsions of Intralipid having sharply forward directed Henyey-Greenstein indicatrices. The detected forward-propagating light power spatial distribution is described analytically, for relatively large or small “optical depth”, in the so-called small-angle approximation. It is shown, in particular, that near the entrance of the laser beam into the turbid medium, when the receiver aperture size exceeds the beam radius, the on-axis detected light power decreases exponentially with the depth in the medium, with the absorption coefficient as decay factor. At larger depth, another exponential-fall-off region exists along the beam axis, where the extinction coefficient is the decay factor. Further, a third in-depth region exists, where the decrease of the detected light power is inversely proportional to the depth in power of three or four.

Some experimental results have also been obtained concerning the detected-power cross-sectional radial distribution at different depths along the beam axis. They are consistent in general with the

analytical expressions obtained that are shown to allow one to estimate in principle the extinction, reduced-scattering and absorption coefficients and the g-factor of the investigated media.

The investigations performed and the results obtained are important for the development of new methods and techniques for more accurate determination of the optical parameters of turbid media such as tissues and experimental tissue-like phantoms. They would also be useful in the process of establishing the laws governing the radiative transfer inside the optically investigated biological objects.

#### ACKNOWLEDGEMENTS

This work has been supported in part by the Bulgarian National Science Fund under contract DO 02-112/08. One of the authors (IB) is thankful to the World Federation of Scientists (WFS) and the World Laboratory, Geneva, Swiss for the financial support.

#### REFERENCES

- [1] A. F. Fercher, W. Drexler, C.K. Hitzenberger, T. Lasser, Rep. Prog. Phys. 66, 239–303 (2003).
- [2] A.P. Gibson, J.C. Hebden, S.R. Arridge, Phys. Med. Biol. 50, R1–R43 (2005).
- [3] H.G. Bezerra, M.A. Costa, G. Guagliumi, A.M. Rollins, D.I. Simon, J. Am. Coll. Cardiol. Intv. 2, 1035-1046, doi:10.1016/j.jcin.2009.06.019 (2009).
- [4] S.D. Campbell, S. Menon, G. Rutherford, Q. Su, R. Grobe, Las. Phys. 17, 117-123 (2007).
- [5] R. Michels, F. Foschum, A. Kienle, Optics Express 16, 5907-5925 (2008).
- [6] P. Di Ninni, F. Martelli, G. Zaccanti, Proc. SPIE, vol. 7906, paper # 79060M (2011).

Poster Presentations – Biophotonics P.BP.8

## Comparison of beetroot extracts originating from several sites using Time Resolved Laser Induced Fluorescence Spectroscopy

M.S. Rabasovic<sup>1</sup>, D. Sevic<sup>1</sup>, M. Terzic<sup>2</sup> and B.P. Marinkovic<sup>1</sup>

<sup>1</sup>*Institute of Physics,  
University of Belgrade, Serbia*

<sup>2</sup>*Faculty of Science,  
University of Novi Sad., Serbia*

e-mail: bratislav.marinkovic@ipb.ac.rs

Beetroot (*Beta Vulgaris*) juice contains a large number of fluorophores which can fluoresce [1, 2]. Betanin (C<sub>24</sub>H<sub>27</sub>N<sub>2</sub>O<sub>13</sub>) makes up 75-95% of the total colouring matter found in the beet root, therefore it is used as a natural food coloring agent [3]. There is a growing interest in beet root extracts analysis, see [4] and references therein. On the other hand, there is only limited information about beetroot obtained without sample preparation and/or extraction of components from sample.

In this work we continue our study presented in [5], analyzing and comparing beet root extracts originating from several sites, using time resolved laser-induced fluorescence (TR-LIF) technique to measure fluorescence of samples at different excitation wavelength (340-475 nm) and for different sample dilutions. The fluorescence signals were detected without any special treatment of the red beet juice. The measurements can be a useful tool to provide information on changes in juice constituents, and can be used to compare varieties of beetroots. Fluorescence excitation-emission spectroscopy is also applied in this study to characterize the fresh juice of beetroot.

The time resolved fluorescence emission spectra of beetroot extract were acquired using a streak camera (Hamamatsu model C4334-01). Pulsed light excitation is provided by a tunable Nd-YAG OPO laser system (Vibrant model 266 made by Opotek, Inc.). The output of the OPO can be continuously tuned over a spectral range from 320 nm to 475 nm.

A detailed description and some of the preliminary results of our experimental set up are published recently [5-7].

#### REFERENCES

- [1] F. Gandia-Herrero, F. Garcia-Carmona, J. Escibano, J. Chromatogr. A, 1078, 83 (2005).
- [2] F. Gandia-Herrero, F. Garcia-Carmona, J. Escibano, Food Research International 38, 879 (2005).
- [3] H. M. C. Azeredo, A. N. Santos, A. C. R. Souza, Kenya C. B. Mendes, M. I. R. Andrade, Am. J. Food Technol. 2 (4), 307 (2007).
- [4] B. Nemzer, Z. Pietrowsky, A. Sporna, P. Stalica, W. Thresher, T. Michalowski, S. Wibraniec, Food Chemistry 127, 42 (2011).
- [5] M.S. Rabasovic, D. Sevic, M. Terzic, S. Savic Sevic, B. Muric, D. Pantelic, B.P. Marinkovic, Acta Physica Polonica A 116, 570 (2009).
- [6] M. Terzic, B.P. Marinkovic, D. Sevic, J. Jureta, A.R. Milosavljevic, Facta Universitatis, Series Phys. Chem. Technol. 6, 105 (2008).
- [7] D. Sevic, M.S. Rabasovic, B.P. Marinkovic, to appear in IEEE Transactions on Plasma Science, Vol. 39, Special Issue of Images in Plasma Science, (2011).

Poster Presentations – Biophotonics P.BP.9

### **Study of the thermal denaturation of S-layer protein from *Lactobacillus salivarius***

**L. Lighezan<sup>1</sup>, R. Georgieva<sup>2</sup> and A. Neagu<sup>3</sup>**

<sup>1</sup>*West University of Timisoara, Faculty of Physics,  
Timisoara, Romania*

<sup>2</sup>*“Stephan Angeloff” Bulgarian Academy of Science, Institute of Microbiology,  
Sofia, Bulgaria*

<sup>3</sup>*“Victor Babes” University of Medicine and Pharmacy,  
Timisoara, Romania*

e-mail: llighezan@physics.uvt.ro

S-layer proteins display intrinsic self-assembly property, forming monomolecular crystalline arrays [1, 2], which have been identified as outermost structures of the cell envelope in many organisms [3, 4]. The biological functions of S-layer proteins are not completely understood. It is assumed that S-layer proteins act as protective coats, cell shape determinants, molecular and ion traps, adhesion sites for exoenzymes, as well as structures involved in cell adhesion and surface recognition [1, 2].

It is known that the S-layer protein subunits are non-covalently linked to each other, as well as to the supporting cell wall, and can be disintegrated into monomers by denaturing agents or by cation substitution [1]. Using circular dichroism (CD) spectroscopy, in this work, we have studied the thermal denaturation of an S-layer peptide, extracted from *Lactobacillus salivarius*.

The far and near UV CD spectra of the S-layer peptide have been collected and the temperature dependence of the circular dichroism in the far and near UV spectral domains has been analyzed. The variable temperature results show that the secondary and tertiary structures of peptide change irreversibly due to the heating of the sample. After the cooling of the heated sample, the secondary and tertiary structures are partially recovered.

We have also found that the peptide unfolding depends on the sample concentration and on the rate of change temperature. Taken together, these properties concerning the thermal behavior of the S-layer protein could be important for a better understanding of the protein structure and function.

## REFERENCES

- [1] M. Sara, U. B. Sleytr, J. Bacteriol. 182, 859 (2000).
- [2] U. B. Sleytr, T. J. Beveridge, Trends Microbiol. 7, 253 (1999).
- [3] P. Messner, U. B. Sleytr, Adv. Microbiol. Physiol. 33, 213 (1992).
- [4] U. B. Sleytr, P. Messner, Ann. Rev. Microbiol. 37, 311 (1983).

# Optoelectronics and Optocommunications

Poster Presentations – Optoelectronics and Optocommunications P.OE.1

## Electric field enhancement in silicon slotted optical ring microresonators

B. Radjenović<sup>1</sup>, B. Milanović<sup>2</sup>, and M. Radmilović-Radjenović<sup>1</sup>

<sup>1</sup>*Institute of Physics, University of Belgrade,  
Pregrevica 118, Belgrade, Serbia*

<sup>2</sup>*Military Academy,  
Pavla Jurišića Šturma 33, Belgrade, Serbia  
e-mail:bradjeno@ipb.ac.rs*

Slotted waveguide structures have attracted significant research interests since they were first proposed [1]. Such slotted configurations exploit the fact that the introduction of a sub-wavelength slot in conventional slab waveguides leads to an extremely high electric field confinement inside the slot region. Various functional devices with complicated designs, such as ring resonators [2], have been made with the slot structures for potential optical communications or sensing applications.

In this paper we have investigated numerically parameters of practical interest such as bending loss, peak field localization, power confinement in various regions of the slotted optical ring microresonators waveguide structure shown in Fig. 1. The system consists of a ring (with a 60nm wide slot) and a bus waveguides made of silicon on the SiO<sub>2</sub> substrate. Presented results are obtained using 3D frequency-domain finite element method, where computational domain is closed using perfectly matched layers approach.

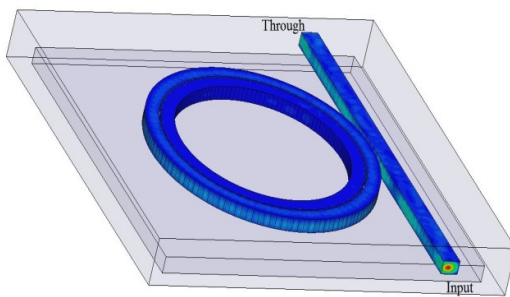


Figure 1.

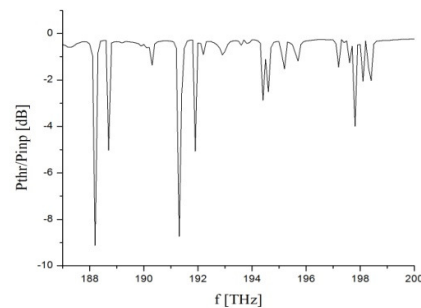


Figure 2.

The calculations are performed in the 187-200 [THz] (1.5-1.6 [μm]) spectral range with the step of 100GHz, for different slot positions. In Fig.1 we present the magnetic field distribution for the central slot position, at the first minimum (188.2 THz) of the transmission coefficient of the input bus (shown in Fig.2). The obtained results are compared with the 2D simulations for similar system based on the coupled mode theory (CMT) [3], and some limitations of the CMT are discussed. Also, it is shown that electromagnetic field confinement strongly depends on the slot position, in accordance with [4].

## REFERENCES

- [1] V. R. Almeida, Q. Xu, C. A. Barios, and M. Lipson, *Optics Letters* 29, 1209 (2004).
- [2] T. Baehr-Jones, M. Hochberg, C. Walker, and A. Scherer, *Applied Physics Letters* 86, 081101:1–3 (2005).
- [3] K. Hiremath, *OPTICS EXPRESS* 19, 8641-8655(2011).
- [4] P. Anderson, B.Schmidt, and M.Lipson, *OPTICS EXPRESS* 14, 9197–9202 (2006).

Poster Presentations – Optoelectronics and Optocommunications P.OE.2

## **A simple fiber optic inclination sensor based on the refraction of light**

J. Bajić<sup>1</sup>, D. Stupar<sup>1</sup>, A. Joža<sup>1</sup>, M. Slankamenac<sup>1</sup> and M. Živanov<sup>1</sup>

<sup>1</sup>*Faculty of Technical Sciences,  
Novi Sad, Serbia  
e-mail: drstupar@uns.ac.rs*

In scientific papers, there are many implementations of inclination sensors such as resistive [1], capacitive [2], inductive [3-5] and optical [6-10] sensors. The paper presents a relatively simple and low-cost plastic fiber optic inclination sensor based on refraction of light through medium. The sensor is cylindrical shaped and made of plastic with water as a liquid and two plastic optical fibers. At the center of the top and bottom base of the cylinder are plastic optical fibers connected to transmitter and receiver which are realized with ultra bright red LED and phototransistor, respectively. Sensor housing is filled with water to half of the height of the cylinder. The sensor is based on the Fresnel refraction on the boundary surface of two media inside sensor. The sensor is mounted on a precise manual rotation stage. As angle of the rotation stage increases, angle of boundary surface water-air in relation to fibers is changed. This causes change in intensity of received light in dependence on angle. In this paper the characteristic of the sensor measured in steps of 5 degrees is also given. Measured characteristic is symmetric in respect to 180 degrees. It has four linear regions and each linear region extends along 30 degrees. Immunity to electromagnetic interference is the advantage of this sensor realization compared to the resistive, capacitive and inductive. In the paper [10] is described fiber optic inclination sensor with mercury as a liquid, but with a different principle of operation. The advantage of our realization compared to the aforementioned is that in our solution we are using non-toxic materials.

## REFERENCES

- [1] C. H. Lin, S. M. Kuo, *Sensor Actuat. A-Phys.* 143, (2008).
- [2] D. Benz, T. Botzelmann, H.Kuck, D. Warkentin, *Sensor Actuat. A-Phys.* 123 (2005).
- [3] R. Olaru, D.D. Dragoi, *Sensor Actuat. A-Phys.* 120 (2005).
- [4] O. Baltag, D. Constandache, A. Salceanu, *Sensor Actuat. A-Phys.* 81 (2000).
- [5] R. Oiaru, C. Cotae, *Sensor Actuat A-Phys* 59 (1997).
- [6] R. Ragazzoni, S. R. Restaino, *Opt. Commun.* 137 (1997).
- [7] H. Bao, X. Dong, C. Zhao, L. Shao, C. C. Chan, P. Shum, *Opt. Commun.* 283 (2010).
- [8] H. Bao, X. Dong, L. Shao, C.Zhao, S. Jin, *Opt. Commun.* 283 (2010).
- [9] Y. Zhao, J. Yang, B. Peng, S. Yang, *Opt. Laser Technol.* 37 (2005).
- [10] A. Abu\_Al\_Aish, M. Rehman, *MASAUM Journal of Basic and Applied Sciences*, (2009).

## Tunneling times characterizing the electron transport through a multiple quantum well system with Rashba SOI

D.-M. Bălțățeanu

*West University of Timișoara, Faculty of Physics, Bd. V. Pârvan,  
No.4, 300223, Timișoara, Romania  
e-mail: bdmrancel@yahoo.com*

This paper deals with the tunneling of electrons through a quantum system with many barriers and asymmetric wells in an external and constant electric field. Due to the asymmetry of the confining potential in the growth direction, an internal electric field appears, perpendicular on the heterostructure layers. So one gets faced with the Rashba spin-orbit interaction (SOI), which creates a spin-splitting of the energy levels. Moreover, the transmission coefficient through the quantum heterostructure depends on the spin direction. The purpose of the paper is to compute some of the characteristic times corresponding to the electron tunneling through the considered system. The dependence of such times on the spin branches has also been discussed.

### REFERENCES:

- [1] E. I. Rashba, *Sov. Phys. Solid State* 2, 1109 (1960).
- [2] E.A. de Andrada e Silva, G.C. La Rocca, F. Bassani, *Phys. Rev. B* 55, 16293 (1997).
- [3] M. Erić, J. Radovanović, V. Milanović, Z. Ikonić, D. Indjin, *J. Appl. Phys.* 103, 083701 (2008).
- [4] M. Büttiker, R. Landauer, *Phys. Rev. Lett.* 49, 1739 (1982).
- [5] M. Büttiker, *Phys. Rev. B* 27, 6178 (1983).
- [6] C. R. Leavens, G. C. Aers, *Phys. Rev. B* 39, 1202 (1989).

## Monte Carlo simulation of Goos-Hänchen shifts in multimode step-index plastic optical fibers

M. S. Kovačević<sup>1</sup>, A. Djordjevich<sup>2</sup> and D. Nikezić<sup>1</sup>

<sup>1</sup>*Faculty of Science, Department of Physics, University of Kragujevac, Serbia*  
<sup>2</sup>*City University of Hong Kong, Tat Chee Avenue, Kowloon, Hong Kong*  
e-mail: kovac@kg.ac.rs

In this paper, the step-profile plastic optical fiber (POF) has been considered to give a quantitative example of how Goos-Hänchen (GH) shift effects on the ray transit time for traveling in axial distance  $z$ . The application of the three dimensional ray-tracing method based on Monte Carlo simulation reported earlier [1], has been adapted in order to study the importance of GH shift correction on pulse dispersion in POFs. The GH shift is considered as an accumulated effect along the length of the optical fiber. The GH shift corrections to pulse dispersion in POF are only significant when the angle  $\theta$  is near the critical angle  $\theta_c$ .

### REFERENCES

- [1] M. S. Kovacevic, D. Nikezic, and A. Djordjevich, *Appl. Opt.* 44, 3898 (2005).
- [2] A. W. Snyder and J. D. Love, *Applied Optics*, 15 (1), 236 (1976).
- [3] N. S. Kapany, J. J. Burke, *Optical Waveguides*, Academic Press, New York (1972).
- [4] W. A. Gambling, D. N. Payne, H. Matsumura, M. Medlicott, *E. Lett.* 10 (7), 99 (1974).
- [5] K. Thyagarajan and B. P. Pal, *J. Opt. Fiber Commun. Rep.* 4, 173 (2007).
- [6] K. F. Barrell and C. Pask, *Appl. Opt.* 19 (8), 1298 (1980).

## An analysis of modal dispersion in plastic optical fibers having W-shaped refractive index

M. S. Kovačević<sup>1</sup>, A. Djordjevich<sup>2</sup>

<sup>1</sup>*Faculty of Science, Department of Physics, Kragujevac, Serbia*

<sup>2</sup>*City University of Hong Kong, Tat Chee Avenue, Kowloon, Hong Kong*  
e-mail: kovac@kg.ac.rs

Plastic optical fibers (POFs) are highly promising transmission media for future short-range applications including in LANs, multi-node bus networks, sensors, power delivery systems, and light guides (as in toys, entertainment and medical devices). This paper presents the effect of the refractive index valley at boundary core and cladding on the group delay in W-shaped POFs. For this purpose we derive the analytical expression that allow calculating the temporal broadening due to the fact that different rays take different amounts of time to propagate through the fiber. Finally, we carry out a comprehensive numerical analysis in order to investigate of dependence of modal dispersion on the depth of the index valley. We concluded that, in the case where  $NA = 0.24$  with  $\rho = 1.5$ , the index exponent  $q = 1.96$  is value that is corresponding to minimum pulse dispersion.

### REFERENCES

- [1] Y. Koike, K. Koike, J. Polym Sci Part B: Polym Phys. 49, 2 (2011).
- [2] Y. Koike, M. Asai, NPG Asia Mat. 1 (1), 22 (2009).
- [3] J. Zubia, G. Aldabaldetrek, G. Durana, J. Arrue, F. Jimenez, Laser Photonics Rev. 2 (3), 182 (2008).
- [4] K. Takahashi, T. Ishigure, J Light. Technol. 24 (9), 2867 (2006).
- [5] T. Ishigure, H. Endo, K. Ohodoko, K. Takahashi, Y. Koike, J. Lightwave Technol. 23 (4), 1754 (2005).
- [6] ] T. Ishigure, H. Endo, K. Ohodoko, K. Takahashi, Y. Koike, IEEE Photonic Tech. L. 16 (9), 2081 (2004).

## Explicit finite difference solution of the power flow equation in W-type optical fibers

A. Simović<sup>1</sup>, S. Savović<sup>1</sup> and A. Djordjevich<sup>2</sup>

<sup>1</sup>*Faculty of Science, Kragujevac, Serbia*

<sup>2</sup>*City University of Hong Kong, Hong Kong, China*  
e-mail: asimovic@kg.ac.rs

Using the power flow equation, we have calculated spatial transients of power distribution as well as a steady state distribution for the mode coupling condition from guided to leaky modes in a W-type optical fiber. A numerical solution has been obtained by the explicit finite difference method. Results show that power distribution in W-type optical fiber depends both on the intermediate layer width and the coupling strength. W-shaped index profile of optical fibers is effective in reducing modal dispersion and therefore in improving the fiber bandwidth.

## Calculation of the frequency response and bandwidth in step-index plastic optical fibers using the time-dependent power flow equation

B. Drljaja<sup>1,2</sup>, S. Savović<sup>1</sup> and A. Djordjevich<sup>3</sup>

<sup>1</sup>Faculty of Science, Kragujevac, Serbia

<sup>2</sup>Faculty of Science, Kosovska Mitrovica, Serbia

<sup>3</sup>City University of Hong Kong, Hong Kong, China

e-mail: brdrljaca@gmail.com

The power flow equation is employed to calculate frequency response and bandwidth in addition to mode coupling and mode-dependent attenuation in step-index plastic optical fibers. The frequency response is specified as a function of distance from the input fiber end. A good agreement between our analytical results and experimental results obtained previously is seen. Mode-dependent attenuation and mode dispersion and coupling are known to be strong in plastic optical fibers, leading to major implications for their frequency response in data transmission systems.

## FSR adjustment of silicone rib racetrack resonator

T. Keča<sup>1</sup>, P. Matavulj<sup>2</sup>, W. Headley<sup>3</sup> and G. Mashanovich<sup>3</sup>

<sup>1</sup>ICT college of vocational studies, Belgrade, Serbia

<sup>2</sup>Faculty of Electrical Engineering, University of Belgrade, Serbia

<sup>3</sup>Advanced Technology Institute, University of Surrey, Guildford, UK

e-mail: tatjana.keca@ict.edu.rs

One of the most important parameter describing the quality of components and devices in photonics is a free spectral range (FSR). It is also used to define finesse which represent the estimate of device quality. The larger FSR and finesse means the better quality of the device. In addition, larger FSR is preferred in telecommunication, since devices operate on a single wavelength.

The adjustment of FSR for resulting outgoing power for both incidental modes can be carried out by altering two basic geometric parameters of a racetrack resonator: coupling length and racetrack radius. The objective is to adjust geometric parameters so that FSR coincides with the existing experimental FSR obtained for Silicon-On-Insulator (SOI) rib racetrack resonator with the following nominal geometric parameters: coupling length 500 $\mu\text{m}$ , waveguide width 1 $\mu\text{m}$  and racetrack radii 100, 200 or 300 $\mu\text{m}$ . Operating wavelength is 1.55 $\mu\text{m}$ .

This paper presents analytically obtained FSR dependences regarding geometric parameters. On the basis of those dependences, the pairs of geometric parameters values that coincide with experimental results have been obtained. This procedure gives the possibility to estimate FSR for different geometric parameters, as well as for prediction of device functionality.

### REFERENCES

- [1] W. R. Headley, "Optical Ring Resonators in Silicon-On-Insulator", PhD Thesis, Univ. Surrey, UK (2005).
- [2] W. Lui, T. Hirono, K. Yokoyama, W. P. Huang, J. Lightwave Technol. 16, 929 (1998).
- [3] G. Cusmai, F. Morichetti, P. Rosotti, R. Costa, A. Melloni, Opt. Quant. El. 37, 343-258 (2005).
- [4] F. Morichetti, A. Melloni, M. Martinelli, J. Lightwave Technol. 24, 537 (2006).
- [5] T. Keča, P. Matavulj, W. Headley, G. Mashanovich, MediNano-3 2010, Belgrade.

## Modeling of Carrier Dynamics in Multi-Quantum Well Semiconductor Optical Amplifiers

A. Totović, J.V. Crnjanski, M.M. Krstić and D.M. Gvozdić  
*School of Electrical Engineering,*  
*University of Belgrade, Serbia*  
e-mail: gvozdic@etf.rs

For a long time wavelength-division-multiplexed (WDM) passive optical networks (PONs) have been considered as an ultimate solution for the next-generation broadband access networks capable of providing speeds higher than 10Gb/s to each subscriber. A lot of effort has been invested on trying to develop a low-cost WDM-PON based on the sources in the optical network unit (ONU) that are “color-free” or wavelength independent. Recently, in order to overcome this problem, several proposals have been offered. One possible approach is to remodulate the downstream signal at each ONU. A saturated reflective semiconductor optical amplifier (R-SOA) modulator [1] is used to remodulate the high speed modulated downstream signal [2]. However, until now, these networks have been implemented to operate at the moderate speeds due to the limited bandwidth of directly modulated colorless transmitters. The bandwidth of R-SOA based on the bulk III-V materials is limited by the carrier lifetime and it is only about 2GHz. At the time being, R-SOA can be directly modulated up to 10 Gb/s only by using electronic equalization techniques [2].

In this paper we investigate carrier dynamics in a multi-quantum well (MQW) SOA and methods to speed up SOA response as well as its recovery time. We base our study on the model of the rate equations for the carrier density in the bulk and the bound states of MQW. The model takes into account the gain dependence on the well carrier density in the regime of saturation. In the case of the linearized gain dependence on the carrier density, solutions of the rate equations can be obtained in a closed analytical form. This provides possibility to analyze the carrier density and gain recovery analytically in dependence on various input parameters as are modulation current, carrier capture and escape time, carrier radiative and nonradiative recombination time, differential gain and optical confinement factor etc. Our analysis shows that besides the capture and escape time, SOA’s response and recovery times significantly depends on differential gain.

### REFERENCES:

- [1] H. Takesue, T. Sugie, IEEE J. Lightw. Technol. 21, 2546 (2003).
- [2] K.J. Cho, Y. Takushima, Y.C. Chung IEEE Photonics Technol. Lett. 20, 1533 (2008).

## Intersubband absorption in quantum dashes with various cross-section profiles

J.V. Crnjanski

*School of Electrical Engineering,  
University of Belgrade, Serbia  
e-mail: jasna.crnjanski@etf.rs*

Self-organized growth mechanisms have been investigated widely for the last decade. Although self-organization provides high quality growth of low-dimensional structures, it usually means limited control of the absolute structure size, in contrast to the lithographic techniques of pattern definition [1]. Moreover, it leads to a wide stochastic size distribution and thus, to an energy spreading of the confined subbands and consequently broadening of the ensemble absorption or gain spectrum [2], [3]. Depending on the material system and growth conditions (temperature and growth rates), self-assembled quantum dashes (QDHs) may have various cross-section profiles, as well as different mean values and standard deviations of the size distribution. Usually, the size distribution is approximated with a Gaussian function [3] or with a bimodal distribution consisting of two or three Gaussian functions [4]. In the case of InAs/InP dashes, the cross section profile can be approximated with a semi-parabolic [5] or trapezoidal shape [4], whereas InAs/InAlGaAs dashes are not truncated and have full triangle-like cross section [1]. Moreover, in order to simplify the calculation of the electronic band structure, the semi-parabolic cross section profile is often approximated with an equivalent rectangular shape chosen in such a way to preserve the same area as in case of the semi-parabolic profile [3], [5].

The shape and the size of a nanostructure may significantly affect electronic and therefore optical properties of the nanostructure. However, self-assembled nanostructures, such as quantum dashes, usually have irregular edges of the transversal cross section, and in some cases it is uncertain what shape is the best approximation of the dash cross section. In this work, we investigate the influence of QDH cross section profile on intersubband absorption in the conduction band of quantum dashes, taking into account fluctuation of their size, described by a Gaussian distribution [1]. In order to determine the optical intersubband absorption of a QDH ensemble with given cross section profile, we separately calculate absorption for each dash size in the ensemble at room temperature, taking into account the influence of the wetting layer. Then, we calculate the ensemble average (absorption per dash) by adding together the previously calculated QDHs absorptions, weighted by the probability of finding the QDH with corresponding dimensions in the ensemble [2]. In order to make a fair comparison of the ensemble absorption with differently shaped QDHs, we assume that each corresponding element in the ensembles for semi-parabolic, trapezoidal, triangle and rectangular QDH shape have the same area. Calculation is performed for InAs well material, which is grown on and surrounded by GaAs. For the central dash dimension ( $14 \times 3$  nm) in the ensemble, the difference in the intersubband absorption spectra for equivalent parabolic and trapezoidal cross section is negligible, while spectra for corresponding triangular and rectangular profiles exhibit red shift ( $\sim 5$  meV) and blue shift ( $\sim 3$  meV), respectively, with approximately the same peak absorption.

### REFERENCES

- [1] J. P. Reithmaier, G. Eisenstein, A. Forchel, Proc. of IEEE 95, 1779 (2007).
- [2] J. Crnjanski, D. Gvozdić, Appl. Phys. Lett. 97, 091906 (2010).
- [3] J.H. Wei, K.S. Chan, J. Appl. Phys. 97, 123524 (2005).
- [4] B. S. Ooi, H. S. Djie, Y. Wang, C.-L. Tan, J. C. M. Hwang, X.-M. Fang, J. M. Fastenau, A. W. K. Liu, G. T. Dang, W. H. Chang, IEEE J. Selected. Top. Quantum Electron. 14, 1230 (2008).
- [5] M. Gioannini, IEEE J. Quantum Electron. 40, 364 (2004).

## Interface shape studies in Bridgman growth of multicrystalline silicon

O. Bunoiu, M. Stef, A. Popescu and D. Vizman  
*Physics Faculty, West University of Timisoara, Bd. V. Parvan 4, 300223*  
*Timisoara, Romania*  
e-mail:stef@quantum.physics.uvt.ro

According to the European Photovoltaic Industry Association (EPIA) SET for 2020-study [1] solar energy could supply as much as 12% of EU electricity demand by 2020 – up from less than 1% at present. The main challenges in the production of multicrystalline silicon ingots are to maintain the purity of the silicon raw material and to determine optimal values for different growth parameters in order to control the growth process during directional solidification and to obtain satisfactory crystal quality. The ingot casting method for the crystallization of multi-crystalline silicon for solar cells was developed in the 80-ties [2].

The key point here is the control of grain growth during directional solidification of multicrystalline silicon which is strongly related with the solid-liquid interface shape. For this purpose silicon crystals were obtained using a Bridgman equipment. The equipment is designed for fundamental research of solidification processes in crucibles of maximum 3cm diameter. Numerical simulations were performed in order to optimize the temperature field in the Bridgman apparatus for crystallization of silicon. The comparison between numerical results and experimental measured temperature distributions are presented. Multicrystalline silicon was obtained for different growth parameters (temperature gradients – in the melt and in the solid- and pulling rates) and concerning the experimental results the focus was on the determination of the solidification interface shape .

Acknowledgements:Dr. Jochen Friedrich from Fraunhofer Institute IISB, Erlangen, Germany for useful discussions and permanent support of our crystal growth research activities, The European Social Fund through the Sectoral Operational Program for Human Resources Development 2007-2013 for financial support under the project POSDRU/88/1.5/S/49516 coordinated by West University of Timisoara and the Romanian Ministry of Education and Research for financial support under the grant CONSIL C1-02.

### REFERENCES

[1] <http://www.setfor2020.eu/>.

[2] D. Helmreich, *The Wacker Ingot Casting Process, Materials Processing–Theory and Practices*, 6, Silicon Processing for Photovoltaics II, North-Holland, Amsterdam, 97, (1987).

## Modulation Response and Bandwidth of Injection-Locked Fabry-Perot Laser Diodes

A.G.R.Zlitni, M.M. Krstić and D.M. Gvozdić  
*School of Electrical Engineering, University of Belgrade, Serbia*  
e-mail:gvozdic@etf.rs

The injection locking is an advanced technique which finds a lot of applications in the fields of optical communications and optical signal processing. Some recent applications of the injection locking are related to the next-generation of wavelength-division-multiplexed (WDM) passive optical networks (PONs), in which upstream transmission from an optical network unit to the central office is achieved by injection-locked transmitter [1] instead of more expensive tunable laser. Moreover, the theoretical and experimental investigations have proved that modulation response of injection-locked lasers can be significantly improved compared to the free-running lasers [2]. In addition, the technique of injection-locking can ensure single mode operation, reduce the linewidth of a free-running laser, and eliminate mode partition noise, mode hopping, and frequency chirp from modulated lasers [2].

In this work we study dependence of the modulation response and corresponding  $-3\text{dB}$  bandwidth of side-mode injection-locked Fabry-Perot (FP) laser diodes (LDs) on master laser injection power and frequency detuning between the master and the slave FP-LD laser. Our analysis is based on the small-signal modulation response, derived from the set of linearized multimode rate equations, which besides the carrier rate and photon-density-rate equations for unlocked modes, comprises the photon density and phase rate equations for injection-locked side mode. The modulation response is investigated in two important cases. In the first case, the model comprises two longitudinal modes, the central and the injection-locked side-mode, while in the second case, all longitudinal modes (locked and unlocked modes) are taken into account. Both cases lead to the similar conclusions, although there are some differences which will be discussed in the paper.

Our investigation shows that for low bias currents of the slave laser (close to the threshold current  $I_{\text{th}}$ ), low injection powers of the master laser (less than  $-10\text{dBm}$ ) and injection-locked modes close to the central mode, modulation response exhibits resonant peak, which is not sufficient to improve the bandwidth of the laser compared to the free-running case. The enhancement can not be seen either for larger injection powers, since the influence of the resonant poles disappear. A significant improvement of the bandwidth can be achieved for somewhat larger bias currents (e.g.  $I \approx 3I_{\text{th}}$  or larger). In this case, for weak or moderate detuning (e.g.  $|\Delta\omega| \leq 7\Omega$ , where  $\Omega = 10^{10}$  rad/s), the stable locking as well as the resonant peak occurs for medium injection powers (from  $0\text{ dBm}$  to  $4\text{ dBm}$  for  $I \approx 3I_{\text{th}}$ ), leading to the bandwidth enhancement by factor 2 or even 3 compared to the free-running case. For even larger injection powers the bandwidth of the slave laser rapidly decreases, leading to the bandwidth deterioration compared to the free-running case. This result indicates that for a fixed but weak detuning, there is the optimum injection power, for which the bandwidth has the maximum. For larger detuning or higher order injection-locked side modes (e.g.,  $> 20$ ) this optimum rapidly decreases and becomes of the order of the bandwidth in the free-running regime. An increase of the bias current increases the upper limit of the injection power for which the bandwidth can be enhanced.

The detuning significantly affects the bandwidth. For a negative detuning and low or medium injection powers the bandwidth is smaller than for positive detuning, while for larger injection powers, the situation is reversed. Moreover, the bandwidth exhibits the maximum versus detuning. This provides possibility to find the optimum injection power and the detuning for which the bandwidth may reach the maximum.

### REFERENCES

- [1] N. Kashima, IEEE J. Lightw. Technol. 24, 3045 (2006).
- [2] X.Jin, S.-L. Chuang, Solid-State Electronics 50, 1141 (2006).

## Long-Period Gratings in PCF Fabricated by Fs Laser Pulses

M. D. Petrovic<sup>1</sup>, A. Danicic<sup>1</sup>, T. Allsop<sup>2</sup> and J. Petrovic<sup>1</sup>

<sup>1</sup>*Vinca Institute of Nuclear Sciences, Belgrade, Serbia*

<sup>2</sup>*Photonics Research Group, Aston University, Birmingham, UK,*

e-mail: jovanap@vin.bg.ac.rs

Long-period gratings (LPGs) written in all-silica photonic crystal fibres (PCFs) have been used as sensors of refractive index, strain or temperature [1]. Several direct fabrication methods have been proposed: electric arc, laser-induced hole collapse, femtosecond (fs) laser-pulse and mechanical inscription. As these methods do not require doping or hydrogenation, the mono-material composition of the gratings allows for studies of the modification of the silica during inscription.

In this poster, we present a numerical and experimental study of the fabrication and properties of the fs-laser inscribed LPGs in endlessly single mode PCF [2]. Due to the scattering of the laser beam by the holes, these gratings are characteristically birefringent. Here, we find the grating index profile and use the birefringence to quantify both the fibre-specific fabrication parameters and the general fs-inscription parameter that relates the laser pulse energy to the refractive index change in the silica.

We first present the numerical model that calculates the intensity distribution of the writing beam in the PCF and verify its validity by comparing the results to the profiles of fabricated gratings. Using the generated index profile we obtain the grating birefringence as a function of the parameter that relates the laser pulse energy to the amplitude of the index change. The fit to the measured birefringence gives the value of this parameter. We further study the dependence of the grating birefringence on the fibre orientation and identify the inscription conditions that generate highly birefringent gratings. Finally, we compare the performance of these gratings with the birefringent gratings written in other fibres.

### REFERENCES

- [1] H. Dobb et al., *Opt. Comm.* 260, 184 (2006).
- [2] T. Allsop et al., to be published in *JOSA B* (2011).

## Design of up-converters for silicon solar cells based on nonpolar a-plane GaN/AlGaIn quantum well structures

S. Radosavljević<sup>1</sup>, J. Radovanović<sup>1</sup>, V. Milanović<sup>1</sup> and S. Tomić<sup>2</sup>

<sup>1</sup>*School of Electrical Engineering,*

*University of Belgrade, Serbia*

<sup>2</sup>*University of Salford, UK*

e-mail: radovanovic@etf.rs

We present a procedure for the optimized design of GaN/AlGaIn quantum well (QW) based up-converter for silicon solar cells, aimed at making a better use of the solar spectrum [1-3]. One of the major obstacles for high-efficiency power conversion of the sun light with conventional semiconductor materials is that only photons with energies close to that of the semiconductor energy gap ( $E_g$ ) are effectively converted into electron-hole pairs. A prospective solution is to place another device component, “light converter”, in front of an existing solar cell (SC) to absorb the photons with energy lower than  $E_g$  and re-emit the light at higher energy in order to match the region where SC exhibits a very good spectral response (up-conversion) [4-6]. In quantum well structures this can be

achieved by utilizing nonlinear optical effects based on intersubband transitions. Optimization of up-converter may be performed by maximization of the second order susceptibility derived from the density matrix formalism [7].

In our procedure, based on the use of global optimization tools [8-10], we vary the structural parameters of nonpolar-nitride quantum well in search of the best QW profile, offering highest value of the relevant nonlinear susceptibility. This particular combination of materials provides a large enough conduction band offset to accommodate three bound states with sufficient energy spacing [11,12], as required for the frequency up-conversion. For calculating the electronic states we used a one band model that takes into consideration the effects of strain and band nonparabolicity [13,14]. In one-step quantum wells the following input arguments are needed for evaluating the susceptibility: the widths of step and well layers and the content of AlN in the step regions. The best solution is determined by using the generic algorithm optimization tool for varying these parameters, subject to physical and technological constraints, thus enabling us to obtain a realistic optimized quantum-well profile.

#### ACKNOWLEDGEMENTS

This work was supported by the Ministry of Science (Republic of Serbia), ev. no.III 45010.

#### REFERENCES

- [1] M. Green , Prog. Photovoltaics 9, 123 (2001).
- [2] RR. King, Nat. Photonics 2, 284 (2008).
- [3] S. Tomić, T.S. Jones, NM. Harrison, Appl. Phys. Lett. 26, 263105 (2008).
- [4] T. Trupke, M. Green, P. Wurfel, J. Appl. Phys. 92, 1668 (2002).
- [5] T. Trupke, M. Green, P. Wurfel, J. Appl. Phys. 92, 4117 (2002).
- [6] Y. Yi, L. Zhu, Z. Shuai, Macromol. Theor. Simul. 17, 12 (2008).
- [7] RV. Boyd, Nonlinear Optics, Academic Press - Elsevier Science, 129, (2003).
- [8] G. Goldoni and F. Rossi, Opt. Lett. 25, 1025 (2000).
- [9] A. Franceschetti A. and Zunger, Nature 402, 60 (1999).
- [10] J. Radovanović, V. Milanović, Z. Ikonić, D. Indjin, J. Appl. Phys. 99, 73905 (2006).
- [11] S. Schulz et al., Phys. Rev. B 82,125318 (2010).
- [12] T. J. Badcock et al., J. Appl. Phys. 105, 123112 (2009).
- [13] S. Tomić, AG. Sunderland, IJ. Bush, J. Mater. Chem. 16, 1963 (2006).
- [14] C. Sirtori, F. Capasso, I. Faist, S. Scandolo, Phys. Rev. B 50, 8663 (1994).

Poster Presentations – Optoelectronics and Optocommunications P.OE.15

### **Evanescent field fiber-optic gas sensor using high index sol-gel nanoporous layer**

N. Raicevic<sup>1</sup>, A. Matthias<sup>2</sup>, D. Kip<sup>1</sup> and J. Deubener<sup>2</sup>

<sup>1</sup>*Faculty of Electrical Engineering,  
Helmut Schmidt University Hamburg, Germany*

<sup>2</sup>*Faculty of Natural and Materials Science  
Clausthal University of Technology, Germany*

e-mail: raicevic@hsu-hh.de

In this paper we introduce a new model for a spurious gas sensor, for example for CO<sub>2</sub> detection. The detection method of the sensor is based on absorption spectroscopy and evanescent field sensing [1] using an optical waveguide. The presence of CO<sub>2</sub> molecules in an (evanescent) electromagnetic field of a specific resonant frequency leads to a loss of optical power that is guided in the waveguide. Here not only energy absorbed at the resonant frequency but also higher harmonics may be used. One of the higher harmonics that drives vibration transitions of CO<sub>2</sub> corresponds to a wavelength of 1.58 nm.

Because of cheap and widely available light sources and detectors in this range, we utilized absorption in this spectral region for CO<sub>2</sub> detection.

A main part of the optical waveguide sensor is a TiO<sub>2</sub> layer which is formed by the sol-gel dip-coating technique [3] on an optical fiber. Its purpose is both, guiding the light and increasing the interaction volume of light with gas molecules by using the huge surface of the nanoporous TiO<sub>2</sub> layer. Titanium oxide is chosen because of its high optical quality and high refractive index. The sol-gel method which is applied by the dip-coating technique forms uniform layers with excellent optical properties. The thickness of the waveguiding layers can be tailored by the speed of withdrawing the substrate from the sol-gel solution and by adjusting the viscosity of the solution. Layers can be formed at plain surfaces, cylinders and spheres. Here, as a physical support for the thin TiO<sub>2</sub> film, a single-mode optical fiber is used. In this way it thus provides a cheap substrate material with low optical absorption in the wavelength region of interest.

Due to adsorption CO<sub>2</sub> molecules will attach preferentially to the TiO<sub>2</sub> surface. This enables strong interaction of the gas molecules with the evanescent electromagnetic field of the high-refractive-index waveguide, TiO<sub>2</sub> on silica glass. A huge increase of the effective surface area is achieved by introducing nanometer-sized pores in the TiO<sub>2</sub> coating, while at the same time these pores will not influence the general guiding characteristics of the TiO<sub>2</sub> layer.

In order to overcome coupling problems of light into the thin coated layer, the end of the optical fiber used as a substrate is tapered and broken by purpose at the waist. After tapering the TiO<sub>2</sub> layer is formed over the whole fiber-taper area. Smooth changes of the fiber's diameter due to tapering, lead to smooth changes of the TiO<sub>2</sub> thickness, which will however not affect the characteristics of light coupled at the fiber tip and afterwards guided in TiO<sub>2</sub> layer.

In this paper we report on our results to realize an optimized geometry of tapered fiber and thickness and refractive index of the coated layer according to experimentally realizable values. To compare the results the numerical simulations an analysis of the mode propagation is done by FD-BPM [3].

#### REFERENCES

- [1] <http://arxiv.org/abs/cond-mat/0701264v2>
- [2] L.L. Hench and J. K. West, Chem. Rev. 90, 33 (1990).
- [3] J. Yamauchi, T. Ando, Y. Akimoto et al., Fiber and Integrated Optics 15, 353 (1996).

## Vortex solitons near boundaries of photonic lattices

D. Jović<sup>1,2</sup>, R. Jovanović<sup>1</sup>, C. Denz<sup>2</sup> and M. Belić<sup>3</sup>

<sup>1</sup> *Institute of Physics, P.O. Box 68, University of Belgrade, Serbia*

<sup>2</sup> *Institut für Angewandte Physik and Center for Nonlinear Science (CeNoS), Westfälische Wilhelms-Universität Münster, 48149 Münster, Germany*

<sup>3</sup> *Texas A & M University at Qatar, P.O. Box 23874 Doha, Qatar*  
e-mail: rakabog@yahoo.com

Self-trapped nonlinear surface states (surface solitons) propagating along the interfaces of different media have attracted a great interest in optical systems [1, 2]. Recently, special attention has been devoted to the nonlinear surface vortex solitons. Such solitons were demonstrated experimentally at the surface of an optically induced 2D photonic lattice [3]; they are also observed at the interface of two different optical lattices imprinted in Kerr-type focusing nonlinear media [4].

Here we report on the existence and properties of vortex solitons at the edge and in the corner of two-dimensional triangular photonic lattices. We describe novel types of discrete vortex solitons as well as the ring surface vortex solitons, localized in the lattice corners or at its edges. Stable surface vortex solitons exist only in the form of a discrete six-lobe solution at the edge of the triangular photonic lattice. Other solutions are observed, in the form of ring vortex and discrete solitons with two or three lobes that oscillate during propagation in a way that neighboring lobes exchange power. We observe dynamical instabilities of surface vortex solitons, for higher beam powers. We focus more attention on the study of dynamical properties of such solitons. Angular momentum transfer of such solutions during propagation is investigated in some detail.

### REFERENCES

- [1] Yu. S. Kivshar, *Laser Phys. Lett.* 5, 703713 (2008).
- [2] S. Suntsov et al., *J. Nonlinear Opt. Phys. Mater.* 16, 401 (2007).
- [3] D. Song, C. Lou, K.J.H. Law, L. Tang, Z. Ye, P.G. Kevrekidis, J. Xu, Z. Chen, *Opt. Express* 18, 5873 (2010).
- [4] Y.V. Kartashov, A.A. Egorov, V.A. Vysloukh, L. Torner, *Opt. Express* 14, 4049 (2006).

## Tunability of band gaps in the biopolymer photonic crystals

S. Savic-Sevic<sup>1</sup>, D. Pantelic<sup>1</sup> and B. Jelenkovic<sup>1</sup>

<sup>1</sup> *Institute of Physics,  
Belgrade, Serbia*

e-mail: savic@ipb.ac.rs

Photonic crystals are dielectric materials that exhibit band gaps (BG) in which electromagnetic wave propagation is forbidden [1]. Several photonic band-gap materials such as dichromated gelatin [2, 3], polymers with TiO<sub>2</sub> [4] and photoresists [5, 6] have been used for fabrication of photonic structures using holographic techniques. Here we report the fabrication of photonic crystals using the optical holography.

One-dimensional photonic crystals were fabricated as volume reflection holograms. The hologram was obtained by interference of two oppositely directed beams inside the emulsion. The interference pattern consists of planes parallel to the substrate surface with spacing  $d = \lambda/2n$ , where  $\lambda$  is the wavelength of the laser source and  $n$  is the refractive index of the recording material. The pullulan (a linear polysaccharide of biologic origin), sensitized with ammonium dichromate, is used in this study as a recording medium. A single-frequency, diode pumped Nd-YAG laser, at 532 nm, is used for exposure.

We have found that the position of the band gap can be tuned by changing the exposure. The spectral measurements show that the band gap centre shifts towards the longer wavelength with decreasing exposure. The tuning is a consequence of the different amounts of swelling of photosensitive material. Efficient tuning the position of the band gap for about is obtained. These results are important as they present a convenient way to move the center wavelength of band gap of the photonic crystal, thus making a tunable filter.

#### REFERENCES

- [1] J. D. Joannopoulos, R. D. Meade, J. N. Winn, Photonic crystals, Princeton (1995).
- [2] R. Ma, J. Xu, W. Y. Tam, Applied Physics letters 89, 081116-1 (2006).
- [3] Z. Ye, J. Zheng, D. Liu, S. Pei, Physics Letters A 299, 313 (2002).
- [4] D. T. Sharp et al., Opt. and Quantum Electronics 34, 3 (2002).
- [5] T. Ohira, T. Segawa, K. Nagai, K. Utaka, M. Nakao, Jpn. J. Appl. Phys. 41, 1085 (2002).
- [6] Y. Miklyaev, D. Meisel, A. Blanco, G. Freymann, Appl. Phys.Lett. 82, 1284 (2003).

Poster Presentations – Photonic Crystals P.PC.3

### **Transition of Anderson localization behavior from one dimensional to two dimensional photonic lattices**

D. Jović<sup>1,2</sup>, M. Belić<sup>2</sup>, C. Denz<sup>3</sup> and Yu. S. Kivshar<sup>4</sup>

<sup>1</sup> *Institute of Physics, P.O. Box 68, University of Belgrade, Serbia*

<sup>2</sup> *Texas A & M University at Qatar, P.O. Box 23874 Doha, Qatar*

<sup>3</sup> *Institut für Angewandte Physik and Center for Nonlinear Science (CeNoS), Westfälische Wilhelms-Universität Münster, 48149 Münster, Germany*

<sup>4</sup> *Nonlinear Physics Center, Research School of Physics and Engineering, Australian National University, Canberra ACT 0200, Australia*

e-mail: milivoj.belic@qatar.tamu.edu

Anderson localization is the absence of diffusion of waves in a *disordered* medium [1]. It is a general wave phenomenon that applies to the transport of electromagnetic waves, acoustic waves, quantum waves, spin waves, etc. It has become a central part of recent investigations of discrete, photonic, band-gap lattices with random structures. Experimental realizations of transverse Anderson localization were reported in two-dimensional (2D) [2], and one-dimensional (1D) photonic lattices [3]. It has also been observed by localization of a Bose-Einstein condensate in a 1D disordered optical potential [4].

We investigated Anderson localization in the stripe geometry when the lattice has a finite extend into one dimension but infinite in the other. Depending on the width of the stripe we may trace a crossover between 1D and 2D cases which are characterized by different localization lengths. First, we studied the limiting cases of 1D and 2D photonic lattices. We use a periodic square lattice potential defined as a sum of Gaussian beams. To observe Anderson localization we include disorder in such lattice using random lattice intensity and also random lattice period. We found that Anderson localization in linear regime is more pronounced in the case of 2D lattice than in 1D lattice. But in nonlinear system, it is

not the case. In different nonlinear regimes, there are also cases when 1D localization is more pronounced comparing to 2D localization.

Next, to consider the crossover between 1D and 2D lattices, we used the same square lattice potential and keep fixed lattice period in one transverse direction but change it in another one. With such geometry, we can study transition effects, and with sufficient large lattice period along another transverse direction, we observe 1D case. The localization is less pronounced in intermediate cases then in both 1D and 2D for linear regime, but in nonlinear case it depends on the strength on nonlinearity.

#### REFERENCES

- [1] P. W. Anderson, Phys. Rev. 109, 1492 (1958).
- [2] T. Schwartz, G. Bartal, S. Fishman, M. Segev, Nature 446, 52 (2007).
- [3] Y. Lahini, A. Avidan, F. Pozzi, M. Sorel, R. Morandotti, D. N. Christodoulides, Y. Silberberg, Phys. Rev. Lett. 100, 013906 (2008).
- [4] J. Billy, V. Josse, Z. Zuo, A. Bernard, B. Hambrecht, P. Lugan, D. Clément, L. Sanchez-Palencia, P. Bouyer, A. Aspect, Nature (London) 453, 891 (2008).

## Holography

Poster Presentations – Holography P.HG.1

### **Reconstruction of silver-halide volume reflection holograms at the wavelengths of recording**

B. Ivanov, M. Shopova, E. Stoykov and, V. Sainov  
*Institute of Optical Materials and Technologies,  
Bulgarian Academy of Sciences  
Acad.G.Bonchev Str., Bl.101,1113 Sofia, Bulgaria  
e-mail: mariana\_k\_sh@abv.bg*

A crucial task in multicolor holographic recording onto silver-halide light sensitive materials is to realize reconstruction at the wavelengths of recording. Typical for these materials, when used for RGB recording of volume reflection (Denisyuk's) holograms, is the shrinkage of the layers, leading to a shift of diffraction peaks towards lower wavelengths in reconstruction approximately at 20 nm in the blue, 50 nm in the green and 60 nm in the red spectral regions. To compensate the shrinkage of the layers and to ensure reconstruction of the Bragg reflection holograms at the wavelengths of recording, suitable swelling has to be performed before final drying of the holograms. For the purpose, the holograms are put in a bath of water solution of collagen hydrolizate at different concentrations.

The report presents the recent results, obtained for swelling of holograms recorded at wavelengths in the red, green and blue spectral regions on a single plate. The cases of successive and simultaneous irradiation of the holographic plate with the laser light from the used three lasers are compared. Experiments on repeatability of the swelling procedure are also provided. Ultra-fine grain panchromatic silver-halide emulsion for recording of RGB volume reflection holograms, production of IOMT-BAS is used for the experiments. The emulsion, created by the so called "double stream" technology, is characterized with 10 nm average size of initial silver halide grains. This ensures high values of resolution, diffraction efficiency and signal-to-noise ratio of holographic recording. The used sensitizers for the red and green spectral regions are selected to achieve maximal absorption and maximal hologram's recording sensitivity respectively at 632.8 and 532 nm. Natural emulsion sensitivity is used for recording in the blue spectral region (400 – 442 nm). Chemical processing of the

exposed plates includes standard for silver-halide emulsion procedures - development to form amplitude modulation of holographic recording and bleaching for translation to phase volume reflection holograms as a final product. Diffraction efficiency of bleached single exposure volume reflection holograms in red, green and blue has values higher than 50% for exposure energy about  $2.0 \text{ mW/cm}^2$  both for the CW and pulse lasers. The developed ultra-fine grain panchromatic silver-halide emulsion with improved characteristics is suitable for recording of high quality multicolor volume reflection holograms, as well as for recording of synthesized reflection holograms in holoprinters.

**Keywords:** Silver-halide holographic emulsion, reflection holograms, RGB holographic recording, swelling.

Poster Presentations – Holography P.HG.2

## **Generation of sinusoidal fringes with a holographic phase grating and a phase-only Spatial light Modulator**

N.Berberova, E. Stoykova and V. Sainov

*Institute of Optical Materials and Technologies, Bulgarian Academy of Sciences,  
Acad. G. Bonchev Str., bl.101, 1113 Sofia, P.O. Box 95, BULGARIA,  
e-mail: natali.berberova@gmail.com*

Generation of sinusoidal fringes is a crucial issue in many phase-measuring techniques for distant determination of the surface relief of 3D objects. Using of phase gratings with coherent illumination has the advantage of providing a large measurement volume. In the present work we analyze the quality of fringes generated with two sinusoidal phase gratings. The first grating is recorded on a silver-halide holographic plate by means of Michelson interferometer. The spatial resolution of the used silver-halide material is greater than 6000 lines per millimeter. The second grating is formed as a sinusoidal phase variation on a LCoS phase-only reflective display with a resolution of 1920x1080 pixels, pixel pitch  $8 \mu\text{m}$  and 256 phase levels.

Two contradictory requirements should be fulfilled for acceptable quality of fringes. In the first place, the influence of higher harmonics should be negligible to ensure satisfactory phase retrieval accuracy. The contribution of higher harmonics of fringes increases with the modulation parameter which defines the contrast of the grating phase distribution. In the second place, accurate measurement entails comparatively high contrast of the generated fringes which requires increase of the modulation parameter. Frequency content of the generated with both gratings fringes is compared on the basis of the calculated Fresnel diffraction pattern, taking in account that the sinusoidal phase distribution in the case of the spatial light modulator is both sampled and quantized. The optimum values of the modulation parameter of the gratings are determined for both cases from simulation of surface relief measurement. Experimental spectra of the generated fringes are also provided.

**Keywords:** sinusoidal phase grating, SLM, surface relief measurement.

## High Resolution Solution Dot Matrix Holograms Generation

B. Zarkov and D. Pantelić  
*Institute of Physics, Belgrade, Serbia*  
 e-mail: zarkov@ipb.ac.rs

The holography is a technique that enables permanent record of 3D color pictures. Due to its sub-micronics structure, holograms are remarkable safety elements which are very difficult to counterfeit. Dot-matrix technology, as one of the commonly used methods, represents substantial obstacle to all types of fraudulent activities. This kind of holograms is mainly used for the purpose of protection against forgery of checks, cards, passports, etc. Such a high resolution technics enable also engineering of 2D and 3D structures leading potentially to the construction of metamaterials. In this paper we describe the high resolution holographic structures obtained by dot matrix device of novel construction.

This device consists of mechanical, electrical and optical components which were driven via control and customized recording software. As a source of coherent light emission we used diode pumped solid state laser with 473 nm wavelength and 50 mW output power. The motorized XY table was used for positioning photosensitive material with resolution up to 25 nm. By using mirrors and prisms, we separated two parallel laser beams to desired distance and introduced them into microscope objective. We put different photosensitive materials like pullulan and photoresist in the objective focus in order to obtain interference patterns of coupled laser beams. Each 15 μm diameter elliptical dot recorded in such way corresponds to microscopic diffraction grating with 1 μm periodicity.

With such sophisticated device we obtained high resolution security hologram and we will be able to generated novel metamaterial structure.

### REFERENCES:

- [1] L. Yaotang, W. Tianji, Y. Shining, Z. Shichao, F. Shaowu, W. Huangrong, Proceedings of SPIE, 3559 (1998).
- [2] S. Lih Yeh, Optical engineering 45, 095801 (2006).
- [3] C. K. Lee et al., Applied Optics 39, 1 (2000).

## Full-field stress analysis by holographic phase-stepping implementation of the photoelastic-coating method

T. Lyubenova<sup>1</sup>, E. Stoykova<sup>1</sup>, B. Ivanov<sup>1</sup>, W. Van Paepegem<sup>2</sup>, A. Degrieck<sup>2</sup> and V. Sainov<sup>1</sup>  
<sup>1</sup>*Institute of Optical Materials and Technologies, Bulgarian Academy of Sciences,  
 Acad. G. Bonchev Str., bl.101, 1113 Sofia, P.O. Box 95, Bulgaria,*  
<sup>2</sup>*Ghent University, Dept. of Mechanical Construction and Production,  
 Sint-Pietersnieuwstraat 41, 9000 Gent, Belgium*  
 e-mail: t\_lyubenova@yahoo.com

A holographic phase-shifting realization of the photoelastic-coating method is an effective approach to separate the stress components over the tested specimen due to its easier and faster implementation in comparison with the oblique-incidence method, the strip coating method and the strain gage separation method. For the purpose, a series of six photoelastic fringe patterns are recorded at different preliminary known orientations of the polarization elements in a circular polariscope to build both isochromatic and isoclinic phase maps which give the loci of points with a constant difference of

principal stresses and constant principal stress direction respectively. In addition, holographic recording of four fringe patterns is applied for retrieval of isopachic fringes which give the sum of principal stresses. If a two-load phase-shifting technique is applied for unambiguous phase retrieval of all photoelastic parameters required for full-field stress analysis, the number of the fringe patterns used for the final calculation of the stress components doubles. This increases the requirements set on the accuracy of the phase retrieval. Therefore the reliable stress separation crucially depends on the signal-to-noise ratio in the recorded fringe patterns. The easiest way to perform a combined polariscopic and holographic measurement for full-field stress analysis is to use a laser light source. However, the speckle noise at coherent illumination violates the requirement for high signal-to-noise ratio in the recorded patterns and worsens the accurate phase estimation and unwrapping. To answer the question how the speckle noise affects the phase retrieval of isochromatics, isoclinics and isopachics we solved two tasks in the presented report: i) modelling of the phase-shifting photoelastic measurement based on calculation of the complex amplitudes in a Mach-Zender interferometer combined with a circular polariscope; ii) comparison of different denoising algorithms with and without normalization by processing simulated and experimental fringe patterns. The latter were recorded at pure tensile load for PhotoStress coated samples with different mechanical stress concentrators.

**Keywords:** stress separation, photo-elastic coating, speckle

#### REFERENCES

[1] Z. Lei, H. Yun, D. Yun, Y. Kang, *Opt. Las. Eng.* 45, 77 (2007).

## *Quantum Optics*

Poster Presentations – Quantum Optics P.QO.1

### **Free photon as a bound state system and consequence on electron**

N.V.Delić<sup>1</sup>, J.P. Štrajčić<sup>1</sup>, S. Armačić<sup>1</sup>, S. Cvetković<sup>2</sup>, I.J. Štrajčić<sup>1</sup>,  
V. Holodkov<sup>3</sup> and B.Markoski<sup>4</sup>

<sup>1</sup> *Department of Physics, Faculty of Sciences, University of Novi Sad, Vojvodina – Serbia,*

<sup>2</sup> *Faculty of Agriculture, University of Novi Sad, Vojvodina – Serbia,*

<sup>3</sup> *Faculty of Sport and Tourism, Novi Sad, „Metropoliten“ University, Belgrade – Serbia,*

<sup>4</sup> *University of Novi Sad, Technical faculty of Zrenjanin, Zrenjanin, Serbia*

e-mail: nenad.delic@df.uns.ac.rs

There are two problems of interpretation of mathematical theories; it is primarily their translation into the language of human communication and other matter lies in the circumstances that the cognitive range of quantum physics boundary between descriptions and explanations of phenomena are not clear. In connection with this fact is the hypothesis that the photon is a bound state of neutrino and antineutrino. This hypothesis has been sent to CEWQO Symposium 2010 [1]. Consequence of this paradigm: The hypothesis that the photon bound states of the neutrino and antineutrino has resulted in the first place that there are three types of photons, due to the fact that there are three types of neutrinos: electron, muon and tau neutrino. The present viewpoint in science is that the photons differ in their energies, and taking into account the fact of equivalence of matter and energy, the different types of energy we can join different types of material photon.

$$\gamma_e = (\nu_e + \bar{\nu}_e) = \nu_e \bar{\nu}_e \quad \gamma_\mu = (\nu_\mu + \bar{\nu}_\mu) = \nu_\mu \bar{\nu}_\mu \quad \gamma_\tau = (\nu_\tau + \bar{\nu}_\tau) = \nu_\tau \bar{\nu}_\tau. \quad (1)$$

It is important to note that the operation + means bound states, which may not be valid energy conservation law (comes to the transfer of energy into information which is responsible for 17 layer of consciousness, which enables nonlocality of quantum theory). Here it is necessary to introduce one more assumption about the electron bound states. From the standpoint of current science known facts about W minus bosons is “W-bosons decay to produce either a quark and a differently charged antiquark or a charged lepton and a neutrino (or antineutrino).” This conclusion should be replaced with the hypothesis that the electron is bound states of W minus bosons and neutrinos.

$$e^- = (W^- + \nu_e) = W^- \nu_e. \quad (2)$$

The fact that the electron mass around 160 000 times smaller than the associated weight W minus boson has so far resulted in the negative W boson decays into an electron and electron antineutrino [3]. From the perspective of our interpretation, of minus W boson, cannot exist independently, in order to survive is linked electron neutrino from photon in cosmic ray (other particle is electron antineutrino is detect) and provides a stable electron structure of the material. Come up with Wave-energy-information transformation into a stable material (it must be made to work to form a stable substance, and this requires energy) in our view that energy conservation law is valid. From the perspective of our interpretation, the graviton is a hypothetical elementary particle responsible for equations (2) that mediates the force of gravitation in the framework of quantum field theory. If it exists, the graviton must be masless (because the gravitational force has unlimited range) and must have a spin of 2. Equation (2) is satisfied for spin number.

#### REFERENCES

- [1] <http://www.st-andrews.ac.uk/~cewqo10/submission/762a2.pdf>.  
 [2] N.V. Delić, J.P.Šetrajčić, D.Lj.Mirjanić, Z.Ivanković, D.Martinov, S.Jokić, I.Petrevska–Đukić, D.Tešanović, S.Pelemiš, „Micro Electronic and Mechanical Systems”, ISBN 978-953-307-027-8, pp. 493-514, Ed.Kenici Takahata, *IN-TECH*, Croatia 2009.  
<http://www.intechopen.com/books/show/title/micro-electronic-and-mechanical-systems>.  
 [3] <http://www.hep.ucl.ac.uk/~jpc/all/ulthesis/node45.html>.

## **Radiation transitions from Rydberg states of lithium atoms in a blackbody radiation of environment**

I.L. Glukhov and V.D. Ovsianikov

<sup>1</sup>*Department of Physics, Voronezh State University, Voronezh, 394006, Russian Federation*  
 e-mail: [glukhovofficial@mail.ru](mailto:glukhovofficial@mail.ru)

Lithium atoms are the simplest single-valence-electron atoms with hydrogen-like spectrum of bound-state energies

$$E_{nl} = -1/2\nu^2,$$

determined by an effective principal quantum number  $\nu = n_r + \lambda + 1$  with  $n_r$ , an integer radial quantum number.  $\lambda$  stands for the angular momentum  $l$ , which for S-, P- and D-states is a non-integer effective angular-momentum quantum number. For Li atoms  $\lambda$  becomes close to integer  $l$  only for states with higher angular momentums,  $\lambda = l \geq 3$ . The distinction from the hydrogen energy spectrum results in essential difference of radiation properties of the Rydberg states with  $l < 3$ . In particular, the spontaneous decay rate of the P-series is more than one order smaller than those of hydrogen and helium atoms [1], while the rate of S-state spontaneous decay is twice as big as that of the hydrogen atoms, and only the D-state natural decay rates become comparable with those of hydrogen. Yet more significant departure from hydrogen appears in particular properties of the three different radiation processes: (i) decay, (ii) excitation and (iii) ionization, induced in the Rydberg-state lithium atoms by the blackbody radiation (BBR) of environment. The most important of these differences is caused by

the irregular behaviour of the  $nS$ -state ionization cross section. This irregularity starts from the threshold ionization of the lowest states. The cross section falls down with the growth of the principal quantum number  $n$ , up to  $n=33-34$  [2,3]. Starting from  $n=35$ , the cross section of the threshold ionization begins to grow up with  $n$  following a power law,  $\sigma_{nl}^{thr} \propto n^q$ , with the exponent  $q > q_0$  where  $q_0 = 5/3$  is the exponent, characteristic of the asymptotic behaviour of the Rydberg-state ionization cross-section, as the semiclassical theory predicts for all Rydberg series independently of the angular momentum  $l$  [4]. The smallness of the ionization cross section makes negligibly small the contribution of ionization to the BBR-induced broadening of the  $nS$ -states. The principal role in the BBR-induced broadening belongs to bound-bound transitions: downward (decays) for the S-series and upward (excitations) for the P- and D-series. For example, at room temperature (300 K) the BBR-induced broadening of the 61S-state equals about 93% of the natural width ( $\Gamma_{61S}^{sp} = 5328 \text{ s}^{-1}$ ). 70.7% of this belongs to the contribution of decays and 22.8% is due to the excitations. The contribution of the BBR-induced ionization here does not exceed 0.001% of  $\Gamma_{61S}^{sp}$ .

Simple analytical approximations for the fractional probabilities of the BBR-induced photo-processes are proposed, which e.g., for decay (excitation) may be written as

$$R_{nl}^{d(e)}(T) = \Gamma_{nl}^{d(e)}(T) / \Gamma_{nl}^{sp} = \frac{a_0^{d(e)} + a_1^{d(e)}x + a_2^{d(e)}x^2}{n^2 [\exp(x^3) - 1]}$$

where  $x^3 = 315780/n^3T$  is the ratio of the energy of transitions between neighbour Rydberg levels  $\Delta E_{nl} \approx 1/n^3$  and the thermal energy  $kT = T/315780$  (in atomic units). The coefficients  $a_i^{d(e)}$  and their very smooth dependence on temperature are determined from the standard curve polynomial fit procedure. The error of the approximation equations in the region of  $x < 1$  is below 2%.

#### REFERENCES

- [1] Glukhov I.L., Nekipelov E.A. and Ovsiannikov V.D. J. Phys. B. 43, 125002 (2010).
- [2] Aymar M., Luc-Koenig E. and Farnoux F.C. J. Phys. B. 9, 1279 (1976).
- [3] Ovsiannikov V.D., Glukhov I.L. and Nekipelov E.A. Optics and Spectrosc. 111, 25 (2011).
- [4] Delone N. B., Goreslavsky S. P. and Krainov V. P. J. Phys. B. 27, 4403 (1994).

Poster Presentations – Quantum Optics P.QO.3

## Simple analytical expressions for analysis of the phase-dependent electromagnetically induced transparency

J. Dimitrijević and D. Arsenović

*Institute of Physics, University of Belgrade, Pregrevica 118, 11080 Serbia*

e-mail: jelena.dimitrijevic@ipb.ac.rs

We study double- $\Lambda$  atomic scheme that interacts with four laser light beams so that the closed loop of radiation-induced transitions is formed. When specific relations for field phases, frequencies and amplitudes are satisfied, coherent superpositions (so called “dark states”) can be formed in a double- $\Lambda$ , which leads to the well known effect of electromagnetically induced transparency (EIT). If the interaction scheme in a double- $\Lambda$  system is such that closed loop is formed, the relative phase of the laser light fields becomes very important [1]. We here analyze the effect of the lasers’ relative phase on the overall EIT profile.

Theoretical study of interactions of lasers with a double- $\Lambda$  atomic scheme is commonly done by solving optical Bloch equations (OBEs). We here use perturbative method [2] to solve OBEs, where the interaction of lasers with double- $\Lambda$  is considered a perturbation. Advantage of perturbative method

is that it generally produces simpler solutions and analytical expressions can be obtained. We present analytical expressions for the lower-order corrections of the EIT signal. Our results show that the EIT by perturbative method can be approximated by the sum of products of complex Lorentzians. Through these expressions we see in which way relative phase affects overall EIT profile.

#### REFERENCES

- [1] E. A. Korsunsky, D. V. Kosachiov, Phys. Rev. A 60, 6 (1999).
- [2] J. Dimitrijević, D. Arsenović, B. M. Jelenković, New J. Phys. 13, 033010 (2011).

Poster Presentations – Quantum Optics P.QO.4

### **Comparison of double- $\Lambda$ atomic scheme with single- and two-fold coupled transitions**

D. Arsenović and J. Dimitrijević

*Institute of Physics, University of Belgrade, Pregrevica 118, 11080 Serbia*

e-mail: jelena.dimitrijevic@ipb.ac.rs

Four-level double- $\Lambda$  atomic scheme i.e., two  $\Lambda$  systems sharing the same two ground levels, that interacts with four laser light fields is studied theoretically. Peculiarity is that each of the two ground states can be coupled to each excited state by two laser light fields. Certain energy difference exists between excited-state levels. We consider this energy small enough, so that laser resonant to either one transition can also couple the other transition. We test whether coupling of the more detuned laser is not non-negligible. Multiply connected states were also recently analyzed (and the comparison with the experiment was presented), but for the simpler, two and three level atomic schemes [1].

Theoretical treatment of the double- $\Lambda$  atomic scheme is commonly done by solving optical Bloch equations (OBEs). When rotating-wave approximation (RWA) is applied, OBEs become, by their form, a set of linear differential equations with constant coefficients. Theoretical treatment of the interaction scheme treated here leads to OBEs with coefficients that are not constant, but oscillate with time, even after RWA is applied. Under certain assumptions, the approximation can be used where the time-dependent coefficients are averaged over their periods [1]. The method yields new system of equations (similar to standard OBEs), but with more independent variables and can also be solved in a usual way. The results presented here analyze validity of this approximation by comparing results for the double- $\Lambda$  atomic scheme with single- and two-fold coupled transitions. We test whether in the limit of large energy splitting between excited-state levels both approaches lead to similar results.

#### REFERENCES

- [1] D.N. Stacey, D.M. Lucas, D.T.C. Allcock et al., J. Phys. B: At. Mol. Opt. Phys. 41, 085502 (2008).

## A quantum phase operator on the von Neumann lattice

Lj. Davidović<sup>1</sup>, M Davidović<sup>2</sup> and M. Davidović<sup>3</sup>

<sup>1</sup>*Institute of Physics, University of Belgrade, Serbia*

<sup>2</sup> *Vinca Institute of Nuclear Sciences, University of Belgrade, Serbia*

<sup>3</sup>*Faculty of Civil Engineering, University of Belgrade, Serbia*

e-mail: milena@grf.bg.ac.rs

Using the results from [1], where some difficulties related to the definition of non entire functions of the creation and annihilation operators present in the literature - were avoided, we analyze a new quantum phase operator defined on the von Neumann lattice- as proportional to the difference of logarithms of creation and annihilation operators. We compare phase distributions for some characteristic states obtained with this new operator and some other results for phase distributions obtained with earlier approaches. We discuss the obtained results.

### REFERENCES

[1] Lj. Davidovic, D. Arsenovic, M. Davidovic, D. Davidovic, J. Phys. A: Math. Theor. 42, 23 (2009).

## Narrowing of EIT resonance in the configuration of counter-propagation laser beams

I. S. Radojičić<sup>1</sup>, Z. D. Grujić<sup>1,2</sup>, M. M. Lekić<sup>1</sup>, D. V. Lukić<sup>1</sup> and B. M. Jelenković<sup>1</sup>

<sup>1</sup>*Institute of Physics, Belgrade, Serbia*

<sup>2</sup>*Department of Physics, University of Fribourg, CH-1700 Fribourg, Switzerland*

e-mail: ivanrad@ipb.ac.rs

We present effects of Ramsey method of separated oscillatory fields (pump and probe) on electromagnetically induced transparency (EIT). Both pump and probe lasers are locked to the  $F_g = 2 \rightarrow F_c = 1$  in  $D_1$  line transitions of  $^{87}\text{Rb}$ . Effects are analyzed in the Hanle configuration and in a room temperature Rb vapor cell. The pump laser beam is used for creation and the probe laser beam for detection of the coherence between ground-state Zeeman sublevels.

We show that EIT can be obtained with spatially separated and counter-propagating pump and probe beams. In comparison with the single laser beam, substantial narrowing of the probe Hanle EIT is obtained due to temporal evolution of the pump induced Zeeman coherence and later probed by the probe laser. The interference between atomic coherences and the probe laser are confirmed from changes of the resonances line shape with the angle between linearly polarized pump and probe laser beams, i.e., due to different initial phases of the atomic coherences. These results are compared with results obtained with co-propagating pump and probe laser beam [1], and in counter-propagating scheme we have overcome problems due to scattered pump beam light that was mixed with probe beam on photo detector. This allowed us to use lower light power in probe beam and to obtain slightly narrower resonances.

### REFERENCES

[1] Grujić, M. Mijailović, D. Arsenović, B. M. Jelenković, Phys. Rev. A 78, 063816-1 (2008).

## Influence of Ramsey effects on Electromagnetically Induced Transparency and Slow Light in Hot Rubidium Vapor

S. N. Nikolic<sup>1</sup>, N.M. Lucic<sup>1</sup>, A.J. Krmpot<sup>1</sup>, S.M. Cuk<sup>1</sup>, M. Radonjic<sup>1</sup> and B.M. Jelenkovic<sup>1</sup>

<sup>1</sup>*Institute of Physics, Belgrade, Serbia*

e-mail: stankon@ipb.ac.rs

Coherent population trapping (CPT) is a coherent superposition of atomic levels of long lived hyperfine states, while Electromagnetically induced transparency (EIT) [1], nonlinear magneto-optical rotation of polarization, and slow light [2] are quantum optical phenomena, related to CPT. Our experimental realization of EIT is based on Zeeman coherences between magnetic sublevels of hyperfine level of rubidium electronic ground state. Slow light effect of the probe laser pulse, in the presence of a resonant, strong pump laser beam is due to a high dispersion, centered at a EIT peak, which hereafter leads to very low group velocity of the light pulse.

In our experiment, we derive two optical fields of different circular polarizations from a single laser beam locked to the transition  $5^2S_{1/2}, F_g=2 \rightarrow 5^2P_{1/2}, F_c=1$  in  $^{87}\text{Rb}$ . Zeeman coherences between magnetic sublevels whose numbers differ by 2 were generated by  $\sigma_+$  and  $\sigma_-$  laser light. Gaussian like pulse of  $\sigma_-$  circular polarization (probe) was obtained by applying voltage pulse to the Pockels cell, i.e.,  $\text{LiNbO}_3$  crystal. This pulse co-propagates with much stronger optical field of  $\sigma_+$  circular polarization through hot Rb cell filled with 30 Torr of Ne buffer gas. These two fields yield to electromagnetically induced transparency and to slower probe pulse propagation due to low group velocity. We define fractional time delay as a ratio of an absolute time delay of the slow light pulse to its temporal length.

We investigated experimentally and theoretically effects of separated excitation fields on probe EIT linewidths and time delay of probe pulse. Due to atom diffusion out and back again in the laser beam, atomic coherence spends time in a “dark” making conditions for Ramsey effect on resonance line narrowing. This effect can be seen by using single probe laser pulse. We enhanced Ramsey effect by applying successive probe pulses thus allowing more atoms in the superposition state to evolve in the “dark” before the second excitation pulse. We have done thorough investigation of various experimental parameters in order to achieve highly contrasted and narrow EIT resonances as well as the minimal values of group velocity and fractional time delay of polarization light pulses. We changed total laser intensity, the ratio of  $\sigma_-$  light power to the  $\sigma_+$  light power, duration of the probe pulse, time interval between subsequent probe pulses and temperature of the Rb cell. We showed that there is an important influence of all these parameters on EIT and slow light features. One of the possible applications of such experiment is the preparation of the system so that storage of light [3] could be achieved as a first step to quantum information processing and atomic quantum memory.

### REFERENCES

- [1] M. Fleischhauer, A. Imamoglu, J. P. Marangos, *Rev. Mod. Phys.* 77, 633 (2005).
- [2] Hau L. V. et al., *Nature (London)* 397, 594 (1999).
- [3] D. F. Phillips et al., *Phys. Rev. Lett.* 86, 783 (2001).

## Acoustic and visual display of photons: a demonstration device

T. L. Dimitrova<sup>1,2</sup>, A. Lechkov<sup>3</sup>, Ts. Grigorova<sup>3</sup>, and A. Weis<sup>2</sup>

<sup>1</sup>*Faculty of Physics, University of Plovdiv, Tzar Assen Str. 24, 4000 Plovdiv, Bulgaria*

<sup>2</sup>*Department of Physics, University of Fribourg, CH-1700 Fribourg, Switzerland*

<sup>3</sup>*Departments of Electronics, Technical University, 61 St. Petersburg Bul., 4000 Plovdiv, Bulgaria*  
e-mail: tldimitrova@abv.bg

We will present a handheld device for rendering the signals produced by individual photons. The device is intended to be used for lecture (or public) demonstrations of the discrete nature of light. It is based on a Hamamatsu type H10722-01 photomultiplier (PM) which contains a controllable high voltage supply and a pulse preamplifier [1]. The PM operates on  $\pm 5$  V, which is supplied by rechargeable batteries. A simple electronic discriminator circuit allows the analog pulses of varying amplitudes produced by the PM to be converted into digital TTL pulses.

Light enters the device through a narrow solid angle collimator made of 0.3 mm diameter apertures. Two interference filters (10 nm bandpass) inserted between the apertures prevent overloading the PM. The apertures and filters are held in a removable collimator block that is mounted onto the PM using Hamamatsu's type A10030 adapter block [2]. The collimator, PM, and batteries are mounted in a handheld housing. Small potentiometers allow the individual control of the PM's high voltage and the discriminator level.

Electric pulses produced by individual photons in the PM are rendered acoustically by a small loudspeaker built into the housing. Output connectors allow the pulse signals to be displayed by an external amplifier/loudspeaker system, an oscilloscope, or to be further processed by pulse counting electronics.

Besides its use as a standalone device that demonstrates photon pulses, the device has a number of interesting other applications in teaching: When using a collimator block with interference filters that pass only a specific spectral line one can demonstrate the remote sensing of chemical elements, such as the presence of mercury (identified by its 546.1 nm green line) in a fluorescence light tube or a street lamp. When pointing the device at a distant surface illuminated by an enlarged laser spot, one may demonstrate the proportionality relation between the brightness of the spot and the photon click rate. When increasing the incident radiation such that the average photon rate exceeds the inverse of the pulse widths ( $\approx 20$   $\mu$ s), the individual pulses pile up to form a fluctuating continuous signal that is well suited for illustrating the concept of shot noise and for making quantitative measurements thereof. The collimator/PM assembly is routinely used by us in our demonstration experiments on the wave-particle duality of light [3] and the phenomenon of quantum erasing [4,5].

Acknowledgements:

The authors thank the financial support of the SNF Scopes program (grant No. IZ73Z0-127942-1).

### REFERENCES

- [1] <http://sales.hamamatsu.com/index.php?id=13226587>.
- [2] [http://jp.hamamatsu.com/products/sensor-etd/3006/A10030-01/index\\_en.html](http://jp.hamamatsu.com/products/sensor-etd/3006/A10030-01/index_en.html).
- [3] T. L. Dimitrova and A. Weis, *Am. J. Phys.*, 76, 137 (2008).
- [4] T. L. Dimitrova and A. Weis, *Eur. J. Phys.*, 31, 625 (2010).
- [5] T. L. Dimitrova and A. Weis, submitted to *Eur. J. Phys.*

**Constrained quantum dynamics and coarse-grained description of a quantum system of nonlinear oscillators**

M. Radonjić, S. Prvanović and N. Burić  
*Institute of Physics, University of Belgrade, Pregrevica 118*  
*Belgrade, Serbia*  
e-mail: buric@ipb.ac.rs

Constrained Hamiltonian dynamics [1,2] is exploited to provide the mathematical framework of a coarse-grained description of the quantum system of nonlinear interacting oscillators [3]. The classical system has finite dimensional phase-space and the quantum system viewed as the Hamiltonian system is infinite dimensional in an essential way. Kinematical and dynamical properties of the classical system are obtained from the quantum one via the two step procedure consisting of a coarse-graining followed by classical limit. The coarse-graining is mathematically treated as an equivalence relation on the set of quantum states, and as a result emerges the classical phase-space. The equivalence relation imposes a constraint on the Hamiltonian dynamics of the quantum system. The constraints preserve constant and minimal quantum fluctuations of the canonical observables. The formulation of the most appropriate finite set of constraints that fulfill the goal is not straightforward and involves the nonlinear interaction potential. Resulting constrained Hamiltonian system on the coherent state constrained manifold represents the coarse-grained description of the quantum system of oscillators. The system differs from the classical system with the same potential only in the terms that are arbitrary small in the classical i.e. macroscopic limit.

The procedure can be used to obtain other classical systems from the corresponding coarse-grained quantum systems in the corresponding classical limit.

This work is partly supported by the Serbian Ministry of Science contracts No. 171017, 171028, 171038 and 45016.

REFERENCES

- [1] N. Burić, *Ann. Phys. (NY)* 233, 17 (2008).
- [2] D.C. Brody, A.C.T. Gustavsson, L.P. Hughston, *J. Phys. A* 41, 475301 (2008).
- [3] Milan Radonjić, Slobodan Prvanović, Nikola Burić, submitted to *Physical Review A*.

## Rb Magneto-Optical Trap and Temperature Measurement by Shaking of the Cold Cloud of Atoms

I. Temelkov<sup>1,2</sup>, G. Dobrev<sup>1,2</sup>, E. Dimova<sup>1</sup>, A. Pashov<sup>2</sup>, K. Blagoev<sup>1</sup> and N. Vitanov<sup>2</sup>

<sup>1</sup>*Institute of Solid State Physics, Bulgarian Academy of Sciences  
Sofia, Bulgaria*

<sup>2</sup>*Faculty of Physics, Sofia University  
Sofia, Bulgaria*

e-mail: edimova@issp.bas.bg

Recently in the Institute of Solid State Physics, Bulgarian Academy of Sciences in collaboration with groups from Faculty of Physics of Sofia University, rubidium atoms (85Rb and 87Rb) were cooled and trapped in a standard 3D magneto-optical trap (MOT). A systematic characterization of the rubidium MOT in terms of the total number of trapped atoms versus several laser intensities, laser detuning, and magnetic field gradients have been done. The total amount of fluorescence emitted by the cold atoms has been measured with a calibrated photodiode subtending a known solid angle, while a high-speed video camera connected to a computer via an image acquisition board is used to monitor the size and the shape of the atomic cloud. The temperature measurements are made by a method of shaking MOT [1,2].

### REFERENCES

- [1] Kohns, P Buch, W. Suptitz, C. Csambal, W. Ertmer, *Europhys. Lett.* 22, 517 (1993).
- [2] M.I. den Hertog, “Measuring the temperature of a Rb MOT using an oscillating magnetic field”, Thesis, (2004).

## Quantum Fluctuations in Dipolar Bose Gases

A. Lima<sup>1</sup> and A. Pelster<sup>2,3</sup>

<sup>1</sup>*Institute for Theoretical Physics, Free University of Berlin, Germany,*

<sup>2</sup>*Department of Physics, University of Duisburg-Essen, Germany*

<sup>3</sup>*Department of Physics, University of Bielefeld, Germany*

e-mail: axel.pelster@fu-berlin.de

We investigate the influence of quantum fluctuations upon dipolar Bose gases by means of the Bogoliubov-de Gennes theory. Thereby, we make use of the local density approximation to evaluate the dipolar exchange interaction between the condensate and the excited particles. This allows to obtain the Bogoliubov spectrum analytically in the limit of large particle numbers. After discussing the condensate depletion and the ground-state energy correction, we derive quantum corrected equations of motion for harmonically trapped dipolar Bose gases by using superfluid hydrodynamics. These equations are subsequently applied to analyze the equilibrium configuration, the low-lying oscillation frequencies, and the time-of-flight dynamics. We find that both atomic magnetic and molecular electric dipolar systems offer promising scenarios for detecting beyond mean-field effects.

### REFERENCES

- [1] A. Lima and A. Pelster, eprint: arXiv:1103.4128.

## From spatially periodic states with lattice periodicity to states with the double lattice period in Bose-Einstein condensates in an optical lattice

G. Gligorić<sup>1,2</sup>, A. Maluckov<sup>3</sup>, Lj. Hadžievski<sup>1</sup> and B. A. Malomed<sup>4</sup>

<sup>1</sup>*Vinca Institute of Nuclear Sciences, Belgrade, Serbia*

<sup>3</sup>*Max-Planck-Institut für Physik komplexer Systeme, Dresden, Germany*

<sup>2</sup>*Faculty of Sciences and Mathematics, University of Niš, Serbia*

<sup>4</sup>*School of Electrical Engineering, Faculty of Engineering, Tel Aviv University, Israel*

e-mail: goran79@vinca.rs

The properties of dipolar Bose-Einstein condensates (BEC) in optical lattice have been in a research focus during past few years [1], [2]. Here we study dipolar BEC in an one-dimensional very deep optical lattice, modeling the system by discrete nonlinear Schrödinger equation with dipole-dipole interaction term [1]. We demonstrate the existence of stationary states with periods equal to twice that of the optical lattice. Their occurrence coincides with the onset of dynamical instability of states of the usual Bloch form with the lattice periodicity (continuous-wave, cw solution) [3]. Actually, the changing of their stability at critical value of the system parameter gives rise to two double periodic solution (DPS) branches which are stable with respect to the mentioned perturbation. In general, in the anti-continuum limit (very deep optical lattice) the supercritical pitchfork bifurcation is associated with this transformation.

The exact form of the period-doubled solutions is found and main conclusions are derived analytically by the variational approach and numerically. To generate spatial doubled periodic pattern in the model the presence of local (contact) or/and nonlocal (dipole-dipole) interaction was needed. It is shown that the DPS occurs in the form of unstaggered or staggered periodic pattern with a twice of the lattice periodicity. Except in the anti-continuum limit the DPSs are unstable with respect to arbitrary small perturbation.

Dynamical calculations show two interesting points for very deep lattices. In the presence of a small perturbation with a twice lattice period, the DPS pattern conserves its form and the cw solution evolves into the double periodic breathing pattern in the long time limit (the order of a few dozens of milliseconds which corresponds to the experimentally reached life times of the dipolar BECs). This period doubling patterns can be also related with the framework of the so called Peierls instability which occurs in the spatially periodic electron systems in the condensate matter physics and leads to transition from conduction to isolator phase. Therefore, studies of this kind of problem in the dipolar BEC could be also interesting in more general point of view, than the physics of ultracold gases is.

### REFERENCES

- [1] G. Gligorić, A. Maluckov, Lj. Hadžievski, B. A. Malomed, *Physical Review A* 78, 063615 (2008).
- [2] S. Müller, J. Billy, E. A. Henn, H. Kadau, A. Griesmaier, M. Jona-Lasinio, L. Santos, T. Pfau, arXiv:1105.5015v1.
- [3] M. Machholm, A. Nicolin, C. J. Pethick H. Smith, *Physical Review A* 69, 043604 (2004).

# *Laser Induced Material Modifications*

Poster Presentations – Laser Induced Material Modifications P.LIM.1

## **Microstructural changes of Nimonic-263 superalloy arisen by laser beam action**

S. Petronić<sup>1</sup>, A. Kovačević<sup>2</sup>, A. Milosavljević<sup>3</sup> and A. Sedmak<sup>3</sup>

<sup>1</sup>*Innovation Center of the Machine Engineering Faculty, University of Belgrade, Belgrade, Serbia*

<sup>2</sup>*Institute of Physics, University of Belgrade, Belgrade, Serbia*

<sup>3</sup>*Machine Engineering Faculty, University of Belgrade, Belgrade, Serbia*

e-mail: aleksander.kovacevic@ipb.ac.rs

The interaction with laser beams can ameliorate the micro-hardness of many materials, among which the superalloys are attractive and new. Nimonic-263 superalloy is widely used in harsh surroundings (elevated temperature and pressure) due to its robust characteristics. Laser treatments induce the changes in the microstructure of superalloys including the formation of nano-particles [1, 2]. We have investigated the microstructure changes of Nimonic-263 surface occurring after laser treatments (mechanical and thermomechanical), with the aim to improve the mechanical properties of the material.

For the mechanical treatment, the absorbent material was applied to the surface, and the samples were submerged in the transparent liquid and exposed to laser beam radiation. For the thermomechanical treatment, the laser beam action occurred directly on the material. The treatments of the surface were performed with pulses of Ti:Sapphire and Nd<sup>3+</sup>:YAG laser beams with various repetition rates.

The microstructure changes arisen in the material after laser beam interaction with the samples were observed by scanning electron microscopy and analyzed by energo-dispersive spectrometry. Different structural morphologies and various forming clusters of micro-constituents were noticed, analyzed and – from technological point of view – labeled as wanted or unwanted. Grain size of the clusters was measured and the micro-hardness Vickers-tests were performed. The results were analyzed and discussed. The investigations are intended to contribute to the study on the level of the microstructure changes due to the laser processing, in order to obtain better mechanical properties of superalloys.

Acknowledgements: This work is supported by the Ministry of Science of the Republic of Serbia under contract III45016.

### REFERENCES

- [1] A. Milosavljević, S. Petronić, M. Srećković, A. Kovačević, A. Krmpot, K. Kovačević, *Acta Phys. Pol. A* 116, 553 (2009).
- [2] S. Petronić, S. Drecun-Nešić, A. Milosavljević, A. Sedmak, M. Popović, A. Kovačević, *Acta Phys. Pol. A* 116, 550 (2009).

## Surface modification of Ti-based nanocomposite multilayer structures by laser beam irradiation

S. Petrović<sup>1</sup>, B. Salatić<sup>2</sup>, D. Peruško<sup>1</sup>, M. Panjan<sup>3</sup>, D. Pantelić<sup>2</sup>, B. Gaković<sup>1</sup>  
B. Jelenković<sup>2</sup> and M. Trtica<sup>1</sup>

<sup>1</sup>*Institute of Nuclear Sciences Vinča, POB 522, 11001 Belgrade, Serbia*

<sup>2</sup>*Institute of Physics Belgrade, University of Belgrade, Prigrevica 118, 11080 Belgrade, Serbia*

<sup>3</sup>*Jožef Stefan Institute, Jamova 39, 1000 Ljubljana, Slovenia*

e-mail: spetro@vinca.rs

Titanium-aluminum and titanium-nickel are well known alloys with very good physicochemical characteristics such as thermo chemical stability for high temperature wear and corrosion protection. Multilayered nanometric thin films, composed of titanium and aluminum/nickel, are attractive due to their unusual phase compositions, which are not attributed to uniform bulk of the single metals. Conventional mechanical micro/nano structuring of such multilayered composites is difficult and application of a focused laser beam is often the solution.

Nano composites in form of alternating nanolayers were created by physical vacuum deposition (PVD). Deposition of Al/Ti and Ni/Ti on silicone substrate, were conducted in a single vacuum run, by switching sputtering from one metallic target to the other. Total thickness of the deposited structures was ~250 nm, each consisting of 10 individual layers. Laser surface modification /processing of samples were done by a focused Er,Yb,Cr-glass laser. The wavelength was 1540 nm, pulse duration 60 ns and pulse energy from 2 to 10 mJ. The irradiation was conducted in air. Before and after the laser irradiation, surface morphology of the samples was monitored by optical microscopy (OM) and scanning electron microscopy (SEM). Chemical and phase composition were determined by X-ray photoelectron spectroscopy (XPS). Profilometer was used to characterize topographic changes of the modified areas.

The surface modification of samples was investigated after one, two, five or ten pulses with the constant energy per pulse. In the experiment, energy density was varied from 10 to 20 Jcm<sup>-2</sup>. During irradiation of (Al/Ti)/Si and (Ni/Ti)/Si systems with nanosecond laser pulses, the main part of the absorbed energy was rapidly transformed into heat which, depending on energy density, caused melting, phase transformation, material ejection, ablation, etc. For applied pulse number-energy density combination, the surface changes of the (Al/Ti)/Si and (Ni/Ti)/Si can be clearly recognized. For both systems surface changes/phenomena can be summarized as: (i) intensive removal of surface material with crater like characteristics; (ii) appearance of hydrodynamic features, resolidified droplets in near and farther periphery; (iii) sporadic cracking and, (iv) manifestation of spark-like plasma in front of the target after first and subsequent pulses. The differences in laser surface modification between both systems were evident.

Morphological changes of (Ni/Ti)/Si system included partial modification of the silicon substrate in the form of polygonal/mosaic structures and appearance of hydrodynamic features in the shape of nano-globules. This result indicated recrystallization and redeposition of the system components. For the (Al/Ti)/Si multilayer, showed amorphisation of the irradiated region. At the constant laser fluence and same number of pulses, the craters were slightly deeper for (Ni/Ti)/Si than for (Al/Ti)/Si system. It was also found that ablation rate in case of (Ni/Ti)/Si system was greater than ablation rate for the (Al/Ti)/Si system. Different shape and dimension of the formed craters for both systems, as well as the absence of specific structure on the Si substrate in the case of (Al/Ti)/Si system, are mainly due to different thermo physical properties of the building components, especially low melting point of aluminum.

**Femtosecond laser ablation of alumina (Al<sub>2</sub>O<sub>3</sub>) from a multilayered coating**

B. Gaković<sup>1</sup>, C. Radu<sup>2</sup>, M. Zamfirescu<sup>2</sup>, B. Radak<sup>1</sup>, M. Trtica<sup>1</sup>, S. Petrović<sup>1</sup>, J. Stašić<sup>1</sup>, M. Čekada<sup>3</sup>  
and I.N. Mihailescu<sup>2</sup>

<sup>1</sup>*Institute of Nuclear Sciences Vinča, University of Belgrade, POB 522, 11001 Belgrade, Serbia*

<sup>2</sup>*National Institute for Lasers, Plasma and Radiation Physics, POB MG-36, Magurele, Ilfov, Romania*

<sup>3</sup>*Jožef Stefan Institute, Jamova 39, 1000 Ljubljana, Slovenia*

e-mail: biljagak@vinca.rs

Femtosecond laser pulses at low fluences can generally produce conditions for no dissipation of laser beam energy out of the irradiated area, due to highly excited electrons that facilitate Coulomb explosion and, consequently, direct ablation. Irradiation by short laser pulses provides unique possibilities for high precision material processing. Due to rapid energy delivery to the material surface, heat-affected zones in the irradiated targets are strongly localized with minimal residual damage, which can allow generation of well-defined nano- micro- structures of high quality and reproducibility. For producing controllable features, the parameter of special importance is the damage threshold fluence (Dth(1)) of a single pulse. This value depends on the properties of the material and on the laser pulse parameters. In the present work we investigated the effects of single femtosecond laser pulses by varying energy per pulse, on multilayered protective coatings. The coating was composed of alumina ceramic (Al<sub>2</sub>O<sub>3</sub>) top layer over titanium aluminium nitride single layer (TiAlN). The optimal conditions at which the irradiation by a single laser pulse produced partial exfoliation of the top layer were recorded. Partial exfoliation in the form of regularly distributed micro holes could be useful, for example, as a “bed” for solid lubricant in tools manufacturing, in microelectronics, etc.

The laser used was a Ti:sapphire equipped with a chirped pulse amplification (CPA) system (Clark-MRX 2101). The wavelength of the amplified output beam was 775 nm, with 200 fs pulse duration. The pulse energy ranged from 0.5 to 50 μJ. The spatial profile of the beam was Gaussian, and the irradiations were performed in air. The linearly polarized beam was focused with a 75 mm focus lens and directed perpendicular to the target surface. The experimental sample, multilayered protective coating of Al<sub>2</sub>O<sub>3</sub> and TiAlN (total thickness 2.4 μm) was deposited on a steel substrate by the PVD sputtering technique.

To determine the damage threshold fluence, a series of laser pulse energies (E) was used. The fluences that corresponded to pulse energies used ranged from 0.1 to 7.0 J cm<sup>-2</sup>. The procedure was computer controlled. Before and after laser irradiation, the sample was characterized by several analytical techniques. The coating was analysed by energy-dispersive X-ray and Auger electron spectroscopy (EDXS and AES). Detailed analyses of the surface morphology were performed by scanning electron microscopy (SEM&EDX). Profilometry was used for estimating the damaged/ablated area diameters, depths and for morphology analysis. The damage/ablation threshold for these multilayered coatings was found to be Dth (1)=1.2 μJ or F(1) =0.22 J cm<sup>-2</sup>. The top 1.4 μm Al<sub>2</sub>O<sub>3</sub> layer was ablated within the range of fluences from 0.22 to 1.90 J cm<sup>-2</sup>, without affecting the remaining TiAlN layer.

## Laser based observation of water condensation on metal surface

A. Bizjak<sup>1</sup>, D. Horvat<sup>2</sup> and J. Možina<sup>2</sup>

<sup>1</sup>*IHS, Krško, Slovenia*

<sup>2</sup>*Faculty of Mechanical Engineering, University of Ljubljana, Slovenia*

e-mail: darja.horvat@fs.uni-lj.si

In this contribution we have studied experimentally and in controlled conditions the condensation of water on the surface of a metal. The measurement was fully laser supported, from surface preparation through laser treatment to the laser evaporation of condensed water and to optodynamic response measurements with a laser deflection probe.

When light is rapidly absorbed in matter nonstationary phenomena occur which together constitute optodynamic response of the material [1]. It consists of a wide range of phenomena such as heating, expansion, deformation, vaporization, ablation, formation of shock and sound waves in the material and the surrounding area, etc.. When nanosecond Er: YAG laser pulses are absorbed in water rapid heating occurs, which can be followed by evaporation, explosive boiling [2] and removal of material (ablation). The wavelength emitted by Er: YAG laser (2940 nm) lies in the part of the spectrum, where there is a maximum in water absorption and is often used in scientific and technological applications related to water, such as biological and medical fields. Optodynamic waves which are created following the absorption of a laser pulse in the material and the surrounding area are a rich source of information about the phenomenon. They can be detected with a laser deflection probe, which has the advantage of being non-contact and having a wide frequency response, limited only by the characteristics of the detection electronics.

The surface was cooled to a constant temperature below the dew point. Condensation was studied as a dynamic phenomenon, from the beginning of accumulation of water on a dry surface until equilibrium quantity of water on the surface is reached under given conditions. Er:YAG pulses were also used as a laser cleaning tool [3] for prior drying of the experimental area. After the water was allowed to condense on the metal surface for a prescribed time interval we illuminated it with a single laser pulse and detected the resulting optodynamic waves with a laser deflection probe in the surrounding air. The relationship between the optodynamic response and condensation dynamics was examined by changing the measurement parameters such as surface temperature, humidity of the ambient air and the time of condensation.

### REFERENCES

- [1] D. Horvat, R. Petkovšek, J. Možina, *Meas. sci. technol.*, 21, 035301-1 (2010).
- [2] A. A. Samokhin, V. I. Vovchenko, N. N. Il'ichev, P. V. Shapkin, *Laser Phy.* 19, 187 (2009).
- [3] V. Bregar, J. Možina, *Appl. Surf. Sci.*, 185, 277 (2002).

# Post-Deadline Contributions

---

Poster Presentations – Metamaterials P.MM.6

## Investigation of Group Delay in Transmission Lines Consisting of Reconfigurable Split-Ring Resonators

R. Bojanic, B. Jokanovic and V. Milosevic  
*Institute of Physics,  
Belgrade, Serbia  
e-mail:radovan@ipb.ac.rs*

Reconfigurable, multi band devices play an important role in modern wireless systems. A number of papers published so far presents the application of split-ring resonators (SRRs) in design of multi band filters operating simultaneously in two or three frequency bands [1-2]. Despite that concept we investigate different spatial arrangements of split-ring resonators, obtained by rotating individual split-rings, which can be done electronically. It was shown that twisting the angle between SRRs significantly influences the electromagnetic properties and operating frequency range and can be use as additional degree of freedom in design of tunable multi band devices from microwaves to terahertz. [3].

In this work we present theoretical and experimental results of the effective electromagnetic parameters [4-5] for different transmission lines consisting of coupled split-ring resonators. We investigate how the effective electromagnetic parameters and group delay depend on the angle between SRRs. Three different shapes of SRRs: square, rectangular and meander type, which have the same length, are considered in order to maximize group delay per one unit cell. It was shown that unit cells with SRRs placed symmetrically in respect to transmission line exhibit considerably smaller

group index  $n_g$  ( $n_g = \frac{c}{v_g} = n + \omega \frac{dn}{d\omega}$ ) and consequently the smaller group delay  $\tau_g$  ( $\tau_g = -\frac{d\phi(\omega)}{d\omega}$ ),

than if a little asymmetry is introduced by twisting the resonators by 90 degrees. It is noticed that if mutual position of gaps in square SRRs changes from 0 to 180 degrees in respect to transmission line, the group delay exhibits variation of more than four times (from 0.75ns to 3.1ns). The variation of group delay is even more pronounced in case of rectangular SRRs and reaches almost six times (from 0.78ns to 4.7ns). At the same time group velocity of light can be reduced by factor of 600 with relatively low losses.

In order to verify simulated results, different configurations of SRRs coupled with microstrip line are fabricated and measured in microwave range from 4GHz to 10GHz. The measured transmission and reflection coefficients as well as the extracted effective parameters show a very good agreement with simulations.

### REFERENCES

- [1] Fan, J. W., C. H. Liang, and X. W. Dai, Progress In Electromagnetics Research, PIER 75, 285 (2007).
- [2] R.H. Geschke, B. Jokanovic and P. Meyer, IEEE Trans. on MTT 59, 1500 (2011).

- [3] V. Milosevic, B. Jokanovic, B. Kolundzija, 4th International Congress on Advanced Electromagnetic Materials in Microwaves and Optics, Metamaterials, 537-539 (2010).
- [4] Shau-Gang Mao, Shiou-Li Chen, Chen-Wei Huang, IEEE Trans. Microwave Theory Tech. 53, 1515 (2005).
- [5] S. Ponjavic, B. Jokanovic, R. Geschke, 3rd International Congress on Advanced Electromagnetic Materials in Microwaves and Optics, Metamaterials, 794-797 (2009).

# Author Index

---

Abdou-Ahmed M.	63	Bergmair I.	85
Abramovich A.	30	Berzinsh A.	105
Affolderbach C.	38, 103, 110	Bessièrè A.	36
Akram A.	30	Bessodes M.	36
Aktsipetrov O.A.	90	Bison G.	39
Aleksic B.N.	99, 100	Bizjak A.	155
Aleksic N.	28, 46, 98	Blagoev K.	150
Aleksic N.B.	99, 100	Blažić L.	118, 119, 120
Alexeenko A.A.	89	Bliznakova I.	122
Alic N.	41	Blondeau J-P.	45
Al-Jibbouri H.	56	Boeva R.	111
Allegre O.J.	58	Bogdanović G.	121
Allix M.	45	Bojanic R.	156
Allsop T.	134	Božić M.	54
Ameloot M.	90	Brik M.G.	70
Andreici E.-L.	78	Brunner R.	44
Antić Ž.	70, 71	Buck V.	82
Arnaković S.	142	Bulgakova N.M.	31
Arsenović D.	144, 145	Bunoiu O.	132
Arsoski V.	73	Burić N.	149
Auzinsh M.	105	Busuladžić M.	91, 92
Avram C.N.	70, 78	Cantelar E.	22
Avram N.M.	70, 78	Cartaleva S.	109
Avramov L.	122	Castagna N.	39, 106
Bajcsy M.	23	Cataliotti F.S.	29
Bajić J.	52, 126	Čekada M.	154
Balaž A.	56	Čerkić A.	91, 92
Bălăţeanu D.-M.	127	Cetin A.	49
Bandi T.	38, 103	Cevizovic D.	79
Banica R.	61, 72	Chembo Y.K.	50
Barnakov Y.	88	Chen F.	22
Becker W.	91	Chen G.	28
Belenky A.	30	Chipouline A.	38
Belic M.	28, 97, 98, 99, 137, 138	Cholley N.	50
Beličev P.P.	86, 102	Christodoulides D.	21
Benayas A.	22	Chu S.	26
Berberova N.	140	Crnjanski J.V.	130, 131

Cuk S.M.	147	Fedotova O.	46, 112
Čukarić N.	73	Feldhaus J.	47
Cvetković S.	142	Ferber R.	105
Damljanović V.	75	Ferrera M.	26
Damnjanovic V.	80	Fidanovski Z.	114
Danicic A.	115, 134	Freysz E.	112
Davidović Lj.	146	Gahbauer F.	105
Davidović M.	54, 146	Gajić R.	75, 81, 85, 90
De Clercq B.	90	Gaković B.	153, 154
de Rooij N.F.	110	Galliou S.	50
Dean P.	42	Galovic S.	79, 107
Dearden G.	32, 58	Gansch R.	44
Degert J.	112	Gazibegović-Busuladžić A.	91, 92
Degrieck A.	141	Gensch M.	47
Delić N.V.	142	Georges P.	63
Denkova D.	90	Georgieva R.	124
Denz C.	137, 138	Gillijns W.	90
Deubener J.	135	Gligorić G.	95, 151
Diaci J.	33	Glukhov I.L.	55, 143
Dimitrijević J.	144, 145	Glushko O.	44
Dimitrova T.L.	68, 148	Glushkov A.V.	53, 113
Dimova E.	150	Goldner P.	63
Djerdj I.	84	Gourier D.	36
Djordjevich A.	127, 128, 129	Grabiec M.	45
Dmitruk I.M.	88, 89	Graf T.	63
Dobrev G.	150	Grigorova Ts.	148
Dong N.N.	22	Grozescu I.	61, 72
Đorđević M.	121	Gruet F.	38
Đorđević V.	70, 71	Gruia A.S.	70
Drachev V.P.	22	Grujić M.	80
Dramićanin M.D.	70, 71	Grujic Z.	39, 116
Dreischuh T.	122	Grujić Z.D.	146
Drljača B.	129	Gurdev L.	122
Druon F.	63	Gusavac P.	107
Duchesne D.	26	Gvozdić D.M.	130, 133
Dzierżęga K.	45	Hadžievski Lj.	59, 95, 96, 86, 151
Edwardson S.P.	32	Hangyo M.	19
Edwardson S.P.	58	Hasović E.	91, 92
Eftimov T.	68	Headley W.	129
Elazar J.	66, 80	Hingerl K.	85
Ellis B.	23	Hmima A.	50
Enache C.	72	Holodkov V.	142
Faatz B.	47	Horvat D.	155
Faraon A.	23	Ikonić Z.	115
Fearon E.	32	Ilić I.	86, 102

Ilic J.	114, 117	Kochev V.	121
Indjin D.	115	Kopeika N.S.	30
Ishiguro S.	59	Kostadinov I.K.	104
Isić G.	81, 85	Kostić R.	74, 75, 95
Ivanov B.	139, 141	Kotko A.V.	89
Ivanov G.	68	Kovačević A.	121, 152
Ivašcu S.	78	Kovačević M.S.	127, 128
Jacinto C.	22	Krasteva A.	109
Jaffres A.	63	Krmpot A.J.	147
Jakovljević M.	81, 85	Krsmanović R.M.	70, 71
Jakšić Z.	69, 84	Krstić M.M.	130, 133
Jaque D.	22	Krumnow C.	56
Jelenkovic B.	137, 153	Kuang Z.	32
Jelenković B.M.	146, 147	Larger L.	50
Jevremović D.	121	Latinovic Z.	117
Jeyaram Y.	90	Lazarides N.	37
Jhozaki T.	30	Lechkov A.	148
Jin C.	67	Lecointre A.	36
Jokanovic B.	83,156	Lee C.	67
Joseph H.	30	Lekić M.M.	146
Jovanic P.	117	Levanon A.	30
Jovanović D.	71	Lifante G.	22
Jovanović D.J.	70	Lighezan L.	124
Jovanović R.	97, 137	Lim Y.L.	34
Jović D.	97, 137, 138	Lima A.	150
Joža A.	126	Little B.E.	26
Kalchmair S.	44	Liu D.	32
Kalvans L.	105	Loiseau P.	63
Kantardžić I.	119, 120	Lončar M.	18
Kar A.K.	22	Lucic N.M.	147
Karnakis D.	32	Lukić D.V.	146
Kasprzak M.	39, 116	Lupan O.	62
Kearsley A.	32	Lyubenova T.	141
Keča T.	129	Majumdar A.	23
Kevrekidis P.G.	18	Maldiney T.	36
Khasanov O.	46, 112	Malomed B.A.	28, 95, 96, 151
Khetselius O.Yu.	98	Maluckov A.	95, 96, 151
Kılıckaya M.S.	49	Manojlovic L.	52
Kim E.	23	Marinkovic B.P.	108, 123
Kim H.	67	Markoski B.	142
Kip D.	135	Markovic D.	118
Kirilov V.I.	104	Mashanovich G.	129
Kivshar Yu.S.	138	Matavulj P.	129
Kliese R.	34	Matković A.	81
Knowles P.	39, 116	Matthey R.	38

Matthias A.	135	Ovsiannikov V.D.	55, 143
Meisels R.	44	Paepegem W.Van	141
Mellor L.	58	Panić B.	65, 72
Merkle M.	114	Panjan M.	153
Miclau M.	61	Pantelić D.	65, 72, 118, 137, 141, 153
Mihailescu I.N.	154	Papageorge A.	23
Miladinović T.B.	93, 94	Park S.	67
Milanović B.	51, 66, 125	Pashov A.	150
Milanovic D.	57	Pasquazi A.	26
Milanović V.	86, 87, 115, 134	Pauporté T.	62
Mileti G.	38, 103, 110	Pavlovic N.B.	101
Miletic D.	38, 103	Pavlyuchenko E.	50
Milosavljevic A.	57, 152	Peccianti M.	26
Milošević D.B.	91, 92	Peeters F.M.	73, 80
Milosevic V.	156	Pellaton M.	38, 110
Mima K.	30	Pellerin N.	45
Miret J.J.	69	Pellerin S.	45
Miron I.	61, 72	Pelster A.	56, 150
Mitrovic M.	83	Perrie W.	32, 58
Momcilovic M.	57	Peruško D.	57, 153
Moorhouse C.	32	Petkov S.	76
Morandotti R.	26	Petkov V.	90
Moshchalkov V.V.	90	Petkova P.	75, 76
Moss D.J.	26	Pétremand Y.	110
Mottay E.	63	Petronić S.	57, 152
Mozers A.	105	Petrov N.	109
Možina J.	33, 155	Petrovic J.	134
Murić B.	65, 72, 118	Petrović M.	98
Naether U.	48	Petrovic M.D.	95, 134
Nagatomo H.	30	Petrovic N.	97
Neagu A.	124	Petrović S.	153, 154
Nedkov V.	76	Pinchuk A.O.	89
Nesic M.	107	Popescu A.	132
Nicoara I.	64	Popovic A.	79
Nikezić D.	127	Popović Z.	84
Nikolić Lj.	59	Popovic M.	107
Nikolić M.G.	70, 71	Prepelitsa G.P.	98
Nikolic S.N.	147	Prvanović S.	97, 149
Nikolov M.	111	Puškar T.	118, 119, 120, 121
Nistora R.	76	Rabasovic M.S.	108, 123
Oberlé J.	112	Radak B.	154
Odžak S.	92	Radjenović B.	51, 125
Opalevs D.	105	Radmilović-Radjenović M.	51, 125
Oros A.	117	Radojičić I.S.	146
Ostojić S.	114	Radonjić M.	147, 149

Radosavljević S.	134	Soskic Z.	79, 107
Radovanović J.	86, 87, 115, 134	Spiridonov I.	111
Radu C.	154	Sreckovic M.	114, 117
Radulović M.M.	93, 94	Stanciu M.L.	74
Raicevic N.	135	Stašić J.	154
Rakić A.D.	34	Stef M.	64, 132
Ralević U.	81	Stepić M.	48, 102
Ramović S.	87	Stevanović J.M.	93, 94
Razzari L.	26	Stojanović D.	74, 82, 95
Ricaud S.	63	Stojanovic N.	47
Richard C.	36	Stojanovic Z.	79
Ristić V.M.	93, 94	Stojanović-Krasić M.	96
Ritz D.	63	Stoyanov D.	122
Ródenas A.	22	Stoykov E.	139
Rozban D.	30	Stoykova E.	140, 141
Rusetsky G.	46	Strasser G.	44
Rusetsky G.	112	Strinić A.	97, 98
Sainov V.	139, 140, 141	Stupar D.	52, 126
Sakagami H.	30	Suganuma A.	63
Salatić B.	153	Sukhorukov A.	46
Saltiel S.	109	Sunahara A.	30
Salzenstein P.	50	Svinarenko A.A.	98, 113
Sambles J.R.	25	Tacheva J.	76
Sarkisyan D.	109	Tadić M.	73, 80
Savic-Sevic S.	118, 137	Taguchi T.	30
Savović S.	128, 129	Tan Y.	22
Scherman D.	36	Tasić M.	119, 120
Schneidmiller E.	47	Tavella F.	47
Sedmak A.	152	Teixeira A.	101
Segev M.	20	Temelkov I.	150
Sergeev A.	28	Temelkov K.A.	104
Šetrajčić I.J.	142	Terzic M.	108, 123
Šetrajčić J.P.	142	Themelis S.I.	104
Sevic D.	108, 123	Thomsom R.R.	22
Shambat G.	23	Todorov P.	109
Shopova M.	111, 139	Tomić Lj.	66
Silhanek A.V.	90	Tomić S.	40, 134
Silva W.F.	22	Torchia G.A.	22
Simović A.	128	Totović A.	130
Skarka V.	99, 100	Trtica M.	153, 154
Škorić M.M.	59	Tsironis G.P.	37
Slankamenac M.	52, 126	Ucgun E.	49
Slaveeva S.I.	104	Ursu D.H.	61
Slavov D.	109	Vaida M.	74, 77
Soltani M.T.	76	Valev V.K.	90

Vankov O.	122	Watkins K.	32
Vaseva K.	109	Watkins K.G.	58
Vasić B.	85, 90	Weichelt B.	63
Vasile M.	61, 72	Weis A.	39, 106, 116, 148
Vasiljević D.	65, 72, 118, 119, 120	Wilson S.J.	34
Vázquez de Aldana J.	22	Woehrl N.	82
Verbiest T.	90	Wolak A.	45
Verdal J.	89	Yadid-Pecht O.	30
Vereb G.	35	Yeshchenko O.A.	88, 89
Veron O.	45	Yitzhaky Y.	30
Viana B.	36, 62, 63	Yurkov M.V.	47
Vicencio R.A.	48	Zahreddine H.	97
Vidal S.	112	Zamfirescu M.	154
Vidanović I.	56	Zapata-Rodriguez C.J.	69
Vitanov N.	150	Zarenia M.	80
Vizman D.	132	Zarkov B.	141
Vladimirova L.	121	Zarkov B.G.	100
Voss A.	63	Zarubin M.	50
Vuchkov N.K.	104	Živanov M.	52, 126
Vučković J.	23	Zlitni A.G.R.	133
Vujčić Z.	101		
Vuković S.M.	69		